Development of Novel Cysteine Synthase M and Lysine Ɛ-Aminotransferase Inhibitors Targeting Dormant Stages of *Mycobacterium tuberculosis*

THESIS

Submitted in partial fulfilment

of the requirements for the degree of

DOCTOR OF PHILOSOPHY

by

R. RESHMA SRI LAKSHMI

ID No 2012PH47063H

Under the supervision of

D. SRIRAM

BITS Pilani

Pilani | Dubai | Goa | Hyderabad

BIRLA INSTITUTE OF TECHNOLOGY & SCIENCE, PILANI

2017

BIRLA INSTITUTE OF TECHNOLOGY & SCIENCE, PILANI

CERTIFICATE

This is to certify that the thesis entitled "**Development of Novel Cysteine Synthase M and Lysine Ɛ-Aminotransferase Inhibitors Targeting Dormant Stages of *Mycobacterium tuberculosis***" and submitted by **R. RESHMA SRI LAKSHMI** ID No. **2012PH47063H** for award of Ph.D. of the Institute embodies original work done by her under my supervision.

Signature of the supervisor :

Name in capital letters   : **D. SRIRAM**

Designation   : **Professor**

Date:

Acknowledgement

This thesis is the end of my journey in obtaining my Ph.D. In this wonderful journey there are numerous people whose continuous support, encouragement and guidance helped me to successfully complete my thesis. I would take this opportunity to express my gratitude to each and every one who made my stay in BITS memorable.

*My first thanks must go out to my adviser, HOD of pharmacy department **Prof. D. Sriram** for the continuous support of my Ph.D. study and research, for his patience, motivation, enthusiasm and immense knowledge. His guidance helped me in all the time of research and writing of this thesis. Our interactions were always quite informal and friendly. I consider myself quite fortunate to have had such an understanding and caring adviser, throughout the course of my research at the Institute. The work environment given to me under him, the experiences gained from him and his creative working culture are treasured and will be remembered throughout my life.*

*I gratefully acknowledge my DAC member **Prof. A. Sajeli Begum** for her understanding, encouragement and personal attention which have provided good and smooth basis for my Ph.D. tenure.*

*I deeply acknowledge and my heartfelt thanks to **Dr. Balaram Gosh**, Department of Pharmacy, BITS, Pilani-Hyderabad campus, for his valuable suggestions, guidance and precious time which he offered me throughout my research. And I indeed very thankful for his support during practical sessions.*

*I would like to thank my parents **R V Ramakrishnam Raju** and **R V Lakshmi**, my brother **Rajesh Varma** and his wife **Geetha bhavani** who have given their blessings for the great desire to see me succeed and get the highest degree in education. It is only their vision, support and encouragement which always helped me in keeping my morale high. I dedicate this thesis to my father for his unconditional love and care.*

*I take this opportunity to thank **Prof. Souvik Bhattacharya**, Vice-Chancellor (BITS) and Director **Prof. G Sundar** (Hyderabad campus), for allowing me to carry out my doctoral research work in the institute.*

Date   *R Reshma Sri Lakshmi*

DEDICATION

This thesis is dedicated to my beloved father, **R V Ramakrishnam Raju**.

Abstract

Tuberculosis still remains the leading cause of death worldwide. The major obstacles in the path to end TB are resistance, persistence and coinfection. One third of world population acts as reservoir of torpid noncontagious form of disease. Available treatment strategies have many drawbacks like longer treatment period, side effects, drug interactions which result in patient noncompliance. In present work we thrived to develop inhibitors against dormant targets namely- Cysteine synthase M and Lysine ε-amino transferase.

By high throughput screening approach leads were identified for CysM which were taken for further optimization by synthesis and biological evaluation. Among 54 compounds tested, compounds **RK_01** 3-(3-(3,4-Dichlorophenyl)ureido)benzoic acid and **RK_03** 4-(3-([1,1'-Biphenyl]-3-yl)ureido)-2-hydroxybenzoic acid were active against replicating and non replicating stages of mycobacteria. **RK_01** when tested for enzyme inhibitory assays showed an IC_{50} of 0.48 μM.

For second target, LAT 3 libraries comprising a total of 61 compounds were prepared by lead derivatization approach. In cyclobutyl series of 18 compounds, **RL_33** 2-hydroxy-2-(1-(3-(4-nitrophenyl)thioureido)cyclobutyl)acetic acid emerged as most potent compound with an IC_{50} of 2.09 ± 0.21μM. **RL_37** was found to be more potent in dormant models such as nutrient starvation, biofilm. Among 22 benzthiazole inhibitors **RR_22** (E)-4-(5-(2-(benzo[d]thiazol-2-yl)-2-cyanovinyl)thiophen-2-yl)isophthalicacid emerged as potent molecule with LAT IC_{50} of 2.62 μM. It has a significant log reduction of 2.9 and 2.3 fold against nutrient starved and biofilm forming mycobacteria. In last series belonging to quinoline class, compounds **RS_21** and **RS_30** were found to be more potent with IC_{50} values of 0.74 ± 0.16 and 0.74 ± 0.34 μM respectively. But **RS_10** 2-(4-(quinolin-4-yl)piperazin-1-yl)-N-(pyridin-2-ylmethyl)acetamide results show that it is equally effective as standard drugs against active stage of TB additionally it has an advantage of potency against persistent phase of TB by inhibiting dormant target LAT.

We believe that present class of inhibitors owing to their potency and efficacy against persistent TB would be able to meet the urge for new antitubercular drugs.

Table of contents

LIST OF TABLES

LIST OF FIGURES

LIST OF ABBREVIATIONS

μg	:	Microgram
μL	:	Microlitre
μM	:	Micromolar
^{13}C NMR	:	Carbon Nuclear Magnetic Resonance
^{1}H NMR	:	Proton Nuclear Magnetic Resonance
3D	:	Three Dimensional
ANOVA	:	Analysis of Variance
Ala	:	Alanine
Arg	:	Arginine
ATP	:	Adenosine Triphosphate
(BOC)$_2$O	:	Di-tert-butyl dicarbonate
BSA	:	Bovine serum albumin
CDCl$_3$	:	Chloroform deuterated
CysM	:	Cysteine synthase M
CysK	:	Cysteine synthase K
d	:	Doublet
DCM	:	Dichloromethane
dd	:	Doublet of doublet
DMF	:	*N*,*N*-Dimethylformamide
DMSO	:	Dimethyl sulfoxide
DMSO-d$_6$	:	Dimethyl sulphoxide deuterated
DOTS	:	Directly Observed Treatment, Short course
DRC	:	Dose Response Curve

E	:	Ethambutol
EMA	:	European Medical Agency
ESI	:	Electron Spray Ionization
Et$_3$N	:	Triethylamine
EtOH	:	Ethanol
FDA	:	Food and drug administration
GABA	:	γ-aminobutyrate aminotransferase
H/ INH	:	Isoniazid
HEPES	:	4-(2-Hydroxyethyl)-1-Piperazineethanesulfonic acid
HIV	:	Human Immuno Deficiency Virus
HPLC	:	High Pressure Liquid Chromatography
IC$_{50}$	:	Half Maximal Inhibitory Concentration
ITC	:	Iso Thermal Calorimetry
J	:	Coupling constant
KCl	:	Potassium chloride
kDa	:	Kilodalton
KOH	:	Potassium hydroxide
LAT	:	Lysine ε-amino transferase
LB	:	Luria Broth
LCMS	:	Liquid chromatography–Mass Spectrometry
LHS	:	Left Hand Side
m	:	Multiplet
M.p	:	Melting point
MDR-TB	:	Multidrug-Resistant Tuberculosis
MeOH	:	Methanol

mg	:	Milligram
MgCl$_2$	:	Magnesium chloride
MHz	:	Mega hertz
MIC	:	Minimum Inhibitory Concentration
mL	:	Milliliter
Mmol	:	Millimole
Msm	:	*Mycobacterium smegmatis*
Mtb	:	*Mycobacterium tuberculosis*
MTT	:	(4,5-Dimethylthiazol-2-yl)-2,5-diphenyltetrazolium bromide
MW	:	Microwave
NaCl	:	Sodium chloride
NADH	:	Nicotinamide Adenine Dinucleotide
nM	:	Nanomolar
NRP	:	non-replicating persistence
OADC	:	Oleic Albumin Dextrose Catalase
OASS	:	O-acetylserine sulfhydrylase
OAT	:	Ornithine aminotransferase
OD	:	Optical density
OPS	:	O-phosphoserine
P	:	Para
PDB	:	Protein Data Bank
Ppm	:	Parts per million
PLP	:	Pyridoxal pyrophosphate
R/Rif	:	Rifampicin
ROI	:	Reactive oxygen intermediate

RNS	:	Reactive nitrogen species
Rpm	:	Rotations per minute
RPMI	:	Roswell Park Memorial Institute
Rt	:	Room temperature
S	:	Singlet
SAR	:	Structure Activity Relationship
SDS-PAGE	:	Sodium Dodecyl Sulphate- Polyacrylamide Gel Electrophoresis
t	:	Triplet
TAE	:	Trisbase, Acetic acid, EDTA mixture
TB	:	Tuberculosis
TFA	:	Trifluoroacetic acid
THF	:	Tetrahydrofuran
TLC	:	Thin-layer chromatography
TMS	:	Trimethylsilane
UV	:	Ultraviolet
WHO	:	World Health Organization
XDR-TB	:	Extensively Drug-Resistant Tuberculosis
XP	:	Extra Precision
Z	:	Pyrazinamide
δ	:	Chemical shift

Nature is that lovely lady to whom we owe polio, leprosy, smallpox, syphilis, tuberculosis, cancer. In spite of availability of large number of antibiotics and vaccine for treatment still every 15 seconds one person die out of TB and 8 million new cases are reported every year [WHO Global tuberculosis report, 2016]. TB is aptly referred to as consumption, phthisis, wasting disease, King's Evil, captain of deaths as it is leading cause of deaths worldwide. TB is caused by nonmotile, acid-fast, obligate aerobe namely *Mycobacterium tuberculosis*. "TB Anywhere Is TB Everywhere" because it spreads mainly by inhalation of aerosols containing the tubercle bacilli. Each aerosol droplet contains 1 - 400 bacilli which is enough to cause infection (infectious dose is 1-200 bacilli) [Sakamoto, K. 2012, Daniel, T. M., et al., 2006].

Mtb mainly resides in respiratory system i.e., alveoli of lungs. Once infected host may develop symptoms of disease (active infection) or bacilli may reside in granuloma (latent infection) [Smith, I. 2003]. The symptoms of disease are variable and most commonly found symptoms include coughing, fatigue, malaise, wasting, finger clubbing, low grade fever accompanied by chills and night sweats, hemoptysis, dyspnea or orthopnea (in severe stages), anemia and leukocytosis [Knechel NA, *et al*., 2009, Payne, D. J., *et al*., 2013].

One third of population acts as reservoir of TB as they are carrying *Mtb* inside without symptoms of the disease. The risk of development to active TB is about 5-10% in life time and it can be aggravated by factors such as coinfection with HIV, use of immunosuppressant, Diabetes mellitus, cancer, malnutrition, aging, smoking, and alcohol consumption [Lin, P. L., *et al*., 2010].
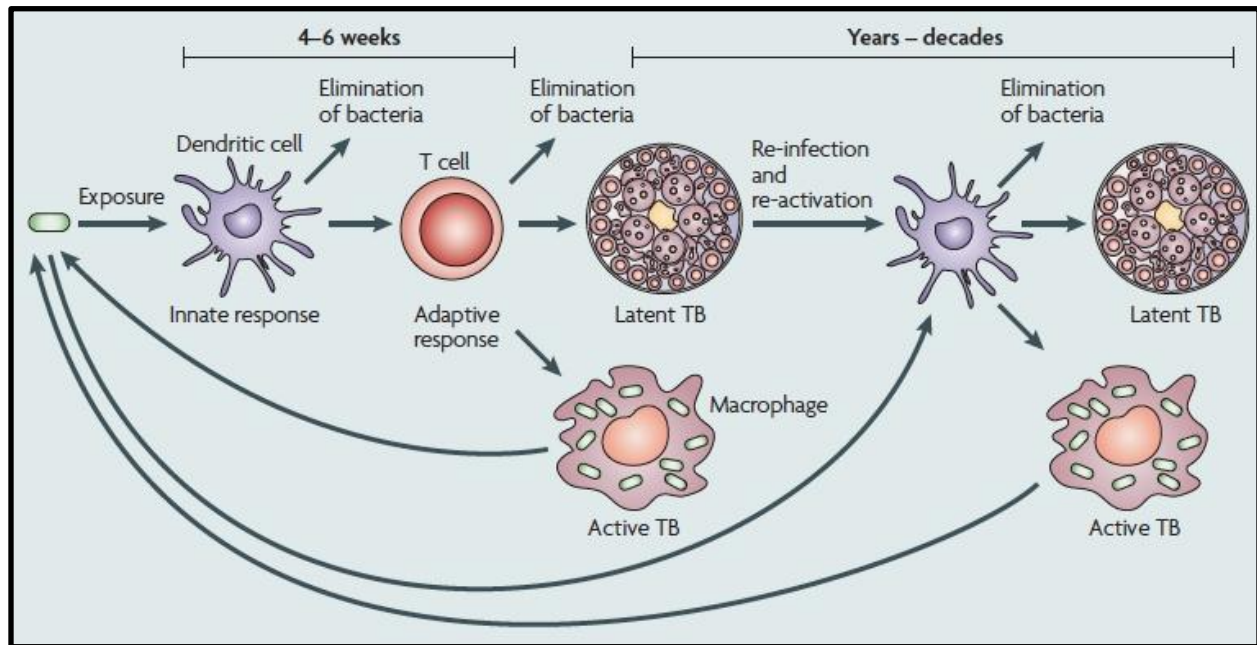
Fig 1.1: Pathophysiology of Tuberculosis [Young, D., *et al*., 2008].

1.1. Latent Tuberculosis –Granuloma formation:

Granuloma formation is hall mark of pulmonary tuberculosis and can be defined as compact, organized aggregates of immune cells consisting of blood-derived infected and uninfected macrophages, foamy macrophages, epithelioid cells (uniquely differentiated macrophages), and multinucleated giant cells (Langerhans cells) surrounded by a ring of lymphocytes. Granuloma has dual contradictory rule as it controls the progression of disease as well as acts as niche for survival of *Mtb* [Silva Miranda, M. *et al*., 2012, Rubin, E. J. 2009].
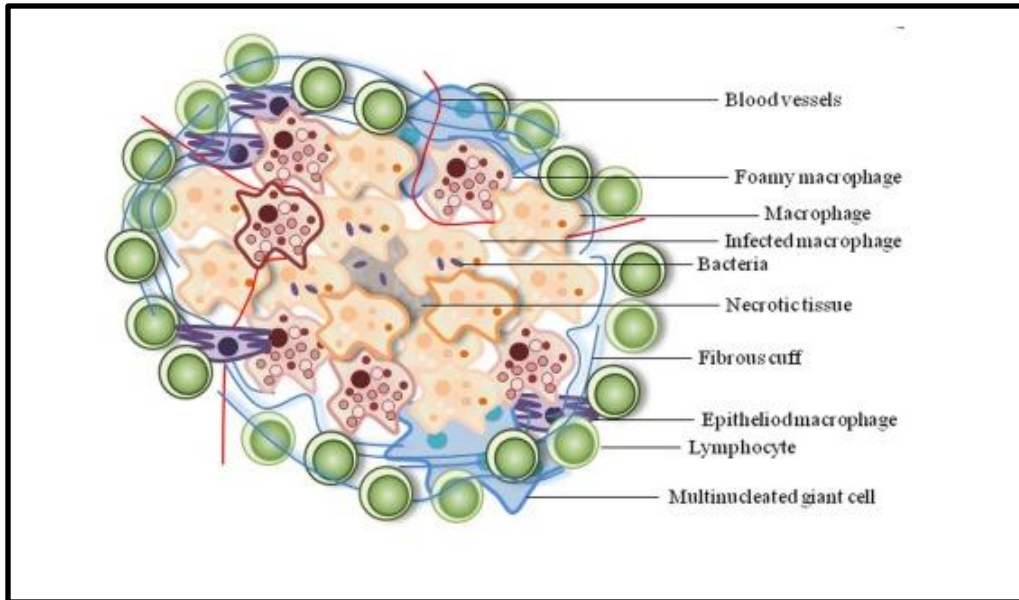
Fig 1.2: Environment of Granuloma [Guirado, E., *et al*., 2013].

Bacilli after entering through respiratory route invade immune cells such as alveolar macrophages, type 2 pneumocytes, and polymorphonuclear neutrophils. Infected macrophages stimulate events leading to production of pro and anti-inflammatory cytokines and chemokines which in turn initiates phagocytes and recruits mononuclear leukocytes into the site of infection. All these events lead to accumulation of cells around bacilli resulting in formation of granuloma. The granuloma is maintained by delayed type of hypersensitivity response produced by stimulating antigens and lipids. Necrosis happens in center of granuloma leading to accumulation of protein and lipid rich caseum. During chronic infection granuloma are calicified. A balance of pro-inflammatory and anti-inflammatory immune responses is essential for maintaining latent TB. One the balance is disturbed progression to active TB occurs causing symptoms of TB. *Mtb* can survive dormant in granuloma for many decades till the conditions seem favorable for infection. This ability to survive in adverse conditions is the secret for success of TB. In the microenvironment of granuloma *Mtb* faces challenges such as hypoxia, nutrient starvation, and oxidative stress. To combat this stress *Mtb* enters into dormancy characterized by changes in phenotype, genotype and metabolism [Guirado, E., *et al*., 2013, Rubin, E. J. 2009, Lin, P. L., *et al*., 2010].

3

1.2. History of tuberculosis treatment:

Streptomycin isolated from *Streptomyces griesus* was the first antibiotic for treatment of TB. Indiscriminate use of it led to development of resistance which was combated by use of Para-amino salicylic acid, Isoniazid, Pyrazinamide, Cycloserine and Kanamycin in combination [Coxon, G. D., *et al*., 2012]. The major drawback of this therapy was longer treatment duration of 18 months or more. This disadvantage was overcomed with new therapy comprising of Iisoniazid, Rifampicin, Pyrazinamide and Ethambutol for 6-9 months. Rifabutin has replaced the role of rifampicin in treatment regimen for HIV patients as the latter has drug interaction with protease inhibitors [Zumla, A., *et al*., 2013]. Currently available drugs are classified into 5 classes based on their efficacy, chemical nature and side effects. Group I are generally used for treatment of susceptible strains of TB whereas group II - IV are preserved for resistant strains [Zumla A., *et al*., 2013 and 2014].

FIRST LINE DRUGS	GROUP 1 (oral)	Isoniazid, Rifampicin, Pyrazinamide, Ethambutol, Rifapentine or Rifabutin
SECOND LINE DRUGS	GROUP 2 (injectable amino glycosides, poly peptides)	Streptomycin, Kanamycin, Amikacin, Capreomycin, Viomycin
	GROUP 3 (oral & injectable fluoro quinolones)	Ciprofloxacin, Levofloxacin, Moxifloxacin, Ofloxacin, Gatifloxacin
	GROUP 4 (oral)	p-Amino salicylic acid, Cycloserine, Terizidone, Ethionamide,Prothionamide, Thioacetazone, Linezolid
THIRD LINE DRUGS	GROUP 5	Clofazimine, Linezolid, Clarithromycin, Amoxycillin + Clavulanate, Imipenem + Cilastatin

Table 1.1: Classification of drugs used for TB treatment.
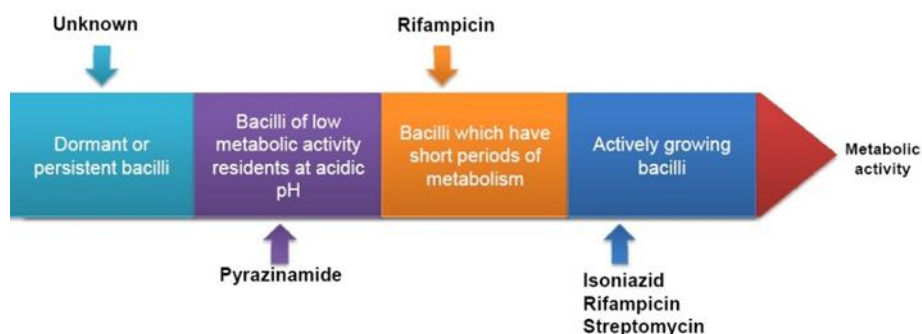
Fig 1.3: Mechanism of action of known drugs.

1.3. Current Tuberculosis Regimen:

WHO recommends standard regimen of antibiotics in DOTS therapy for newly infected individuals for period of 6 months which covers 2 phases [Ginsberg, A. M., *et al*., 2007]. The primary phase i.e., Intensive phase treatment involves use of Isoniazid (H), Rifampicin (R), Pyrazinamide (Z), Ethambutol (E) and Streptomycin for a period of 2 months; the latter phase namely Continuation phase involves use of Isoniazid and Rifampicin for 4 months to completely eliminate bacteria and avoid development of resistance [Dover, L. G., *et al*., 2011]. WHO recommended doses of first line drugs for adults are as follows.

| | Recommended dose | | | |
| | Daily | | 3 times per week | |
Drug	**Dose and range** (mg/kg body weight)	**Maximum (mg)**	**Dose and range** (mg/kg body weight)	**Daily maximum (mg)**
Isoniazid	5 (4-6)	300	10 (8-12)	900
Rifampicin	10 (8-12)	600	10 (8-12)	600
Pyrazinamide	25 (20-30)	-	35 (30-40)	-
Ethambutol	15 (15-20)	-	30 (25-35)	-
Streptomycin	15 (12-18)		15 (12-18)	1000

Table 1.2: WHO recommended therapy for treatment of TB.

For new patients with INH resistance intensive phase lasts for 2 months with use of HRZE and continuation phase involves HRE for 4 months. In case of HIV infected patients with TB, TB therapy is started prior to Clotrimoxazole and antiretroviral therapy. Drugs used for treatment of MDR TB have been classified into 5 groups based on their efficacy. The standard regimen for treatment of MDR TB consists of 8 months of Pyrazinamide, Kanamycin, Ofloxacin,

Protionamide, and Cycloserine, followed by 12 months of Ofloxacin, Protionamide, and Cycloserine [WHO Guidelines for treatment of tuberculosis fourth edition-2010, Sharma, S. K., *et al*., 2013].

Group	Drugs (abbreviations)
Group 1 : First-line oral agents	Pyrazinamide (Z) Ethambutol (E) Rifabutin (Rfb)
Group 2 : Injectable agents	Kanamycin (Km) Amikacin (Am) Capreomycin (Cm) Streptomycin (S)
Group 3 : Fluoroquinolones	Levofloxacin (Lfx) Moxifloxacin (Mfx) Ofloxacin (Ofx)
Group 4 : Oral bacteriostatic second-line drugs	p-Amino salicylic acid (PAS) Cycloserine (Cs) Terizidone (Trd) Ethionamide (Eto) Protionamide (Pto)
Group 5 : Agents with unclear role in treatment of drug resistant-TB	Clofazimine (Cfz) Linezolid (Lzd) Amoxicillin/Clavulanate (Amx/Clv) Thioacetazone (Thz) Imipenem/Cilastatin (Ipm/Cln) High dose Isoniazid (High dose H) Clarithromycin (Clr)

Table 1.3: Drugs used for treatment of resistant TB.

1.4. Present scenario of Tuberculosis:

Manmade amplification of TB led to emergence of resistant forms of TB such as MDR TB and XDR TB. Tuberculosis is termed MDR TB (multi drug resistant) if it is resistant to Isoniazid or Rifampicin [Green, K., *et al*., 2013] Treatment of MDR strains is limited due to lesser options, expensive, less potency and more side effects. XDR TB [Haydel, S. E., *et al*., 2010, Parida, S.

K., *et al*., 2015] (extensive drug resistant) [Dheda, K., et al., 2010, O'Donnell, M. R., *et al*., 2013] is MDR TB having additional resistance to any of the Fluoroquinolones (such as Levofloxacin or Moxifloxacin) and to at least one of three injectable second-line drugs (Amikacin, Capreomycin or Kanamycin).

As per WHO report, 2015 witnessed 1.4 million deaths worldwide because of TB which makes TB as leading cause of death. 0.4 million HIV patients died because of TB. Incidence of new TB patients is 10.4 million in 2015 out of which 11% are coinfected with HIV. In 2015 4,80,000 people were found to have MDR TB and 1,00,000 people developed resistance to Rifampicin. 9.5 % cases of MDR TB patients are found to have XDR TB. The **Fig1.4** illustrates the list of countries with three TB burdens from 2016-20 [WHO Global tuberculosis report, 2016].
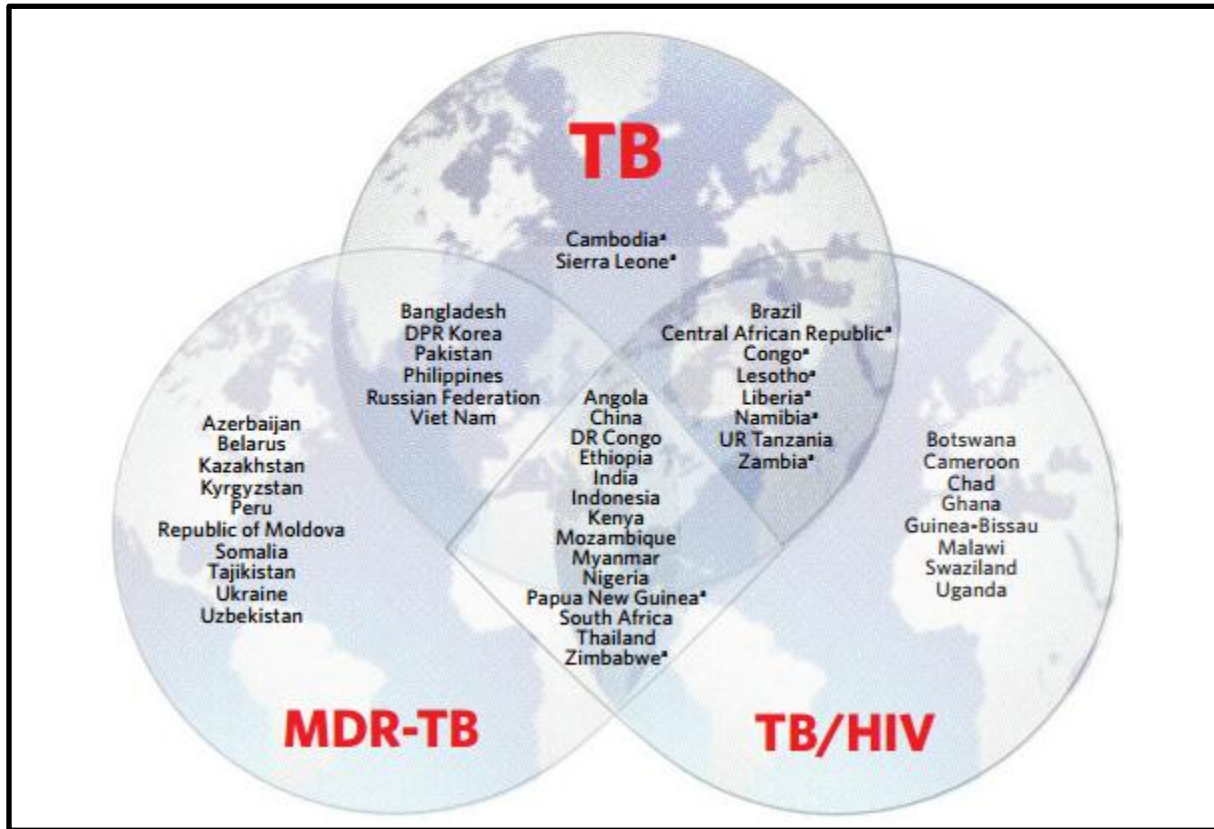
Fig 1.4: Prevalence of TB world wide.

The other major problem with TB treatment is persistence i.e., ability of bacilli to survive in dormant metabolically inactive stage. One third of world population is infected with latent tuberculosis. Most of the drugs available act on metabolically active stages of bacilli [CDC

report 2012]. The standard treatment regimen available for latent TB is use of Isoniazid for 6 – 9 months or Rifampin for 4 months or Isoniazid and Rifapentine for 3 months [Jasmer, R. M., 2002]. The current therapies are lengthy and have associated side effects so there is growing need for new antibacterial agents with more efficacy and potency against resistant and persistent TB. The new agents are also expected to lower duration of therapy.

1.5. TB drug development pipeline:

Due to enormous efforts in area of TB more than 50 rapid diagnostic tests, 15 vaccine candidates and 2 drugs (Bedaquiline and Delamanid) successfully entered clinical trials in the last decade. Apart from development of new drugs researchers are focusing on repurposing of existing drugs for treatment of susceptible, resistant and latent forms of *Mtb*. Examples of repurposed drugs include Linezolid, Meropenem-Clavulanate, Sulfamethoxazole and Mefloquine. Linezolid belonging to oxazolidinone class is effective against MDR and XDR forms of TB at a dose of 300 – 600 mg per day. But long term use is restricted due to associated neurotoxicity, which can be overcomed by using in combination with Clarithromycin. Another derivative from same class Sutezolid is more attractive due to more tolerance and is under development. Meropenem-Clavulanate and Sulfamethoxazole were also found to be effective against MDR and XDR forms of TB [WHO Global tuberculosis report, 2016].
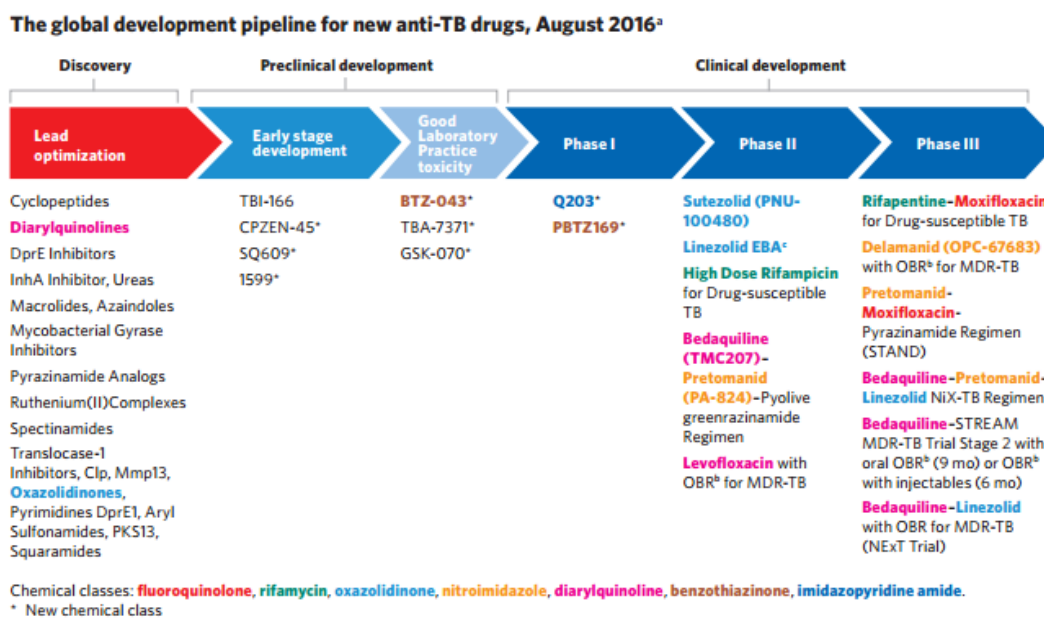
Fig 1.5: Drug development pipeline for TB.

Bedaquiline, Delamanid, Pretomanid, Sutezolid, Q203, SQ109 and Benzothiazinones fall under category of new drugs. Bedaquiline was approved in Dec, 2012 by US FDA for treatment of MDR TB as it targets the proton pump of ATP synthesis. It is superior to Isoniazid and Rifampicin in murine model and also reduces treatment duration to 2 months. Delamanid and Pretomanid are nitroimidazole derivatives under phase 3 clinical trials. SQ109 is an analogue of Ethambutol and is effective against susceptible and resistant forms of TB. It acts by targeting MmpL3 and protein synthesis. Benzothiazinones are in preclinical phase of development and acts by inhibiting cell wall synthesis. PBTZ169 a piperazine containing benzothiazinone is compatible with all TB drugs and appears to have synergies with Bedaquiline and Clofazimine. It is phase I clinical trial for treatment of susceptible and resistant forms of TB. Q203 belongs to imidazopyridine class which acts by inhibiting synthesis and inhibition of ATP. It is under phase I trials [D'Ambrosio, L., 2015].

Global alliance for TB drug [Gupta, P., *et al*., 2004] development extensively works on development of new treatment a regimen that shortens treatment duration and effective against resistant, latent forms of bacteria [Burki, T., et al 2014, Shehzad, A., et al., 2013]. Based on findings in NC-003 trail, combination of Bedaquiline, Pretomanid and Pyrazanamide are now taken further for phase IIB studies. END TB trail organized by Global TB alliance scheduled to start at end of this year evaluates efficacy of Bedaquiline or Delamanid, Moxifloxacin or Levofloxacin and Pyrazinamide + Linezolid or Clofazimine against MDR TB. Other trail TB-PRACTECAL will evaluate safety and efficacy of 6 months regimen consisting of Bedaquiline, Pretomanid and Linezolid with or without Moxifloxacin againt MDR and XDR TB [Lienhardt, C., *et al*., 2010 and 2012, Villemagne, B., *et al*., 2012]. Vigorous efforts are made for development of vaccines to prevent infection or to prevent primary progression to disease or reactivation of latent TB. DAR 901, Ad5 Ag85A, TB/FLU-04L and MVA85A (Aerosol) are few examples of vaccines under phase I trials.

Thorough literature review was done on two targets involved in the study namely- Cysteine synthase M and Lysine Ɛ-aminotransferase. Cysteine synthesis is crucial for intracellular survival of *Mtb* during dormancy. Cysteine serves as prime source for synthesis of mycothiol, essential component involved in redox defense by *Mtb*. Three major pathways are involved in biosynthesis of cysteine which differ in substrate and sulfur donor. Studies revealed that CysM is upregulated in response to hypoxia, oxidative stress and starvation conditions.

LAT is a PLP dependent enzyme involved in catabolism of lysine. It was found to be upregulated in nutrient starvation conditions. It has major role in persistence and antibiotic tolerance.

2.1. Target I - Cysteine synthase M (CysM):

In granuloma *Mtb* is exposed to various stresses such as hypoxia, oxidative stress and depletion of nutrients [Dorhoi, A., *et al*., 2011]. To combat ROI and RNS, *Mtb* needs redox defense and this is primarily maintained by mycothiol [Sareen, D., *et al*., 2003 and Bhaskar, A., *et al*., 2014]. Sulfhydryl group of mycothiol is derived from cysteine so its biosynthesis depends on the availability of cysteine. Cysteine is also required for the repair of iron–sulfur center containing proteins, damaged by reactive ROS and RNI species. Hence during dormancy metabolic pathways related to sulfate assimilation and cysteine biosynthesis are upregulated [Schnappinger, D., *et al*., 2003, Voskuil, M. I., *et al*., 2004]. Enzymes from these pathways have therefore been suggested as potential targets for new antimycobacterial compounds as these pathways are absent in humans. Potent inhibitors of adenosine-5′-phosphosulfate reductase were found to possess bactericidal activity [Voskuil, M. I., *et al*., 2004].

To date, three pyridoxal-phosphate (PLP)-dependent cysteine synthases have been characterized in *M. tuberculosis* (**Fig 2.1**). CysK1, a bonafide O-acetylserine sulfhydrylase (OASS), uses O-acetylserine and hydrogen-sulfide from the APS/PAPS pathway for the synthesis of cysteine [Schnell, R., *et al*., 2005]. CysM on the other hand utilizes O-phosphoserine (OPS) together with a small sulfur delivery protein CysO, which contains a thiocarboxylated carboxy terminus

[Burns, K. E., *et al*., 2005, Ågren, D., *et al*., 2008]. A third putative cysteine synthase, CysK2, also utilizes OPS as acceptor substrate and is able to produce cysteine with hydrogen-sulfide as sulfur donor. However, this enzyme shows a preference for thiosulfate, leading to S-sulfocysteine as the primary product, and is thought to be involved in redox-signaling [Steiner, E. M., *et al*., 2014].
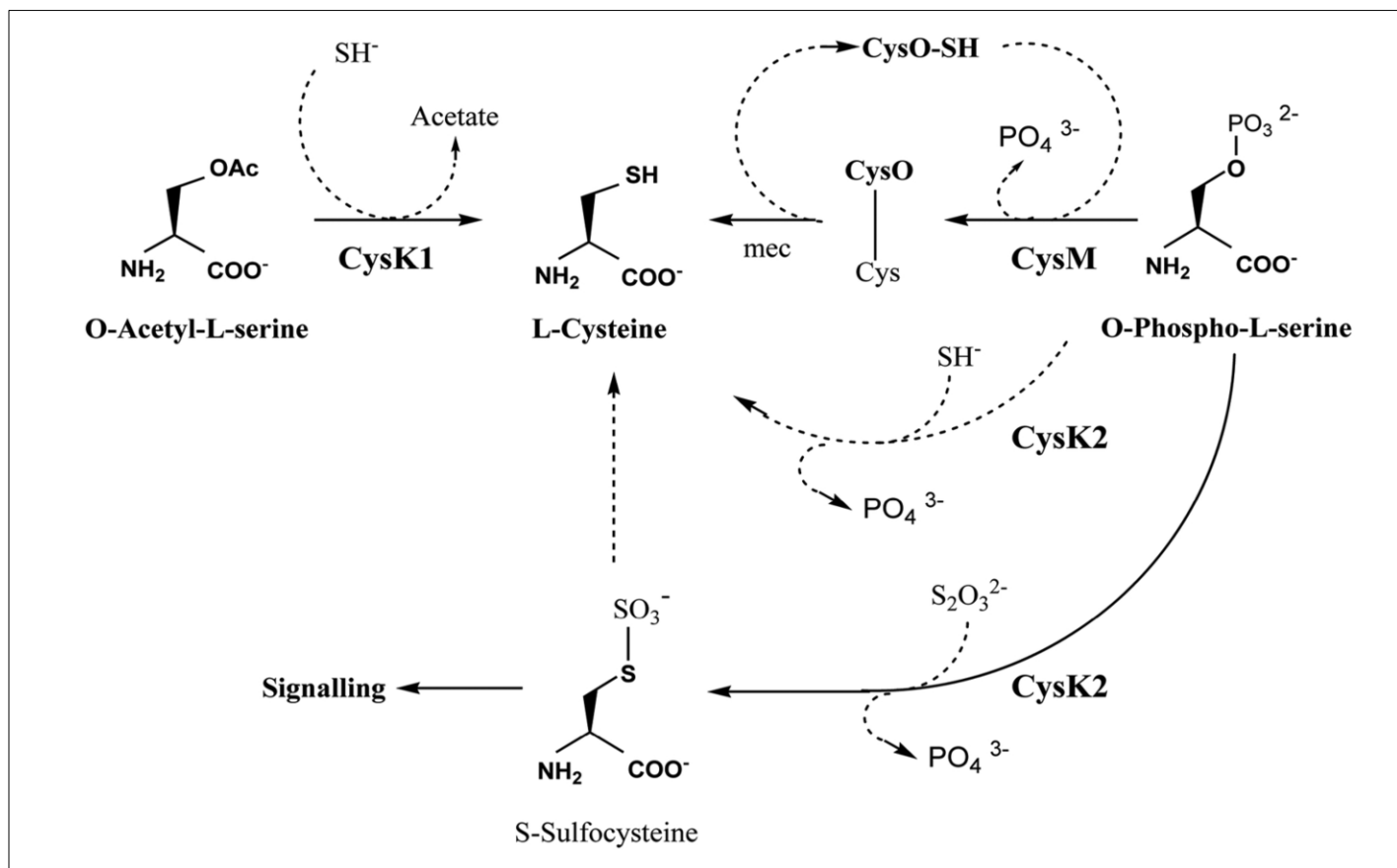
Fig 2.1: Three major pathways involved in cysteine biosynthesis.

The three enzymes involved exhibits similarity in amino acid sequence. CysK1 and CysM has 37% sequence identity where as CysK2 has less similarity of 26% with CysK1 and CysM [Zeng, L., *et al*., 2013]. Denovo L-cysteine biosynthesis in plants, eubacteria, and some archaea is similar to MTB except that they are devoid of OPS pathway [Ågren, D., *et al*., 2008].

CysM is a type II PLP dependent enzyme exhibiting substrate specificity to OPS by hydrogen bond interaction of Arg220 with phosphate group. Site directed mutagenesis of Arg 220 led to loss of OPS recognition capacity. It was found to independent of O-acetyl serine and sulfate

reduction pathways [Ågren, D., *et al*., 2009]. The proteins CysM (Rv1336), CysO (Rv1335), and mec (Rv1334) operating in the OPS-dependent cysteine biosynthesis pathway are encoded in the same transcriptional unit in the H37Rv genome. This pathway is crucial in persistent phase of *Mtb* because OPS is more stable than OAS and thiocarboxylates are more resistant to oxidation than thiols. Mutants carrying a transposon insertion in cysM were shown to be attenuated in macrophages and in a mouse tuberculosis model. Inhibition of CysM alone cannot effect survival of *Mtb* complete inhibition of cysteine pathway requires at least two inhibitors for the two different branches of biosynthesis of this amino acid [Schnell, R., *et al*., 2015].

2.1.1. Cysteine synthase M pathway:

CysM reacts with O-phosphoserine (OPS) to form α-amino acrylate intermediate (species III). In next step a nucleophilic attack of CysO-SH on the amino acrylate followed by a S,N-acyl shift results in the formation of a CysO-cysteine adduct, which is subsequently hydrolyzed by the Zn^{2+}dependent hydrolase Mec$^+$. CysO, a 93 amino acid containing protein serves as a source of sulfur instead of sulfide derived from sulfate reduction pathway. Binding of CysO-SH induces conformational changes in CysM i.e., domain rotation and ordering of C-terminal residues, rendering active site inaccessible from solvent. Reaction with OPS is 600 times faster than with OAS indicating selectivity towards substrate [Ågren, D., *et al*., 2009].
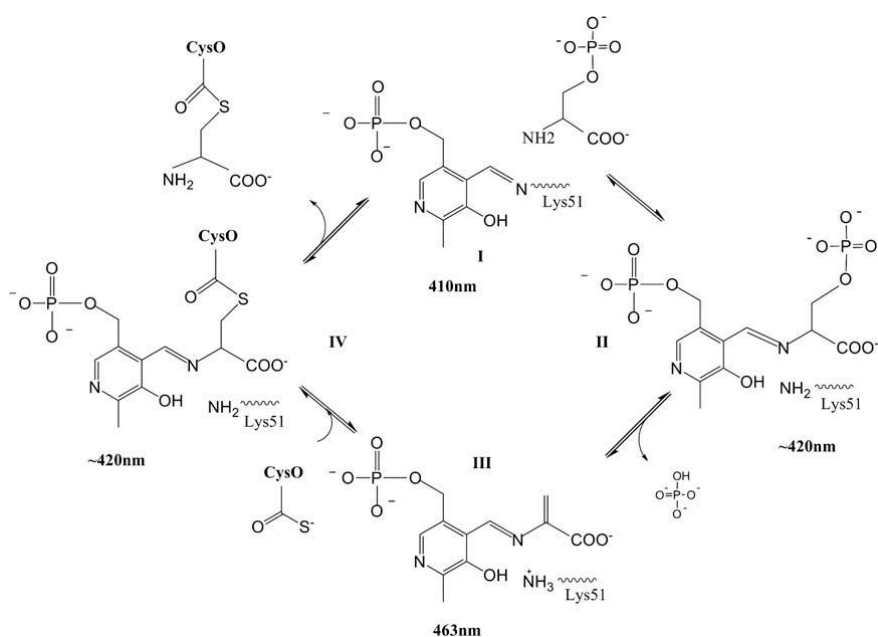
Fig 2.2: Cysteine synthase M mechanism of action.

2.1.2. Structural aspects of CysM:

X-ray crystallographic structure of CysM (2.1 Å resolution) exhibits typical fold of type II PLP dependent enzymes. It is a homodimer in solution and crystal form. Each monomer has two domains and the PLP binding site is formed in a cleft between the C-terminal ends of the β-sheets of the two domains within one subunit. PLP will be bound covalently to Lys51 of active site. Differences in primary and tertiary structures of CysK1 and CysM are responsible for differences in substrate specificities and stabilization of the amino acrylate intermediate. Arg 220 in active site is responsible for switch from OAS to OPS in CysM. Replacement of Arg with Ala resulted in 600 fold decrease in rate of reaction but reaction with sulfur donor is unaffected indicating its role in OPS binding.

Crystal structures of CysM had revealed an open conformation, with the bound cofactor accessible from the bulk solution, and a closed conformation, where two active site loops and the C-terminal residues fold over the active site making it inaccessible. Closed confirmation cannot accommodate PLP due to steric factors. This confirmation restricts the exposure of active site to ROS and RNS making the amino acrylate intermediate more stable than in case of CysK1 from *Mtb* and CysM from *E.coli*. Owing to this advantage and also more stable CysO as sulfur donor makes this pathway more favorable in oxidative stress.
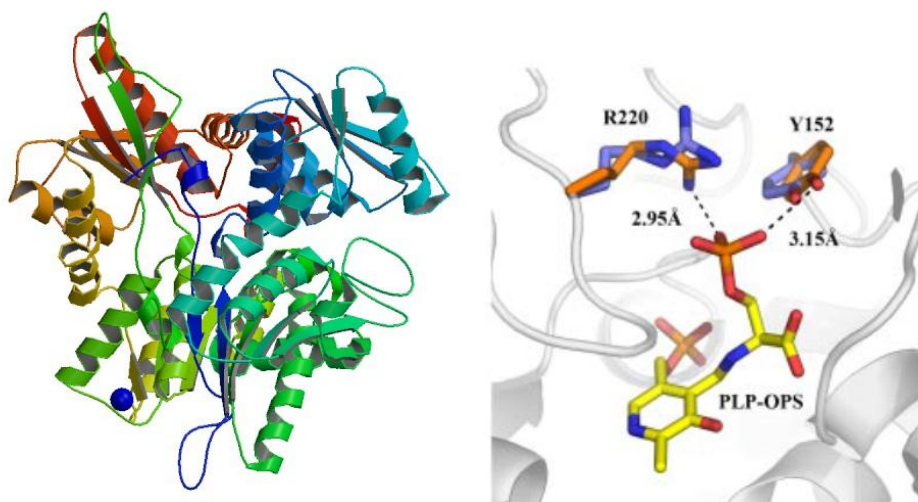
Fig 2.3: PDB structure of CysM and Active site analysis.

All major differences in the structures between the two chains are found at the entrance of the active site and involve three surface loops, L-6 (residues 103–108) including the following helix, L-8 (residues 124–132) and L-15 (residues 210–229). In particular L-15 undergoes complete rearrangement, with a maximum displacement of the tip of the loop by 14 Å. Another important structural change occurs at the C-terminus, where the chain, which is disordered in the subunits showing the open conformation, adopts a well-defined conformation and extends the C-terminal helix by one turn. The last C-terminal amino acids (residues 319-GQLWA- 323) are inserted into the active site cleft. This five residue - long sequence is located between the substrate – carboxylate binding loop (residues 78–82), a segment of the mobile loop L - 15, the N-terminus of helix-8 (residues 264–285) and helix-9 (residues 298–304). The carbonyl oxygen atom of Gln320 forms a hydrogen bond with the backbone amide nitrogen of Thr303. The side chain of Trp322 is stacking against Pro 210 and its main chain amide is engaged in a hydrogen bonding interaction with the main chain carbonyl oxygen atom of Glu214. The oxygen atoms of the terminal carboxyl group are within hydrogen bonding distance to the backbone amide of Asn81 and two water molecules located at the active site. The distance between the nitrogen of the internal aldimine linkage and the closest carboxylate oxygen atom is 3.5 Å. Overall the conformational changes in subunit B result in a closed conformation which renders the active site completely inaccessible to the solvent.

The carboxyl - oxygen atoms of the amino acrylate form hydrogen bonds to the backbone oxygen of Ser79, to the side chain of Thr82 and to carboxy terminus of Ala32. The amino acrylate intermediate formed in CysM is more stable than CysK1 and CysM from *E.coli*. The C-terminal tail acts a plug which protects amino acrylate from oxidative stress and nucleophiles such as sulfide. If last residues in CysM are removed CysO binding is impaired and opening of channel occurs resulting in diffusion of oxidants or nulceophiles to active site. The structure of CysM and CysM bound to CysO is almost similar. Differences in the structures are as follows - loop L-15 undergoes a large conformational change upon binding to CysO and forms the majority of the interaction with CysO. The five C-terminal residues remain inserted into the active site, but the conformation of this polypeptide segment and in particular the interactions of the side chains with residues from the active site pocket are different. N-terminal domain comprising residues 72–152 is shifted towards the active site (about 8 Å maximum distance between equivalent Ca atoms) in the CysM-CysO complex [Ågren, D., *et al*., 2008].

2.2. Target II – Lysine Ɛ-aminotransferase (LAT):

2.2.1. Role of LAT in dormancy

LAT in *Mtb* is expressed by gene Rv3290c and was involved in lysine catabolism. LAT is the member of pyridoxal 5-phosphate (PLP) vitamin B6 dependent aminotransferase family of enzymes [Hayashi H., 1995], which have been divided into several fold types on the basis of structural and evolutionary relatedness. Fold type 1 enzymes are mostly studied and are aspartate aminotransferase (AAT). They are further subdivided into two groups as aspartate aminotransferase belonging to subgroup I [Hayashi H., et al., 1995], LAT a member of subgroup II of fold type I aminotransferases that include ornithine aminotransferase (OAT) and γ-aminobutyrate aminotransferase (GABA).
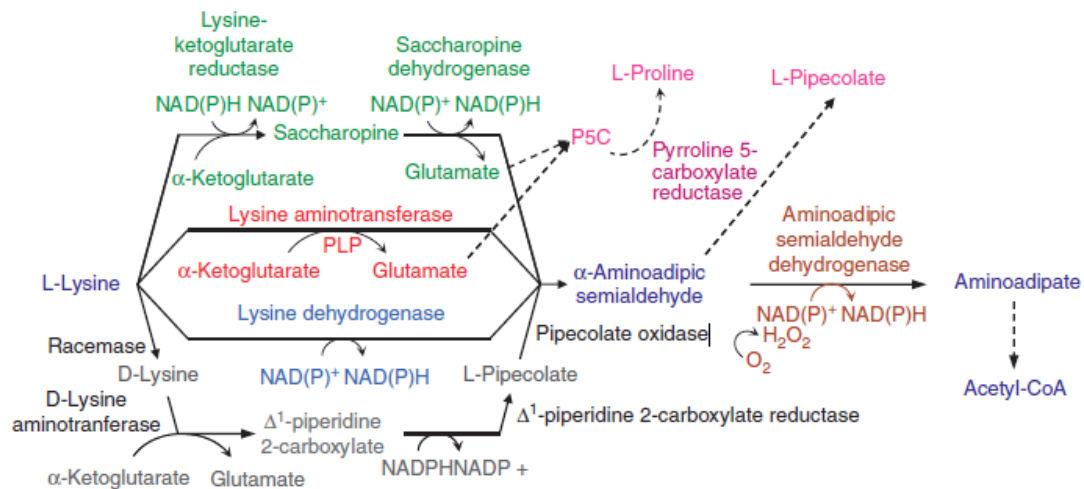
Fig 2.4: The four pathways used by prokaryotes to catabolize lysine to AASA [Neshich, I. A., et al., 2013] .

In β-lactum antibiotic producing bacteria LAT catalyzes first step in antibiotic production. In prokaryotes LAT is involved in regulation of osmotic stress by production of pipecolate [Neshich, I. A., et al., 2013]. It lies within the genomic region upstream of sigF involved in mycobacterial stress response. In *Mtb* LAT was found to be up-regulated over 40-fold in nutrient starved and hypoxia models [Betts J.C., et al, 2002]. Another study revealed the adaption of the pathogenic bacteria to stationary phase and non-replicating persistence (NRP) showed that LAT was up-regulated. Its regulation level on the other hand decreased long-term latency.

LAT was found to be involved in persister formation and antibiotic tolerance especially to norfloxacin. Knock out studies revealed that LAT plays a crucial role in expression of *lrpA* gene which in turn regulates biosynthesis of amino acids. Guanosine 3′,5′ -bispyrophosphate (p)ppGpp is upregulated in starved condition which stimulates LRP so amino acid homeostasis will be maintained as shown in **Fig 2.5** [Duan, X., et al, 2016].
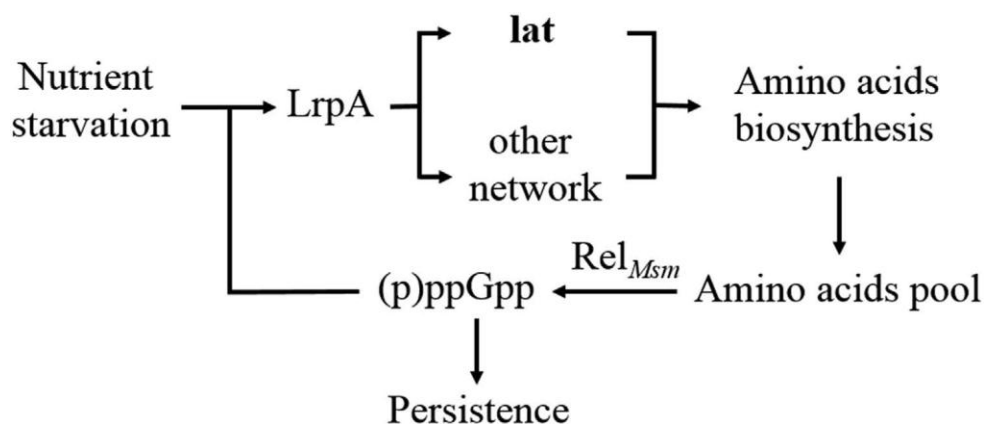
Fig 2.5: Role of LAT in TB persistence.

2.2.2. Mechanism of LAT

LAT is a PLP dependent type II enzyme which catalyzes reversible transamination of lysine and α- ketoglutaric acid. LAT exists as monomer or homodimer and each subunit has molecular weight of ~50 kDa. It was proposed that the overall reaction of this enzyme family follows Ping-Pong Bi-Bi mechanism [Velick S.F., et al., 1962]. This is a special multi-substrate reaction in which two substrates and two products with an enzyme react with one substrate to form a product and modify the enzyme. Later, reacting with the second substrate leads to a final product and regeneration the original enzyme. The terminal amino group of L-lysine was enzymatically transferred to α -ketoglutarate to yield α -aminoadipate-6-semialdehyde which was immediately converted into intramolecularly dehydrated form δ-piperidine-6-carboxylic acid [Tripathi, S. M., et al., 2006].

Reaction -1
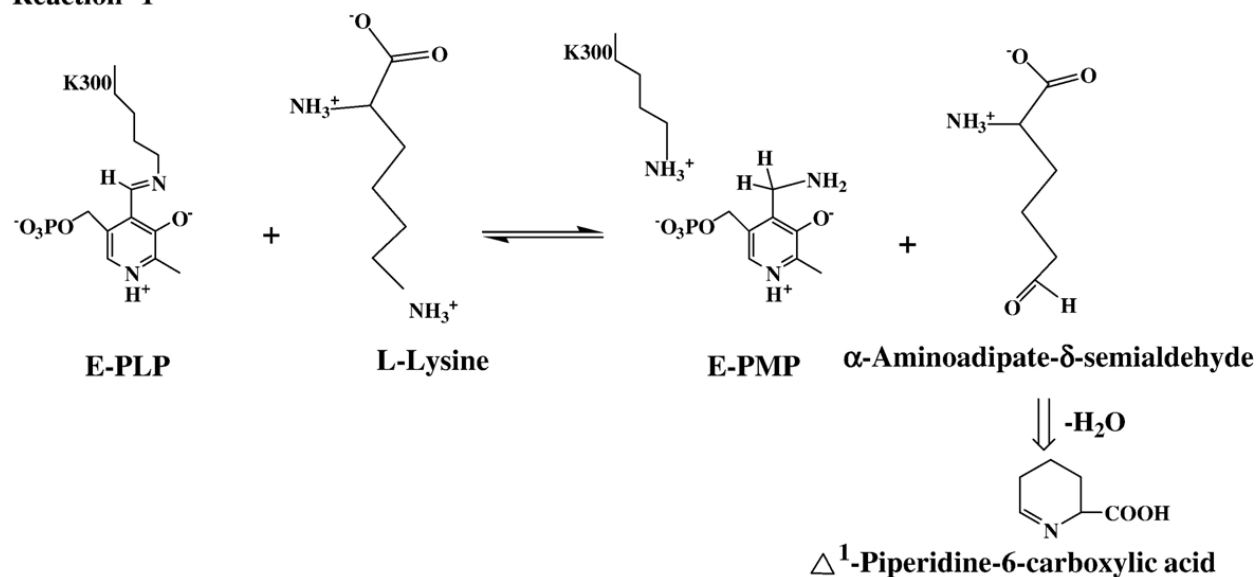
Reaction-2
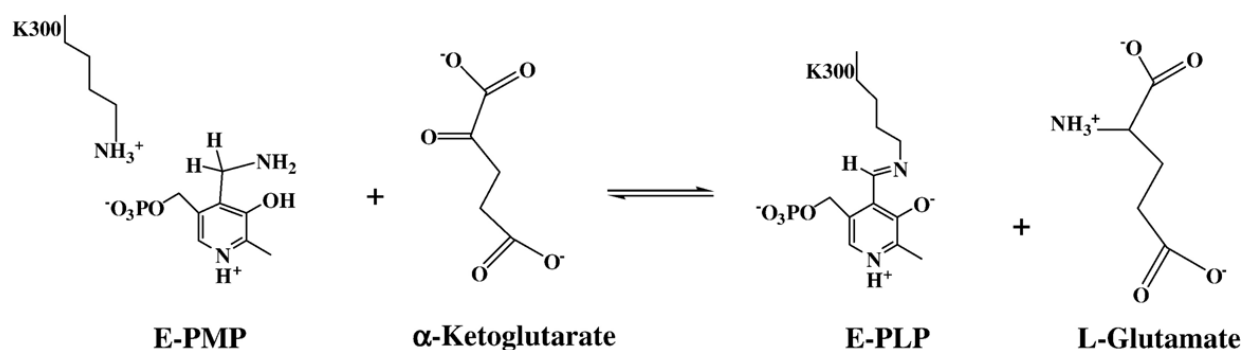
Fig 2.6: Mechanism of action of LAT enzyme in *Mtb*.

2.2.3. Active site analysis of LAT

In the X-ray structure of LAT enzyme it was found in two forms. Internal aldimine and external aldimine form with L-lysine bound with PLP as a substrate and α-ketoglutarate in its bound form towards LAT. The internal aldimine form of the enzyme exhibited the characteristic Schiff's base linkage with Lys300 in the active site of this enzyme. Residues bound with PLP were Gly128, Ala129, Phe167, His168, Glu238, Asp271, Val273 and Gln274. The two residues Ser329 and Thr330 formed a symmetry-related dimer. N1 of PLP was stabilized by the interaction with the invariant residue Asp 271. The phosphate moiety of PLP anchored the co-factor with hydrogen bond interaction with Thr330, Gly128 and Ala129 and was also involved in water mediated interactions. In the PMP-bound form, there was a change when compared with

17

internal aldimine structure. Additional interaction of this internal aldimine was compared with the external aldimine which involved interaction with N4 atom of PMP hydrogen bonded with Lys300, Gln243 and a water molecule.
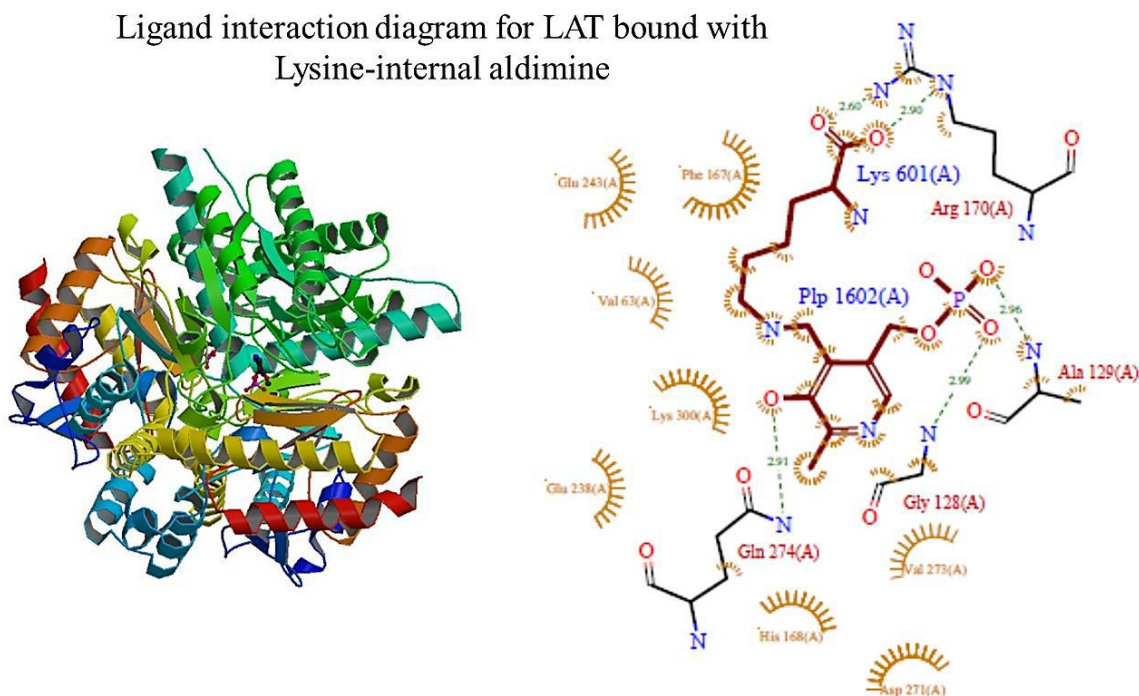
Fig 2.7: PDB structure of LAT bound to lysine and interaction profile of internal aldimine.

The external aldimine form of this enzyme was formed due to presence of excess of substrate. It was expected that the enzyme bound with PMP released the product as an imine form between α-aminoadipate-δ-semialdehyde and PMP [Tripathi S.M., et al., 2006]. The carboxylate group of L-lysine was stabilized by bidentate hydrogen bonds with invariant Arg170. The PLP-lysine is naturally stabilized by an internal bond while the non-polar lysine atoms from Cα-Cε extended into the pocket involving Val63, Lys300, Ser329 and Thr 330. Glu243 in this enzyme will shielded the positively charged invariant Arg422 by creating a salt-bridge with the residues. Conceivably Arg422 also prevented the carboxylic group of the substrate L-lysine from interaction inorder to avoid unwanted transamination at the α-amino group which was important for reaction specificity. Also, Cγ-Cδ atoms of this residue showed Van der Waals interaction with Cδ and Cε atoms of the substrate. With the breakage of Schiff base, the active site of this enzyme was stabilized by the interaction with Thr330 [Tripathi S.M., et al., 2006]. Arg170 was

conserved across the large family of PLP-dependent enzymes whereas; Glu243 was conserved among selected subgroup II enzymes. α-ketoglutarate was bound with the enzyme making interaction of O-1 and O-2 with the invariant Arg422 at one end and O-3 and O-4 to the conserved Arg170 residue at the other end [Tripathi S.M., et al., 2006]. Asn328 from the dimeric counterpart was also involved in interaction with O-3 of the substrate α-ketoglutarate and water mediated interactions.
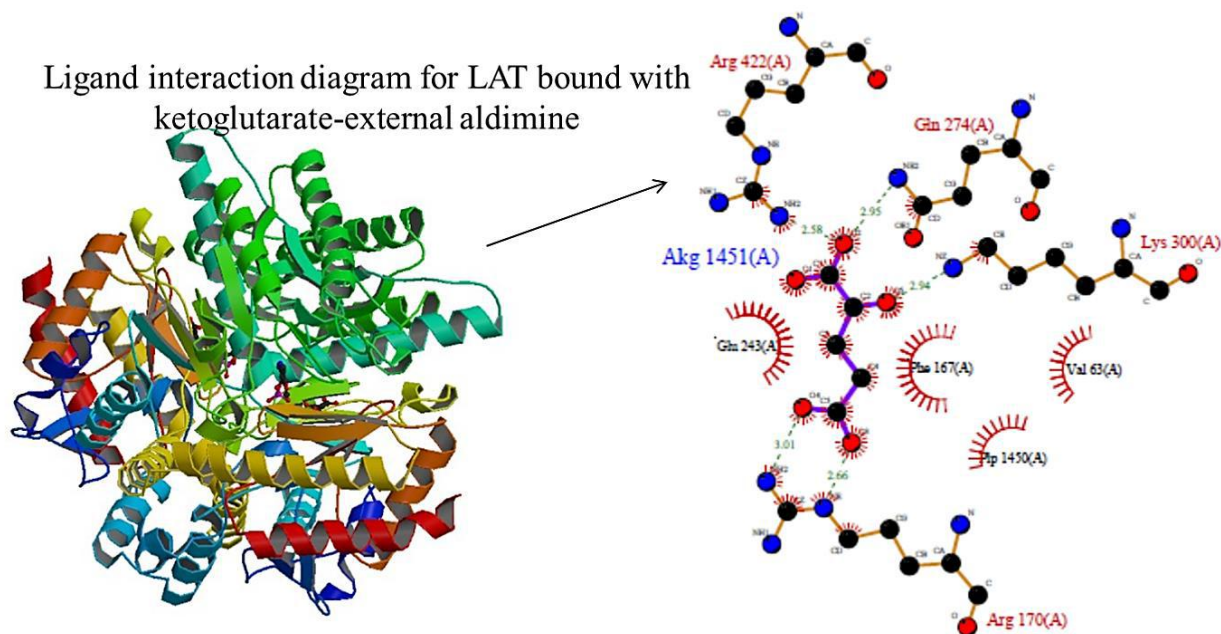
Fig 2.8: PDB structure of LAT bound to ketoglutarate and Interaction profile with external aldimine.

2.2.4. Inhibitors for LAT

Tripathi et.al., 2008 by pharmacophore mapping and 3-D flexible searches identified hexahydro isoindole-1,3-dione and cyclohexylmethyl amine derivatives as novel inhibitors for *Mtb* LAT. Other inhibitors reported till date are shown in the **Fig 2.9** below [Samala, G., et al., 2014, Devi, P. B., et al., 2015, 2016]-
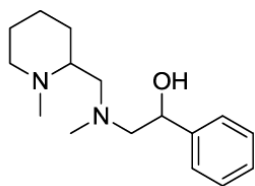
IC$_{50}$: 200 μM
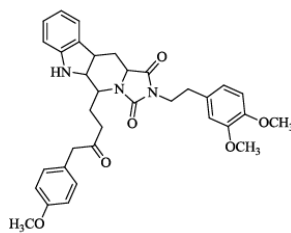
IC$_{60}$: 500 μM
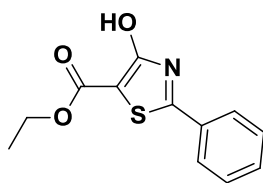
IC$_{50}$: 5.32 μM
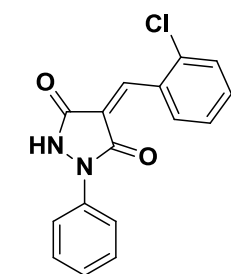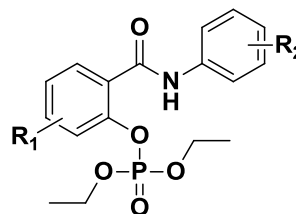
IC$_{50}$: 0.81 μM
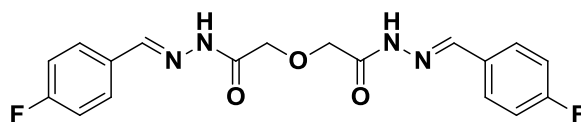
IC$_{50}$: 11.45 μM

Fig 2.9: Inhibitors reported till date with their inhibitory potencies.

3.1. Objective

Current TB treatment is based on a combination of drugs that were developed mostly in the central decades of the last century. Cure rates are high for drug sensitive strains of *M. tuberculosis* when the recommended complex and lengthy treatment protocols are adhered to. However the difficulty in correctly prescribing and adhering to these protocols, the emergence of *M. tuberculosis* strains resistant to multiple drugs, and drug-drug interactions that interfere with optimal treatment of HIV and TB co-infected patients have generated a pressing need for improved TB therapies. Together with the ominous global burden of TB, these shortcomings of current treatment have contributed to a renewed interest in the development of improved drugs and protocols for the treatment of TB. With the emergence of mycobacterial multiple drug resistance during the treatment of TB, CysM, LAT might present alternative targets for new antibacterial agents.

The main objectives of the proposed work are:

1. Lead identification and expansion for inhibition of Cysteine synthase M and Lysine ε-aminotransferase to target dormant phase of *Mycobacterium tuberculosis*.

2. Synthesis and characterisation of the designed compounds using various synthetic protocols and analytical techniques.

3. a. To evaluate inhibitory potency of the synthesized compounds by CysM enzymatic assays.

   b. To evaluate inhibitory potency of the synthesized compounds by LAT enzymatic assays.

4. To undertake *in vitro* anti-mycobacterial screening of the synthesized compounds against *Mtb* by MABA assay and to perform cytotoxicity studies of the compounds.

5. *In vivo* evaluation of anti-mycobacterial potency of the synthesized compounds in *M.marinum* induced Zebra fish model.

6. To determine the efficacy of synthesized compounds against persistent phase of bacteria using nutrient starved culture of *Mtb* and biofilm forming *Mtb*.

7. To evaluate nature and type of kill from kill kinetics curve determined in nutrient starved conditions.

8. To evaluate potency of LAT inhibitors against human 3D granuloma model.

9. To co-crystallize the potent CysM leads with CysM protein.

3.2. Plan of work

The plan of work was classified into following categories:

3.2.1. Lead identification and expansion

For designing the new anti-tubercular agents we followed two approaches:

1. *High throughput screening for CysM*

2. *Molecular derivatization strategy for LAT*

3.2.2. Synthesis and characterization of designed molecules

Synthesis: The molecules designed with either of the above approaches were taken up for synthesis in our laboratory using previously reported methodologies available in literature for structurally related molecules. Wherever possible we carried out reactions using microwave assisted methods for less exposure of hazardous chemicals/vapours to the environment. Most of the synthesized molecules were purified by trituration, recrystallization techniques and flash chromatography with lesser amount of solvents for eco-friendly conditions.

Characterization: Characterization of the synthesized compounds were carried out by ^{1}H NMR, ^{13}C NMR, HPLC, LC-MS and elemental analysis.

3.2.3. *In vitro* enzyme inhibitory potency

3.2.3.a. *In vitro* CysM inhibitory potency: Synthesised CysM inhibitors were evaluated for their inhibitory potency using spectrofluorometric method, mass analysis and spectrophotometric methods.

3.2.3.b. *In vitro* LAT inhibitory potency: Synthesised LAT inhibitors were evaluated for their inhibitory potency using spectrophotometric evaluation of end products adapted to 96-well plate format.

3.2.4. *In vitro Mtb* activity studies

All the synthesized compounds were further screened for their *in vitro* antimycobacterial activity against *Mtb* H_{37}Rv (ATCC27294) by using micro plate alamar blue assay (MABA) method.

3.2.5. *In vitro* cytotoxicity screening

The synthesized compounds were also screened for their *in vitro* cytotoxicity against RAW 264.7 cell line (mouse leukemic monocyte macrophage) using 3-(4,5-dimethylthiazol-2-yl)-2,5-diphenyltetrazolium bromide (MTT) assay.

3.2.6. *In vivo* anti-mycobacterial screening using adult zebra fish

The synthesized compounds were evaluated for *in vivo* studies using adult zebra fish model, against *Mycobacterium marinum* strain (ATCC BAA-535) grown at 30 °C in Middlebrook 7H9 broth. The reduction in bacterial count was evaluated by MPN assay.

3.2.7. Nutrient starvation model

Synthesized compounds were further studied in dormant model of *Mtb* as reported by J. C. Betts, *et.al.,* 2002 i.e.,Nutrient starvation model. The reduction in bacterial count was evaluated by MPN assay.

3.2.8. Biofilm model of persistent phase

Synthesized compounds were further studied in dormant model of *Mtb* as reported by Kulak K, *et.al.,* 2012 The reduction in bacterial count was evaluated by MPN assay.

3.2.9. Kill kinetic curve

To determine nature of kill and factors influencing kill potency of compounds was determined against nutrient starved culture at different time points. The reduction in bacterial count was evaluated by MPN assay.

3.2.10. Human 3D granuloma model

As this model mimics *in vivo* conditions of dormancy and lesion environment the most potent molecules of series were evaluated against persistent phase in granuloma. Reduction in bacterial count and % Rifampicin resistance was determined at the end of study using the procedure reported.

3.2.11. Structure determination of CysM inhibitor complex

The most potent CysM leads were also attempted to co-crystallize with the CysM protein to understand the binding pattern in more detail.

4.1. Development of novel inhibitors targeting *Mycobacterium tuberculosis* acting through the inhibition of Cysteine synthase M and Lysine aminotransferase.

4.1.1. Development of novel inhibitors targeting *Mycobacterium tuberculosis* acting through the inhibition of Cysteine synthase M

Till date no inhibitors were reported for CysM for *Mycobacterium tuberculosis* we employed screening of small molecules from Chemical Biology Consortium Sweden. The CysM small molecule screening was performed by monitoring the fluorescence of the PLP cofactor. A library of 17312 compounds were screened at a single concentration of 10 µM in the presence of 2 µM CysM. Compounds that showed an increase in fluorescence by ≥30% were identified as hits. The process of screening and hit selection was depicted in **Fig 4.1** below.

PLP fluorescence based HTS — Library of 17312 compounds screened at 10µM

> 30% fluorescence — 431 initial hits

Hit confirmation — 49 compounds exhibit dose dependent binding

Chemical feasibility — 23 compounds for DRC ,ITC and enzymatic assays
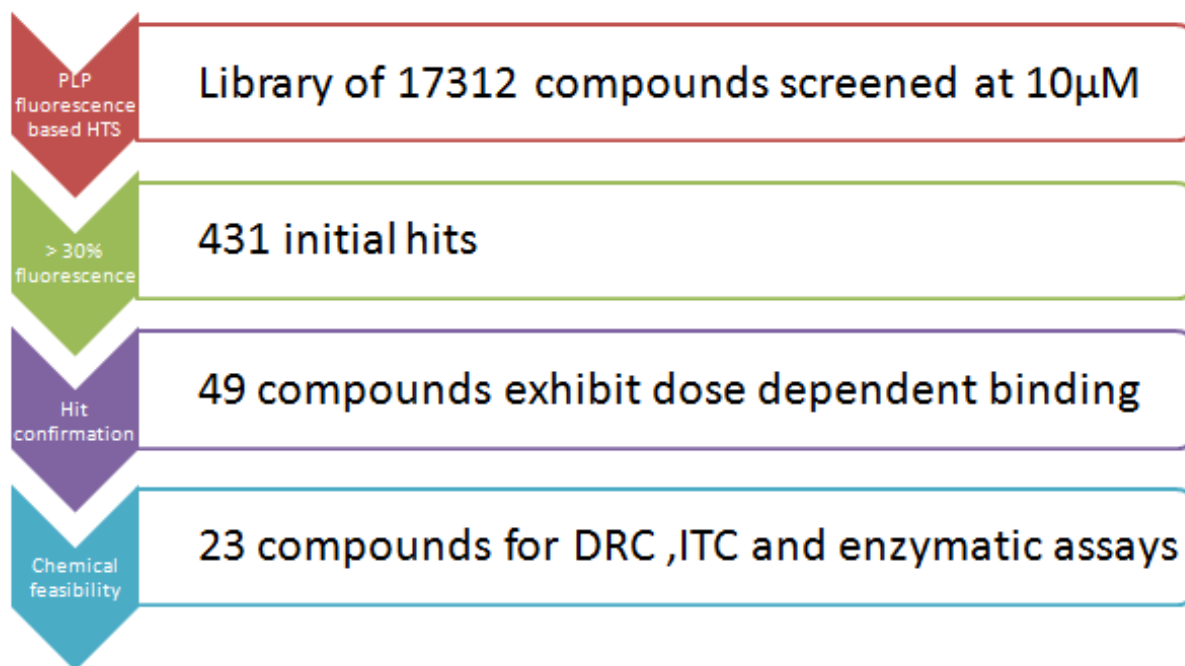
Fig 4.1: Small molecule screening and hit selection procedure

4.1.1.1. Protein production and purification:

Recombinant CysM and thiocarboxylated CysO were produced in *E. coli* strain BL21 (DE3) using a pET-28a vector and purified as previously described [Ågren et al., 2008]. The protein concentration was determined by the Bradford method using bovine serum albumin as standard and purity assessed by SDS-PAGE. The protein aliquots were flash-frozen in liquid nitrogen and stored at -80°C until further use.

CysK1 and CysK2 were produced and purified as described [Schnell, *et. al.,* 2007; Steiner, *et. al.,* 2014]. A plasmid expressing human cystahionine beta synthase (CBSA) was obtained from the Structural Genomics Consortium, Oxford and purified in accordance with published protocols [McCorvie, 2014]. The human SERC protein was produced and purified in *E. coli* (BL21(DE3)) using the expression construct obtained from the Structural Genomics Consortium, Stockholm.

4.1.1.2. Compound handling:

The compound libraries applied in the screening campaign at CBCS consist of a total 17312 compounds. A substantial number of compounds in the screening set were donated by Biovitrum AB in 2010 and originated from both in-house and commercial sources. This screening set was complemented with a set of compounds obtained from Enamine Ltd. All compound libraries were stored as 10 mM stock solutions in Labcyte 384 LDV plates (LP-0200) to enable dispensing using acoustic liquid handling equipment (Labcyte Echo 550).

4.1.1.3. PLP cofactor fluorescence based screening assay:

A single point small molecule screening campaign was carried out based on changes in the PLP cofactor fluorescence upon ligand binding at room temperature in a final volume of 10 μl in black 384-well plates (Corning, 3820). The assay buffer consisted of 25 mM Trizma Base buffered by acetic acid (Tris-Acetate, Sigma Aldrich, 93362) at pH 7.4 and 150 mM NaCl. The assay procedure involved thawing, centrifugation and removing the seal of the assay plates containing 10 nl of the 10 mM compound solutions and DMSO controls (dispensed using an Echo 550 from Labcyte). Next 10 μl of a CysM solution at a concentration of 2 μM in assay buffer was added to columns 1-23 using a MultiDrop Combi reagent dispenser (Thermo

Scientific), resulting in a compound concentration of 10 µM. The final concentration of DMSO in the assay was 0.1% in all samples. Finally the corresponding volume of pre-mixed 10 mM α-ketoglutarate (Sigma Aldrich, 75892) and 2 µM CysM was added to column 24 serving as the positive control for the assay. The plates were shaken on a plate shaker for 5 minutes to allow for compound binding prior to detection of the fluorescence signal in a Victor 3 plate reader (PerkinElmer). A filter at 405 nm was used for the excitation and a filter at 535 nm was used for the emission.

The recorded fluorescence data were processed and analyzed using dedicated templates in Microsoft Excel. Control wells containing only CysM or CysM + α-ketoglutarate were used to calculate Z′ values [Zhang *et al.*, 1999] for each plate (**Fig 4.2** for the Z´ values of all plates in the screen). Compounds that showed an increase in fluorescence by ≥30% were considered as hits that were re-tested in hit confirmation experiments. These experiments were carried out using the same assay volume, but with three different compound concentrations of 2.5, 10 and 40 µM, respectively. For the parallel counter-screening experiments, all conditions were kept the same, except that CysM was omitted from the assay buffer to enable auto-fluorescence measurements of the test compounds. The final concentration of DMSO in the hit confirmation assay was ranging between 0.025 to 0.4 % depending on the tested concentration.
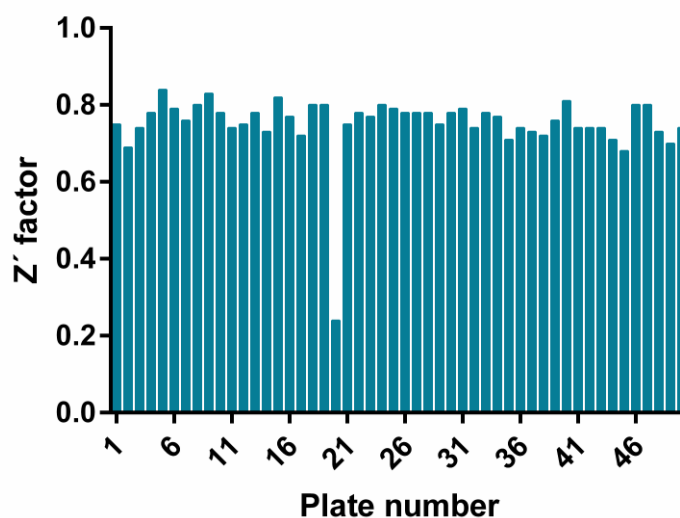
Fig 4.2: Graph showing the Z´ values for all plates in the screening campaign calculated based on the controls in columns 23 and 24 of each plate. In one instance the Z´ factor is 0.24 (plate

20), which is caused by a low response for one out of 16 of the positive controls. Removal of this data point results in a Z´ factor of 0.7 which is in line with the other plates.

The concentration-response experiments were carried out in 96-well black bottom microtiter plates (Costar 3694) in a total volume of 40 µl and the fluorescent signal was detected using a Perkin Elmer Multilabel Reader with excitation at 412 nm and emission at 510 nm. CysM was added to the wells to a final concentration of 2 µM over a range of compound concentrations (0-300 µM) in 25 mM Tris-HCl and 150 mM NaCl at pH 8.0 and incubated for five minutes at room temperature prior to the measurements. All samples were measured together with a blank in which the spontaneous fluorescence was recorded and subsequently subtracted from the signals. The dissociation constants were derived from the hyperbolic fits of the data using GraphPad Prism and the determined K_d values reported as mean ± SD from triplicate experiments. CysK1, CysK2, and human cystathionine β-synthase and phosphoserine-aminotransferase were assayed in a similar manner, using excitation at 430 nm (PLP absorption peak) and emission in the range 460-680 nm with peak at 500 nm.

4.1.1.4. Identification and Purity of compounds from the CBCS compound collection:

The identity and purity were examined for all test compounds that were progressed to concentration-response experiments. This was done by means of high-pressure liquid chromatography coupled to mass spectrometry (HPLC-MS). A 2 µl aliquot of the compound solution was placed in a deep-well plate and diluted with 20 µl of methanol. The plate was then placed in an Agilent 1100 HPLC UV/MS with electrospray ionization (ESI$^+$). The HPLC method that was used for analysis was based on an ACE C8 3 µm column (3.0 mm × 50 mm) and a mobile phase [CH$_3$CN] / [0.1% TFA/H$_2$O]. Solvents were HPLC grade and the absorbance was monitored at 305 ± 90 and 254 nm. Compounds that gave unsatisfactory data were re-analyzed using an alternative method based on a Waters XBridge C18 3.5 µm column (3.0 mm × 50 mm), 3.5 min gradient mobile phase [CH$_3$CN] / [10 mM NH$_4$HCO$_3$/H$_2$O]. The obtained UV peaks were integrated using the instrument software resulting in a list of peaks and their associated masses. The estimated purity was calculated based on the integrated area for the expected mass compared to the areas of all other peaks.

4.1.1.5. Isothermal titration calorimetry:

For isothermal titration calorimetry experiments the buffer of the protein sample was exchanged to 50 mM Hepes buffer pH 8.0, 150 mM NaCl through dialysis using the Slide-A-Lyzer mini dialysis unit of 3500 MWCO (Thermo scientific). The top binders, which showed a $K_d \approx 1$ μM, using the fluorometric PLP assay, were diluted into the final buffer from the protein dialysis. Due to the 0.5% DMSO in the final solution of ligand an equivalent amount of DMSO was also added to the final protein solution prior to running the experiments. Titration was done using a MicroCal ITC200 (MicroCal) by addition of 20 - 25 injections of $1.5 - 2.0$ μl of concentrated ligand solution (initial concentration 500 μM) to the cell containing 280 μl of the protein solution (50 μM). All reactions were done at 20 °C and a 180 s equilibration time was allowed between injections. Data were fitted to a single-site binding model using the MicroCal Origin software.

4.1.1.6. Inhibition of the aminoacrylate intermediate formation:

The influence of the inhibitors on the first half-reaction of CysM was monitored spectrophotometrically at 463 nm, the characteristic wavelength of the aminoacrylate intermediate. The reactions were carried out in a total volume of 100 μl in 25 mM Tris-HCl pH 8.0, 150 mM NaCl following pre-incubation of 12.5 μM CysM with 100 μM compound (5 min, 22°C). Immediately upon the addition of 500 μM OPS the spectra were recorded for 10 - 20 min at 463 nm using a Jasco-V65 spectrophotometer. The k_{obs} were derived from exponential fits to the recorded absorbance data [Ågren, *et. al.,* 2008, Rabeh, *et. al.,* 2005] and compared to the non-inhibited reaction.

4.1.1.7. Inhibition of the covalent CysO-Cysteine adduct formation:

Electrospray ionization mass spectrometry was used to assess the formation of the covalent CysO-cysteine adduct in the second half-reaction of the CysM catalytic cycle in the presence of top HTS hits and their derivatives. The reactions were carried out in 10 μl total volume in 20 mM HEPES pH 7.5 with 5 μM CysM incubated with 400 μM compound and 100 μM CysO-SH (50 μg). Reactions were started with the addition of 500 μM OPS, incubated at 22 °C for 10 min, stopped by the addition of the denaturing buffer (5% acetonitrile, 0.1% formic acid, 2 mM TCEP) and frozen at -20 °C until analysis. The reaction mixtures as well as samples from non-inhibited reaction and un-reacted CysO-SH were loaded on a CapLC system and analyzed by a

Q-TOF mass spectrometer (Waters Corp., Manchester, United Kingdom) as described previously [Sundqvist, *et. al.,* 2007]. Mass spectra of the reaction mixture products were compared to the mass spectrum of the covalent CysO-cysteine adduct (9658.7 Da) as well as the mass spectrum for the un-reacted CysO-SH (9571.6 Da).

4.1.1.8. IC$_{50}$ determination by spectroscopic method:

Multiple turnover enzyme activity assays for CysM using the natural substrates O-phosphoserine and thiocarboxylated CysO (CysO-SH) were based on the spectrophotometric determination of the stoichiometric amount of phosphate ions released using the Malachite-green (MG) reagent [Baykov*, et. al.,* 1988]. The MG stock solution was prepared by slowly adding 60 ml of concentrated H$_2$SO$_4$ to 300 ml of water; the solution was cooled to room temperature and supplemented with 0.44 g of MG. The MG-reagent was composed of 10 parts of colour reagent, 2.5 parts 7.5% (NH$_4$)$_2$MoO$_4$ and 0.2 parts 11% Tween20. Control experiments showed that concentrations of the **RK_01** lower than 100 μM and CysO-SH lower than 50 μM did not interfere with the phosphate read-out.

The enzyme inhibition assay mixtures contained 100 mM Tris-HCl pH 7.5, 1 mM O-phosphoserine, 50 nM CysM, 30 μM CysO-SH, and the **RK_01** at varying concentrations (8 different in 3x dilution steps) from 33.3 μM − 0.0152 μM in total reaction volumes of 200 μl. CysM-free and inhibitor-free control reactions were carried out in parallel. The assays were run in a multi-well plate and were started by the addition of CysM. 30 μl samples were withdrawn from the assay mixtures after 1,2,4,8,12 and 16 minutes, and added to the MG-reagent in the clear-bottom spectrophotometry-plate (Corning 3994). The highly acidic MG-reagent served as a stop-solution and after incubation in the dark for 15 minutes, the color reaction was completed. The absorbance data at 620 nm was recorded using a BIOTEK plate reader. The reaction rates were derived from linear fits to the A$_{620}$ data. A phosphate standard curve was recorded under the same conditions to determine the change in reaction product concentration. The inhibition assay was carried out in triplicates and the relative activities from each assay mixture (setting the non-inhibited reaction as 1.0) were plotted against compound concentration to derive the IC$_{50}$ values from the obtained concentration-response curves.

4.1.1.9. MIC determination:

Bacterial inoculi of *Mycobacterium tuberculosis* H37Rv were prepared from fresh LJ medium and re-suspended in Middlebrook 7H9 broth supplemented with 10% OADC (HiMedia Laboratories). This culture was grown at 37 °C until the turbidity matched with McFarland no.1 turbidity standard. The culture was diluted to 1:25 with media and 100 µL was used as an inoculum. Each drug stock solution was thawed and diluted in Middlebrook 7H9-OADC at four-fold the final highest concentration tested. Serial two-fold dilutions of each drug were prepared directly in a sterile 96-well microtiter plate using 100 µl Middlebrook 7H9-OADC. Each plate also contained wells containing *M. tuberculosis* cultures without addition of the tested compounds and wells with only sterile medium as controls. Sterile water was added to all outer wells to avoid evaporation during incubation. The plate was covered, sealed in plastic bags and incubated at 37 °C. MIC values were determined using the Alamar Blue assay [Collins, *et. al.,* 1997, Franzblau, *et. al.,* 1998]. After 5 days of incubation, 50 µl of 1:1 mixture of alamar blue solution (Sigma Aldrich) and sterile 10% tween 80 (Nice chemicals) were added to each well and the plate was re-incubated overnight (reading on 7th day). A change in color from blue (oxidized state) to pink (reduced) indicated growth of bacteria and the minimum inhibitory concentration (MIC) was defined as the lowest concentration of the compound that prevented this change in color.

4.1.1.10. *In vivo* assay of lead compounds using a nutrient starvation model:

 M. tuberculosis was starved according to a procedure described earlier [Betts, *et. al.* 2002]. A culture of *M. tuberculosis* H37Rv (NIRT, Chennai) grown in Middlebrook 7H9 medium supplemented with OADC was pelleted and washed twice with PBS (Phosphate Buffer Saline, obtained from HiMedia Laboratories). The pellet was resuspended in PBS with out tween in sealed bottles and incubated at 37 °C for 6 weeks. Tween was avoided in nutrient starved culture as *Mtb* has lipase enzyme which can hydrolyse tween to oleic acid which can serve as source of energy or can cause toxicity [Dubos, R. J., *et al.,* 1946, Lyon, R. H., *et al.,* 1963]. Aliquots of these cultures were then treated with standard drugs like Isoniazid, Rifampicin and Moxifloxacin and the lead compounds for 7 days at a concentration of 10 µg/ml. For the determination of CFU the cell suspensions were then diluted 10-fold to 10^{-6} using Middlebrook 7H9 medium supplemented with OADC and 50 µl of each dilution was plated in 48 well plates in triplicates

along with 450 µl of Middlebrook 7H9 medium supplemented with OADC (HiMedia Laboratories). The plates were incubated at 37 °C for 3-4 weeks, after which the wells were examined for visible bacterial growth. The bacterial count was evaluated using standard statistical methods [de Man, 1975].

4.1.1.11. Cytotoxicity assays:

The four cell lines human hepatic cell line-HEPG2 (85011430), mouse macrophages- J774A.1 (91051511), neuroblast of human- SHSY5Y (94030304) and human monocytes-THP-1 (88081201) were obtained from Sigma Aldrich. The cell lines were maintained in the following media supplemented with 1X penicillin/streptomycin (Sigma Aldrich, P4333) and 10% FBS (Sigma Aldrich, P9665): HEPG2, DMEM (Sigma Aldrich, D6429); J774A.1, DMEM (Sigma Aldrich, D6429); SHSY5Y, DMEMF12 (Sigma Aldrich, D6421); THP-1, RPMI (Sigma Aldrich, R8758). The cell lines were passaged two to three times a week and HEPG2 and SHSY5Y cells were dissociated using TrypLE (Life Technologies, 12605010), while J774A.1 cells were dislodged with a scraper.

To determine the cell density for the cytotoxicity experiment 30 µl of a cell suspension was added to a 384-well plate at the following cells per well (14 replicates each): 250, 500, 1000, 2000, and 4000. After 72 hours, 30 µl of CellTiterGlo® (Promega) diluted 1:3 with PBS was added to each well. After 10 minutes of incubation at room temperature the luminescence of each well was recorded on an EnVision (Perkin Elmer).

Prior to the experiment, a source compound plate was prepared containing a three-fold dilution series of up to 28 compounds and a three-fold dilution series of staurosporine using a Bravo Automated Liquid Handling Platform (Agilent). For top concentrations used in the three-fold dilution series, see **Table 4.1**. Single point Staurosporine and DMSO controls (16 each) were also added to the source plate. Assay-ready, 384-well plates (Corning, 3750) were prepared by acoustic transfer of 100 nl from the compound source plate to each well of the assay plate using an Echo Liquid Handler (LabCyte). 30 µl of a cell suspension was then added to the 384-well plates using a Multidrop (Thermo Scientific) at a density of 1000 cells per a well. The plates were placed in humidity chamber in a tissue culture incubator. After 72 hours, 30 µl of CellTiterGlo® (Promega) diluted 1:3 with PBS was added to each well. After 10 minutes

incubation at room temperature the luminescence of each well was recorded on an EnVision (Perkin Elmer). The percent inhibition of cell viability in each well was computed by comparing to the positive (6 µM staurosporine) and the negative (DMSO) controls. Experiments were performed in duplicate. For all plates a Z'- score between the positive and negative controls was calculated and these scores were all greater than 0.55.

Table 4.1: Top concentration of compounds used in viability testing against the four mammalian cell lines.

Compound number	Top concentration in viability testing (µM)
RK_01	33
RK_02	33
RK_03	33
RK_04	50
RK_05	50
RK_06	50
RK_07	50
8	33
13	33
RK_17	50
RK_18	50
RK_19	50
RK_20	50
RK_22	50
23	33
24	33
25	33
26	33
27	33
28	33

29	33
30	33
RK_37	50
RK_42	50
RK_54	50
RK_62	50
71	33
Staurosporine	6

4.1.1.12. Structure determination of enzyme-ligand complexes:

Co-crystallization of protein-inhibitor complexes

Crystallization screening was carried out using a Mosquito crystallization robot and the vapor diffusion method. CysM at a concentration of 21 mg/ml was incubated with 2 mM of the individual compounds for at least 30 min at room temperature prior to setting up the crystallization plates (96-well 3-drop conical flat bottom, Corning) using a Mosquito nanodrop dispenser (TTP Labtech). Two commercially available crystallization screens PACT and JCSG$^+$ (Qiagen) were used with 0.1 μl, 0.15 μl and 0.2 μl of prepared protein-compound solution mixed with 0.2 μl, 0.15 μl and 0.1 μl of the reservoir solution, respectively at 20 °C. Various conditions that resulted in crystals of individual CysM-compound complexes, which appeared within 48-72 h, were further optimized in 24-well format using the hanging drop vapor diffusion technique at 20 °C. Crystal plates were prepared using the same concentration of protein and compound as above in various crystal conditions to obtain larger, single co-crystals of CysM with hit compounds. The cryo solutions were prepared in 20 μl aliquots by mixing 15 μl of a concentrated crystallization solution together with 2 mM compound (1 μl of 100 mM in DMSO) and 4 μl glycerol resulting in 22% glycerol (table 4). The crystals were picked, incubated with the cryo-solution for a few seconds and frozen in liquid nitrogen.

Table 4.2: Crystallization and cryo-protection conditions for the crystals used in the study

CysM complex	Crystallization condition	Drop composition	Cryoprotection
1	0.2 M MgCl$_2$, 0.1 M Bis-Tris pH 5.5, 25% PEG 3350	2:2	0.2 M MgCl$_2$, 0.1 M Bis-Tris pH 5.5, 25% PEG 3350, 2 mM compound, 22% glycerol
2	0.2 M Ammonium acetate, 0.1 M Bis-Tris pH 5.5, 25% PEG 3350	2:2	0.2M Ammonium acetate, 0.1 M Bis-Tris pH 5.5, 25% PEG 3350, 2 mM compound, 22% glycerol
3	0.2 M Ammonium acetate, 0.1 M BT pH 5.5, 25% PEG 3350	2:2	0.2 M Ammonium acetate, 0.1 M Bis-Tris pH 5.5, 25% PEG 3350, 2 mM compound, 22% Glycerol
5	0.2 M MgCl$_2$, 0.1 M MES pH 6, 25% PEG 6000	3:1	0.2 M MgCl$_2$, 0.1 M MES pH 6, PEG 6000, 2 mM compound, 22% Glycerol
6	0.2 M NaCl, 0.1 M Bis-Tris pH 5.5 25% PEG3351	3:1	No cryo
7	0.2 M MgCl$_2$, 0.1 M MES pH 6, 25% PEG 6000	3:1	0.2 M MgCl$_2$, 0.1 M MES pH 6, PEG 6000, 2 mM compound, 22% Glycerol
4	0.2M NH$_4$Cl 0.1M MES pH 6, 20% PEG 6000	3:1	0.2M NH$_4$Cl 0.1M MES pH 6, 20% PEG 6000, 2 mM compound, 9% Glycerol

Crystallographic data collection.

Crystallographic data for CysM complexes with **RK_02**, **RK_05** and **RK_07** were collected at the BL-14 beamline at BESSY (Berlin, Germany), data for CysM in complex with **RK_01**, **RK_03** and **RK_ 06** at beamline ID23-1 and data for CysM in complex with **RK_04** at beamline ID29 of the European Synchrotron Radiation Facility (Grenoble, France). The data were processed by XDS [Kabsch, 2010] and scaled using AIMLESS from the CCP4 suite [Winn et al., 2011]. Table S4 provides a summary of the cell dimensions, space groups and data quality for the CysM-ligand complexes.

Structure determination and refinement

The structures of CysM-inhibitor complexes were determined by molecular replacement using MOLREP [Vagin and Treplakov, 2010] and the coordinates of CysM [Ågren, *et. al.,* 2008] as search model. Crystals of the CysM-ligand complexes were either of space group $P2_12_12_1$ with two polypeptide chains or P1 with four chains in the asymmetric unit. The structures were refined using REFMAC5 [Murshudov, *et. al.,* 2011]. In the reported cases well-defined difference electron densities were observed in the active site, which allowed an unambiguous fit of the ligands. Model building was performed using COOT [Emsley, *et. al..* 2010], interspersed with round of model building. Structure validation was performed with MolProbity [Chen, *et, al.,* 2010]. Statistics for data collection, refinement and the final protein model are given in **Table 4.3**. Figures of the enzyme-ligand complexes were prepared with PyMOL (http://www.pymol.org).

Table 4.3: Statistics of crystallographic data collection and refinement

Ligand	RK_01	RK_02	RK_03	RK_04	RK_05	RK_06	RK_07
PDB code/file	5I7A	5I7R	5I7C	5IW8	5I6D	5I7H	5I7O
Synchrotron, Beamline	BESSY BL-14	ESRF ID23-1	ESRF ID23-1	ESRF ID29	BESSY BL-14	BESSY BL-14	BESSY BL-14
Space group	P1	$P2_12_12_1$	$P2_12_12_1$	$P2_12_12_1$	P1	P1	P1

Unit cell							
a,b,c (Å)	64.5, 76.0, 81.6	72.2, 86.5, 101.6	66.0, 87.5, 98.2	67.2, 87.9, 100.8	64.6, 76.4, 80.9	64.6, 76.1, 80.7	64.3, 75.9, 79.3
α,β,γ(°)	94.7, 108.8, 107.3	90, 90, 90	90, 90, 90	90, 90, 90	94.6, 108.2, 107.6	94.3, 108.3, 107.7	93.7, 108.4, 107.9
Resolution (Å)	47.47-2.08 (2.12-2.08)[a]	55.41-1.73 (1.81-1.73)	66.04-2.70 (2.85-2.70)	53.37-2.04 (2.15-2.04)	47.47-1.64 (1.67-1.64)	49.16-2.57 (2.66-2.57)	47.20-2.49 (2.58-2.49)
No. of unique reflections	80146 (3789)	65578 (9510)	15620 (2185)	38565 (5421)	163557 (7619)	42814 (4258)	45415 (4136)
$I/s(I)$	9.0 (1.9)	19.6 (2.0)	9.1 (2.1)	8.3 (1.9)	12.9 (1.8)	4.4 (1.7)	7.4 (2.0)
Redundancy	2.9 (2.8)	4.5 (4.3)	5.0 (4.9)	5.5 (5.7)	2.4 (2.2)	2.0 (2.0)	2.3 (2.2)
Completeness (%)	97.3 (81.0)	98.3 (98.8)	96.9 (95.2)	99.5 (97.3)	96.9 (90.6)	97.9 (92.6)	97.6 (90.2)
R_{merge}	0.065 (0.426)	0.041 (0.717)	0.131 (0.806)	0.167 (0.819)	0.031 (0.334)	0.158 (0.523)	0.125 (0.533)
Wilson B-value (Å^2)	28.1	25.7	39.1	20.7	18.7	19.6	39.7
Refinement							

R_{cryst}	0.169	0.173	0.212	0.185	0.163	0.201	0.199
R_{free}	0.208	0.206	0.266	0.237	0.186	0.264	0.259
Number of atoms / B-factor Å²							
Overall	9602 / 37.2	4988 / 34.0	4572 / 57.8	5149 / 30.2	9934 / 27.4	9115 / 33.1	9224 / 34.9
Protein	8802 / 36.7	4690 / 33.5	4484 / 58.0	4650 / 29.6	8950 / 26.2	8771 / 33.2	8837 / 35.1
Inhibitor	84 / 31.0	50 / 24.7	52 / 40.6	52 / 23.3	80 / 17.8	80 / 30.2	80 / 30.8
Miscellaneous Ligands	N/A	20 / 42.7 (Acetate ions)	N/A	N/A	12 / 42.0 (Glycerol)	1 / 34.7 (Chloride ion)	N/A
Water	716 / 44.2	228 / 44.8	36 / 37.8	447 / 36.7	892 / 39.8	263 / 29.2	307 / 31.3
Rmsd from ideal geometry							
Bond length (Å)	0.0089	0.0139	0.011	0.011	0.0137	0.0108	0.0097
Bond angles (deg.)	1.358	1.611	1.547	1.487	1.562	1.549	1.377
Ramachandran Plot (%)							
Residues in	1105	597	557	579	1124	1071	1079

preferred regions	(96.9%)	(97.4%)	(96.5%)	(96.0%)	(97.8%)	(95.0%)	(94.45%)
Residues in allowed regions	35 (3.1%)	16 (2.6%)	20 (3.5%)	23 (3.8%)	23 (2.0%)	54 (4.8%)	60 (5.2%)
Outliers	0 (0%)	0 (0%)	0 (0%)	1 (0.2%)	2 (0.2%)	2 (0.2%)	4 (0.35%)

Overall structure of the enzyme-ligand complexes.

Overall the three-dimensional structures of the enzyme complexes are similar to the structure of the unliganded enzyme with r.m.s.d. values for the Cα atoms in the range of 0.7 - 1.4 Å upon superimposition. In chain A of the orthorhombic crystal form (**RK_02-04**) and chains A, B, and C of the triclinic space group (**RK_01, RK_05-07**) the ligand is bound to the enzyme in an open conformation characterized by a disordered active site loop (residues 211 – 227) and a disordered C-terminus, residues (310-323). The disorder of these peptide segments results in an open active site, which renders the inhibitor partially accessible from the solvent. In the B chains of the orthorhombic crystals the active site loop is however well defined in electron density and has folded back over the active site thus shielding the bound ligand from the solvent. Also in chain D of the triclinic space group both active site loop and the C-terminal residues are well defined in density and contribute to ligand binding. The active site loop is folded over the ligand-binding site and the C-terminal residues 320-323 are inserted into the active site cleft. In the main text we will describe enzyme-ligand interactions for the closed conformations as in these structures ligand interactions are fully developed.

4.1.1.13. Synthesis for hit expansion:

The compounds in this study were either cherry-picked from the CBCS compound selection or synthesized. For synthesis, all commercially available chemicals and solvents were used without

further purification. Analytical thin layer chromatography (TLC) was performed on alumina-backed silica gel 40 F254 plates (Merck, Darmstadt, Germany) that were visualized with UV light and $KMnO_4$ solution, and flash column chromatography was carried out on 60 Å (40–63 μm) silica gel. HPLC-MS analyses were run on an Agilent series 6100B system with electrospray ionization (ESI[+]). ^{1}H and ^{13}C NMR spectra were recorded at 400 MHz and 100 MHz respectively on a Bruker AM spectrometer. Chemical shifts are reported in ppm (δ) with reference to TMS as internal standard, and coupling constants J are quoted in Hertz. Elemental analyses were carried out using a Vario MICRO cube in CHN mode.

Scheme 1: Synthesis of *N,N*-diphenylureas (type I inhibitors) and *N,N*-diphenylthioureas

R^1 = COOH; R^2 = OH; R^3 = 4-NO_2; 4-OCH_3; 4-CH_3; 4-Acetyl; 4-Br; 4-Cl; 3-Br; Benzyl; 3,4-Dichloro
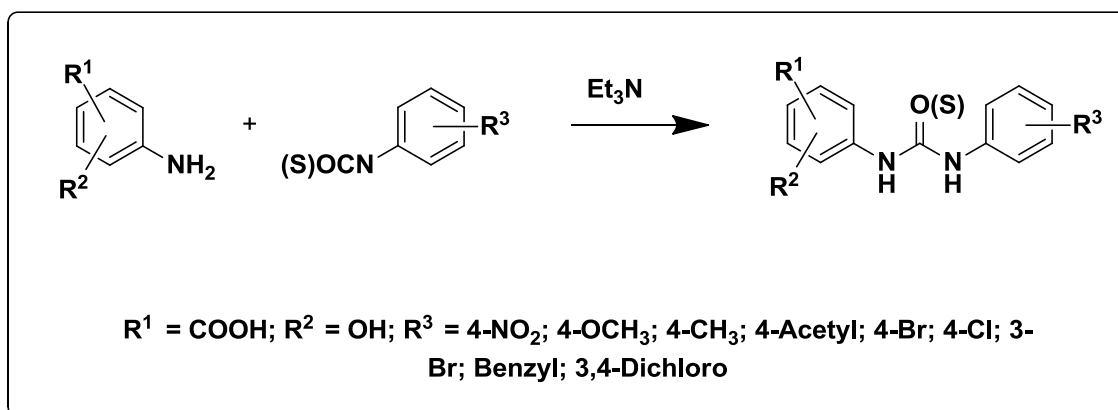
Fig 4.3: Synthetic protocol utilized for the synthesis of type I inhibitors

Scheme 2: Synthesis of type II inhibitors (RHS = biphenyl)

R^3 = 3-Br or 4-Br; R^4 = Phenyl; 4-fluoro phenyl; 2,3-dichloro phenyl; I; 2,5-dimethyl; 3-benzoic acid; 2-pyridyl; 2-fluoro pyridine; pyrimidyl.
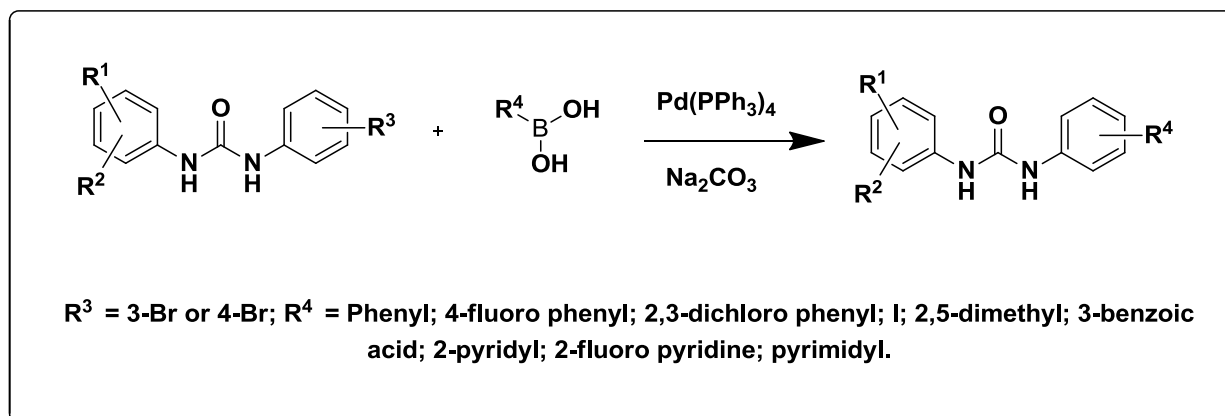
Fig 4.4: Synthetic protocol utilized for the synthesis of type II inhibitors

4.1.1.14. Anti-mycobacterial screening using adult zebra fish:

The most active compound was further evaluated for its *in vivo* activity using adult zebrafish model established by us in a laboratory setup [Sridevi, J. P., *et al*., 2014]. We used *Mycobacterium marinum* strain (ATCC BAA-535) grown at 30 °C in Middlebrook 7H9 broth. Fish were initially weighed and monitored for its locomotor activities and were divided into control and treatment groups (n=6). All the fish were injected by intraperitonial injection with 20 µl of thawed bacterial stocks (around 0.75 million bacteria) [De Man, J. C., *et al*., 1975]. They were observed for lesions, reduction in swimming activities and squamous eruptions in the initial 7 day infection stage which was followed by treatment stage. The drug solutions were prepared based on the fish's body weight and oral dosing amount of 5 µL. Fish were then administered drug orally using micropipette, on each day during the treatment phase and were noted for their recovery symptoms. They were allowed to swim in 1.5 mg/mL solution of kanamycin sulphate before proceeding for sacrifice at the end of study i.e., 14th day. Finally, all of them were sacrificed using homogenization technique and the tissue sample was prepared in Middlebrook 7H9 broth [Salina, E., *et al*., 2014]. The collected homogenate was serially diluted to 10^{-6} times and plated into 48-well plates, incubated at 30 °C for 24 h. The plates were checked for the bacterial counts using graph pad prism software.

4.2.1. Development of novel inhibitors targeting *Mycobacterium tuberculosis* acting through the inhibition of Lysine Ɛ-amino transferase

4.2.1.1. Design of the molecules:

To develop new antitubercular drugs against dormant forms we have used leads identified by screening of BITS-inhouse database against LAT crystallised with lysine (PDB code: 2CJD) and α-ketoglutarate (PDB code: 2CJH). Based on the interaction profile of lead compounds the core moieties were retained and modifications were attempted by molecular derivatization approach to develop library of compounds in each series.

4.2.1.2. Chemistry and methodology:

Reagents and solvents obtained from commercial sources were used without further purification. All the reactions were monitored by thin layer chromatography (TLC) on silica gel 40 F$_{254}$

(Merck, Darmstadt, Germany) coated on aluminium plates. All ^{1}H NMR and ^{13}C NMR spectra were recorded on a Bruker AM-400/300 MHz and 100/75 MHz spectrometer, Bruker Bio Spin Corp., Germany. Chemical shifts are reported in parts per million (ppm) using tetramethyl silane (TMS) as an internal standard. Compounds were purified by Biotage Isolera flash chromatography. Temperatures were reported in degrees celsius and are uncorrected. Compounds were analysed for C, H, N using Elementar and analytical results obtained were found within ± 0.4% of the calculated values for the formula shown. Molecular weights of the synthesized compounds were checked by Shimadzu, LCMS-2020 and the method used was electron spray ionisation (ESI-MS) method.

a) MeNHOMe.HCl, DIEA, HATU, DMF, 0 ºC, 2h; b) LAH, Ether, 0 ºC, 20 min; c) t-Butylisocyanide, pyridine, MDC, TFA, 0 ºC-RT, 8-10 h; d) LiOH, 30 ºC, 1h; e) (i) 6N HCl, 110 ºC, 12h, (ii) IN NaOH, Boc₂O, Dioxane, 0 -30 ºC; f) MeI, K₂CO₃, DMF, 0 -30 ºC, 3 h; g) HCl/Dioxane, MDC, 0 - 30 ºC, 4 h; h) Substituted phenyl isocyantes and isothiocyanates, TEA, MDC, 0 - 30 ºC, 6h; i) LiOH, 3h, THF:H₂O.

X = O, S; R = (CH₃)₂CH; H, F, Cl, Br, NO₂, CH₃, OCH₃, COCH₃.
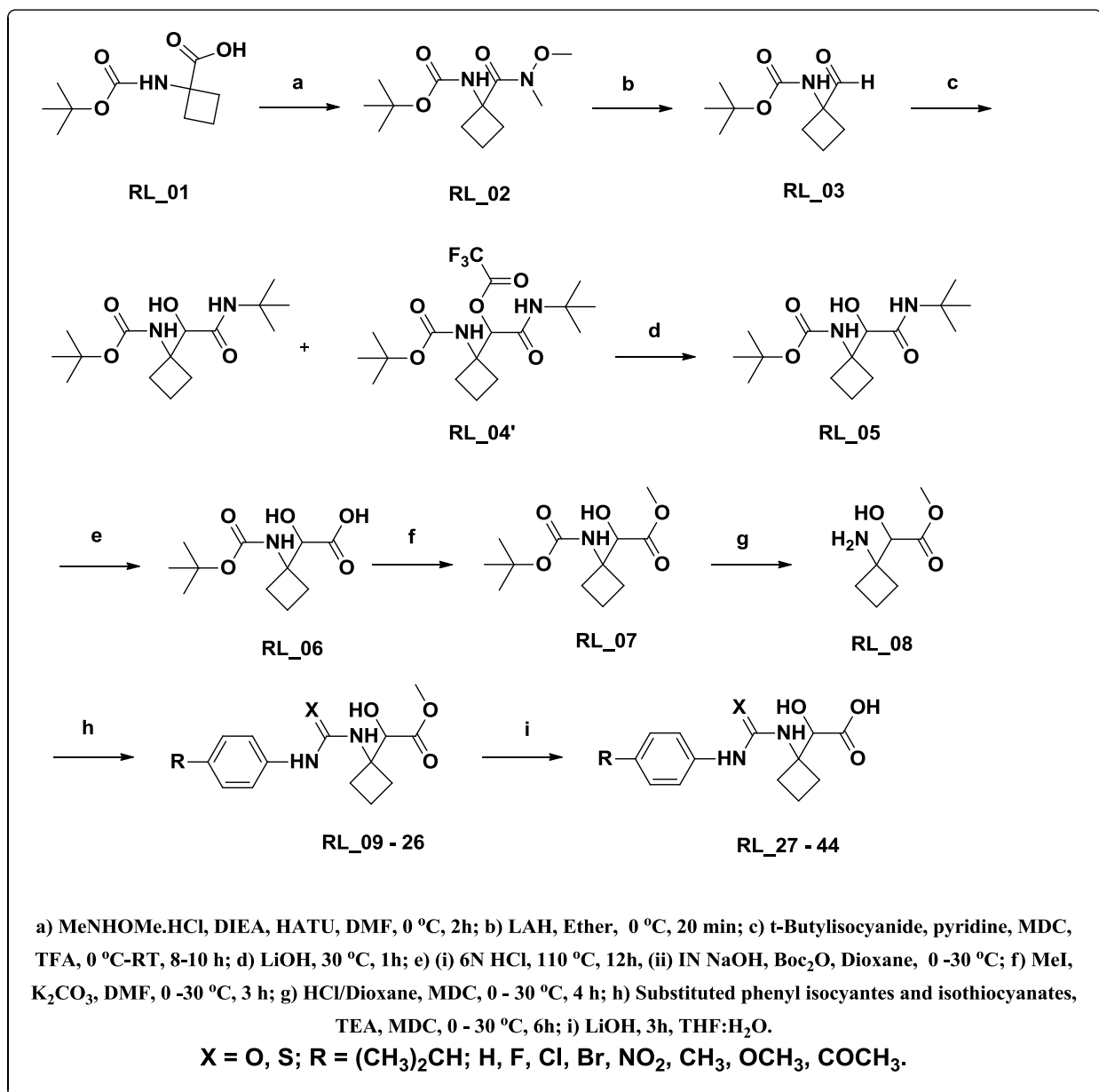
Fig 4.5: Synthetic protocol utilized for the synthesis of molecules **RL_27 – RL_44**

Scheme – 2: Synthesis of Benzthiazole derivatives as potent Mycobacterium tuberculosis LAT inhibitors

a. acetic acid, ethanol b. corresponding aldehyde (R$_1$), piperidine or alcoholic KOH, ethanol.
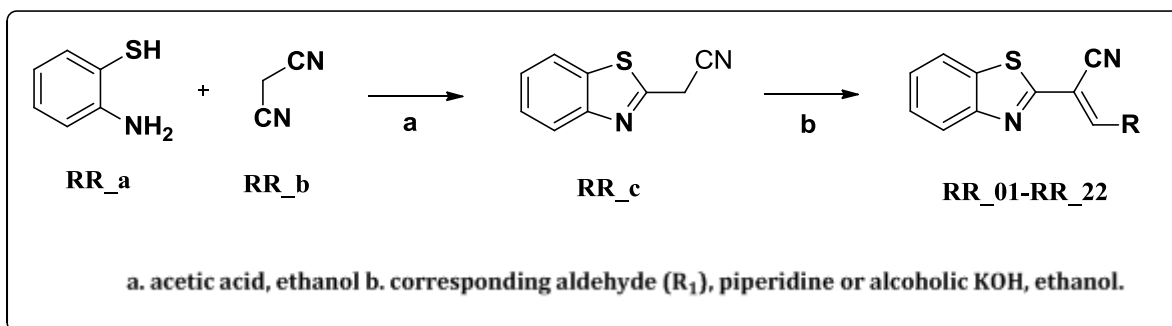
Fig 4.6: Synthetic protocol utilized for the synthesis of molecules **RR_01 – RR_22**

Scheme – 3: Synthesis of Quinoline derivatives as potent Mycobacterium tuberculosis LAT inhibitors

R = H, Cl, CF$_3$; R1 = 2-Pyridyl methyl, 2-Pyridyl ethyl,2-chloro-5-methylpyridine, Benzyl, Phenethyl, 2-thiophene methyl, 2-furan methyl

a. Piperazine, K$_2$CO$_3$, CH$_3$CN, 80 ^{0}C, b. i. methyl bromoacetate, K$_2$CO$_3$, CH$_3$CN, 60 ^{0}C, ii. LiOH (THF:H$_2$O:CH$_3$OH), 30 ^{0}C, c. corresponding amine, propyl phosphonic anhydride, triethylamine, DCM, 30 ^{0}C.
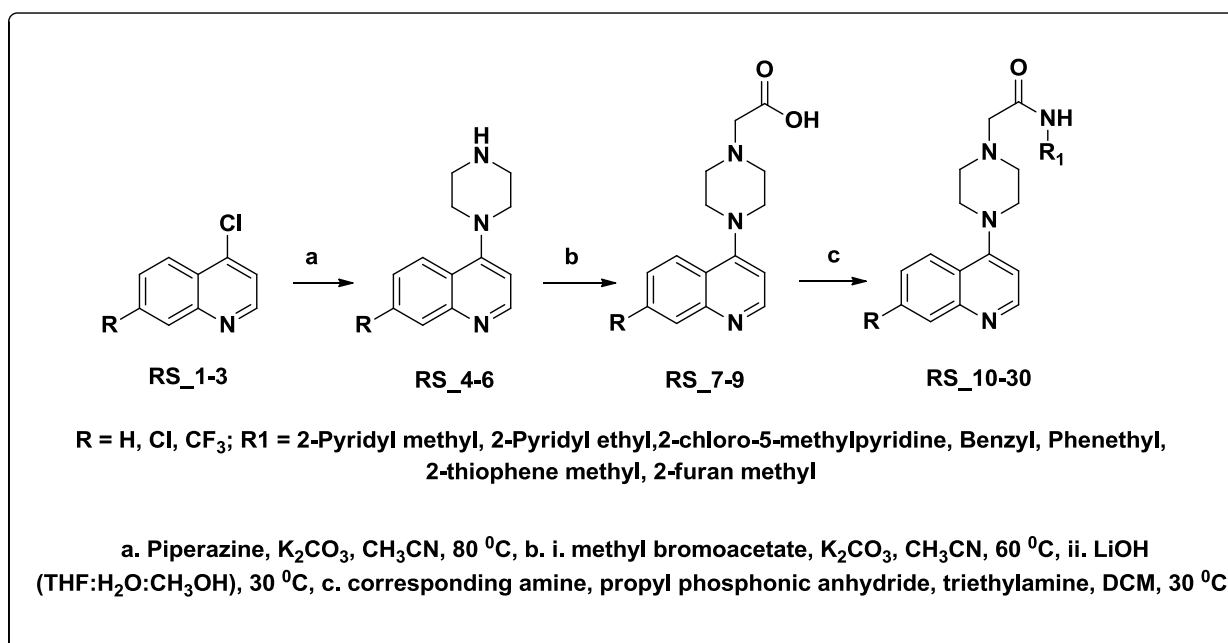
Fig 4.7: Synthetic protocol utilized for the synthesis of molecules **RS_10 – RS_30**

4.2.1.3. Biological screening of synthesized inhibitors

4.2.1.3.1. Cloning and purification of *Mtb* LAT:

Cloning to obtain the target protein *Mtb* LAT was performed as per the earlier reported procedure [Tripathi S.M., *et al*., 2006]. Lysine ε-aminotransferase was PCR amplified using specific forward primer (5'CCCAAGCTTATGGCCGCCGTCGTGAAGTCCGTC3') and reverse primer (5'ATGCAAGCTTACGTCACCACCGGTAACGCGCT3') from *Mtb* genomic DNA. Pfu polymerase was used with 65 °C of primer annealing temperature. PCR products were digested with HindIII and cloned into HindIII site of pET28b vector. Sequence confirmed clones were further transformed into C41 (DE3) cells (Lucigen) for expression studies. Further the transformed colonies were expressed and induced with 0.2 mM IPTG grown in YT media (Yeast extract and Tryptone broth) for 12-16 h at 20 °C. Induced cells were then harvested and lysed by sonication in lysis buffer (50 mM Tris pH-7.2, 300 mM NaCl and 10 mM imidazole) and subsequently centrifugation was done at 10,000 rpm at 4 °C for 45 min for clear extract. Later, the cell extracts were loaded into column (Bio-Rad) and equilibrated with Ni-NTA beads at 4 °C for 3 h. The cell extracts were washed with wash buffer and subsequently the desired protein of interest was eluted with elution buffer containing different concentrations of imidazole from 100 mM to 500 mM. Eluted samples containing the desired protein were identified by SDS PAGE.

4.2.1.3.2. *Mtb* LAT assay:

LAT enzyme was cloned, expressed and purified as per previously reported literature. *Mtb* LAT enzymatic assay was performed in 100 μl volume containing 200 mM phosphate buffer (pH 7.2), 1.5 mM L-lysine, 1.5 mM α-ketoglutarate, 15 μM pyridoxal 5-phosphate with *Mtb* LAT for 1h at 37 °C. The compounds were added to the plates with different concentrations from 50 μM to 0.1 μM. Reactions were terminated by adding 10% trichloroacetic acid in ethanol. The *Mtb* LAT activity was monitored and the end product piperidine-6-carboxylic acid and glutamate was detected at absorbance of 465 nm and 280 nm. Reactions were carried out in a heat-controlled Perkin Elmer Victor X3 spectrophotometer. Further the IC_{50} values were calculated using GraphPad Prism analysis software. The error values in IC_{50}s were derived using non-linear regression mode in Graphpad prism software.

4.2.1.3.3. *In vitro* antimycobacterial potency:

The anti-tubercular potency of the all the molecules synthesised as LAT inhibitors were evaluated by *in vitro* MABA assay against *Mycobacterium tuberculosis* H$_{37}$RV strain following similar protocol to the one utilized for evaluating the anti-tubercular potency of CysM inhibitors.

4.2.1.3.4. Nutrient starvation model:

Synthesized compounds were evaluated against dormant forms of *Mtb* using nutrient starvation model following similar protocol to the one utilized for CysM inhibitors.

4.2.1.3.5. Inhibitory potency against biofilm forming *Mtb*:

4.5 ml of sautons media inoculated with *Mtb* (1:100 dilution) was added in each well and the 12 well plate was covered with lid. Each plate was sealed with several layers of parafilm and were incubated undisturbed in humidified atmosphere at 37 ^{0}C for 5 weeks. To the matured biofilm, compound to be evaluated was injected at desired concentration into media and swirled. For statistically significant results, the antibiotic was injected in four wells. In parallel, same volume of solvent in which the antibiotic was dissolved was injected in other four wells, and the last four wells of the plate were left untouched. The plates were incubated in incubator for 7 days after sealing with parafilm.

At the end of the incubation, the plate was opened and Tween-80 (0.1% volume/volume) was added, swirled and incubated at room temperature for 15 minutes. The content of each well was mixed with pipette several times and transferred to a 15mL conical tube. The contents of the tube were centrifuged at 4000 rpm for 10 minutes at room temperature. The pellet was resuspended in 5mL of fresh wash buffer (PBS with 10% glycerol and 0.05% Tween-80). Washing was repeated three times and the pellet was resuspended in 5mL of wash buffer. The tubes were kept on rocker for overnight at room temperature.

Pass the whole contents of tube through syringe fitted with sterile microtip (2-200µl) for 5-6 times to attain fairly homogenous suspension. The cell suspensions were diluted 10-fold up to 10^{-6} using Middlebrook 7H9 medium supplemented with OADC and 100 µl of each dilutions were plated in 48 well plates in triplicates along with 900 µl of Middlebrook 7H9 medium (HiMedia Laboratories) supplemented with OADC (HiMedia Laboratories). The plates were

46

incubated at 37 °C for 3-4 weeks the wells with visible bacterial growth were counted as positive. The frequency of persisters in the biofilm population was determined by comparing antibiotic treated plates to solvent treated plates [Kulka, K., et al., 2012, Wang, F., et al., 2013].

4.2.1.3.6. Kill kinetics under nutrient starved condition:

M. tuberculosis culture (5ml) with an O.D. of 0.6-1.0 was centrifuged at 2,500 rpm for 15 min. The supernatant was discarded and suspended in 1ml of PBS-Tyloxapol (5 mL 10 % Tyloxapol in 995 mL of PBS). The culture was diluted with PBS-Tyloxapol till it attains O.D. of 0.1 and it was starved for 2 weeks prior to the study.

For each compound to be tested 4 tubes were labeled -3 as concentrations (5, 10, 20 μg/ml) to be tested and one served as DMSO control. To each tube 5ml of PBS-Tyloxapol and 50μl of starved culture were added. To compound tubes 100 μl of stock solution (50x) of compound was added to attain desired concentration. To tube labeled as control 100 μl DMSO was added. The contents of tubes were mixed and incubated at 37 °C. The treated cell suspensions were tested at 0, 7, 14, 21 days intervals. The bacterial suspension was diluted 10-fold up to 10^{-6} using Middlebrook 7H9 medium supplemented with OADC and 100 μl of each dilution were plated in 48 well plates in triplicates along with 900 μl of Middlebrook 7H9 medium (HiMedia Laboratories) supplemented with OADC (HiMedia Laboratories). The plates were incubated at 37 °C for 3-4 weeks the wells with visible bacterial growth were counted as positive. The bacterial count was down by using standard statistical methods using MPN assay [Parish, T., et al., 1998].

4.2.1.3.7. Human 3D granuloma model:

An extracellular matrix (ECM) was prepared by mixing 0.95ml Purecol collagen solution, 50 μl 10x DPBS (Lonza, USA), 4 μl fibronectin (BD Biosciences, USA) and 10 μl 1N NaOH (Sigma, USA) per ml of matrix solution and kept on ice (pH 7.0). PBMC cells were mixed at room temperature (RT) with ECM at $5x10^5$ cells/50 μl/well of 96-well plate. Assuming 5% macrophages in PBMCs, H37Rv strain of *Mtb* was added to the ECM at multiplicities of infection (MOI) of 0.1. ECM was allowed to set by incubating at 37 °C, CO_2 incubator for 45min. RPMI media containing 20% human Serum was added to the set ECM containing PBMCs and *Mtb* and incubated in 37 °C, CO_2 incubator. Media was changed after 2 days.

Once the granulomas were formed, the granulomas were either left untreated or were treated with the compound for 4 days and then with Rifampicin (Rif) for further 3 days. To add compounds media was removed, and media containing the compound was added to the experimental wells for 4 days. Then to some wells Rif was added. After 3 additional days, media was removed and wells treated with 50 μl/well collagenase (Sigma, USA) for 40 min at 37 ^{0}C to isolate host PBMC cells. Samples from five wells were pooled in 1.8ml micro centrifuge tubes and host cells were lyzed with 200 μl of 0.1% triton X-100 solution. *Mtb* pellet was obtained by centrifuging at 3500 Xg for 12 min. the *Mtb* pellet was suspended in 1ml 7H9 media and 10-fold serial dilutions were made in Middlebrook 7H9 media containing 0.05% tween-80 and 100μl samples plated on Middlebrook 7H10 agar plates. Plates were incubated at 37 ^{o}C. Colony forming units (cfu) were determined after four weeks. % Rifampicin-tolerance is calculated by formula - %Rif-tolerance = cfu (Rif)/cfu(untreated) x 100 [Kapoor, N., et al., 2013].

4.2.1.3.8. *In vivo* antimycobacterial evaluation by *Mycobacterium marinum* induced zebra fish model:

The anti-tubercular potency of the potent molecules were evaluated by *in vivo Mycobacterium marinum* induced zebra fish model following similar protocol to the one utilized for evaluating the CysM inhibitors.

4.2.1.3.9. Cytotoxicity studies:

The synthesized compounds were further examined for its cytotoxicity in mouse macrophage cell line (RAW 264.7) at 50 μg/ml concentration. After 48 h of exposure, viability was assessed on the basis of cellular conversion of MTT into a formazan product using the Promega Cell Titer 96 non-radioactive cell proliferation assay. Mouse macrophages were grown in RPMI medium supplemented with 10% fetal bovine serum (FBS), 10,000 units penicillin and 10 mg streptomycin per ml in T25 flasks to attain 80-90% confluency. Cells were scraped and seeded into wells approx 5,000 cells per well in poly-L-lysine coated plates. The microtiter plates were incubated at 37 ^{o}C, 5% CO_2, 95% air and 100% relative humidity for 24 h prior to addition of experimental drugs. The test compounds at 50 μg/ml concentration were then added to cells and incubated at 37 °C for 48 h; later 10 μl of 0.5mg/ml concentration of MTT was added and incubated for 3 h at 37 ^{o}C and the final product formazon crystals were measured at 595nm.

Ciprofloxacin (3% inhibition) and Novobiocin (9.8% inhibition) were used as a standards in this assay [Gerlier D., et al., 1986 and Scudiero D.A., et al., 1988]. The percentage inhibition was calculated from the following formula:

$$\text{Percentage inhibition} = \frac{100 - \text{mean OD sample}}{\text{mean OD day 0}}$$

Results and discussion for development of Mycobacterial Cysteine synthase M inhibitors

5.1. Identification of hits, hit expansion and characterization, biological evaluation of substituted diphenyl urea derivatives as potent *Mycobacterium tuberculosis* Cysteine synthase M inhibitors

5.1.1. Small molecule screening and hit selection

Cysteine has been implicated as an important amino acid in the redox defense of *Mycobacterium tuberculosis*, primarily as a building block of mycothiol. CysM/CysO pathway is the dominant route to cysteine in dormant bacteria to combat stress. Binding of small-molecule ligands to the active site of CysM from *M. tuberculosis* is accompanied by an increase in the fluorescence of the bound cofactor PLP. We exploited this property in a 384-well microplate-based screening assay to identify new small-molecule binders of this enzyme. To this end 17312 chemically diverse and lead- to drug-like compounds [Lipinski (2004) Drug Discovery Today 4, 337] were screened against recombinant CysM at a single concentration of 10 µM at Chemical Biology Consortium Sweden (www.cbcs.se). Compounds that resulted in an arbitrarily chosen fluorescence increase by more than 30% were considered as primary hits that warranted further investigation in concentration-dependent response and counter-assays to remove auto-fluorescent compounds. This selection criterion gave 431 initial hits and a hit rate of 2.4%. Hit confirmation experiments resulted in 20 compounds showing dose-dependent binding to CysM with minimal interference from background fluorescence of the compound itself. Seven of these demonstrated a saturating fluorescence signal in the interval between 2.5 to 40 µM and also showed suitable properties after examination of both pan assay interference compounds [PAINS; Baell, *et. al.,* 2010] and potential aggregator filters [Irwin, *et. al.,* 2015]. Among these seven compound structures, two were closely related urea derivatives of which none had previously appeared as hits in other in-house screens. As further analogues of this scaffold were easily accessible to us

through analogue searches of the CBCS compound collection and from synthesis, we choose to focus our next efforts on this compound series.

The changes in PLP cofactor fluorescence were next used to assess the apparent affinity of the two initial urea hits in full concentration-response curves (**Fig 5.3a),** giving apparent K_d values of 0.95 ± 0.09 μM for **RK_01** and 1.7 ±0.2 μM for **RK_02** (**Table 5.1**), respectively. This characterization was limited to the lower μM range as a CysM concentration of 2 μM was necessary to obtain a reliable signal to background ratio in the assay. Wherever possible (**Fig 5.3**) compounds with K_d values in the lower μ-molar range were therefore re-evaluated by isothermal titration calorimetry (ITC). For **RK_01**, ITC gave a K_d value of 0.32± 0.01 μM (**Table 5.1**), whereas binding of **RK_02** could not be evaluated by ITC. The value of 1.7 ±0.2 μM from the PLP fluorescence experiment thus represents an upper apparent K_d for this compound.
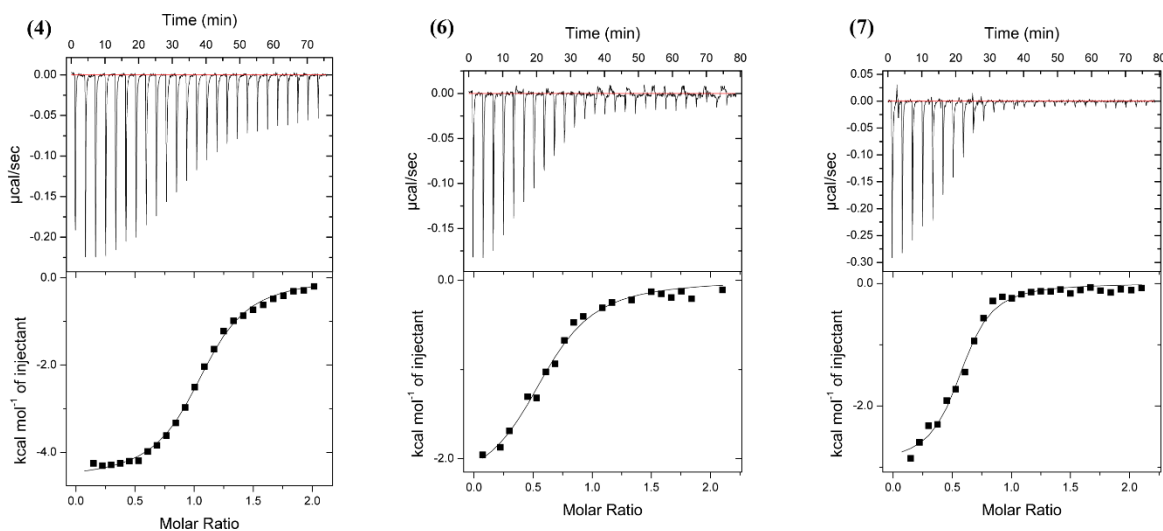
Fig 5.1: Determination of K_d for strong binding inhibitors using ITC.

5.1.2. Hit characterization and expansion

Hit expansion was carried out by several rounds of compound selection/synthesis, where three-dimensional structures of CysM−inhibitor complexes (see below) in combination with biochemical data informed the design of the analogs. The identified hits had urea as a linker bridging two flanking phenyl rings (**Table 5.1**). Based on this scaffold, 17 analogs were selected from the in-house compound collection and small sub-libraries comprising an additional 54

molecules were synthesized. This resulted in a total of 71 analogues that were characterized in the assays described above to derive an initial understanding of the structure-activity relationships (SAR).

The synthetic protocols employed involved the synthesis of urea and thiourea derivatives of the initial hits. To accomplish this 3-amino benzoic acid was coupled with various substituted isocyanates and isothiocyanates. A sub-library of 18 compounds was synthesized, using triethyl amine as organic base and ethanol as solvent at room temperature. To explore the effect of hydroxyl group substitution on the LHS, 4-amino salicylic acid, 5-amino salicylic acid and 4-amino-3-hydroxy benzoic acid were treated with the isocyanates and isothiocyanates [Devi, K., et al., 2014]. In further steps to investigate the effect of substitutions on the RHS phenyl ring, 3-bromo and 4-bromo urea compounds were treated with substituted aromatic boronic acid to facilitate C-C bond formation via a Suzuki cross coupling reaction. This was achieved using tetrakis as catalyst, an acetonitrile:water mixture as solvent, and sodium carbonate as base under microwave irradiation at $110\ ^{o}C$ for 1 h. [Betts et al. Patent no-US 2013/0338361].

General procedure for the synthesis of 3-(3-phenylureido) and 3-(3-phenylthioureido) benzoic acid derivatives.
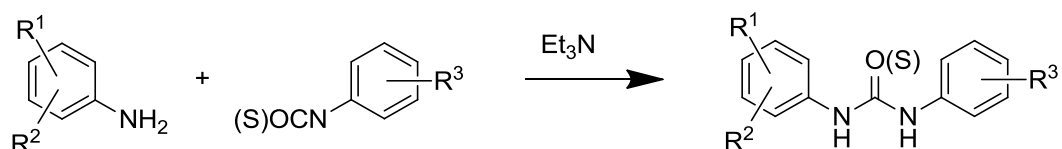
R^1 = COOH; R^2 = OH; R^3 = 4-NO$_2$; 4-OCH$_3$; 4-CH$_3$; 4-Acetyl; 4-Br; 4-Cl; 3-Br; Benzyl; 3,4-Dichloro

Substituted Phenyl isocyanate or isothiocyanate (1 mmol) was added dropwise to a stirred ice-cooled solution of 3-amino benzoic acid or 4-amino salicylic acid or 5-amino salicylic acid or 4-amino-3-hydroxy benzoic acid (1 mmol) and triethylamine (2 mmol) in dry ethanol. Reaction progress was monitored by TLC and HPLC-MS. After 24 h, solvent was evaporated under reduced pressure and the resulting residue was diluted with aq. sodium bicarbonate and the mixture was filtered. The filtrate was acidified with 2N hydrochloric acid and the precipitate was filtered and recrystallized in ethanol to yield the respective (thio)urea derivatives.

General procedure for the synthesis of biphenyl urea derivatives:
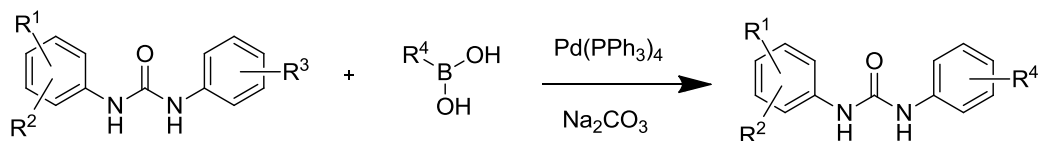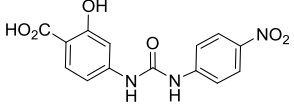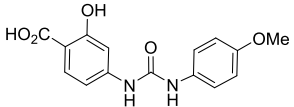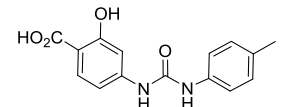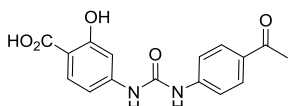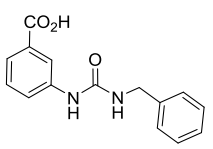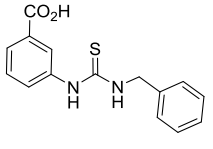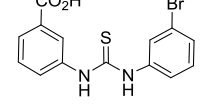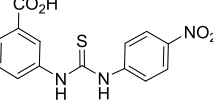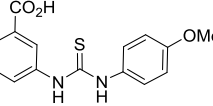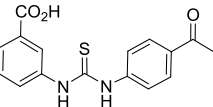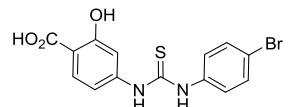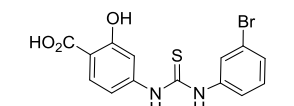
R^3 = 3-Br or 4-Br; R^4 = Phenyl; 4-fluoro phenyl; 2,3-dichloro phenyl; I; 2,5-dimethyl; 3-benzoic acid; 2-pyridyl; 2-fluoro pyridine; pyrimidyl.

Substituted(3-(4-bromophenyl)ureido)benzoic acid (1 mmol), corresponding boronic acid (2 mmol), sodium carbonate (2M solution) (4 mmol) and Tetrakis (0.06 mmol) were taken in acetonitrile and irradiated in microwave at 100 °C for 1 h (monitored by TLC and LCMS for completion). The reaction mixture was passed through celite and washed with methanol. The filtrate was concentrated and purified by column chromatography using hexane:ethyl acetate as eluent to get the desired product in good yield.

Table 5.1: Physicochemical properties of Urea and thio urea derivatives (Type I inhibitors)

Cmpd.	Structure	Yield (%)	Molecular formula	Molecular weight	Melting point (°C)
RK_01		75.5	C$_{14}$H$_{10}$Cl$_2$N$_2$O$_3$	325.15	119 – 121
RK_05		71.1	C$_{15}$H$_{14}$N$_2$O$_3$	270.28	242 – 244
RK_06		80.3	C$_{14}$H$_{11}$BrN$_2$O$_3$	335.15	275 – 277
RK_07		78.8	C$_{14}$H$_{11}$ClN$_2$O$_3$	290.70	279 – 281
RK_09		70.0	C$_{14}$H$_{10}$Cl$_2$N$_2$O$_4$	341.15	253 – 255

RK_10		79.0	$C_{14}H_{10}Cl_2N_2O_4$	341.15	131 – 133
RK_11		83.5	$C_{14}H_{10}Cl_2N_2O_4$	341.15	131 – 133
RK_12		78.23	$C_{14}H_{11}ClN_2O_2S$	306.77	195 – 197
RK_17		83.76	$C_{14}H_{11}N_3O_5$	301.25	227 – 229
RK_18		80.0	$C_{15}H_{14}N_2O_4$	286.28	259 – 261
RK_19		79.1	$C_{16}H_{14}N_2O_4$	298.29	228 – 230
RK_20		78.5	$C_{15}H_{14}N_2O_2S$	286.35	203 – 205
RK_21		86.3	$C_{14}H_{11}BrN_2O_2S$	351.22	189 – 191
RK_22		80.5	$C_{14}H_{11}BrN_2O_3$	335.15	184 – 186
RK_31		73.7	$C_{14}H_{11}BrN_2O_4$	351.15	211 – 213
RK_32		79.4	$C_{14}H_{11}BrN_2O_4$	351.15	236 – 238
RK_33		70.0	$C_{14}H_{11}ClN_2O_4$	306.70	204 – 206

RK_34		84.5	$C_{14}H_{11}N_3O_6$	317.25	181 – 183
RK_35		80.0	$C_{15}H_{14}N_2O_5$	302.28	247 – 249
RK_36		70.6	$C_{15}H_{14}N_2O_4$	286.28	221 – 223
RK_37		84.3	$C_{16}H_{14}N_2O_5$	314.29	195 – 197
RK_38		69.0	$C_{15}H_{14}N_2O_3$	270.28	253 – 255
RK_39		75.2	$C_{15}H_{14}N_2O_2S$	286.35	214 – 216
RK_40		80.5	$C_{14}H_{11}BrN_2O_2S$	351.22	163 – 165
RK_41		78.7	$C_{14}H_{11}N_3O_4S$	317.32	161 – 163
RK_42		80.7	$C_{15}H_{14}N_2O_3S$	302.35	199 – 201
RK_43		62.4	$C_{16}H_{14}N_2O_3S$	314.36	191 – 193
RK_44		51.3	$C_{14}H_{11}BrN_2O_3S$	367.22	225 – 227
RK_45		69.6	$C_{14}H_{11}BrN_2O_3S$	367.22	162 – 164
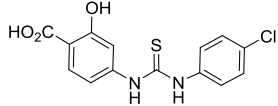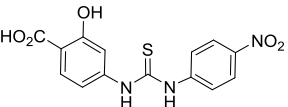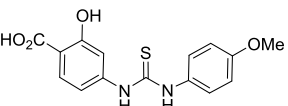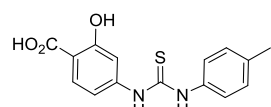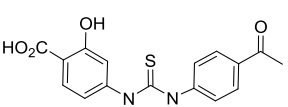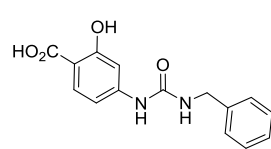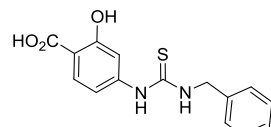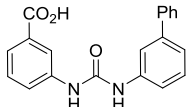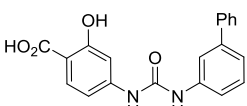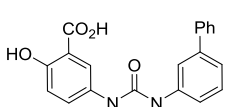
Cmpd.	Structure	Yield (%)	Molecular formula	Molecular weight	Melting point (°C)
RK_46		58.8	$C_{14}H_{11}ClN_2O_3S$	322.77	175 – 177
RK_47		72.1	$C_{14}H_{11}N_3O_5S$	333.32	173 – 175
RK_48		85.1	$C_{15}H_{14}N_2O_4S$	318.35	185 – 187
RK_49		82.0	$C_{15}H_{14}N_2O_3S$	302.35	163 – 165
RK_50		63.0	$C_{16}H_{14}N_2O_4S$	330.36	231 – 233
RK_51		79.2	$C_{15}H_{14}N_2O_4$	286.28	180 – 182
RK_52		73.4	$C_{15}H_{14}N_2O_3S$	302.35	192 – 194

Table 5.2: Physicochemical properties of Biphenyl urea derivatives (Type II inhibitors)

Cmpd.	Structure	Yield (%)	Molecular formula	Molecular weight	Melting point (°C)
RK_02		31.0	$C_{20}H_{16}N_2O_3$	332.35	229–231
RK_03		43.0	$C_{20}H_{16}N_2O_4$	348.35	210 – 212
RK_04		48.0	$C_{20}H_{16}N_2O_4$	348.35	208 – 210

Compound	Structure	%	Formula	MW	mp (°C)
RK_54		96.0	$C_{20}H_{14}Cl_2N_2O_3$	401.24	215 - 217
RK_55		46.2	$C_{22}H_{20}N_2O_3$	360.41	--
RK_56		39.8	$C_{20}H_{16}N_2O_3$	332.35	193 – 195
RK_57		63.4	$C_{19}H_{14}FN_3O_3$	351.33	--
RK_58		65.2	$C_{20}H_{15}FN_2O_3$	350.34	--
RK_59		71.5	$C_{20}H_{15}FN_2O_3$	350.34	--
RK_60		63.6	$C_{20}H_{14}Cl_2N_2O_3$	401.24	189 - 191
RK_62		38.4	$C_{20}H_{16}N_2O_4$	348.35	198 – 200
RK_63		48.1	$C_{19}H_{15}N_3O_3$	333.34	139 – 141
RK_64		57.4	$C_{19}H_{14}FN_3O_3$	351.33	--
RK_65		51.5	$C_{21}H_{16}N_2O_5$	376.36	--

57

RK_66		45.9	$C_{21}H_{16}N_2O_5$	376.36	182 – 184
RK_67		38.3	$C_{18}H_{14}N_4O_3$	334.33	--
RK_68		44.2	$C_{18}H_{14}N_4O_3$	334.33	--
RK_69		53.4	$C_{22}H_{20}N_2O_3$	360.41	--
RK_70		53.1	$C_{19}H_{15}N_3O_3$	333.34	171 – 173

5.1.3. Characterization of the synthesized molecules

3-(3-(3,4-Dichlorophenyl)ureido)benzoic acid (**RK_01**): The compound was synthesized according to the above general procedure using 3-amino benzoic acid (0.10g, 0.73mmol), 3,4-dichloro phenyl isocyanate (0.14g, 0.73mmol) and triethylamine (0.15g, 1.46mmol) to afford **RK_01** as white solid (0.18g, 75.5 % yield). M.P:119 – 121 °C. ^{1}H NMR (DMSO-d_6): δ 12.96 (br s, 1H), 9.30 (s, 1H), 9.25 (s, 1H), 8.14 (s, 1H), 7.90 (s, 1H), 7.59 (d, J = 8 Hz, 1H), 7.54 (d, J = 8.8 Hz, 1H), 7.44 (t, J = 8 Hz, 1H), 7.37 (m, 2H). ^{13}C NMR (DMSO-d_6): δ 167.2, 152.3, 139.9, 139.6, 131.3, 131.0, 130.5, 129.0, 123.1, 123.0, 122.1, 119.3, 119.0, 118.3. ESI-MS m/z 324.01(M-H)$^+$. Anal Calc'd for $C_{14}H_{10}Cl_2N_2O_3$; C, 51.72; H, 3.10; N, 8.62; Found C, 51.82; H, 3.09; N, 8.64.

3-(3-(p-Tolyl)ureido) benzoic acid (RK_05): The compound was synthesized according to the above general procedure using 3-amino benzoic acid (0.10g, 0.73mmol), p-tolyl isocyanate (0.09g, 0.73mmol) and triethylamine (0.15g, 1.46mmol) to afford **RK_05** as pale yellow solid (0.14g, 71.1 % yield). M.P: 242 – 244 °C. ^{1}H NMR (DMSO-d_6): δ 12.74 (br s, 1H), 9.32 (s, 1H), 8.91 (s, 1H), 8.23 (s, 1H), 7.78 (d, J = 8.2 Hz, 2H), 7.73 – 7.41 (m, 5H), 2.56 (s, 3H). ^{13}C NMR (DMSO-d_6): δ 167.5, 152.7, 142.7,138.9, 138.1, 130.7 (2C), 126.7, 126.3, 124.4, 123.9, 119.8

(2C), 118.2, 22.6. ESI-MS m/z 269.10(M-H)$^+$. Anal Calc'd for $C_{15}H_{14}N_2O_3$; C, 66.66; H, 5.22; N, 10.36; Found C, 66.48; H, 5.24; N, 10.39.

3-(3-(4-Bromophenyl)ureido)benzoic acid (RK_06): The compound was synthesized according to the above general procedure using 3-amino benzoic acid (0.10g, 0.73mmol), 4-chloro phenyl isocyanate (0.11g, 0.73mmol) and triethylamine (0.15g, 1.46mmol) to afford **RK_06** as white solid (0.19g, 80.3 % yield).M.P: 275 – 277 °C. ^{1}H NMR (DMSO-d$_6$): δ 12.63 (br s, 1H), 9.00 (s, 1H), 8.93 (s, 1H), 8.12 (s, 1H), 7.65 (m, 1H), 7.57 (d, J = 8 Hz, 1H), 7.45 – 7.39 (m, 5H). ^{13}C NMR (DMSO-d$_6$): δ 167.3, 152.7, 145.8, 140.9, 133.8 (2C), 129.6, 128.4, 124.1, 122.8, 120.3, 119.6 (2C), 118.5. ESI-MS m/z 334.01 (M-H)$^+$. Anal Calc'd for $C_{14}H_{11}BrN_2O_3$; C, 50.17; H, 3.31; N, 8.36; Found C, 50.32; H, 3.33; N, 8.38.

3-(3-(4-Chlorophenyl)ureido)benzoic acid (RK_07): The compound was synthesized according to the above general procedure using 3-amino benzoic acid (0.10g, 0.73mmol), 4-chloro phenyl isocyanate (0.11g, 0.73mmol) and triethylamine (0.15g, 1.46mmol) to afford **RK_07** as white solid (0.17g, 78.8 % yield). M.P: 279 – 281 °C. ^{1}H NMR (DMSO-d$_6$): δ 12.88 (br s, 1H), 8.98 (s, 1H), 8.89 (s, 1H), 8.15 (s, 1H), 7.88 (d, J = 8 Hz, 2H), 7.68 – 7.36 (m, 5H). ^{13}C NMR (DMSO-d$_6$): δ 168.0, 152.7, 141.9, 139.3, 135.8, 130.3 (2C), 129.6, 128.5, 127.1, 123.4, 121.6, 118.6 (2C). ESI-MS m/z 289.05 (M-H)$^+$. Anal Calc'd for $C_{14}H_{11}ClN_2O_3$; C, 57.84; H, 3.81; N, 9.64; Found C, 57.67; H, 3.82; N, 9.62.

5-(3-(3,4-Dichlorophenyl)ureido)-2-hydroxybenzoic acid (RK_09): The compound was synthesized according to the above general procedure using 5-amino salicylic acid (0.10g, 0.65mmol), 3,4-dichloro phenyl isocyanate (0.12g, 0.65mmol) and triethylamine (0.13g, 1.31mmol) to afford **RK_09** as brown solid (0.16g, 70.0 % yield). M.P: 253 – 255 °C. ^{1}H NMR (DMSO-d$_6$): δ 12.85 (br s, 1H), 9.62 (s, 1H), 9.56 (s, 1H), 8.18 (s, 1H), 8.01 (s, 1H), 7.82 (d, J = 8.2 Hz, 1H), 7.62 – 7.21 (m, 3H), 5.05 (s, 1H). ^{13}C NMR (DMSO-d$_6$): δ 172.2, 162.4, 152.8, 138.7, 138.2, 129.6, 128.7, 127.6, 126.4, 124.4, 122.7, 118.8, 117.9, 116.3. ESI-MS m/z 340.05 (M-H)$^+$. Anal Calc'd for $C_{14}H_{10}Cl_2N_2O_4$; C, 49.29; H, 2.95; N, 8.21; Found C, 49.17; H, 2.96; N, 8.23.

4-(3-(3,4-Dichlorophenyl)ureido)-2-hydroxybenzoic acid (RK_10): The compound was synthesized according to the above general procedure using 4-amino salicylic acid (0.10g,

0.65mmol), 3,4-dichloro phenyl isocyanate (0.12g, 0.65mmol) and triethylamine (0.13g, 1.31mmol) to afford **RK_10** as palebrown solid (0.18g, 79.0 % yield). M.P: 131 – 133 °C. ^{1}H NMR (DMSO-d$_6$): δ 12.82 (br s, 1H), 9.63 (s, 1H), 9.55 (s, 1H), 8.11 (d, J = 8 Hz, 1H), 8.04 (s, 1H), 7.65 – 7.29 (m, 4H), 5.05 (s, 1H). ^{13}C NMR (DMSO-d$_6$): δ 172.2, 162.4, 152.7, 140.4, 138.3, 132.7, 129.6, 129.3, 127.6, 125.28, 123.6, 116.7, 115.8, 104.2. ESI-MS m/z 340.05 (M-H)$^+$. Anal Calc'd for C$_{14}$H$_{10}$Cl$_2$N$_2$O$_4$; C, 49.29; H, 2.95; N, 8.21; Found C, 49.42; H, 2.94; N, 8.23.

4-(3-(3,4-Dichlorophenyl)ureido)-3-hydroxybenzoic acid (RK_11): The compound was synthesized according to the above general procedure using 4-amino-3-hydroxy benzoic acid (0.10g, 0.65mmol) 3,4-dichloro phenyl isocyanate (0.12g, 0.65mmol) and triethylamine (0.13g, 1.31mmol) to afford **RK_11** as Yellow solid (0.19g, 83.5 % yield). M.P: 131 – 133 °C. ^{1}H NMR (DMSO-d$_6$): δ 12.73 (br s, 1H), 9.65 (s, 1H), 9.56 (s, 1H), 8.01 (s, 1H), 7.81 (d, J = 8.4 Hz, 1H), 7.74 (s, 1H), 7.69 – 7.29 (m, 3H), 5.03 (s, 1H). ^{13}C NMR (DMSO-d$_6$): δ 167.2, 152.8, 146.4, 132.5, 128.8, 127.6, 125.6, 124.1, 123.5, 122.6, 118.4, 117.2, 114.6, 112.6. ESI-MS m/z 340.05 (M-H)$^+$. Anal Calc'd for C$_{14}$H$_{10}$Cl$_2$N$_2$O$_4$; C, 49.29; H, 2.95; N, 8.21; Found C, 49.42; H, 2.96; N, 8.19.

3-(3-(4-Chlorophenyl)thioureido)benzoic acid (RK_12): The compound was synthesized according to the above general procedure using 3-amino benzoic acid (0.10g, 0.73mmol), 4-chloro phenyl isothiocyanate (0.12g, 0.73mmol) and triethylamine (0.15g, 1.46mmol) to afford **RK_12** as white solid (0.18g, 78.23 % yield). M.P: 195 – 197 °C. ^{1}H NMR (DMSO-d$_6$): δ 12.68 (br s, 1H), 7.98 (s, 1H), 7.78 (s, 1H), 7.61 (d, J = 8.2 Hz, 1H), 7.55 – 7.18 (m, 4H), 6.85 – 6.67 (m, 3H). ^{13}C NMR (DMSO-d$_6$): δ 180.6, 164.8, 139.5, 137.2, 135.8, 133.6, 129.3 (2C), 127.6 (2C), 127.0, 126.4, 124.2, 123.2. ESI-MS m/z 305.02 (M-H)$^+$. Anal Calc'd for C$_{14}$H$_{11}$ClN$_2$O$_2$S; C, 54.81; H, 3.61; N, 9.13; Found C, 54.93; H, 3.60; N, 9.11.

3-(3-(4-Nitrophenyl)ureido)benzoic acid (RK_17): The compound was synthesized according to the above general procedure using 3-amino benzoic acid (0.10g, 0.73mmol), 4-nitro phenyl isocyanate (0.12g, 0.73mmol) and triethylamine (0.15g, 1.46mmol) to afford **RK_17** as pale yellow solid (0.18g, 83.76 % yield). M.P: 227 – 229 °C. ^{1}H NMR (DMSO-d$_6$): δ 12.71 (br s, 1H), 10.51 (s, 1H), 10.03 (s, 1H), 8.22 (d, J = 9.2 Hz, 1H), 8.13 – 7.96 (m, 3H), 7.73 (d, J = 9.2

Hz, 1H), 7.65 (m, 2H), 7.46 (t, J = 8.4 Hz, 1H). ^{13}C NMR (DMSO-d$_6$): δ 166.2, 152.4, 147.8, 145.6, 144.4, 132.8, 129.1, 128.4, 127.4, 122.2 (2C), 118.8, 117.1 (2C). ESI-MS m/z 300.07 (M-H)$^+$. Anal Calc'd for C$_{14}$H$_{11}$N$_3$O$_5$; C, 55.82; H, 3.68; N, 13.95; Found C, 55.67; H, 3.67; N, 13.99.

3-(3-(4-Methoxyphenyl)ureido) benzoic acid (RK_18): The compound was synthesized according to the above general procedure using 3-amino benzoic acid (0.10g, 0.0.73mmol), 4-methoxy phenyl isocyanate (0.11g, 0.73mmol) and triethylamine (0.15g, 1.46mmol) to afford **RK_18** as pale brown solid (0.17g, 80.0 % yield). M.P: 259 – 261 °C. ^{1}H NMR (DMSO-d$_6$): δ 12.53 (br s, 1H), 9.13 (s, 1H), 8.74 (s, 1H), 8.17 (s, 1H), 7.85 (d, J = 8.2 Hz, 2H), 7.55 – 6.96 (m, 5H), 3.85 (s, 3H). ^{13}C NMR (DMSO-d$_6$): δ 167.3, 154.5, 152.7, 140.2, 132.6, 131.3, 128.9, 122.3, 122.1, 120.1 (2C), 118.6, 113.9 (2C), 55.1. ESI-MS m/z 285.13 (M-H)$^+$. Anal Calc'd for C$_{15}$H$_{14}$N$_2$O$_4$; C, 62.93; H, 4.93; N, 9.79; Found C, 63.14; H, 4.92; N, 9.76.

3-(3-(4-Acetylphenyl)ureido) benzoic acid (RK_19): The compound was synthesized according to the above general procedure using 3-amino benzoic acid (0.10g, 0.73mmol), 4-acetyl phenyl isocyanate (0.12g, 0.73mmol) and triethylamine (0.15g, 1.46mmol) to afford **RK_19** as pale brown solid (0.17g, 79.1 % yield). M.P: 228 – 230 °C. ^{1}H NMR (DMSO-d$_6$): δ 12.46 (br s, 1H), 9.15 (s, 1H), 8.69 (s, 1H), 8.21 (s, 1H), 7.82 (d, J = 8 Hz, 2H), 7.59 – 7.38 (m, 5H), 2.53 (s, 3H). ^{13}C NMR (DMSO-d$_6$): δ 195.6, 164.3, 152.7, 142.5, 143.3, 135.7, 130.3 (2C), 129.6, 129.17, 125.3, 124.7, 119.7 (2C), 117.5, 27.3. ESI-MS m/z 297.10 (M-H)$^+$. Anal Calc'd for C$_{16}$H$_{14}$N$_2$O$_4$; C, 64.42; H, 4.73; N, 9.39; Found C, 64.24; H, 4.72; N, 9.41.

3-(3-(p-Tolyl)thioureido) benzoic acid (RK_20): The compound was synthesized according to the above general procedure using 3-amino benzoic acid (0.10g, 0.73mmol), p-tolyl isothiocyanate (0.11g, 0.73mmol) and triethylamine (0.15g, 1.46mmol) to afford **RK_20** as white solid (0.16g, 78.5 % yield). M.P: 203 – 205 °C. ^{1}H NMR (DMSO-d$_6$): δ 12.51 (br s, 1H), 7.95 (s, 1H), 7.75 (s, 1H), 7.63 (d, J = 8 Hz, 1H), 7.52 – 7.21 (m, 4H), 6.72 – 6.41 (m, 3H), 2.37 (s, 3H). ^{13}C NMR (DMSO-d$_6$): δ 181.6, 167.5, 139.4, 137.3, 136.4, 134.8, 132.7, 130.9 (2C), 129.6, 128.7, 124.4 (2C), 123.7, 20.4. ESI-MS m/z 285.08 (M-H)$^+$. Anal Calc'd for C$_{15}$H$_{14}$N$_2$O$_2$S; C, 62.92; H, 4.93; N, 9.78; Found C, 63.07; H, 4.92; N, 9.76.

3-(3-(4-Bromophenyl)thioureido)benzoic acid (RK_21): The compound was synthesized according to the above general procedure using 3-amino benzoic acid (0.10g, 0.73mmol), 4-bromo phenyl isothiocyanate (0.16g, 0.73mmol) and triethylamine (0.15g, 1.46mmol) to afford **RK_21** as white solid (0.22g, 86.3 % yield). M.P: 189 – 191 °C. ^{1}H NMR (DMSO-d$_6$): δ 12.66 (br s, 1H), 7.93 (s, 1H), 7.78 (s, 1H), 7.65 (d, J = 7.8 Hz, 1H), 7.55 – 7.25 (m, 4H), 6.75 – 6.30 (m, 3H). ^{13}C NMR (DMSO-d$_6$): δ 181.3, 168.7, 139.8, 138.3, 133.8 (3C), 132.6 (2C), 130.7, 129.6, 126.4, 124.27, 121.3. ESI-MS m/z 349.97 (M-H)$^+$. Anal Calc'd for C$_{14}$H$_{11}$BrN$_2$O$_2$S; C, 47.88; H, 3.16; N, 7.98; Found C, 47.76; H, 3.17; N, 8.00.

3-(3-(3-Bromophenyl)ureido)benzoic acid (RK_22): The compound was synthesized according to the above general procedure using 3-amino benzoic acid (0.10g, 0.73mmol), 3-bromo phenyl isocyanate (0.14g, 0.73mmol) and triethylamine (0.15g, 1.46mmol) to afford **RK_22** as white solid (0.21g, 80.5 % yield). M.P: 184 – 186 °C. ^{1}H NMR (DMSO-d$_6$): δ 12.68 (br s, 1H), 9.15 (s, 1H), 9.02 (s, 1H), 8.15(s, 1H), 7.85 (d, J = 8.4 Hz, 2H), 7.76 (s, 1H), 7.52 – 7.28 (m, 4H). ^{13}C NMR (DMSO-d$_6$): δ 167.1, 152.8, 141.5, 140.6, 128.6, 128.1, 126.6, 126.3, 125.9, 125.0, 124.3, 121.7, 119.7, 118.7. ESI-MS m/z 334.01 (M-H)$^+$. Anal Calc'd for C$_{14}$H$_{11}$BrN$_2$O$_3$; C, 50.17; H, 3.31; N, 8.36; Found C, 50.27; H, 3.32; N, 8.34.

4-(3-(4-Bromophenyl)ureido)-2-hydroxybenzoic acid (RK_31): The compound was synthesized according to the above general procedure using 4-amino salicylic acid (0.10g, 0.65mmol), 4-bromo phenyl isocyanate (0.13g, 0.65mmol) and triethylamine (0.13g, 1.31mmol) to afford **RK_31** as Off white solid (0.17g, 73.7 % yield). M.P: 211 – 213 °C. ^{1}H NMR (DMSO-d$_6$): δ 12.65 (br s, 1H), 9.02 (s, 1H), 8.95 (s, 1H), 8.05 (d, J = 8 Hz, 1H), 7.85 – 7.65 (m, 4H), 7.59 (s, 1H), 7.48 (d, J = 7.8 Hz, 1H), 5.01 (s, 1H). ^{13}C NMR (DMSO-d$_6$): δ 172.7, 162.2, 152.9, 139.7, 135.7, 127.2, 126.5 (2C), 120.7, 119.5 (2C), 115.6, 113.3, 104.3. ESI-MS m/z 350.05 (M-H)$^+$. Anal Calc'd for C$_{14}$H$_{11}$BrN$_2$O$_4$; C, 47.89; H, 3.16; N, 7.98; Found C, 47.77; H, 3.17; N, 7.96.

4-(3-(3-Bromophenyl)ureido)-2-hydroxybenzoic acid (RK_32): The compound was synthesized according to the above general procedure using 4-amino salicylic acid (0.10g, 0.65mmol), 3-bromo phenyl isocyanate (0.13g, 0.65mmol) and triethylamine (0.13g, 1.31mmol) to afford **RK_32** as brown solid (0.18g, 79.4 % yield). M.P: 236 – 238 °C. ^{1}H NMR (DMSO-

d$_6$): δ 12.68 (br s, 1H), 9.05 (s, 1H), 8.91 (s, 1H), 8.04 (d, J = 8.2 Hz, 1H), 7.88 (s,1H), 7.62 – 7.25 (m, 5H), 5.03 (s, 1H). ^{13}C NMR (DMSO-d$_6$): δ 172.4, 162.5, 152.2, 140.4, 136.3, 129.4, 127.4, 126.4, 121.7, 119.9, 117.3, 114.7, 112.4, 104.6. ESI-MS m/z 350.05 (M-H)$^+$. Anal Calc'd for C$_{14}$H$_{11}$BrN$_2$O$_4$; C, 47.89; H, 3.16; N, 7.98; Found C, 47.75; H, 3.15; N, 8.00.

4-(3-(4-Chlorophenyl)ureido)-2-hydroxybenzoic acid (RK_33): The compound was synthesized according to the above general procedure using 4-amino salicylic acid (0.10g, 0.65mmol), 4-chloro phenyl isocyanate (0.10g, 0.65mmol) and triethylamine (0.13g, 1.31mmol) to afford **RK_33** as off white solid (0.14g, 70.0 % yield). M.P: 204 – 206 °C. ^{1}H NMR (DMSO-d$_6$): δ 12.63 (br s, 1H), 8.99 (s, 1H), 8.90 (s, 1H), 8.05 (d, J = 8.2 Hz, 1H), 7.82 – 7.45 (m, 5H), 7.38 (d, J = 8.2 Hz, 1H), 5.01 (s, 1H). ^{13}C NMR (DMSO-d$_6$): δ 172.8, 162.4, 152.7, 140.8, 136.3, 132.1, 130.4, 127.5 (2C), 119.8 (2C), 116.7, 112.5, 104.1. ESI-MS m/z 305.02 (M-H)$^+$. Anal Calc'd for C$_{14}$H$_{11}$ClN$_2$O$_4$; C, 54.83; H, 3.62; N, 9.13; Found C, 54.68; H, 3.63; N, 9.11.

2-Hydroxy-4-(3-(4-nitrophenyl)ureido)benzoic acid (RK_34): The compound was synthesized according to the above general procedure using 4-amino salicylic acid (0.10g, 0.65mmol), 4-nitro phenyl isocyanate (0.11g, 0.65mmol) and triethylamine (0.13g, 1.31mmol) to afford **RK_34** as yellow solid (0.18g, 84.5 % yield). M.P: 181 – 183 °C. ^{1}H NMR (DMSO-d$_6$): δ 12.67 (br s, 1H), 9.03 (s, 1H), 8.93 (s, 1H), 8.18 (d, J = 8.2 Hz, 2H), 7.98 (d, J = 8.2 Hz, 1H), 7.93 (d, J = 8 Hz, 2H), 7.62 – 7.51 (m, 2H), 5.05 (s, 1H). ^{13}C NMR (DMSO-d$_6$): δ 172.2, 162.8, 152.7, 142.9, 140.6, 138.7, 129.5, 120.6 (2C), 116.4 (2C), 112.7, 110.5, 104.2. ESI-MS m/z 316.06 (M-H)$^+$. Anal Calc'd for C$_{14}$H$_{11}$N$_3$O$_6$; C, 53.00; H, 3.49; N, 13.24; Found C, 52.87; H, 3.48; N, 13.27.

2-Hydroxy-4-(3-(4-methoxyphenyl)ureido)benzoic acid (RK_35): The compound was synthesized according to the above general procedure using 4-amino salicylic acid (0.10g, 0.65mmol), 4-methoxy phenyl isocyanate (0.09g, 0.65mmol) and triethylamine (0.13g, 1.31mmol) to afford **RK_35** as pale brown solid (0.16g, 80.0 % yield). M.P: 247 – 249 °C. ^{1}H NMR (DMSO-d$_6$): δ 12.69 (br s, 1H), 9.04 (s, 1H), 8.96 (s, 1H), 8.05 (d, J = 8.4 Hz, 1H), 7.63 – 7.49 (m, 3H), 7.45 (d, J = 7.8 Hz, 1H), 7.05 (m, 2H), 5.03 (s, 1H), 3.88 (s, 3H). ^{13}C NMR (DMSO-d$_6$): δ 172.5, 162.3, 152.7, 153.6, 144.7, 135.8, 133.6, 121.1 (2C), 116.9 (2C), 115.8,

114.3, 104.3, 56.7. ESI-MS m/z 301.09 (M-H)$^+$. Anal Calc'd for $C_{15}H_{14}N_2O_5$; C, 59.60; H, 4.67; N, 9.27; Found C, 59.44; H, 4.66; N, 9.29.

2-Hydroxy-4-(3-(p-tolyl)ureido) benzoic acid (RK_36): The compound was synthesized according to the above general procedure using 4-amino salicylic acid (0.10g, 0.65mmol), p-tolyl isocyanate (0.09g, 0.65mmol) and triethylamine (0.13g, 1.31mmol) to afford **RK_36** as white solid (0.13g, 70.6 % yield). M.P: 221 – 223 °C. ^{1}H NMR (DMSO-d$_6$): δ 12.62 (br s, 1H), 9.01 (s, 1H), 8.98 (s, 1H), 8.01 (d, J = 8.2 Hz, 1H), 7.65 – 7.58 (m, 3H), 7.46 (d, J = 8 Hz, 1H), 7.33 (m, 2H), 5.01 (s, 1H), 2.38 (s, 3H). ^{13}C NMR (DMSO-d$_6$): δ 172.3, 162.9, 152.9, 145.2, 139.8, 138.8, 134.7, 132.7 (2C), 125.4 (2C), 116.8, 115.4, 104.4, 22.6. ESI-MS m/z 285.10 (M-H)$^+$. Anal Calc'd for $C_{15}H_{14}N_2O_4$; C, 62.93; H, 4.93; N, 9.79; Found C, 63.09; H, 4.94; N, 9.81.

4-(3-(4-Acetylphenyl)ureido)-2-hydroxybenzoic acid (RK_37): The compound was synthesized according to the above general procedure using 4-amino salicylic acid (0.10g, 0.65mmol), 4-acetyl phenyl isocyanate (0.11g, 0.65mmol) and triethylamine (0.13g, 1.31mmol) to afford **RK_37** as yellow solid (0.17g, 84.3 % yield). M.P: 195 – 197 °C. ^{1}H NMR (DMSO-d$_6$): δ 12.65 (br s, 1H), 9.03 (s, 1H), 8.95 (s, 1H), 8.05 (d, J = 8 Hz, 1H), 7.89 – 7.65 (m, 5H), 7.48 (d, J = 7.8 Hz, 1H), 5.02 (s, 1H), 2.53 (s, 3H). ^{13}C NMR (DMSO-d$_6$): δ 199.8, 172.8, 162.3, 152.5, 144.6, 142.1, 134.4, 129.7, 127.9 (2C), 118.4 (2C), 112.4, 111.5, 103.9, 25.7. ESI-MS m/z 313.10 (M-H)$^+$. Anal Calc'd for $C_{16}H_{14}N_2O_5$; C, 61.14; H, 4.49; N, 8.91; Found C,61.13; H, 4.48; N, 8.88.

3-(3-Benzylureido)benzoic acid (RK_38): The compound was synthesized according to the above general procedure using 3-amino benzoic acid (0.10g, 0.73mmol), benzyl isocyanate (0.09g, 0.73mmol) and triethylamine (0.15g, 1.46mmol) to afford **RK_38** as white solid (0.14g, 69.0 % yield). M.P: 253 – 255 °C. ^{1}H NMR (DMSO-d$_6$): δ 12.54 (br s, 1H), 9.17 (s, 1H), 8.96 (s, 1H), 8.14 (s, 1H), 7.71 (d, J = 8.2 Hz, 2H), 7.52 – 7.26 (m, 6H), 4.51 (s, 2H). ^{13}C NMR (DMSO-d$_6$): δ 167.6, 153.0, 145.3, 139.6, 129.2, 129.0, 128.7 (2C), 127.3 (2C), 126.6, 125.7, 124.3, 118.7, 43.2. ESI-MS m/z 269.11 (M-H)$^+$. Anal Calc'd for $C_{15}H_{14}N_2O_3$; C, 66.66; H, 5.22; N, 10.36; Found C, 66.84; H, 5.20; N, 10.34.

3-(3-Benzylthioureido)benzoic acid (RK_39): The compound was synthesized according to the above general procedure using 3-amino benzoic acid (0.10g, 0.73mmol), benzyl isothiocyanate

(0.11g,0.73mmol) and triethylamine (0.15g, 1.46mmol) to afford **RK_39** as white solid (0.16g, 75.2 % yield). M.P: 214 – 216 °C. ^{1}H NMR (DMSO-d$_6$): δ 12.58 (br s, 1H), 7.92 (s, 1H), 7.75 (s, 1H), 7.61 (d, J = 8 Hz, 1H), 7.55 – 7.41 (m, 2H), 7.39 – 7.27 (m, 6H), 4.55 (s, 2H). ^{13}C NMR (DMSO-d$_6$): δ 181.3, 167.8, 139.1, 138.8, 134.6, 131.0, 129.3 (2C), 128.7, 128.2, 124.8 (2C), 123.3, 123.9, 48.6. ESI-MS m/z 285.08 (M-H)$^{+}$. Anal Calc'd for C$_{15}$H$_{14}$N$_2$O$_2$S; C, 62.92; H, 4.93; N, 9.78; Found C, 62.75; H, 4.94; N, 9.80.

3-(3-(3-Bromophenyl)thioureido)benzoic acid (RK_40): The compound was synthesized according to the above general procedure using 3-amino benzoic acid (0.10g, 0.73mmol), 3-bromo phenyl isothiocyanate (0.16g, 0.73mmol) and triethylamine (0.15g, 1.46mmol) to afford **RK_40** as white solid (0.21g, 80.5 % yield). M.P: 163 – 165 °C. ^{1}H NMR (DMSO-d$_6$): δ 12.66 (br s, 1H), 7.91 (s, 1H), 7.79 (s, 1H), 7.65 (d, J = 8.2 Hz, 1H), 7.55 (m, 1H), 7.33 (s,1H) 7.01 – 6.81 (m, 2H), 6.79 (d, J = 8.0 Hz, 1H), 6.75 – 6.52 (m, 2H).^{13}C NMR (DMSO-d$_6$): δ 182.6, 167.5, 140.8, 138.8, 135.8, 132.7, 130.3, 130.0, 129.3, 128.3, 126.8, 125.6, 124.4, 120.6. ESI-MS m/z 349.97 (M-H)$^{+}$. Anal Calc'd for C$_{14}$H$_{11}$BrN$_2$O$_2$S; C, 47.88; H, 3.16; N, 7.98; Found C, 48.01; H, 3.15; N, 7.99.

3-(3-(4-Nitrophenyl)thioureido)benzoic acid (RK_41): The compound was synthesized according to the above general procedure using 3-amino benzoic acid (0.10g, 0.73mmol), 4-nitro phenyl isothiocyanate (0.13g, 0.73mmol) and triethylamine (0.15g, 1.46mmol) to afford **RK_41** as yellow solid (0.18g, 78.7 % yield). M.P: 161 – 163 °C. ^{1}H NMR (DMSO-d$_6$): δ 12.69 (br s, 1H), 8.08 (d, J = 8.2 Hz, 2H), 7.93 (s, 1H), 7.81 (s, 1H), 7.52 – 6.93 (m, 4H), 6.7 (d, J = 8 Hz, 2H). ^{13}C NMR (DMSO-d$_6$): δ 182.7, 167.2, 146.9, 145.8, 139.4, 132.6, 129.6, 128.8, 126.3, 124.8, 122.4 (2C), 122.3 (2C). ESI-MS m/z 316.05 (M-H)$^{+}$. Anal Calc'd for C$_{14}$H$_{11}$N$_3$O$_4$S; C, 52.99; H, 3.49; N, 13.24; Found C, 53.12; H, 3.48; N, 13.28.

3-(3-(4-Methoxyphenyl)thioureido) benzoic acid (RK_42): The compound was synthesized according to the above general procedure using 3-amino benzoic acid (0.10g, 0.73mmol), 4-methoxy phenyl isothiocyanate (0.12g, 0.73mmol) and triethylamine (0.15g, 1.46mmol) to afford **RK_42** as white solid (0.18g, 80.7 % yield). M.P: 199 – 201 °C. ^{1}H NMR (DMSO-d$_6$): δ 12.61 (br s, 1H), 7.95 (s, 1H), 7.81 (s, 1H), 7.67 (d, J = 8.4 Hz, 1H), 7.59 – 7.18 (m, 2H), 6.81 – 6.72 (m, 3H), 6.45 (d, J = 8 Hz, 2H), 3.89 (s, 3H). ^{13}C NMR (DMSO-d$_6$): δ 182.3, 167.7, 162.3,

139.4, 133.82, 132.0, 130.7, 129.9, 125.5 (2C), 123.2, 122.7 , 111.2 (2C), 56.2. ESI-MS *m/z* 301.07 (M-H)$^+$. Anal Calc'd for $C_{15}H_{14}N_2O_3S$; C, 59.59; H, 4.67; N, 9.27; Found C, 59.74; H, 4.66; N, 9.24.

3-(3-(4-Acetylphenyl)thioureido) benzoic acid (RK_43): The compound was synthesized according to the above general procedure using 3-amino benzoic acid (0.10g, 0.73mmol), 4-acetyl phenyl isothiocyanate (0.13g, 0.73mmol) and triethylamine (0.15g, 1.46mmol) to afford **RK_43** as white solid (0.14g, 62.4 % yield). M.P: 191 – 193 °C. ^{1}H NMR (DMSO-d$_6$): δ 12.51 (br s, 1H), 7.92 (s, 1H), 7.86 (s, 1H), 7.75 (d, *J* = 8 Hz, 2H), 7.66 (d, *J* = 8.2 Hz, 1H), 7.55 – 6.85 (m, 3H), 6.64 (d, *J* = 8 Hz, 2H), 2.53 (s, 3H).. ^{13}C NMR (DMSO-d$_6$): δ 199.4, 181.8, 167.4, 145.4, 136.4 (2C), 134.8, 130.2 (2C), 129.2, 128.5, 127.6 (2C), 127.2, 126.9, 25.7. ESI-MS *m/z* 313.07 (M-H)$^+$. Anal Calc'd for $C_{16}H_{14}N_2O_3S$; C, 61.13; H, 4.49; N, 8.91; Found C, 61.06; H, 4.50; N, 8.89.

4-(3-(4-Bromophenyl)thioureido)-2-hydroxybenzoic acid (RK_44): The compound was synthesized according to the above general procedure using 4-amino salicylic acid (0.10g, 0.65mmol), 4-bromo phenyl isothiocyanate (0.14g, 0.65mmol) and triethylamine (0.13g, 1.31mmol) to afford **RK_44** as pale red solid (0.12g, 51.3 % yield). M.P: 225 – 227 °C. ^{1}H NMR (DMSO-d$_6$): δ 12.55 (br s, 1H), 7.96 (s, 1H), 7.77 (s, 1H), 7.72 (d, *J* = 8.4 Hz, 1H), 7.43 (m, 2H), 6.82 – 6.63 (m, 3H), 6.33 (d, *J* = 8.2 Hz, 1H), 5.02 (s, 1H).^{13}C NMR (DMSO-d$_6$): δ 181.8, 172.5, 162.5, 140.3, 134.8, 128.6 (2C), 128.2 (2C), 128.3, 118.6, 115.4, 112.3, 108.3. ESI-MS *m/z* 366.22 (M-H)$^+$. Anal Calc'd for $C_{14}H_{11}BrN_2O_3S$; C, 45.79; H, 3.02; N, 7.63; Found C, 45.68; H, 3.03; N, 7.62.

4-(3-(3-Bromophenyl)thioureido)-2-hydroxybenzoic acid (RK_45): The compound was synthesized according to the above general procedure using 4-amino salicylic acid (0.10g, 0.65mmol), 3-bromo phenyl isothiocyanate (0.14g, 0.65mmol) and triethylamine (0.13g, 1.31mmol) to afford **RK_45** as pale yellow solid (0.17g, 69.6 % yield). M.P: 162 – 164 °C. ^{1}H NMR (DMSO-d$_6$): δ 12.59 (br s, 1H), 7.91 (s, 1H), 7.79 (s, 1H), 7.68 (d, *J* = 8 Hz, 1H), 7.21 – 6.52 (m, 5H), 6.38 (d, *J* = 8.2 Hz, 1H), 5.05 (s, 1H). ^{13}C NMR (DMSO-d$_6$): δ 182.2, 172.4, 162.8, 141.5, 136.9, 129.8, 126.2, 125.8, 124.5, 122.0, 119.4, 115.1, 112.4, 108.5. ESI-MS *m/z*

366.22 (M-H)$^+$. Anal Calc'd for $C_{14}H_{11}BrN_2O_3S$; C, 45.79; H, 3.02; N, 7.63; Found C, 45.91; H, 3.01; N, 7.61.

4-(3-(4-Chlorophenyl)thioureido)-2-hydroxybenzoic acid (RK_46): The compound was synthesized according to the above general procedure using 4-amino salicylic acid (0.10g, 0.65mmol), 4-chloro phenyl isothiocyanate (0.17g, 0.65mmol) and triethylamine (0.13g, 1.31mmol) to afford **RK_46** as Off white solid (0.12g, 58.8 % yield). M.P: 175 – 177 °C. ^{1}H NMR (DMSO-d$_6$): δ 12.63 (br s, 1H), 7.95 (s, 1H), 7.74 (s, 1H), 7.72 (d, J = 8.4 Hz, 1H), 7.36 (m, 2H), 6.73 – 6.37 (m, 3H), 6.29 (d, J = 8.2 Hz, 1H), 5.01 (s, 1H). ^{13}C NMR (DMSO-d$_6$): δ 182.9, 172.4, 162.4, 145.3, 139.1, 135.9, 129.4, 127.7 (2C), 125.3 (2C), 115.8, 112.5, 108.3. ESI-MS m/z 321.02 (M-H)$^+$. Anal Calc'd for $C_{14}H_{11}ClN_2O_3S$; C, 52.10; H, 3.44; N, 8.68; Found C, 52.23; H, 3.45; N, 8.66.

2-Hydroxy-4-(3-(4-nitrophenyl)thioureido)benzoic acid (RK_47): The compound was synthesized according to the above general procedure using 4-amino salicylic acid (0.10g, 0.65mmol), 4-nitro phenyl isothiocyanate (0.12g, 0.65mmol) and triethylamine (0.13g, 1.31mmol) to afford **RK_47** as yellow solid (0.16g, 72.1 % yield). M.P: 173 – 175 °C. ^{1}H NMR (DMSO-d$_6$): δ 12.65 (br s, 1H), 8.01 (s, 1H), 7.98 (s, 1H), 7.85 (d, J = 8 Hz, 2H), 7.75 (d, J = 8.2 Hz, 1H), 6.95 – 6.72 (m, 3H), 6.43 (d, J = 8.2 Hz, 1H), 5.03 (s, 1H). ^{13}C NMR (DMSO-d$_6$): δ 181.2, 172.3, 162.8, 148.7, 145.9, 145.3, 129.6, 122.4 (2C), 121.8 (2C), 120.6, 116.3, 108.8. ESI-MS m/z 332.04 (M-H)$^+$. Anal Calc'd for $C_{14}H_{11}N_3O_5S$; C, 50.45; H, 3.33; N, 12.61; Found C, 50.58; H, 3.34; N, 12.57.

2-Hydroxy-4-(3-(4-methoxyphenyl)thioureido)benzoic acid (RK_48): The compound was synthesized according to the above general procedure using 4-amino salicylic acid (0.10g, 0.65mmol), 4-methoxy phenyl isothiocyanate (0.11g, 0.65mmol) and triethylamine (0.13g, 1.31mmol) to afford **RK_48** as white solid (0.18g, 85.1 % yield). M.P: 185 – 187 °C. ^{1}H NMR (DMSO-d$_6$): δ 12.61 (br s, 1H), 7.92 (s, 1H), 7.88 (s, 1H), 7.82 (d, J = 8 Hz, 1H), 6.85 (d, J = 8.2 Hz, 2H), 6.65 – 6.43 (m, 3H), 6.39 (d, J = 8.2 Hz, 1H), 5.04 (s, 1H), 3.85 (s, 3H).^{13}C NMR (DMSO-d$_6$): δ 181.4, 172.3, 162.7, 158.7, 140.5, 136.8, 134.9, 130.5 (2C), 121.4, 116.3 (2C), 112.4, 108.4, 56.3. ESI-MS m/z 317.07 (M-H)$^+$. Anal Calc'd for $C_{15}H_{14}N_2O_4S$; C, 56.59; H, 4.43; N, 8.80; Found C, 56.73; H, 4.42; N, 8.78.

2-Hydroxy-4-(3-(p-tolyl)thioureido) benzoic acid (RK_49): The compound was synthesized according to the above general procedure using 4-amino salicylic acid (0.10g, 0.65mmol), p-tolyl isocyanate (0.09g, 0.65mmol) and triethylamine (0.13g, 1.31mmol) to afford **RK_49** as white solid (0.16g, 82.0 % yield). M.P: 163 – 165 °C. ^{1}H NMR (DMSO-d$_6$): δ 12.63 (br s, 1H), 7.95 (s, 1H), 7.85 (s, 1H), 7.75 (d, J = 8.2 Hz, 1H), 7.08 (d, J = 8.2 Hz, 2H), 6.63 – 6.49 (m, 3H), 6.32 (d, J = 8 Hz, 1H), 5.03 (s, 1H), 2.39 (s, 3H). ^{13}C NMR (DMSO-d$_6$): δ 181.4, 172.5, 162.3, 148.3, 139.6, 136.9, 134.3, 130.9 (2C), 128.4 (2C), 120.5, 116.4, 109.7, 22.5. ESI-MS m/z 301.08 (M-H)$^+$. Anal Calc'd for C$_{15}$H$_{14}$N$_2$O$_3$S; C, 59.59; H, 4.67; N, 9.27; Found C, 59.43; H, 4.68; N, 9.25.

4-(3-(4-Acetylphenyl)thioureido)-2-hydroxybenzoic acid (RK_50): The compound was synthesized according to the above general procedure using 4-amino salicylic acid (0.10g, 0.65mmol), 4-acetyl phenyl isothiocyanate (0.12g, 0.65mmol) and triethylamine (0.13g, 1.31mmol) to afford **RK_50** as pale yellow solid (0.14g, 63.0 % yield). M.P: 231 – 233 °C. ^{1}H NMR (DMSO-d$_6$): δ 12.66 (br s, 1H), 7.93 (s, 1H), 7.88 (s, 1H), 7.83 (d, J = 8.4 Hz, 1H), 7.75 (d, J = 8 Hz, 2H), 6.81 – 6.43 (m, 3H), 6.38 (d, J = 8.2 Hz, 1H), 5.05 (s, 1H), 2.52 (s, 3H). ^{13}C NMR (DMSO-d$_6$): δ 199.8, 182.6, 172.1, 162.2, 145.7, 143.2, 139.6, 129.9, 127.6 (2C), 124.7 (2C), 118.6, 112.3, 106.8, 25.7. ESI-MS m/z 329.06 (M-H)$^+$. Anal Calc'd for C$_{16}$H$_{14}$N$_2$O$_4$S; C, 58.17; H, 4.27; N, 8.48; Found C, 58.32; H, 4.26; N, 8.50.

4-(3-Benzylureido)-2-hydroxybenzoic acid (RK_51): The compound was synthesized according to the above general procedure using 4-amino salicylic acid (0.10g, 0.65mmol), benzyl isocyanate (0.09g, 0.65mmol) and triethylamine (0.13g, 1.31mmol) to afford **RK_51** as pale yellow solid (0.15g, 79.2 % yield). M.P: 180 – 182 °C. ^{1}H NMR (DMSO-d$_6$): δ 12.61 (br s, 1H), 8.08 (d, J = 8.6 Hz, 1H), 7.91 (s, 1H), 7.85 (s, 1H), 7.65 (s,1H), 7.52 (d, J = 8 Hz, 1H), 7.48 – 7.27 (m,5H), 5.05 (s, 1H), 4.56 (s, 2H). ^{13}C NMR (DMSO-d$_6$): δ 172.4, 162.7, 152.9, 144.4, 139.3, 134.8, 130.5 (2C), 128.4 (2C), 127.7, 115.7, 113.7, 104.3, 43.7. ESI-MS m/z 285.10 (M-H)$^+$. Anal Calc'd for C$_{15}$H$_{14}$N$_2$O$_4$; C, 62.93; H, 4.93; N, 9.79; Found C, 63.09; H, 4.94; N, 9.81.

4-(3-Benzylthioureido)-2-hydroxybenzoic acid (RK_52): The compound was synthesized according to the above general procedure using 4-amino salicylic acid (0.10g, 0.65mmol), benzyl isothiocyanate (0.09g, 0.65mmol) and triethylamine (0.13g, 1.31mmol) to afford **RK_52** as white solid (0.15g, 73.4 % yield). M.P: 192 – 194 °C. ^{1}H NMR (DMSO-d$_6$): δ 12.64 (br s, 1H),

7.92 (s, 1H), 7.88 (s, 1H), 7.76 (d, J = 8.2 Hz, 1H), 7.45 – 6.42 (m, 6H), 6.32 (d, J = 8.4 Hz, 1H), 5.02 (s, 1H), 4.52 (s, 2H). ^{13}C NMR (DMSO-d$_6$): δ 180.5, 172.3, 162.4, 146.7, 139.6, 129.6, 125.7 (2C), 123.4 (2C), 122.8, 114.4, 112.8, 108.2, 48.4. ESI-MS m/z 301.07 (M-H)$^+$. Anal Calc'd for C$_{15}$H$_{14}$N$_2$O$_3$S; C, 59.59; H, 4.67; N, 9.27; Found C, 59.43; H, 4.66; N, 9.30.

3-(3-([1,1'-Biphenyl]-3-yl)ureido) benzoic acid (RK_02): The compound was prepared according to the general procedure using 3-(3-(3-bromophenyl)ureido)benzoic acid **(RK_22)** (0.1 g, 0.24 mmol), phenyl boronic acid (0.057 g, 0.47 mmol), Na$_2$CO$_3$ (0.1g, 0.96mmol) and Tetrakis (0.019, 0.016mmol) to afford **RK_02** as a white solid (0.025 g, 31.0 % yield) M.P. 229–231 °C. ^{1}H NMR (DMSO-d$_6$): δ 12.8 (br s, 1H), 9.54 (s, 1H), 9.48 (s, 1H), 8.13 (s, 1H), 8.03 (s, 1H), 7.99 – 7.79 (m, 2H), 7.64 – 7.32 (m, 9H). ^{13}C NMR (DMSO-d$_6$): δ 167.2, 152.6, 144.6, 141.2, 140.6, 135.8, 130.2 (2C), 129.8, 129.0, 128.5, 127.9, 127.6 (2C), 126.4, 126.3, 124.5, 122.2, 121.8, 120.6. EI-MS m/z: 331.01 (M-H)$^+$. Anal Calc'd for C$_{20}$H$_{16}$N$_2$O$_3$: C, 72.28; H, 4.85; N, 8.43. Found: C, 72.46; H, 4.86; N, 8.41.

4-(3-([1,1'-Biphenyl]-3-yl)ureido)-2-hydroxybenzoic acid (RK_03): The compound was prepared according to the general procedure using 4-(3-(3-bromophenyl)ureido)-2-hydroxybenzoic acid **(RK_32)** (0.1 g, 0.28 mmol), phenyl boronic acid (0.069 g, 0.56 mmol), Na$_2$CO$_3$ (0.12g, 1.12 mmol) and Tetrakis (0.021 g, 0.019 mmol)to afford **RK_03** as a white solid (0.042 g, 43 % yield). MP: 210 – 212 °C. ^{1}H NMR (DMSO-d$_6$): δ 12.86 (br s, 1H), 9.68 (s, 1H), 9.57 (s, 1H), 7.87 (s, 1H), 7.66 (t, J = 8 Hz, 3H), 7.50 – 7.35 (m, 5H), 7.26 (d, J = 7.6 Hz, 1H), 7.03 (s, 1H), 6.84 (d, J = 7.2, 1H), 4.63 (s, 1H). ^{13}C NMR (DMSO-d$_6$): δ 172.6, 162.9, 152.6, 143.6, 140.7, 140.6, 140.4, 130.6, 129.3, 128.9 (2C), 127.4, 126.6 (2C), 120.0, 117.2, 116.4, 113.2, 107.1, 104.5. EI-MS m/z: 347.01 (M-H)$^+$. Anal Calc'd for C$_{20}$H$_{16}$N$_2$O$_4$: C, 68.96; H, 4.63; N, 8.04; Found C, 69.13; H, 4.62; N, 8.03.

5-(3-([1,1'-Biphenyl]-3-yl)ureido)-2-hydroxybenzoic acid (RK_04): The compound was prepared according to the general procedure using 5-(3-(3-bromophenyl)ureido)-2-hydroxybenzoic acid (0.1 g, 0.28 mmol), phenyl boronic acid (0.069 g, 0.56 mmol), Na$_2$CO$_3$ (0.12g, 1.12 mmol) and Tetrakis (0.021 g, 0.019 mmol) to afford **RK_04** as brown solid (0.048 g, 48 % yield). MP: 208 – 210 °C. ^{1}H NMR (DMSO-d$_6$): δ 12.79 (br s, 1H), 9.55 (s, 1H), 9.49 (s, 1H), 8.12 (s, 1H), 8.05 (s, 1H), 7.93 (d, J = 8.2 Hz, 1H), 7.65 – 7.01 (m, 9H), 5.03 (s, 1H). ^{13}C NMR (DMSO-d$_6$): δ 172.3, 162.2, 152.5, 139.6, 139.0, 137.8, 137.5, 130.6, 130.2 (2C), 129.5,

128.3 (2C), 128.2, 124.6, 122.8, 121.6, 120.5, 118.7, 117.7. EI-MS m/z: 347.01 (M-H)$^{+}$. Anal Calc'd for $C_{20}H_{16}N_2O_4$: C, 68.96; H, 4.63; N, 8.04; Found C, 69.10; H, 4.64; N, 8.02.

3-(3-(2',3'-Dichloro-[1,1'-biphenyl]-4-yl)ureido)benzoic acid (RK_54): The compound was prepared according to the general procedure using 3-(3-(4-bromophenyl)ureido)benzoic acid **(RK_06)** (0.1 g, 0.24 mmol), 2,3 dichloro phenyl boronic acid (0.089 g, 0.47 mmol), Na_2CO_3 (0.1g, 0.96mmol) and Tetrakis (0.019, 0.016mmol) to afford **RK_54** as brown solid (0.068 g, 96% yield). M.P: 215 - 217 °C. ^{1}H NMR (DMSO-d$_6$): δ 12.85 (br s, 1H), 9.58 (s, 1H), 9.51 (s, 1H), 8.14 (s, 1H), 8.01 − 7.98 (m, 2H), 7.82 (d, J = 8.2 Hz, 2H), 7.75 (d, J = 8 Hz, 2H), 7.64 − 7.39 (m, 4H). ^{13}C NMR (DMSO-d$_6$): δ 167.6, 152.4, 144.3, 143.7, 139.6, 135.6, 134.6, 132.2, 130.2, 129.6, 129.2, 129.0 (2C), 128.2, 127.5, 126.8, 125.4, 122.3, 120.6 (2C). EI-MS m/z: 400.01 (M-H)$^{+}$. Anal Calc'd for $C_{20}H_{14}Cl_2N_2O_3$: C, 59.87; H, 3.52; N, 6.98; Found C, 60.02; H, 3.53; N, 6.99.

3-(3-(2',5'-Dimethyl-[1,1'-biphenyl]-4-yl)ureido)benzoic acid (RK_55): The compound was prepared according to the general procedure using 3-(3-(4-bromophenyl)ureido)benzoic acid **(RK_06)** (0.1 g, 0.24 mmol), 2,5 dimethyl phenyl boronic acid (0.07 g, 0.47 mmol), Na_2CO_3 (0.1g, 0.96mmol) and Tetrakis (0.019, 0.016mmol) to afford **RK_55** as dark brown liquid (0.04 g, 46% yield). ^{1}H NMR (DMSO-d$_6$): δ 12.87 (br s, 1H), 9.60 (s, 1H), 9.54 (s, 1H), 8.11 (s, 1H), 8.00 − 7.95 (m, 2H), 7.85 (d, J = 8.4 Hz, 2H), 7.72 (d, J = 8.2 Hz, 2H), 7.61 − 7.23 (m, 4H) 2.34 (s, 3H), 2.36 (s, 3H). ^{13}C NMR (DMSO-d$_6$): δ 167.6, 152.57, 144.6, 139.5, 136.5, 134.3 (2C), 133.6, 133.2, 130.2, 129.6, 128.9 (2C), 128.1, 126.9, 126.2, 124.1, 122.6, 120.6 (2C), 22.1, 20.1. EI-MS m/z: 359.03 (M-H)$^{+}$. Anal Calc'd for $C_{22}H_{20}N_2O_3$: C, 73.32; H, 5.59; N, 7.77; Found C, 73.54; H, 5.58; N, 7.79.

3-(3-([1,1'-Biphenyl]-4-yl)ureido)benzoic acid (RK_56): The compound was prepared according to the general procedure using 3-(3-(4-bromophenyl)ureido)benzoic acid **(RK_06)** (0.1 g, 0.24 mmol), phenyl boronic acid (0.057 g, 0.47 mmol), Na_2CO_3 (0.1g, 0.96mmol) and Tetrakis (0.019, 0.016mmol) to afford **RK_56** as pale brown solid (0.031 g, 39% yield). M.P 193 − 195°C. ^{1}H NMR (DMSO-d$_6$): δ 12.88 (br s, 1H), 9.55 (s, 1H), 9.49 (s, 1H), 8.15 (s, 1H), 7.98 − 7.88 (m, 2H), 7.76 (d, J = 8 Hz, 2H), 7.68 (d, J = 8.2 Hz, 2H), 7.59 − 7.35 (m, 6H). ^{13}C NMR (DMSO-d$_6$): δ 167.9, 152.6, 144.6, 141.7, 140.9, 139.5, 130.2 (2C), 129.6, 129.2, 128.9 (2C),

127.9 (2C), 127.3, 126.9, 126.2, 122.1, 120.5 (2C). EI-MS m/z: 331.00 (M-H)$^+$. Anal Calc'd for C$_{20}$H$_{16}$N$_2$O$_3$: C, 72.28; H, 4.85; N, 8.43. Found: C, 72.46; H, 4.84; N, 8.42.

3-(3-(3-(6-Fluoropyridin-3-yl)phenyl)ureido)benzoic acid (RK_57): The compound was prepared according to the general procedure using 3-(3-(3-bromophenyl)ureido)benzoic acid **(RK_22)** (0.1 g, 0.24 mmol), 2-Fluoropyridine-5-boronic acid (0.066 g, 0.47 mmol), Na$_2$CO$_3$ (0.1g, 0.96mmol) and Tetrakis (0.019, 0.016mmol) to afford **RK_57** as brown oil (0.053 g, 63% yield). ^{1}H NMR (DMSO-d$_6$): δ 12.84 (br s, 1H), 9.54 (s, 1H), 9.50 (s, 1H), 8.31 (s, 1H), 8.19 (m, 1H), 8.13 (s, 1H), 8.65 (s, 1H), 8.02 – 7.95 (m, 2H), 7.71 – 7.31 (m, 5H). ^{13}C NMR (DMSO-d$_6$): δ 167.7, 161.6, 152.6, 142.2, 140.9, 139.6, 137.8, 137.2, 136.6, 130.3, 129.6, 129.2, 127.5, 126.2, 122.7, 121.9, 121.6, 120.5, 110.6. EI-MS m/z: 350.05 (M-H)$^+$. Anal Calc'd for C$_{19}$H$_{14}$FN$_3$O$_3$: C, 64.95; H, 4.02; N, 11.96; Found C, 65.12; H, 4.06; N, 11.99.

3-(3-(4'-Fluoro-[1,1'-biphenyl]-3-yl)ureido)benzoic acid (RK_58): The compound was prepared according to the general procedure using 3-(3-(3-bromophenyl)ureido)benzoic acid **(RK_22)** (0.1 g, 0.24 mmol), 4-fluoro-phenyl boronic acid (0.065 g, 0.47 mmol), Na$_2$CO$_3$ (0.1g, 0.96mmol) and Tetrakis (0.019, 0.016mmol) to afford **RK_58** as brown gummy liquid (0.055g, 65% yield). ^{1}H NMR (DMSO-d$_6$): δ 12.85 (br s, 1H), 9.55 (s, 1H), 9.48 (s, 1H), 8.15 (s, 1H), 8.05 (s, 1H), 7.98 – 7.43 (m, 5H), 7.35 (d, J = 8.2 Hz, 2H), 7.28 (d, J = 8.4 Hz, 2H), 7.18 (d, J = 8 Hz, 1H). ^{13}C NMR (DMSO-d$_6$): δ 167.7, 162.8, 152.6, 144.6, 140.2, 137.7, 137.7, 130.4 (2C), 129.5, 128.8, 127.9, 125.9, 125.7, 124.9, 122.3, 121.6, 120.4, 115.6 (2C). EI-MS m/z: 349.03 (M-H)$^+$. Anal Calc'd for C$_{20}$H$_{15}$FN$_2$O$_3$: C, 68.57; H, 4.32; N, 8.00; Found: C, 68.38; H, 4.33; N, 8.02.

3-(3-(4'-Fluoro-[1,1'-biphenyl]-4-yl)ureido)benzoic acid (RK_59): The compound was prepared according to the general procedure using 3-(3-(4-bromophenyl)ureido)benzoic acid **(RK_06)** (0.1 g, 0.24 mmol), 4-fluoro-phenyl boronic acid (0.065 g, 0.47 mmol), Na$_2$CO$_3$ (0.1g, 0.96mmol) and Tetrakis (0.019, 0.016mmol) to afford **RK_59** as dark brown oil (0.060g, 71% yield). ^{1}H NMR (DMSO-d$_6$): δ 12.86 (br s, 1H), 9.56 (s, 1H), 9.51 (s, 1H), 8.18 (s, 1H), 7.95 (m, 2H), 7.85 (d, J = 8.6 Hz, 2H), 7.73 (d, J = 8.4 Hz, 2H), 7.59 (m, 1H), 7.48 (d, J = 8 Hz, 2H), 7.25 (d, J = 8 Hz, 2H). ^{13}C NMR (DMSO-d$_6$): δ 167.6, 162.1, 152.6, 144.5, 140.3, 139.5, 137.3, 132.6 (2C), 129.5, 129.1, 128.7 (2C), 126.5, 126.2, 122.5, 120.5 (2C), 117.3 (2C). EI-MS m/z: 349.02

(M-H)$^+$. Anal Calc'd for $C_{20}H_{15}FN_2O_3$: C, 68.57; H, 4.32; N, 8.00; Found: C, 68.39; H, 4.33; N, 7.98.

3-(3-(2',3'-Dichloro-[1,1'-biphenyl]-3-yl)ureido)benzoic acid (RK_60): The compound was prepared according to the general procedure using 3-(3-(3-bromophenyl)ureido)benzoic acid **(RK_22)** (0.1 g, 0.24 mmol), 2,3 dichloro phenyl boronic acid (0.089 g, 0.47 mmol), Na_2CO_3 (0.1g, 0.96mmol) and Tetrakis (0.019, 0.016mmol) to afford **RK_60** as brown solid (0.061 g, 63% yield). M.P: 189 - 191 °C. ^{1}H NMR (DMSO-d$_6$): δ 12.84 (br s, 1H), 9.55 (s, 1H), 9.50 (s, 1H), 8.13 (s, 1H), 8.09 (s, 1H), 8.02 - 7.96 (m, 2H), 7.82 – 7.31 (m, 7H). ^{13}C NMR (DMSO-d$_6$): δ 167.8, 152.3, 144.5, 143.9, 137.9, 136.9, 132.6, 130.3, 129.7, 129.2, 128.3, 128.6, 127.6, 127.2, 126.6, 125.2, 124.3, 122.1, 121.6, 120.5. EI-MS m/z: 400.01 (M-H)$^+$. Anal Calc'd for $C_{20}H_{14}Cl_2N_2O_3$: C, 59.87; H, 3.52; N, 6.98; Found C, 60.01; H, 3.51; N, 6.99.

4-(3-([1,1'-Biphenyl]-3-yl)ureido)-3-hydroxybenzoic acid (RK_62): The compound was prepared according to the general procedure using 4-(3-(3-bromophenyl)ureido)-3-hydroxybenzoic acid (0.1 g, 0.28 mmol), phenyl boronic acid (0.069 g, 0.56 mmol), Na_2CO_3 (0.12g, 1.12 mmol) and Tetrakis (0.021 g, 0.019 mmol) to afford **RK_62** as brown solid (0.037 g, 38 % yield). MP: 198 – 200 °C. ^{1}H NMR (DMSO-d$_6$): δ 12.81 (br s, 1H), 9.57 (s, 1H), 9.49 (s, 1H), 8.11 (s, 1H), 7.88 (d, J = 8 Hz, 1H), 7.75 (s, 1H), 7.63 (d, J = 8 Hz, 1H), 7.59 – 7.51 (m, 2H), 7.49 (d, J = 8 Hz, 2H), 7.46 (d, J = 8.2 Hz, 2H), 7.39 – 7.25 (m, 2H), 5.04 (s, 1H). ^{13}C NMR (DMSO-d$_6$): δ 170.3, 152.5, 150.2, 139.9, 138.9, 136.6, 132.73, 130.5, 130.2 (2C), 128.6 (2C), 128.4, 127.8, 124.7, 124.2, 123.6, 121.2, 120.6, 117.2. EI-MS m/z: 347.06 (M-H)$^+$. Anal Calc'd for $C_{20}H_{16}N_2O_4$: C, 68.96; H, 4.63; N, 8.04; Found C, 68.77; H, 4.64; N, 8.06.

3-(3-(3-(Pyridin-2-yl)phenyl)ureido)benzoic acid (RK_63): The compound was prepared according to the general procedure using 3-(3-(3-bromophenyl)ureido)benzoic acid **(RK_22)** (0.1 g, 0.24 mmol), pyridine-2-boronic acid (0.057 g, 0.47 mmol), Na_2CO_3 (0.1g, 0.96mmol) and Tetrakis (0.019, 0.016mmol) to afford **RK_63** as Pale yellow solid (0.038 g, 48% yield). MP: 139 – 141 °C. ^{1}H NMR (DMSO-d$_6$): δ 12.81 (br s, 1H), 9.57 (s, 1H), 9.51 (s, 1H), 8.21 (s, 1H), 8.16 (m, 1H), 8.11 (s, 1H), 8.05 (m, 1H), 8.03 - 7.95 (m, 2H), 7.82 – 7.14 (m, 6H). ^{13}C NMR (DMSO-d$_6$): δ 167.3, 153.5, 152.9, 150.2, 144.9, 138.2, 135.7 (2C), 130.3, 129.5, 129.4, 127.3, 126.8, 124.6, 124.2, 123.6, 121.9, 121.5, 120.6. EI-MS m/z: 332.01 (M-H)$^+$. Anal Calc'd for $C_{19}H_{15}N_3O_3$: C, 68.46; H, 4.54; N, 12.61; Found C, 68.64; H, 4.55; N, 12.59.

3-(3-(4-(6-Fluoropyridin-3-yl)phenyl)ureido)benzoic acid (RK_64): The compound was prepared according to the general procedure using 3-(3-(4-bromophenyl)ureido)benzoic acid **(RK_06)** (0.1 g, 0.24 mmol), 2-Fluoropyridine-5-boronic acid (0.066 g, 0.47 mmol), Na_2CO_3 (0.1g, 0.96mmol) and Tetrakis (0.019, 0.016mmol) to afford **RK_64** as Brown oil (0.048 g, 57 % yield). ^{1}H NMR (DMSO-d_6): δ 12.81 (br s, 1H), 9.61 (s, 1H), 9.57 (s, 1H), 8.25 (s, 1H), 8.19 (m, 1H), 8.16 (s, 1H), 8.02 – 7.95 (m, 2H), 7.84 (d, J = 8.2 Hz, 2H), 7.76 (d, J = 8 Hz, 2H), 7.62 – 7.41 (m, 2H). ^{13}C NMR (DMSO-d_6): δ 167.3, 163.5, 152.1, 143.0, 141.8, 140.3, 139.6, 136.2, 133.4, 129.6, 129.2, 128.5 (2C), 126.5, 126.2, 122.3, 120.5 (2C), 110.6. EI-MS m/z: 350.02 (M-H)$^+$. Anal Calc'd for $C_{19}H_{14}FN_3O_3$: C, 64.95; H, 4.02; N, 11.96; Found C, 65.11; H, 4.03; N, 11.94.

4'-(3-(3-Carboxyphenyl)ureido)-[1,1'-biphenyl]-3-carboxylic acid (RK_65): The compound was prepared according to the general procedure using 3-(3-(4-bromophenyl)ureido)benzoic acid **(RK_06)** (0.1 g, 0.24 mmol), 3 carboxy phenyl boronic acid (0.077 g, 0.47 mmol), Na_2CO_3 (0.1g, 0.96mmol) and Tetrakis (0.019, 0.016mmol) to afford **RK_65** as Brown liquid (0.046 g, 51% yield). ^{1}H NMR (DMSO-d_6): δ 12.88 (br s, 1H), 12.85 (b, 1H), 9.63 (s, 1H), 9.59 (s, 1H), 8.33 (s, 1H), 8.28 (s, 1H), 8.20 (m, 1H), 8.05 - 7.99 (m, 2H), 7.91 (d, J = 8.6 Hz, 2H), 7.88 (m, 1H), 7.81 (d, J = 8 Hz, 2H), 7.75 – 7.61 (m, 2H). ^{13}C NMR (DMSO-d_6): δ 170.3, 167.9, 152.5, 144.6, 142.2, 139.5, 137.9, 133.9, 131.6, 130.2, 130.2, 129.5, 129.4, 128.6 (2C), 127.6, 126.9, 126.2, 122.4, 120.5 (2C). EI-MS m/z: 375.04 (M-H)$^+$. Anal Calc'd for $C_{21}H_{16}N_2O_5$: C, 67.02; H, 4.28; N, 7.44; Found C, 67.20; H, 4.29; N, 7.46.

3'-(3-(3-Carboxyphenyl)ureido)-[1,1'-biphenyl]-3-carboxylic acid (RK_66): The compound was prepared according to the general procedure using 3-(3-(3-bromophenyl)ureido)benzoic acid **(RK_22)** (0.1 g, 0.24 mmol), 3 carboxy phenyl boronic acid (0.077 g, 0.47 mmol), Na_2CO_3 (0.1g, 0.96mmol) and Tetrakis (0.019, 0.016mmol) to afford **RK_66** as Brown solid (0.041 g, 45% yield). MP: 182 – 184 °C. ^{1}H NMR (DMSO-d_6): δ 12.91 (br s, 1H), 12.85 (s, 1H), 9.16 (s, 1H), 9.52 (s, 1H), 8.39 (s, 1H), 8.13 (s, 1H), 8.08 (m, 1H), 8.04 (s, 1H), 7.96 – 7.88 (m, 2H), 7.71 – 7.31 (m, 6H). ^{13}C NMR (DMSO-d_6): δ 170.2, 167.8, 152.9, 142.8, 140.9, 140.2, 138.2, 135.8, 132.2, 131.6, 129.5, 129.2, 128.8, 128.7, 125.5, 125.2, 124.7, 123.9, 122.6, 121.6, 120.6. EI-MS m/z: 375.05 (M-H)$^+$. Anal Calc'd for $C_{21}H_{16}N_2O_5$: C, 67.02; H, 4.28; N, 7.44; Found C, 67.21; H, 4.29; N, 7.46.

3-(3-(4-(Pyrimidin-5-yl)phenyl)ureido)benzoic acid (RK_67): The compound was prepared according to the general procedure using 3-(3-(4-bromophenyl)ureido)benzoic acid 10 **(RK_06)** (0.1 g, 0.24 mmol), pyrimidine 5 boronic acid (0.058 g, 0.47 mmol), Na_2CO_3 (0.1g, 0.96mmol) and Tetrakis (0.019, 0.016mmol) to afford **RK_67** as Brown oil (0.031 g, 38 % yield). ^{1}H NMR (DMSO-d$_6$): δ 12.86 (br s, 1H), 9.65 (s, 1H), 9.60 (s, 1H), 9.34 (s, 1H), 9.06 (s, 2H), 8.13 (s, 1H), 8.01 - 7.94 (m, 2H), 7.86 (d, J = 8.2 Hz, 2H), 7.74 (d, J = 8 Hz, 2H), 7.61 (m, 1H). ^{13}C NMR (DMSO-d$_6$): δ 167.2, 152.7, 149.8, 149.5 (2C), 144.3, 140.2, 132.3, 129.9, 129.4, 129.4, 127.3 (2C), 125.8, 124.9, 122.3, 120.5 (2C). EI-MS m/z: 333.02 (M-H)$^+$. Anal Calc'd for $C_{18}H_{14}N_4O_3$: C, 64.66; H, 4.22; N, 16.76; Found C, 64.49; H, 4.23; N, 16.72.

3-(3-(3-(Pyrimidin-5-yl)phenyl)ureido)benzoic acid (RK_68): The compound was prepared according to the general procedure using 3-(3-(3-bromophenyl)ureido)benzoic acid **(RK_22)** (0.1 g, 0.24 mmol), pyrimidine 5 boronic acid (0.058 g, 0.47 mmol), Na_2CO_3 (0.1g, 0.96mmol) and Tetrakis (0.019, 0.016mmol)to afford **RK_68** as Dark brown liquid (0.035 g, 44% yield). ^{1}H NMR (DMSO-d$_6$): δ 12.85 (br s,1H), 9.68 (s,1H), 9.61 (s,1H), 9.15 (s,1H), 8.51(d, J = 8.2 Hz, 1H), 8.16 (s,1H), 8.11 (d, J = 8 Hz, 1H), 8.03 (s,1H), 7.98–7.89 (m, 2H), 7.71–7.49 (m, 4H). ^{13}C NMR (DMSO-d$_6$): δ 167.4, 152.6, 149.8, 149.5 (2C), 144.5, 136.3, 135.2, 131.3, 129.9, 129.4, 129.4, 127.3 , 125.9, 124.9, 122.3, 120.6, 118.4. EI-MS m/z: 333.02 (M-H)$^+$. Anal Calc'd for $C_{18}H_{14}N_4O_3$: C, 64.66; H, 4.22; N, 16.76; Found C, 64.49; H, 4.23; N, 16.72.

3-(3-(2',5'-Dimethyl-[1,1'-biphenyl]-3-yl)ureido)benzoic acid (RK_69): The compound was prepared according to the general procedure using 3-(3-(3-bromophenyl)ureido)benzoic acid **(RK_22)** (0.1 g, 0.24 mmol), 2,5 dimethyl phenyl boronic acid (0.07 g, 0.47 mmol), Na_2CO_3 (0.1g, 0.96mmol) and Tetrakis (0.019, 0.016mmol) to afford **RK_69** as Brown liquid (0.046 g, 53% yield). ^{1}H NMR (DMSO-d$_6$): δ 12.81 (br s, 1H), 9.66 (s, 1H), 9.58 (s, 1H), 8.15 (s, 1H), 8.04 (s, 1H), 7.98 - 7.89 (m, 2H), 7.69 – 7.01 (m, 7H), 2.35 (s, 6H). ^{13}C NMR (DMSO-d$_6$): δc 167.2, 152.6, 144.2, 136.9, 136.5, 135.7, 134.3, 133.2, 130.3 (2C), 129.6, 128.9, 128.2, 127.2, 126.2, 123.9, 123.7, 122.1, 121.9, 120.5, 22.6, 20.1. EI-MS m/z: 359.00 (M-H)$^+$. Anal Calc'd for $C_{22}H_{20}N_2O_3$: C, 73.32; H, 5.59; N, 7.77; Found C, 73.53; H, 5.58; N, 7.79.
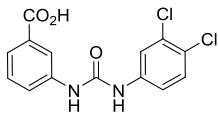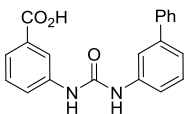
3-(3-(4-(Pyridin-2-yl)phenyl)ureido)benzoic acid (RK_70): The compound was prepared according to the general procedure using 3-(3-(4-bromophenyl)ureido)benzoic acid **(RK_06)** (0.1 g, 0.24 mmol), pyridine-2-boronic acid (0.057 g, 0.47 mmol), Na_2CO_3 (0.1g, 0.96mmol) and
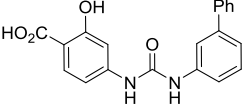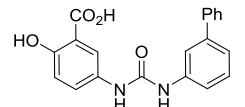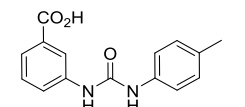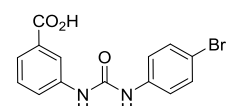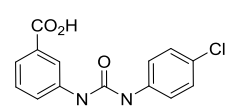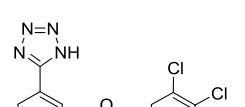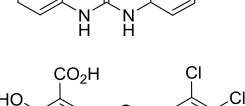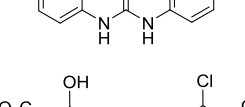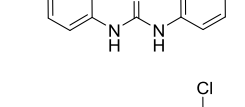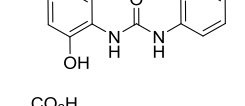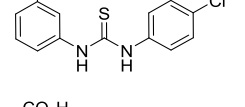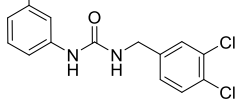
Tetrakis (0.019, 0.016mmol) to afford **RK_70** as brown solid (0.042 g, 53% yield) MP: 171 – 173 °C. ^{1}H NMR (DMSO-d$_6$): δ 12.88 (br s, 1H), 9.59 (s, 1H), 9.51 (s, 1H), 8.22 (m, 1H), 8.14 (s, 1H), 8.05 (d, J = 8 Hz, 2H), 8.03 - 7.92 (m, 2H), 7.89 (d, J = 8.2 Hz, 2H), 7.69 – 7.09 (m, 4H). ^{13}C NMR (DMSO-d$_6$): δ 167.9, 155.7, 152.6, 150.3, 144.5, 139.7, 138.9, 135.3, 129.8, 129.0, 128.1 (2C), 127.2, 126.7, 124.2, 122.5, 121.7, 120.6 (2C). EI-MS m/z: 332.06 (M-H)$^+$. Anal Calc'd for C$_{19}$H$_{15}$N$_3$O$_3$: C, 68.46; H, 4.54; N, 12.61; Found C, 68.28; H, 4.55; N, 12.63.
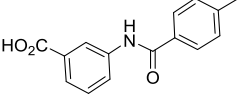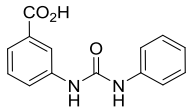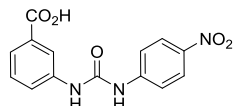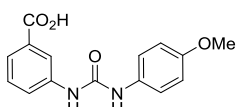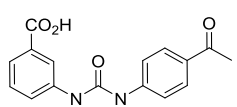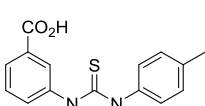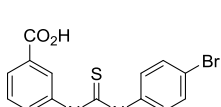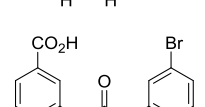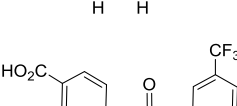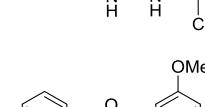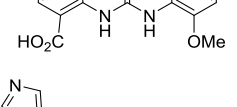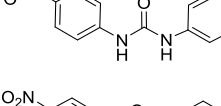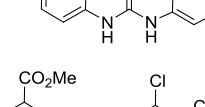
5.1.4. Biological evaluation of synthesized molecules
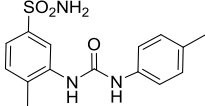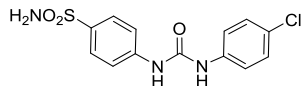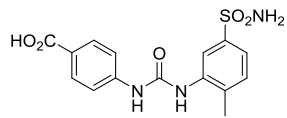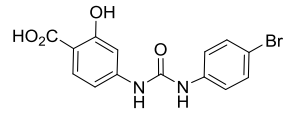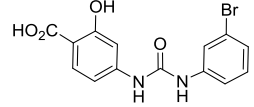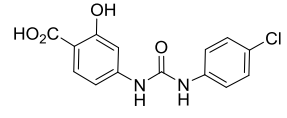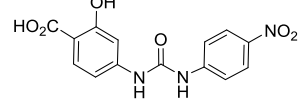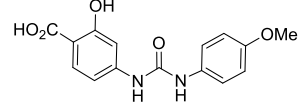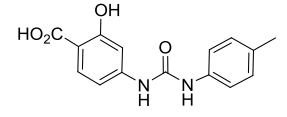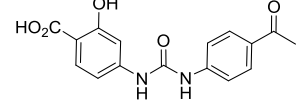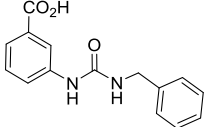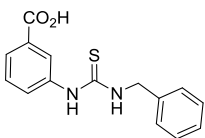
An orthogonal assay was employed to evaluate inhibition of the CysM enzymatic activity by monitoring the α-aminoacrylate intermediate formed in the first half reaction. The second half-reaction of the catalytic cycle of CysM uses thiocarboxylated CysO (CysO-SH) as sulfur donor, leading to the formation of a covalent CysO-cysteine adduct which can be detected by mass spectrometry (Burns 2005, Ågren, *et. al.,* 2008). In order to assess the ability of the best inhibitors of the first half reaction to completely inhibit CysM (i.e. no formation of the covalent CysO-cysteine adduct) the reactions were carried out in the absence and presence of hit compounds and analyzed by ESI-MS. For most active compounds IC$_{50}$ were also determined. The binding modes of seven of the strongest inhibitors were furthermore determined through high-resolution crystal structures of protein-ligand complexes. The most active compounds were tested for antimycobacterial potency by MABA method, nutrient starved *Mtb* and *M. marinum* induced zebra fish model.
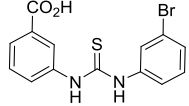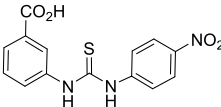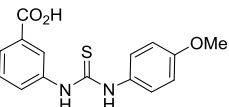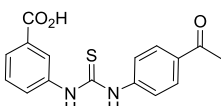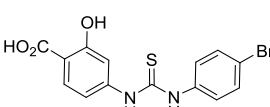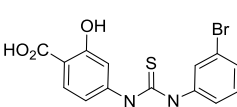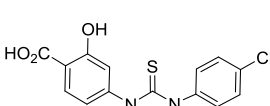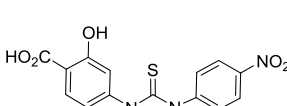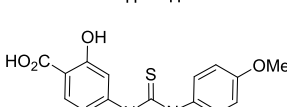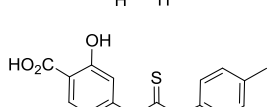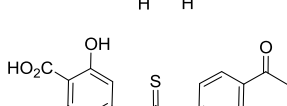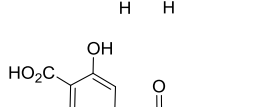
Table 5.3: *In vitro* biological evaluation of the synthesized compounds **RK_01 –71**
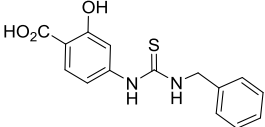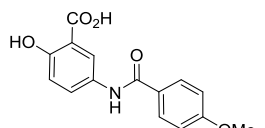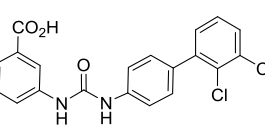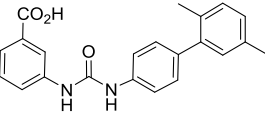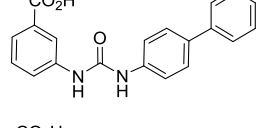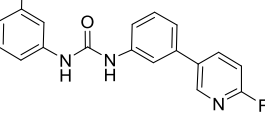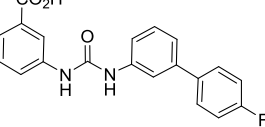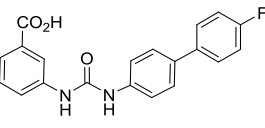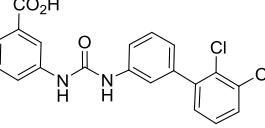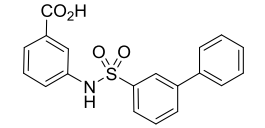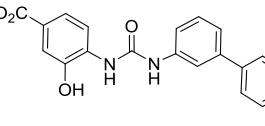
Cmpd.	Structure	K$_d$ (μM)	k$_{obs}$ (min^{-1}) % activity[a]	MIC (μM)
RK_01		0.32[b] ± 0.01	0.10 ± 0.01 0.3	9.6
RK_02		1.7 ± 0.1	0.24 ±0.06 0.6	18.8

RK_03		4.5 ± 0.2	0.48 ± 0.18 1.2	2.2
RK_04		$2.2^{b} \pm 0.1$	0.23 ± 0.05 0.6	ND
RK_05		8.0 ± 0.6	1.92 ± 1.08 4.9	23.1
RK_06		2.1 ± 0.7	0.48 ± 0.12 1.2	18.6
RK_07		1.2 ± 0.1 $3.4^{b} \pm 0.1$	0.24 ± 0.06 0.6	21.5
8		no signal	$> 20^{c}$	ND
RK_09		no signal	$> 20^{c}$	ND
RK_10		no signal	$> 20^{c}$	ND
RK_11		no signal	$> 20^{c}$	ND
RK_12		> 300	$> 20^{c}$	ND
13		> 300	$> 20^{c}$	ND
14		no signal[d]	$> 20^{c}$	ND

15		no signal[d]	> 20[c]	ND
16	CO$_2$H ... phenyl urea	12.9 ± 1.4	1.02 ±0.42 2.6	ND
RK_17	CO$_2$H ... NO$_2$ urea	10.5 ± 1.3	2.22 ±0.54 5.7	20.7
RK_18	CO$_2$H ... OMe urea	11.3 ± 1.5	3.84 ±1.32 9.9	21.8
RK_19	CO$_2$H ... acetyl urea	110.7 ± 7.1	> 20[c]	10.47
RK_20	CO$_2$H ... thiourea tolyl	no signal	> 20[c]	43.65
RK_21	CO$_2$H ... thiourea Br	> 300	> 20[c]	2.22
RK_22	CO$_2$H ... urea Br	20.1 ± 3.1	> 20[c]	35.59
23	HO$_2$C ... CF$_3$, Cl urea	no signal	> 20[c]	ND
24	OMe, HO$_2$C ... OMe urea	no signal	> 20[c]	ND
25	oxazole ... phenyl urea	no signal	> 20[c]	ND
26	O$_2$N ... phenyl urea	no signal	> 20[c]	ND
27	CO$_2$Me ... Cl, Cl urea	no signal	> 20[c]	ND

28		no signal	> 20[c]	ND
29		no signal	> 20[c]	ND
30		no signal	> 20[c]	ND
RK_31		> 300	> 20[c]	71.19
RK_32		no signal	> 20[c]	17.79
RK_33		> 300	> 20[c]	1.27
RK_34		100	> 20[c]	9.85
RK_35		no signal	> 20[c]	5.16
RK_36		no signal	> 20[c]	43.66
RK_37		> 300	> 20[c]	9.94
RK_38		> 300	> 20[c]	5.77
RK_39		> 300	> 20[c]	87.30

78

RK_40		> 300	> 20[c]	18.64
RK_41		> 300	> 20[c]	39.39
RK_42		no signal	> 20[c]	20.67
RK_43		no signal	> 20[c]	2.48
RK_44		no signal	> 20[c]	136.15
RK_45		> 300	> 20[c]	17.02
RK_46		no signal	> 20[c]	38.72
RK_47		>300	> 20[c]	75.00
RK_48		no signal	> 20[c]	19.63
RK_49		no signal	> 20[c]	5.16
RK_50		no signal	> 20[c]	37.83
RK_51		no signal	> 20[c]	5.44

RK_52		no signal	$> 20^c$	10.33
53		no signal	$> 20^c$	ND
RK_54		5.0 ± 0.8	1.26 ± 0.18 3.2	31.24
RK_55		19.5 ± 5.8	2.82 ± 0.30 7.2	17.34
RK_56		37.0 ± 4.8	$> 20^c$	37.61
RK_57		no signal	$> 20^c$	35.57
RK_58		89.9 ± 14.3	$> 20^c$	35.70
RK_59		50.5 ± 26.0	$> 20^c$	35.70
RK_60		222.2 ± 59.5	$> 20^c$	3.90
61		> 300	$> 20^c$	ND
RK_62		no signal	$> 20^c$	5.53

RK_63		no signal	> 20[c]	37.49
RK_64		no signal	> 20[c]	17.79
RK_65		no signal	> 20[c]	33.21
RK_66		no signal	> 20[c]	16.60
RK_67		no signal	> 20[c]	74.77
RK_68		no signal	> 20[c]	174.77
RK_69		no signal	> 20[c]	8.67
RK_70		no signal	> 20[c]	4.68
71		64.9 ± 3.0	2.58 ± 0.43 6.7	ND
INH		--	--	0.4
RIF		--	--	0.5

a: k_{obs} is the first order rate constant for the formation of the α- aminoacrylate intermediate. % activity is the remaining enzymatic activity when compared to the rate constant for the native, non-inhibited enzyme (k_{obs} = 38.92 min^{-1}).

b: determined using ITC

c: due to limitations of the assay only remaining activities lower than 10% can be reliably determined. The term >20% remaining activity indicates weak inhibition or no inhibition.

d: addition of the compound to CysM does not lead to a change in the PLP fluorescence, i.e. suggesting that the compound does not bind.

ND- not determined

5.1.5. Enzymatic assays

Table 5.3 gives a summary of the activity data for all tested molecules collectively these span an affinity range from 300 nM to completely inactive compounds. A significant reduction of the apparent first order rate constants (k_{obs}) was observed for **RK_01** (**Fig 5.2**) and **RK_02** (**Table 5.3**), while the corresponding data for other representatives mirrored the apparent affinities from the PLP-fluorescence assay (**Table 5.3**). In order to assess the ability of the best inhibitors of the first half reaction to completely inhibit CysM (i.e. no formation of the covalent CysO-cysteine adduct) the reactions were carried out in the absence and presence of hit compounds and analyzed by ESI-MS (**Fig 5.2**). The only peaks detected in the presence of **RK_01** and **RK_02** were at ~9571 Da corresponding to the mass of thiocarboxylated CysO (CysO-SH) showing that these compounds completely inhibit CysO-cysteine adduct (9658 Da) formation, i.e. the overall reaction of the enzyme. **RK_03, RK_05-07** showed peaks at both 9571 Da and 9658 Da in different ratios indicating partial inhibition, while **17** showed a main peak at 9658 Da demonstrating no or very limited inhibition of CysO-cysteine adduct formation in the CysM catalyzed reaction compared to the top compounds. For the tightest binding **RK_01** we also determined the IC_{50} value for the overall reaction (**Fig 5.2**), which with 0.48 µM agrees well with the K_d of 0.32 µM determined using ITC.
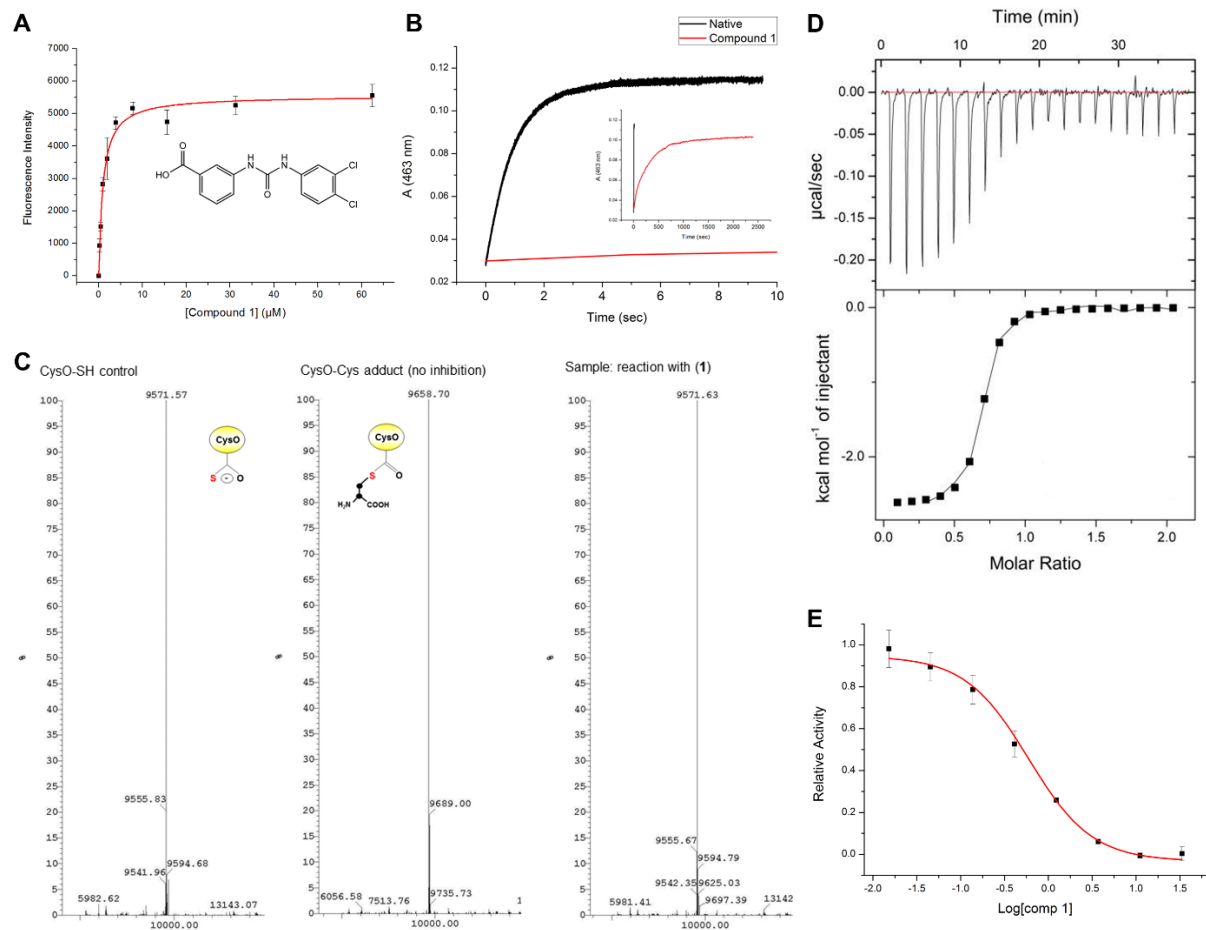
Fig 5.2: *In vitro* characterization of hit compounds, exemplified for **RK_01**. A. Determination of K_d using the PLP fluorescence emission assay. The structure of **RK_01** is inserted in the graph. B. Inhibition of the first half reaction, monitored by following the formation of the α-aminoacrylate intermediate spectrophotometrically at 463 nm. CysM in the presence (red line) and absence (black line) of **RK_01**. The insert shows the same reactions on a longer time-scale. C: Inhibition of the overall CysM reaction by **RK_01** monitored by detection of the reaction product, the CysO-cysteine adduct (9658.7 Da) using ESI-MS mass-spectrometry. D: Determination of K_d using ITC. E: Determination of IC_{50} of **RK_01**.

5.1.6. Enzyme-inhibitor interactions and emerging SAR

The crystal structures of the complexes of CysM with seven inhibitors, **RK_01-07**, were determined by x-ray crystallography to 1.64 – 2.7 Å resolution (**Fig 5.3** and **Table 5.4**). The confirmed small-molecule inhibitors consist of three parts: a left-hand-side substituted phenyl

group (LHS), a central linker part and a right-hand-side aryl group (RHS). In all seven co-crystal structures, the compounds bind in the enzyme active site parallel to the plane of the pyrimidine ring of the PLP cofactor that forms stacking interactions with the urea linker (**Fig 5.3**).

The LHS carboxylate group is consistently positioned in the substrate binding pocket in a similar way as the carboxylate group of the *a*-aminoacrylate intermediate, as previously observed in CysK1 from *M. tuberculosis* [Schnell, *et. al.*, 2007], while the RHS binds into a hydrophobic pocket that extends from the PLP site toward the enzyme surface. The recognition between the enzyme and the linker and RHS, respectively, differs significantly between compounds carrying a RHS phenyl (denoted type I inhibitors) or biphenyl group (type II inhibitors), respectively, at RHS (**Fig 5.4**) as outlined in detail below.

The LHS of inhibitors **RK_01, RK_02, RK_04**−0**7** show similar interactions to residues in the carboxylate binding pocket, i.e. hydrogen bonds to main chain amides of Thr78, Ser79, Asn81 and Thr82 located at the N-terminal of an α-helix (**Fig 5.4**). The interaction between the LHS carboxylate substituent and the enzyme in the carboxylate binding pocket is found in all potent inhibitors of CysM homologues described so far, i.e. CysK1 from *M. tuberculosis* [Poyraz *et. al.,* 2013], OASS from *Haemophilus influenza* [Salsi, *et. al.,* 2010, Amori, *et. al.,* 2012], *Salmonel,la typhimurium* [Pieroni, *et. al.,*2016] and appears to be a hallmark of these enzymes. The exchange of the carboxylic acid group for the tetrazole bioisoster further supports this notion, as this resulted in a complete loss of affinity (**RK_01** *vs* **RK_08**, **Table 5.3**). Further examples reveal that type I inhibitors showed little tolerance for introduction of substituents at LHS. Modifications such as addition of a hydroxyl group and a switch from *m-* to *p*-carboxylate led to loss of binding (**RK_09**−**11**). However, type II inhibitors with the corresponding LHS modifications retained binding affinity and showed considerable inhibitory power (**RK_03**−**04** vs **RK_09**−**10**). This relates to conformational changes in the protein induced by the linker and the RHS of type II inhibitors as discussed below.

We next explored the role of the central linker region. In the crystal structures of CysM with type I inhibitors the carbonyl group of the urea linker interacts with the side chain of Asn221. One of the amides interacts with the terminal carboxyl group of Ala323, inserted into the active site and the second amide forms a hydrogen bond to an internal water molecule. In the structures of type

II inhibitors the carbonyl oxygen of the linker instead forms a hydrogen bond with Arg220 from the mobile active site loop and both amides interact with internal water molecules. To understand the SAR and explore the potential for further optimization of the hit compounds, the urea motif was exchanged for thiourea, sulfonamide or amide linkers. The linker was also extended by a one-carbon elongation, but all these modifications gave inactive or poorly active compounds (**RK_12**-**15**, **Table 5.3**), confirming the importance of the urea hydrogen bonds observed. The difference in activity between urea and thiourea analogs (e.g. **RK_07** vs **RK_12**) may be due to the weaker hydrogen bonding ability of sulfur compared to oxygen and the larger size of the sulfur atom that may affect the angle between the LHS and RHS phenyl groups. Additional examples of thiourea analogues supporting these results are provided in **Table 5.3** (e.g. **RK_20** and **RK_21**).

Significant differences between type I and II inhibitors were also found for the interactions of the enzyme with the RHS. The crystal structures of CysM with **RK_01**, **RK_05**, **RK_06** or **RK_07** are all very similar, with r.m.s.d. values for Cαatoms after superimposition of 0.25-0.3 Å and they also display the same enzyme-ligand interactions. Binding of the type I inhibitors induces a disorder-order transition involving the mobile active site loop (residues 211−227), which folds over the inhibitor binding site and the C-terminal residues that insert into the active site and form important interactions with the linker (**Fig 5.4**). The RHS phenyl group is bound in a hydrophobic pocket denoted pocket A (**Fig 5.4**). The size of this pocket is too small to accommodate inhibitors with a biphenyl substituent, and binding of type II compounds induces a different conformation of the active site loop that increases the size of cavity A by pocket B. The different conformation of the active site loop at the same time prevents insertion of the C-terminus into the active site leading to a change in the interactions of the linker with enzyme residues. The expansion of the binding pocket A with pocket B thus provides sufficient space for the larger biphenyl substituent of **RK_02, RK_03** and **RK_04** (**Fig 5.4**).

The unsubstituted phenyl analog **RK_16** showed an apparent K_d of 12.9 μM, similar to derivatives with the strongly electron-withdrawing p-NO$_2$ substituent and the electron-donating p-OMe group (**RK_17** and **RK_18**) as well as the p-Me analog **RK_05**. However, substitutions with halogens (-Cl **RK_07**, -Br **RK_06**) resulted in a stronger binding, indicating that p-halogens are preferred. Substitution with chloride in both the *para* and *meta*−position resulted in the best

inhibitor **1** with a 40 fold better K_d value than the parent **RK_16**. The electron withdrawing acetyl group had a negative effect on the activity as **RK_19** was a poor inhibitor.

The terminal phenyl group of **RK_02** binds in pocket B and the crystal structures of CysM with **RK_02**, **RK_03** or **RK_04** show that there is little space available in this pocket (less than 4 Å in any direction) for further modifications of this phenyl ring. Consequently substitutions such as -Me, -CO_2H and -F all result in lower affinity or a complete loss of binding (**RK_58**, **RK_66**, and **RK_69**, **Table 5.3**). Exchanging the RHS terminal phenyl ring for a nitrogen heterocycle (pyridine or pyrimidine) (**RK_63**, **RK_68**) led to less active compounds (1-2 orders of magnitude difference in K_d), most likely due to less favorable interactions of these more polar ring systems with the hydrophobic binding pocket.

A.
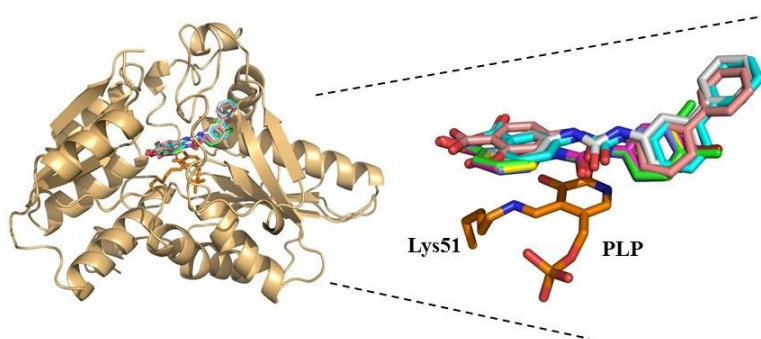
B.
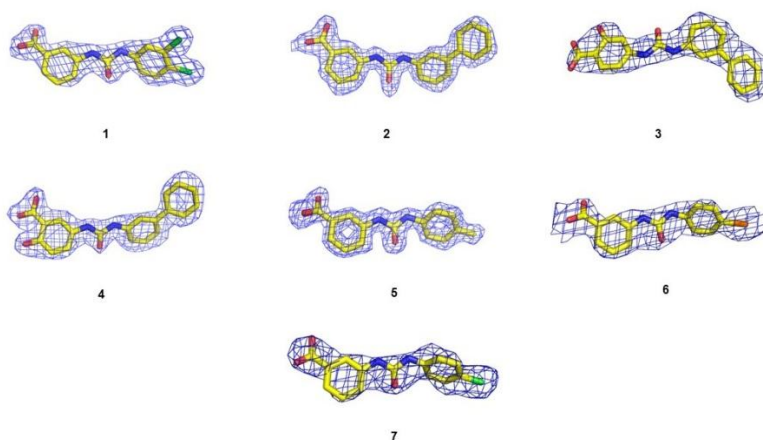
Fig 5.3: Crystal structures of CysM – hit compounds. A. left: Schematic view of the binding of the hit compounds in the active site of CysM. Right: Superposition of the seven structures of CysM- hit complexes illustrating the similar binding modes of the compounds and their position

relative to the PLP cofactor. B. Composite omit 2Fo-Fc maps for the bound inhibitors. The electron density maps are contoured at 1.0Å.
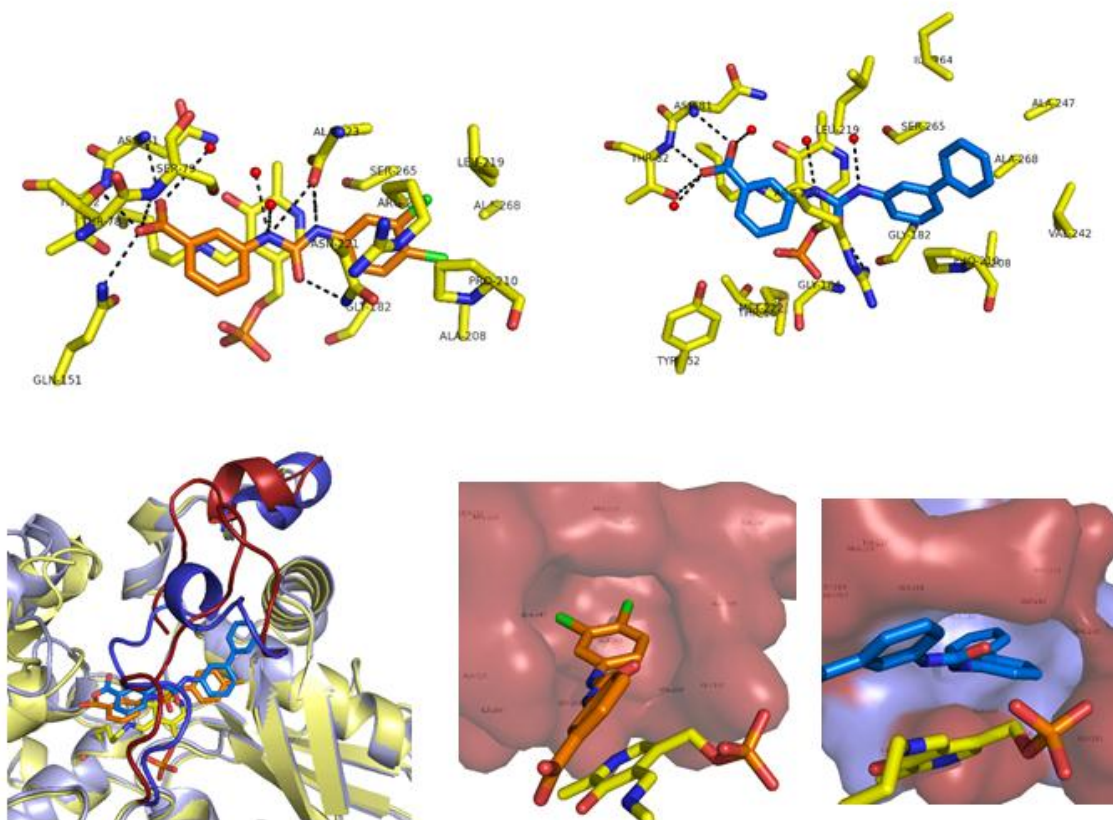
Fig 5.4: Structures of complexes of CysM with representative type I and type II inhibitors. A: Enzyme-ligand interactions in the complex of CysM with **RK_01**. B: Enzyme-ligand interactions in the CysM- **RK_02** complex. Ligands are shown in orange (**1**) and blue (**2**), respectively. Color codes are red for oxygen, blue for nitrogen and yellow for carbon atoms. For the bound inhibitors, carbon atoms are orange (**1**) and blue (**2**), respectively. Hydrogen bonds are indicated by dotted lines. C: Superposition of the CysM - **RK_05** and CysM - **RK_02** complexes illustrating the different conformations of the active site loop (residues 211-227) and the C-terminus in response to differences in substitution of the RHS part of the inhibitor. CysM in complex with **RK_02** is colored in blue, with active site loop and C-terminus in dark blue. CysM in complex with **RK_05** is colored in yellow and the corresponding active site loop and C-terminus in dark red. D: Differently sized binding pockets for RHS in CysM-ligand complexes. Pocket A interacting with the RHS of type I inhibitors. E: Extension of pocket A with pocket B

(blue) to accommodate the large phenyl substituent in type II inhibitors. Note the different position of Leu219 in the two structures, which acts as a gatekeeper to open up pocket B.

5.1.7. Anti-mycobacterial activity and cytotoxicity

The most potent CysM inhibitors were further tested against a growing culture of *M. tuberculosis* and all showed bactericidal effects, with MIC values ranging from 2 – 20 μM (0.7- 6.2 μg/ml) (**Table 5.3**). These observed MIC values are in the low μM range, but do not reach the potency of clinically used drugs such as Isoniazid and Rifampicin. As the gene coding for CysM is predominantly expressed during dormancy (Betts, *et. al.,*2002, Schnappinger, *et. al.,*2003, Voskuil, *et. al.,*2004) this is also not to be expected. We therefore used the nutrient starvation model (Betts et al., 2002) to test the anti-mycobacterial activity of these inhibitors (**Fig 5.6**) under conditions simulating dormancy. In this model **RK_01**, **RK_02**, **RK_03, RK_17** showed anti-mycobacterial potency superior to Rifampicin and Isoniazid, whereas compounds **RK_05, RK_06, RK_07, RK_18** were comparable to these drugs. In an effort to initiate studies of the mechanism of action of these compounds also *in vivo*, we next examined the effect of cysteine complementation during the treatment of nutrient starved cultures of *M. tuberculosis* with **RK_0**1 and **RK_0**3 (**Fig 5.6B**). Addition of cysteine (0.2 mM) led to a complete loss of the bactericidal effect of the two inhibitors. We could not detect any degradation of **RK_0**1 during incubation with cysteine for 24 h using mass-spectrometry, HPLC (**Fig 5.7**), and spectroscopy, thus excluding inactivation of **RK_0**1 by reaction with cysteine as the cause for the loss of antimycobacterial activity. These data point toward cysteine biosynthesis as an important component of the action of **RK_0**1 and **RK_0**3 also *in vivo*. Cytotoxicity assays with these compounds using three different human cell lines and a mouse cell line did not reveal significant cytotoxic effects at concentrations of 10 μM (**Fig 5.5**).
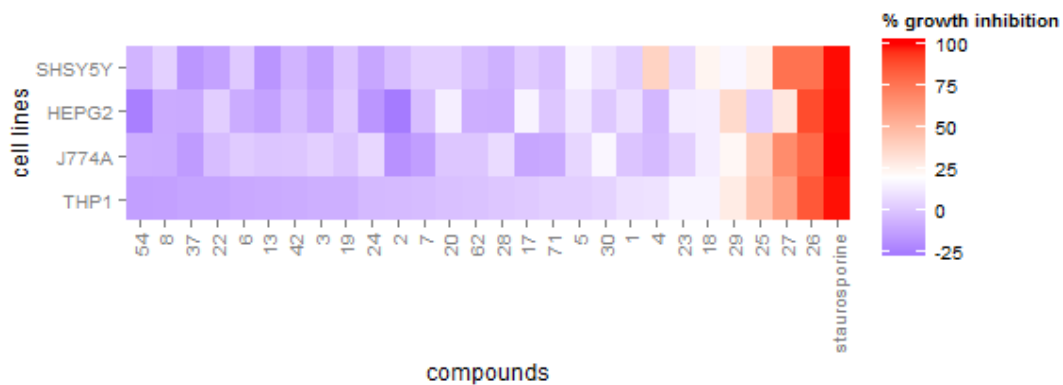
Fig 5.5: Heatmap of the percent growth inhibition across the four cell lines after 72 hour compound treatment at the maximum concentration of each compound tested. Each compound was run in duplicate across the four cell lines.
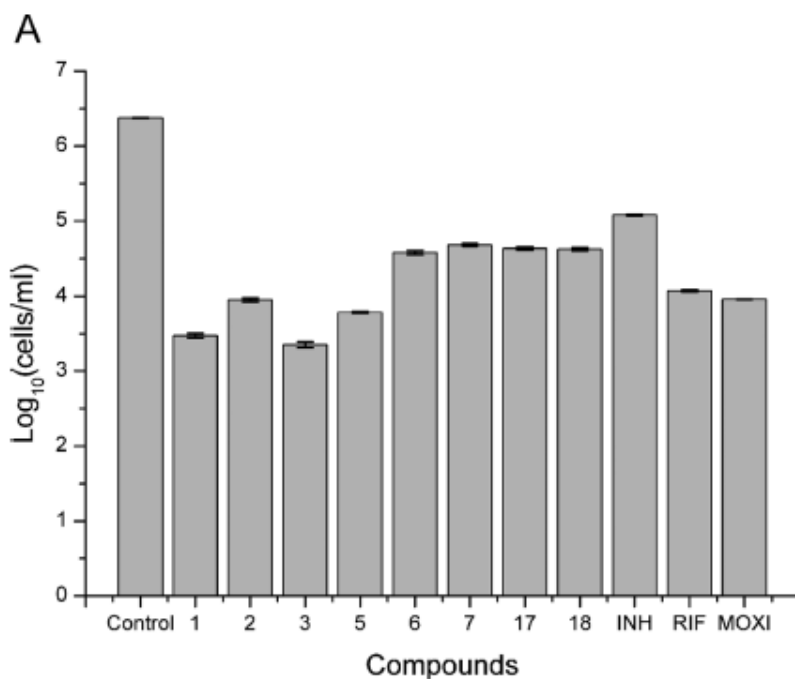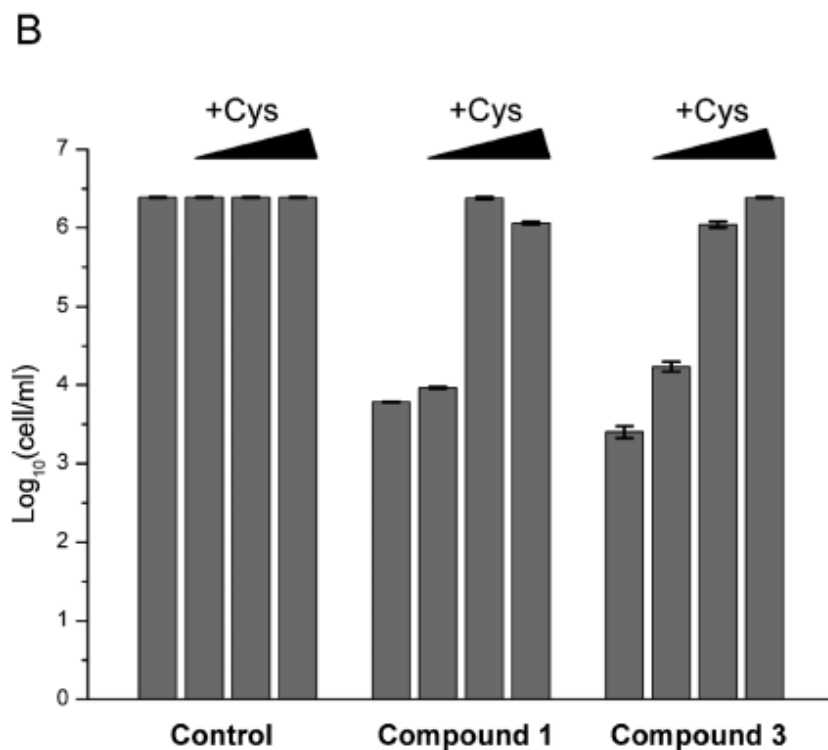
Fig 5.6: (A) Biological activities of the lead compounds against *M. tuberculosis* in the nutrient starvation model. Bacterial count estimation (given as means ± standard deviations from three independent experiments) for control and treated groups was carried out using the MPN (most probable number) assay. **RK_0**1 and **RK_0**3 in particular gave significant inhibition of growth of *M. tuberculosis* in this model as compared to the control ($p < 0.0001$, two way ANOVA using GraphPad Prism Software). (B) Effect of cysteine on bactericidal activities of **RK_0**1 and **RK_0**3. Nutrient-starved cultures of *M. tuberculosis* were split into three groups, control (no compound added (left)), **RK_0**1 (addition of 10 μg/mL 1) and **RK_0**3 (addition of 10 μg/mL 3). For each group, increasing cysteine concentration is indicated from left to right: 0.0, 0.05, 0.2, and 0.5 mM. Bacterial count estimations were obtained as described above. Experiments were carried out in triplicate.
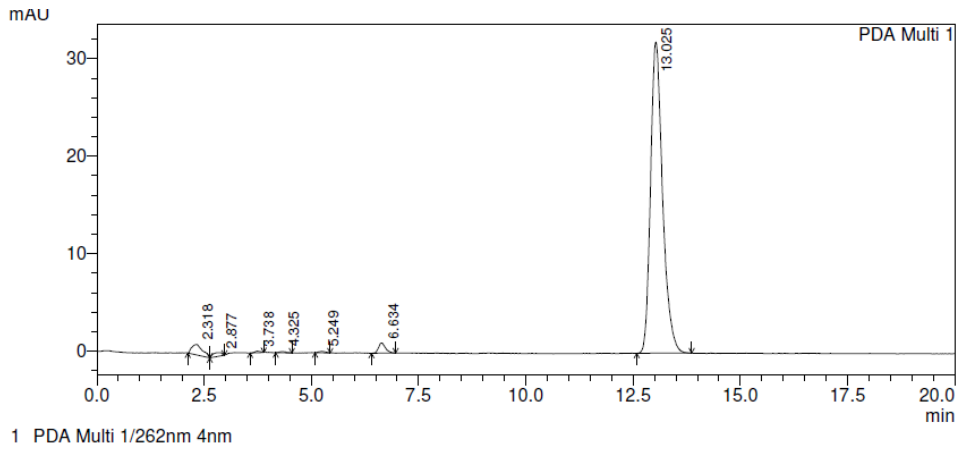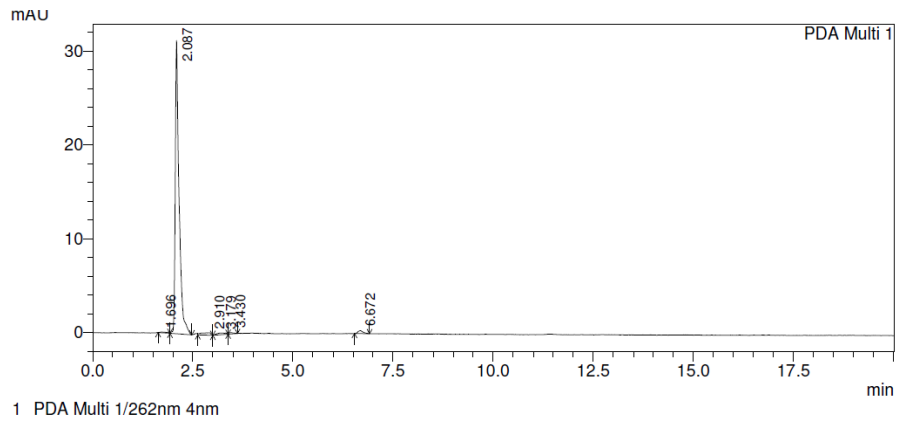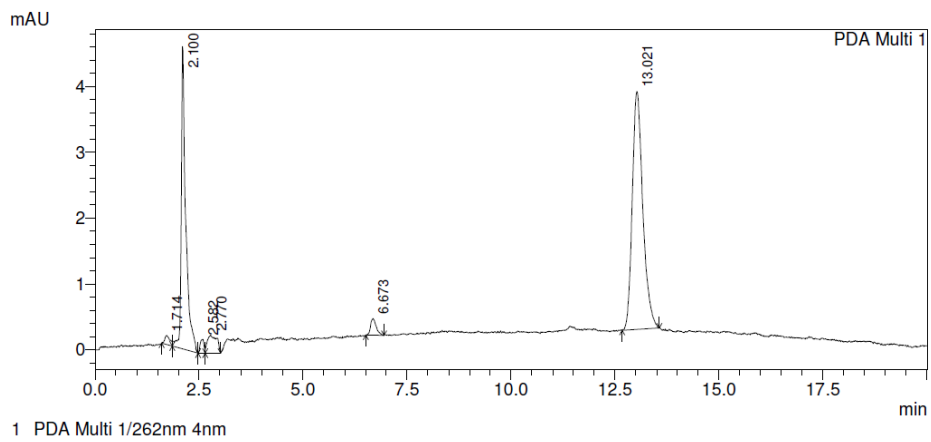
Fig 5.7: HPLC analysis of **RK_0**1 (A), cysteine (B), 24 h post incubation of **RK_0**1 with cysteine (C)

5.1.8. Compound selectivity

De novo cysteine biosynthesis in *M. tuberculosis* is rather complex, with three potential pathways leading to cysteine. Each of these routes contains a specific PLP dependent cysteine synthase, CysK1, CysK2 and CysM [Schnell 2014]. In order to assess the selectivity of the urea-derived inhibitors, we examined the binding and affinity of **RK_01** and **RK_02** to the mycobacterial homologues using the fluorescence–based binding assay. **RK_01** bound to both CysK2 and CysK1, albeit much weaker, returning K_d values of 25.2 μM and 64.3 μM, respectively. **RK_01** thus shows a clear preference for CysM over CysK2 (84 fold) and CysK1 (200-fold) based on these K_d values. **RK_02** gave a K_d of 37.9 μM with CysK1 and does not show any binding to CysK2.

As humans lack the *de novo* biosynthesis pathways to cysteine, these enzymes are particularly attractive as potential targets for new antibiotics. A search of the human genome returned SERC (phosphoserine-aminotransferase, Uniprot AccNr: Q9Y617) that uses O-phosphoserine and α-ketoglutarate as substrates (11% sequence identity) and CBSA (Cystathionine beta-synthase, Uniprot AccNr: P35520) that uses serine and homocysteine as substrates (29% sequence identity) as the closest sequence relatives of CysM. We could not detect any interaction between SERC and **RK_01** or **RK_02**, respectively, using the PLP-fluorescence emission signal. This observation is consistent with the three-dimensional structure of this enzyme (PDB entry 3E77, Structural Genomics Consortium), where the corresponding binding site for the CysM inhibitors is occluded by a tryptophan residue. CBSA on the other hand binds **RK_01** with a K_d of 94 μM, i.e. with approximately 300 times lower affinity compared to the mycobacterial target protein and does not bind **RK_02**. The low affinity of the two hits **RK_01** and **RK_02** for the closest human homologues and the low cytotoxicity suggest that these compounds are suitable starting points for further development.

5.1.9. Anti-mycobacterial screening for most active compound using adult zebrafish

Zebra fish has genetic, physiological and immune (adaptive and innate) related similarities with mammalian host. When infected with *M.marinum* it forms granulomas with central necrosis and hypoxia similar to human. Oxidative stress stimulates the expression of bacterial efflux pumps in active stage of mycobacterium in zebra fish model. Crucial virulence factors, host genes and immune cell types implicated in human *Mtb* pathogenesis are retained in zebrafish–*M.*

marinum model. The natural heterogeneity of the zebrafish population proved to be beneficial as it helps in understanding of genetic differences of different individuals. It also serves as a link between *in vitro* and *in vivo* models as it provides insight into pharmacokinetic and pharmacodynamics parameters. *M. marinum* is relatively safe to humans as it is restricted to topical lesions, has genetic similarity *to Mtb* and also has higher replication rate than *M. tuberculosis*. Activity and dosage of antimycobacterial compounds in zebrafish closely resemble characteristics in humans. Owing to all the mentioned advantages and ease of handling, cost effectiveness zebra fish model can be used for high throughput screening of antimycobacterial agents [Swaim, L. E., et al., 2006, Meijer, A. H. 2016].

The most active compounds were further evaluated for its *in vivo* activity using adult zebrafish model. **RK_01** and **RK_03** exhibited significant log reduction in bacterial load by 2.9 fold and 3 fold respectively and are effective when compared to standard drugs – Isoniazid (1.2 fold), Rifampicin (2.0 fold), Moxifloxacin (2.3 fold) (**Fig 5.8**).
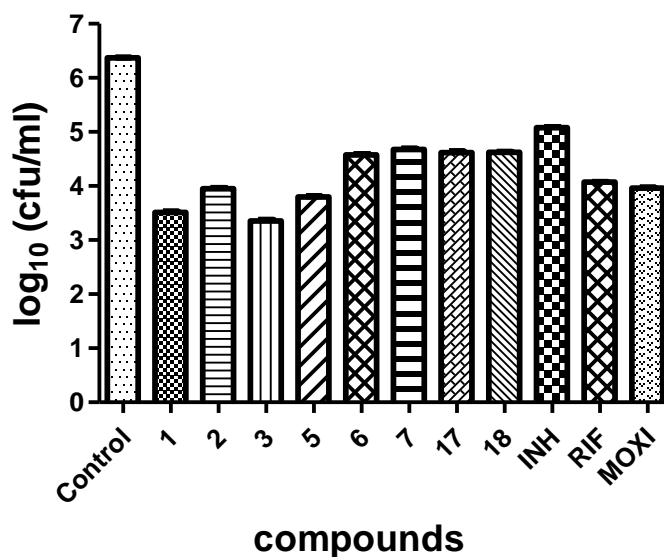
Fig 5.8: Adult zebrafish (*Danio rerio*) was infected with *M. marinum* and was assayed to estimate the infection recovery post-treatment. Bacterial count estimation (Mean ± S.E.M., n = 6) for control and treated groups conducted by using MPN (most probable number) assay. The statistical significance p<0.001) with respect to infected control group has been analyzed by Two-way ANOVA using GraphPad Prism Software.

5.1.10. Highlights of the study

In view of the large number of individuals infected with persistent *M. tuberculosis* worldwide drugs active against the dormant stage of this infectious disease are urgently needed. Indeed most of the anti-mycobacterial drugs in clinical use are not effective in the dormant state of the disease. Significantly, several of the top hits identified in this work display potent antibacterial activity, with four compounds (**RK_01, RK_02, RK_03** and **RK_05**) showing markedly better potency against persistent *M. tuberculosis* compared to first-line drugs in clinical use and thus are promising leads for further development. **RK_0**1 and **RK_0**3 are active against replicating stages of mycobacteria as reflected by their MIC values and zebra fish model results.
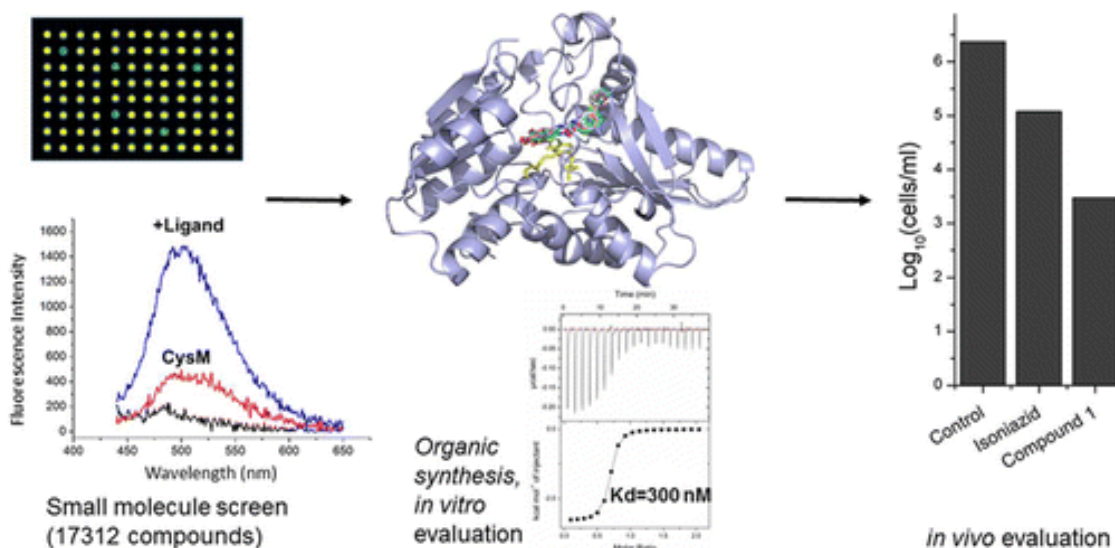
Results and discussion for development of Mycobacterial Lysine aminotransferase inhibitors

6.1. Design, synthesis and biological evaluation of substituted Cyclobutyl derivatives as potent *Mycobacterium tuberculosis* Lysine aminotransferase inhibitors

6.1.1. Design of molecule

In our previous study [Devi PB, *Tuberculosis*, 2015] by screening BITS inhouse data base we identified cyclobutyl scaffold (Lead 10) with an IC_{50} of 8.16 µM. Interaction profiles of boc protected amine and free amine derivative was found to be same (4 hydrogen bonds with Lys300, Arg422 and Gln274) but the boc protected scaffold has lower binding energy (-5.10Kcal/mol) (**Fig 6.1**). To study the effect of various aromatic and aliphatic groups substitutions were made at R position by coupling the free amine with various isocyanates and isothiocyanates to yield respective ureas and thioureas (**Fig 6.2, Table 6.1**).
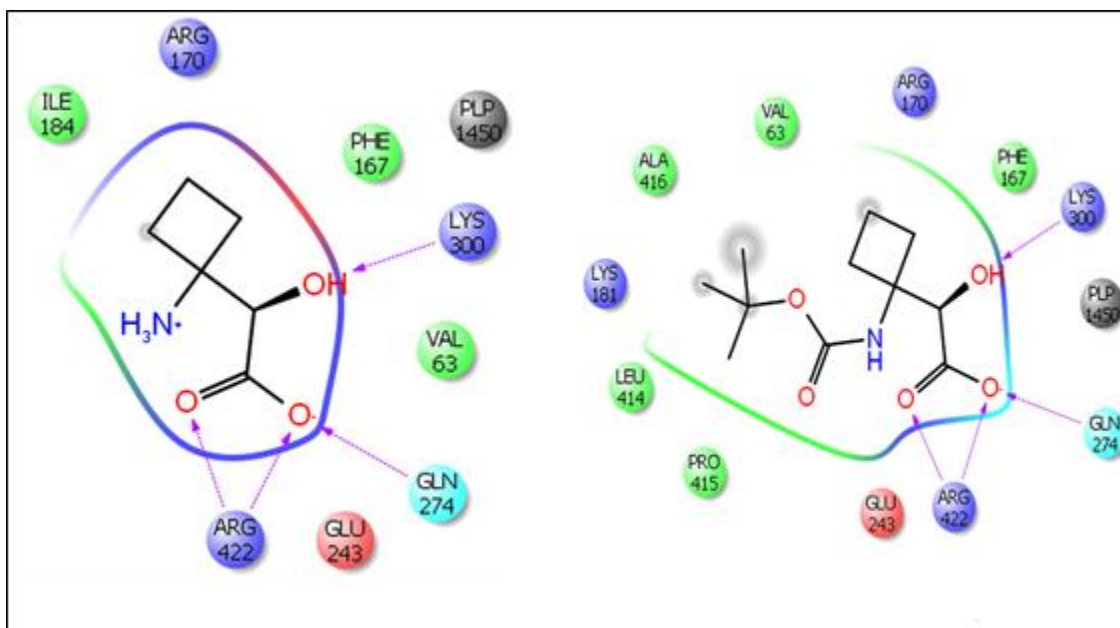
Figure 6.1: Binding pose and its interaction pattern of the compound **S1** and **lead 10.**
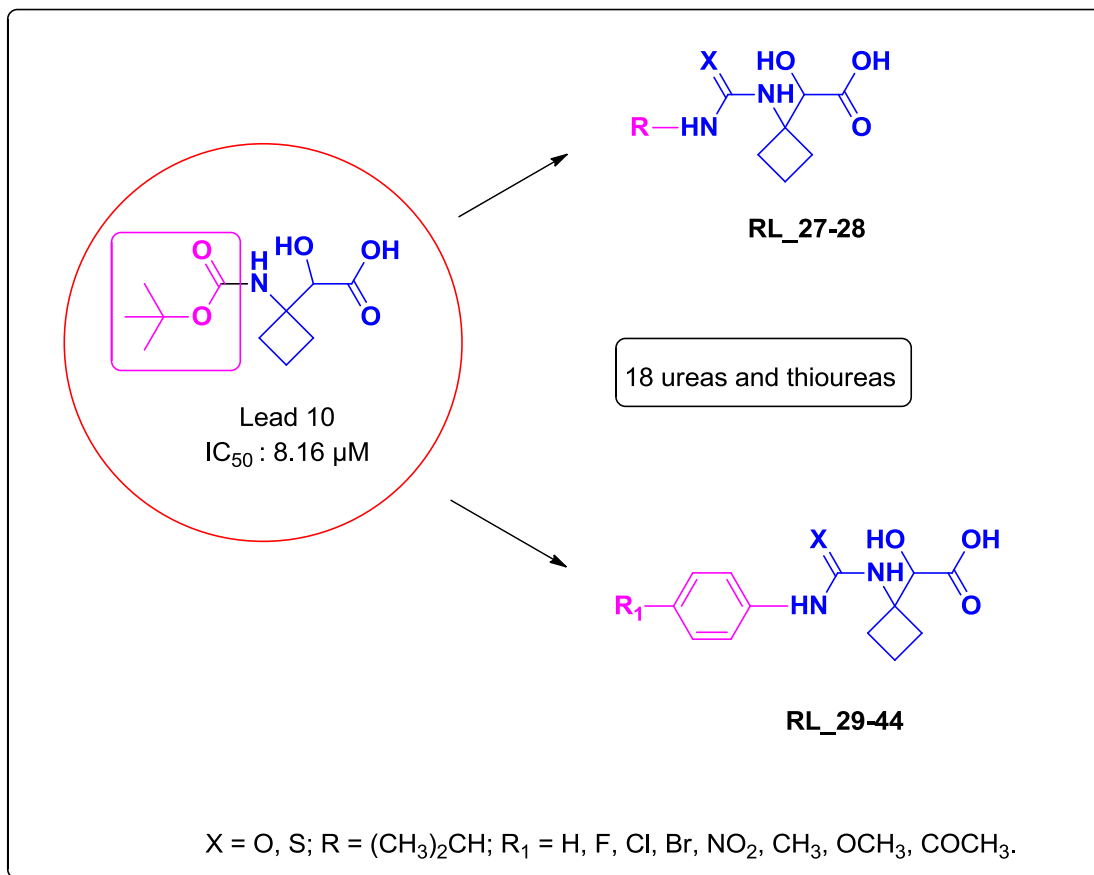
Figure 6.2: Strategy employed for lead expansion

6.1.2. Experimental procedures utilized for the synthesis of RL_27 – RL_44

Interaction profile of lead compound 10 revealed that hydroxyl group and carboxylic acid attached to cyclobutyl nucleus are crucial for hydrogen interactions in the active site. So retaining this part as such, boc group attached to amine was replaced with various aromatic and aliphatic groups. A library of 18 compounds were prepared and evaluated for there *in vitro* inhibitory potential against lysine Ɛ-amino transferase enzyme. The synthetic strategy followed to achieve the target molecule was portrayed in **Fig 4.5.** Synthesis started with commercially available N-Boc-1-aminocyclobutane carboxylic acid (**RL_01**) acid (Sigma Aldrich). In the first step we converted the acid group in **RL_01** to amide via Weinreb synthesis to form Weinreb amide. This was achieved by converting first the acid group to acid chloride. Then treatment of acid chloride with *N,O*-Dimethylhydroxylamine, resulted in nucleophilic acyl substitution resulted in corresponding Weinreb–Nahm amide **RL_02**. Weinreb–Nahm amide is a potential

intermediate in organic synthesis which can be used to prepare ketones and aldehydes. Reduction of Weinreb–Nahm amide with excess of base such as lithium alumunium hydride resulted in corresponding aldehyde. Treatment of **RL_02** with excess of Lithium aluminum hydride at 0° C resulted in aldehyde **RL_03.** The one pot condensation of aldehyde **RL_03**, isocyanide and trifluoroacetic acid resulted in corresponding alpha hydroxyl amide (**RL_05**) by employing Passerini reaction. In this step along with alpha hydroxyl amide (**RL_05**) some percentage of hydroxyl protected with trifluoromethane (**RL_04'**) was formed as byproduct. So the above mixture obtained was on hydrolysis with weak base such as lithium hydroxide given single product alpha hydroxyl amide (**RL_05**). Hydrolysis of t-butyl amide group present in **RL_05** provides alpha hydroxyl carboxylic acid (**RL_06**). Hydrolysis of t-butyl group was achieved by strong acidic conditions, resulted in Boc deprotection. This amine was directly tried to couple with various substituted isocyanates and isothiocyanates to get target molecules with reduced step resulted in failure because of poor solubility of 2-(1-aminocyclobutyl)-2-hydroxyacetic acid. In order to improve the solubility and reaction 2-(1-aminocyclobutyl)-2-hydroxyacetic acid was protected with Boc anhydride. The reason behind selection of Boc anhydride is because of its reactivity with good yield and less side product and also the deprotection can be achieved very easily when compared to other protecting groups. In further step the free carboxylic acid was protected. This was achieved by esterification of carboxylic acid using MeI and K_2CO_3 as base to yield **RL_07**. Deprotection of amine group was achieved using HCl in Dioxane resulted in **RL_08**. In the next step scaffold (**RL_08**) was treated with various substituted isocyanates and isothiocyanates, using weak organic base such as triethylamine to afford ureas and thioureas. The final target molecule was afforded by hydrolysis of methyl ester of substituted ureas and thiourea derivatives using LiOH as base [Ayesa, S. *et. al.,* 2014].

Preparation of *tert*-Butyl (1-(methoxy(methyl)carbamoyl)cyclobutyl)carbamate (RL_02):
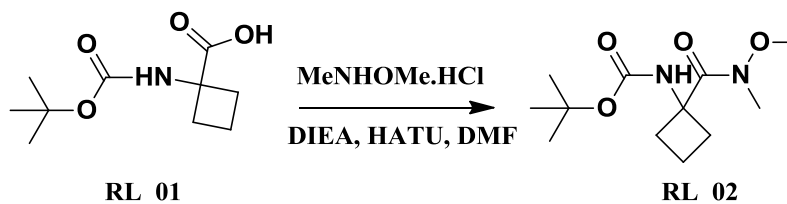
To solution of 1-*tert*-butoxycarbonylamino-cyclobutanecarboxylic acid (**RL_01**) (10gm, 46.46mmol) in dry DMF (50ml), N,O-dimethylhydroxylamine HCl (4.53g, 46.46mmol) and DIEA (24.02g, 185.84mmol) were added. The reaction mixture was cooled to 0 °C for 10min

then HATU (17.67g, 46.46mmol) was added and stirred at 30 $^{\circ}$C for 2 hrs (completion monitored through TLC and LCMS). The solvent was removed under reduced pressure using rota evaporator. The residue was dissolved in ethylacetate (50ml) and washed with aq. Saturated NaHCO$_3$(50ml), 10% citric acid solution (50ml) dried over anhydrous sodium sulphate and concentrated. The crude product was purified by column chromatography to afford **RL_02** (10.21g, 85.08%) as colourless oil. ^{1}H NMR (DMSO-d$_6$):δ_H 6.85 (b, 1H), 3.72 (s, 3H),2.84 (s, 3H),2.38 (m, 2H), 2.01 (m, 2H), 1.83 (m, 2H), 1.36 (s, 9H). ^{13}C NMR (DMSO-d$_6$):δc. 175.3, 157.1, 82.8, 62.7, 57.4, 36.9 (2C), 32.3,25.6 (3C), 12.4. ESI-MS m/z 259.24 (M+1)$^+$. Anal Calcd for C$_{12}$H$_{22}$N$_2$O$_4$; C, 55.80; H, 8.58; N,10.84; Found:; C, 55.72; H, 8.56; N, 10.83.

Preparation of *tert*-Butyl (1-formylcyclobutyl)carbamate (RL_03):

RL_02   RL_03
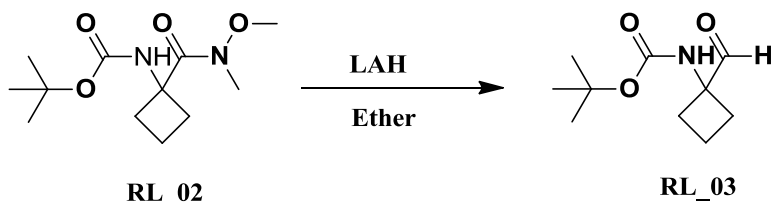
To solution of *tert*-butyl (1-(methoxy(methyl)carbamoyl)cyclobutyl)carbamate (**RL_02**) (10g, 38.71mmol) in diethyl ether (50ml), LiAlH$_4$(1.84g, 48.39mmol) was added at 0 $^{\circ}$C. The solution was stirred for 20min then quenched by adding aq. saturated solution of potassium hydrogen tartaric acid (50ml) and then stirred for 10min(completion monitored through TLC and LCMS). The aqueous phase was extracted thrice with ethylacetate (50ml). The combined organic layers were washed with 0.5M HCl (25ml), aq. saturated NaHCO$_3$ (25ml), brine solution (25ml) then dried over anhydrous sodium sulphate and concentrated. The crude product was purified by column chromatography to afford **3** (5.74g, 74.45%) as white solid. ^{1}H NMR (DMSO-d$_6$):δ_H 9.83 (s, 1H), 6.86 (b, 1H), 2.39 (m, 2H), 1.99 (m, 2H), 1.81 (m, 2H), 1.38 (s, 9H), ^{13}C NMR (DMSO-d$_6$):δc.200.7, 158.3, 82.1, 77.8, 32.6 (2C), 25.8 (3C), 11.2. ESI-MS m/z 200.15 (M+1)$^+$. Anal Calcd for C$_{10}$H$_{17}$NO$_3$; C, 60.28; H, 8.60; N, 7.03; Found:C, 60.20; H, 8.62; N, 7.01.

Preparation of *tert*-Butyl (1-(2-(*tert*-butylamino)-1-hydroxy-2-oxo-ethyl) cyclobutyl) carbamate (RL_05):

RL_03   RL_05
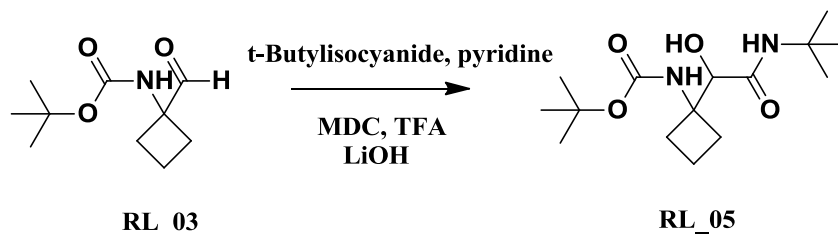
To solution of *tert*-butyl (1-formylcyclobutyl)carbamate (**RL_03**) (5g, 25.09mmol) in DCM (25ml) at 0 °C under nitrogen atmosphere pyridine (10ml), t-butylisocyanide (3.17g, 38.14mmol) and trifluoroacetic acid (5.72g, 50.18mmol) were added. The reaction mixture was allowed to stir at 30 °C for 8 – 10 hrs (completion monitored through TLC and LCMS). The solvent was removed invacuo and residue was dissolved in ethylacetate. The organic layer was washed with 0.5M HCl (15ml), aq. saturated $NaHCO_3$ (15ml), brine solution (15ml) then dried over anhydrous sodium sulphate and concentrated. The resultant crude product was dissolved in MeOH : water (3 :1 ; 10ml), THF (10ml) and 1M LiOH (10ml) were added. The reaction mixture was allowed to stir at 30 °C for 45min (reaction completion monitored through TLC and LCMS). The reaction was then quenched by addition of 1N HCl, water (10ml) and the aqueousphase was extracted with ethylacetate (3*10ml).The organic layer was washed with aq. saturated $NaHCO_3$(20ml), brine solution (20ml) then dried over anhydrous sodium sulphate and concentrated. The resultant product was purified by column chromatography to yield **RL_05** (6.08g, 80.64%) as white solid. ^{1}H NMR (DMSO-d$_6$):δ_H 6.86 (b, 1H), 6.53 (s, 1H), 4.11 (s, 1H), 3.01 (s, 1H), 2.42 (m, 2H), 1.96 (m, 2H), 1.78 (m, 2H), 1.34 (s, 9H), 1.37 (s, 9H). ^{13}C NMR (DMSO-d$_6$):δc 174.5, 157.8, 95.4, 76.2, 63.5, 62.9, 30.1 (3C), 24.3 (5C), 15.8. ESI-MS *m/z* 301.21(M+1)$^+$. Anal Calcd for $C_{15}H_{28}N_2O_4$; C, 59.97; H, 9.40; N, 9.33; Found: C, 60.05; H, 9.42; N,9.31.

Preparation of 2-(1-((*tert*-Butoxycarbonyl)amino)cyclobutyl)-2-hydroxyacetic acid (RL_06):

RL_05   RL_06
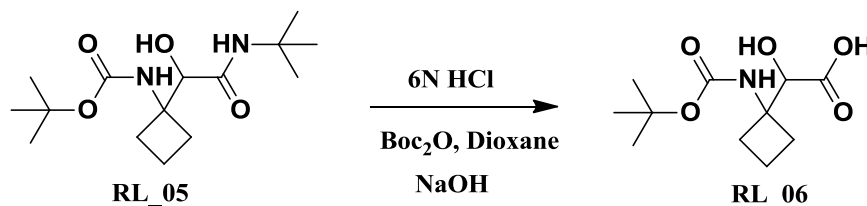
tert-butyl (1-(2-(*tert*-butylamino)-1-hydroxy-2-oxo-ethyl)cyclobutyl)carbamate (**RL_05**) (5g, 16.65mmol) was refluxed with 6N HCl (50ml) for 12hrs (completion monitored through TLC and LCMS). The reaction mixture was concentrated under reduced pressure and residue was stirred with 1M NaOH (30ml) for 15min under vaccum. To the basic solution boc anhydride (7.27g, 33.3mmol) and dioxane (25ml) were added and stirred at 30 $^{\circ}$C for 12 h (completion monitored through TLC and LCMS). The reaction was quenched by adding water (50ml) and adjusting pH to 3 using 1N HCl at 0 $^{\circ}$C. The aqueous phase was extracted with ethylacetate (3*50ml) washed with brine solution (25ml) dried over anhydrous sodium sulphate and concentrated. The obtained crude product was purified by column chromatography to yield **RL_06** (2.93g, 71.81%) as colourless oily liquid. ^{1}H NMR (DMSO-d$_6$):δ_H 12.31 (s, 1H), 6.88(b, 1H), 4.15 (s, 1H), 3.03 (s, 1H), 2.40 (m, 2H), 1.98 (m, 2H), 1.80 (m, 2H), 1.35 (s, 9H).^{13}C NMR (DMSO-d$_6$):δc 171.3, 152.5, 89.3, 75.8, 61.7, 30.2 (2C), 29.8 (3C), 13.2. ESI-MS *m/z* 244.13 (M-1)$^{+}$. Anal Calcd for C$_{11}$H$_{19}$NO$_5$; C, 53.87; H, 7.81; N, 5.71; Found: C, 53.81; H, 7.80; N, 5.72.

Preparation of Methyl 2-(1-(((*tert*-Butoxycarbonyl)amino)cyclobutyl)-2-hydroxyacetate (RL_07):

RL_06   RL_07
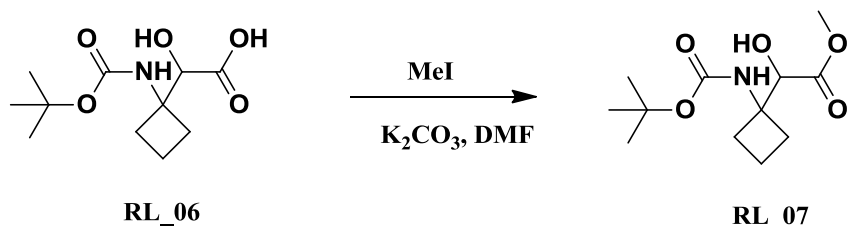
To solution of 2-(1-((*tert*-butoxycarbonyl)amino)cyclobutyl)-2-hydroxyacetic acid (**RL_06**) (2.5g, 8.45mmol) in DMF (5ml) at 0 $^{\circ}$C potassium carbonate (8.45g, 61.14mmol) methyl iodide (4.34g, 141.94mmol) were added and stirred at 30 $^{\circ}$C (completion monitored through TLC and LCMS). The solvent was removed from reaction mixture invacuo and water (10ml) was added to the resulting residue. The aqueous phase was extracted with ethylacetate (3*15ml), washed with brine solution (30ml) dried over anhydrous sodium sulphate and concentrated. The obtained crude product was purified by column chromatography to yield **RL_07** (2.37g, 89.77%) as colourless oily liquid. ^{1}H NMR (DMSO-d$_6$):δ_H 6.90 (b, 1H), 4.10 (s, 1H), 3.72 (s, 3H), 2.98 (s, 1H), 2.35 (m, 2H), 1.92 (m, 2H), 1.74 (m, 2H), 1.31 (s, 9H).^{13}C NMR (DMSO-d$_6$):δc 165.4, 152.3, 90.4, 82.1, 62.3, 54.8, 29.5 (2C), 28.6 (3C), 13.6. ESI-MS *m/z* 260.15 (M+1)$^{+}$. Anal Calcd for C$_{12}$H$_{21}$NO$_5$; C, 55.58; H, 8.16; N, 5.40; Found: C, 55.62; H, 8.15; N, 5.42.

Preparation of Methyl 2-(1-aminocyclobutyl)-2-hydroxyacetate (RL_08):

RL_07   RL_08
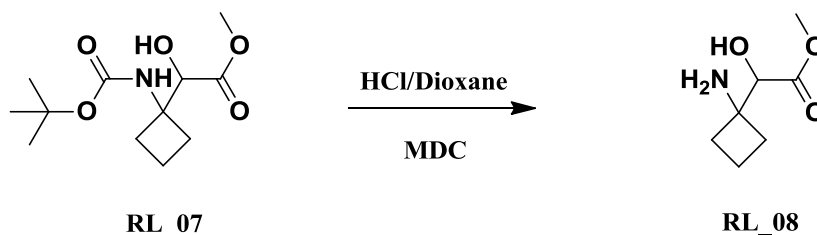
To solution of methyl 2-(1-((*tert*-butoxycarbonyl)amino)cyclobutyl)-2-hydroxyacetate (**RL_ 07**) (2g, 7.71mmol) in DCM, HCl-dioxane (10ml) was added at 0 °C and then allowed to stir at 30 °C for 4 h. After completion of reaction (monitored through TLC and LCMS) solvent was removed under reduced pressure and residue was diluted with water (10ml). Aqueous layer was extracted with ethylacetate (3*15ml) then organic layer was washed with brine solution (20ml), dried over anhydrous sodium sulphate and concentrated. The resultant crude product was purified by column chromatography to yield **RL_08** (0.92g, 74.79%). ^{1}H NMR (DMSO-d$_6$):δ_H 5.09 (s, 2H), 4.08 (s, 1H), 3.75 (s, 3H), 2.97 (s, 1H), 2.32 (m, 2H), 1.87 (m, 2H), 1.72 (m, 2H). ^{13}C NMR (DMSO-d$_6$):δc. 172.5, 93.6, 59.6, 51.7, 34.2 (2C), 12.8. ESI-MS *m/z* 160.12 (M+H)$^+$. Anal Calcd for $C_7H_{13}NO_3$; C, 52.82; H, 8.23; N, 8.80; Found: C, 52.88; H, 8.25; N, 8.81.

Preparation of Methyl-2-hydroxy-2-(1-(3-isopropylthioureido)cyclobutyl)acetate (RL_09):
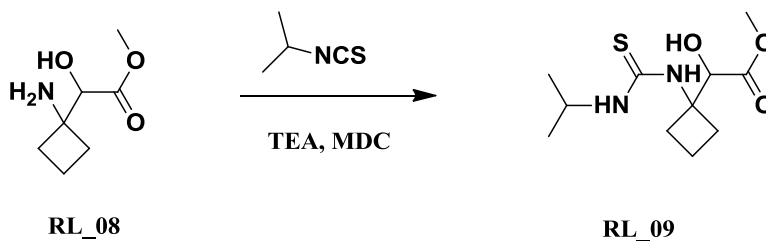
RL_08   RL_09

To a solution of methyl 2-(1-aminocyclobutyl)-2-hydroxyacetate (**RL_08**) (0.15g, 0.94mmol) in dry dichloromethane (3 mL) was added triethyl amine (0.14g, 1.41mmol) and isopropyl isothiocyanate (0.09g, 0.94mmol) at 0 °C and the reaction mixture was slowly warmed to 30 °C and stirred at 30 °C for 6-8 hr (completion monitored through TLC and LCMS). The reaction mixture was washed with water (2 mL), brine (2 mL), dried over anhydrous sodium sulphate and evaporated in vacuo and resultant solid was purified by column chromatography to afford **RL_09** (0.17g, 68%) as off white solid. ^{1}H NMR (DMSO-d$_6$): δ_H. 6.10 (s, 1H), 5.02 (s, 1H), 4.62 (s, 1H), 4.15 (s, 1H), 3.72 (s, 3H), 3.40 (s, 1H), 2.18 (m, 2H), 2.15 (m, 2H), 2.02 (m, 2H), 1.13 (s, 3H), 1.11 (s, 3H). ^{13}C NMR (DMSO-d$_6$): δc 183.9, 172.1, 94.3, 67.8, 53.6 (2C), 30.8 (2C),

25.3 (2C), 15.1. ESI-MS *m/z* 261.14 (M+H)$^+$. Anal Calcd for $C_{11}H_{20}N_2O_3S$; C, 50.75; H, 7.74; N, 10.76; Found C, 50.70; H, 7.76; N, 10.75.

Preparation of Methyl-2-hydroxy-2-(1-(3-isopropylureido)cyclobutyl)acetate (RL_10) :
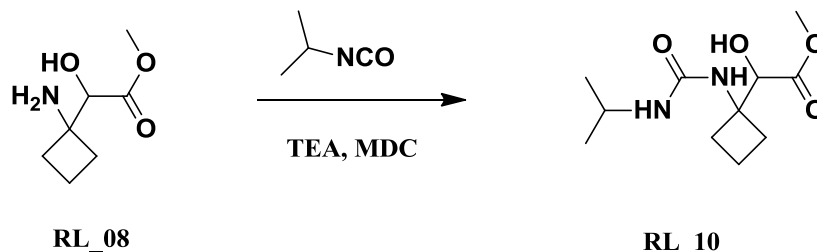
RL_08   **RL_10**

To a solution of methyl 2-(1-aminocyclobutyl)-2-hydroxyacetate (**RL_08**) (0.15g, 0.94mmol) in dry dichloromethane (3 mL) was added triethyl amine (0.14g, 1.41mmol) and isopropyl isocyanate (0.08g, 0.94mmol) at 0 °C and the reaction mixture was slowly warmed to 30 °C and stirred at 30 °C for 6-8 h (completion monitored through TLC and LCMS). The reaction mixture was washed with water (2 mL), brine (2 mL), dried over anhydrous sodium sulphate and evaporated in vacuo and resultant solid was purified by column chromatography to afford **RL_10** (0.15g, 65.22%) as off white solid. ^{1}H NMR (DMSO-d$_6$): δ_H 6.51 (s, 1H), 6.43 (s, 1H), 4.42 (s, 1H), 4.24 (s, 1H), 3.75 (s, 3H), 3.41 (s, 1H), 2.20 (m, 2H), 2.18 (m, 2H), 2.05 (m, 2H), 1.41 (s, 3H), 1.40 (s, 3H).^{13}C NMR (DMSO-d$_6$): δc 168.4, 154.2, 92.6, 64.7, 51.1, 41.7, 29.3 (2C), 21.8 (2C), 12.9. ESI-MS *m/z* 245.15 (M+H)$^+$. Anal Calcd for $C_{11}H_{20}N_2O_4$; C, 54.08; H, 8.25; N, 11.47; Found C, 54.02; H, 8.27; N, 11.45.

General procedure for the synthesis of urea/thiourea derivatives (RL_11-26):

RL_08   **RL_11 - RL_26**
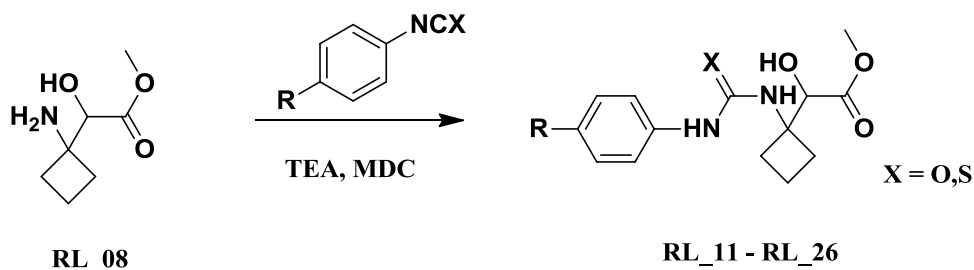
To a solution of methyl 2-(1-aminocyclobutyl)-2-hydroxyacetate (**RL_08**) (1 mmol) in dry dichloromethane (3 mL) was added triethyl amine (1.5 mmol) and the corresponding urea/thiourea (1 mmol) at 0 °C and the reaction mixture was slowly warmed to 30 °C and stirred at 30 °C for 6-8 h (completion monitored through TLC and LCMS). The reaction mixture was washed with water (2 mL), brine (2 mL), dried over anhydrous sodium sulphate and evaporated in vacuo to give the desired product as mentioned below.

102

Methyl-2-hydroxy-2-(1-(3-phenylthioureido)cyclobutyl)acetate (RL_11): The compound was synthesized according to the above general procedure using methyl 2-(1-aminocyclobutyl)-2-hydroxyacetate **(RL_08)** (0.15g, 0.94mmol), phenyl isothiocyanate (0.13g, 0.94mmol) and triethylamine (0.14g, 1.41mmol) to afford **RL_11** (0.2g, 71.43%) as off white solid. ^{1}H NMR (DMSO-d$_6$): δ_H 7.52 (m, 2H), 7.10 (t, J = 7.4 Hz, 2H), 6.78 (m, 1H), 6.27 (s, 1H), 5.13 (s, 1H), 4.12 (s, 1H), 3.69 (s, 3H), 3.29 (s, 1H), 2.14 (m, 2H), 2.10 (m, 2H), 2.02 (m, 2H).^{13}C NMR (DMSO-d$_6$): δc 184.3, 173.4, 135.6, 130.4 (2C), 129.7, 125.4 (2C), 90.3, 65.4, 55.3, 30.3 (2C), 14.9. ESI-MS m/z 295.11 (M+H)$^+$. Anal Calcd for C$_{14}$H$_{18}$N$_2$O$_3$S; C, 57.12; H, 6.16; N, 9.52; Found C, 57.18; H, 6.17; N, 9.54.

Methyl-2-(1-(3-(4-fluorophenyl)thioureido)cyclobutyl)-2-hydroxyacetate (RL_12): The compound was synthesized according to the above general procedure using methyl 2-(1-aminocyclobutyl)-2-hydroxyacetate **(RL_08)** (0.15g, 0.94mmol), 4-fluorophenyl isothiocyanate (0.14g, 0.94mmol) and triethylamine (0.14g, 1.41mmol) to afford **RL_12** (0.22g, 78.57%) as off white solid. ^{1}H NMR (DMSO-d$_6$): δ_H 6.84 (m, 2H), 6.29 (t, J = 8.2 Hz, 2H), 6.24 (s, 1H), 5.11 (s, 1H), 4.07 (s, 1H), 3.65 (s, 3H), 3.25 (s, 1H), 2.13 (m, 2H), 2.10 (m, 2H), 2.05 (m, 2H).^{13}C NMR (DMSO-d$_6$): δc 184.7, 172.5, 165.2, 136.8, 133.2(2C), 117.3(2C), 91.2, 66.4, 54.7, 31.3 (2C), 15.7. ESI-MS m/z 313.12 (M+H)$^+$. Anal Calcd for C$_{14}$H$_{17}$FN$_2$O$_3$S; C, 53.83; H, 5.49; N, 8.97; Found C, 53.77; H, 5.47; N, 8.99.

Methyl-2-(1-(3-(4-chlorophenyl)thioureido)cyclobutyl)-2-hydroxyacetate (RL_13): The compound was synthesized according to the above general procedure using methyl 2-(1-aminocyclobutyl)-2-hydroxyacetate **(RL_08)** (0.15g, 0.94mmol), 4-chlorophenyl isothiocyanate (0.16g, 0.94mmol) and triethylamine (0.14g, 1.41mmol) to afford **RL_13** (0.24g, 77.42%) as off white solid. ^{1}H NMR (DMSO-d$_6$): δ_H 7.14 (m, 2H), 6.70 (t, J = 7.2 Hz, 2H), 6.25 (s, 1H), 5.10 (s, 1H), 4.20 (s, 1H), 3.67 (s, 3H), 3.23 (s, 1H), 2.12 (m, 2H), 2.09 (m, 2H), 2.03 (m, 2H).^{13}C NMR (DMSO-d$_6$): δc 183.5, 171.9, 135.2, 134.8, 132.6 (2C), 129.3 (2C), 92.4, 67.8, 55.3, 32.6 (2C), 13.5. ESI-MS m/z 329.06 (M+H)$^+$. Anal Calcd for C$_{14}$H$_{17}$ClN$_2$O$_3$S; C, 51.14; H, 5.21; N, 8.52; Found C, 51.20; H, 5.23; N, 8.54.

Methyl-2-(1-(3-(4-bromophenyl)thioureido)cyclobutyl)-2-hydroxyacetate (RL_14): The compound was synthesized according to the above general procedure using methyl 2-(1-aminocyclobutyl)-2-hydroxyacetate (**RL_08**) (0.15g, 0.94mmol), 4-bromophenyl isothiocyanate (0.2g, 0.94mmol) and triethylamine (0.14g, 1.41mmol) to afford **RL_14** (0.23g, 65.71%) as off

white solid. ^{1}H NMR (DMSO-d$_6$): δ_H 7.22 (m, 2H), 6.67 (t, J = 7.2 Hz, 2H), 6.28 (s, 1H), 5.14 (s, 1H), 4.09 (s, 1H), 3.62 (s, 3H), 3.18 (s, 1H), 2.09 (m, 2H), 2.04 (m, 2H), 1.96 (m, 2H). ^{13}C NMR (DMSO-d$_6$): δc 180.2, 169.4, 136.3, 129.4 (4C), 120.2, 88.7, 63.5, 50.1, 27.4 (2C), 12.6. ESI-MS m/z 374.02 (M+H)$^+$. Anal Calcd for C$_{14}$H$_{17}$BrN$_2$O$_3$S; C, 45.05; H, 4.59; N, 7.50; Found C, 45.11; H, 4.60; N, 7.51.

Methyl-2-hydroxy-2-(1-(3-(4-nitrophenyl)thioureido)cyclobutyl)acetate (RL_15): The compound was synthesized according to the above general procedure using methyl 2-(1-aminocyclobutyl)-2-hydroxyacetate **(RL_08)** (0.15g, 0.94mmol), 4-nitrophenyl isothiocyanate (0.17g, 0.94mmol) and triethylamine (0.14g, 1.41mmol) to afford **RL_15** (0.23g, 71.88%) as yellow solid. ^{1}H NMR (DMSO-d$_6$): δ_H 7.98 (m, 2H), 6.47 (t, J = 8.2 Hz, 2H), 6.18 (s, 1H), 5.03 (s, 1H), 4.08 (s, 1H), 3.62 (s, 3H), 3.21 (s, 1H), 2.13 (m, 2H), 2.09 (m, 2H), 2.04 (m, 2H). ^{13}C NMR (DMSO-d$_6$): δc 184.8, 172.1, 145.2, 144.6, 125.6 (2C), 124.9 (2C), 92.3, 67.2, 54.6, 32.4(2C), 15.7. ESI-MS m/z 340.09 (M+H)$^+$. Anal Calcd for C$_{14}$H$_{17}$N$_3$O$_5$S; C, 49.55; H, 5.05; N, 12.38; Found C, 49.62; H, 5.03; N, 12.39.

Methyl-2-hydroxy-2-(1-(3-(p-tolyl)thioureido)cyclobutyl)acetate (RL_16): The compound was synthesized according to the above general procedure using methyl 2-(1-aminocyclobutyl)-2-hydroxyacetate (**RL_08)** (0.15g, 0.94mmol), p-tolyl isothiocyanate (0.14g, 0.94mmol) and triethylamine (0.14g, 1.41mmol) to afford **RL_16** (0.22g, 75.86%) as off white solid. ^{1}H NMR (DMSO-d$_6$): δ_H 6.82 (m, 2H), 6.21 (t, J = 7.2 Hz, 2H), 6.20 (s, 1H), 5.09 (s, 1H), 4.06 (s, 1H), 3.62 (s, 3H), 3.21 (s, 1H), 2.28 (s, 3H), 2.10 (m, 2H), 2.04 (m, 2H), 1.96 (m, 2H). ^{13}C NMR (DMSO-d$_6$): δc 180.1, 168.7, 135.6, 133.2, 127.4 (2C), 124.3 (2C), 88.7, 63.6, 50.2, 27.5 (2C), 19.6,12.5. ESI-MS m/z 308.16 (M+H)$^+$. Anal Calcd for C$_{15}$H$_{20}$N$_2$O$_3$S; C, 58.42; H, 6.54; N, 9.08; Found C, 58.48; H, 6.56; N, 9.06.

Methyl-2-hydroxy-2-(1-(3-(4-methoxyphenyl)thioureido)cyclobutyl)acetate (RL_17): The compound was synthesized according to the above general procedure using methyl 2-(1-aminocyclobutyl)-2-hydroxyacetate **(RL_08)** (0.15g, 0.94mmol), 4-methoxyphenyl isothiocyanate (0.16g, 0.94mmol) and triethylamine (0.14g, 1.41mmol) to afford **RL_17** (0.2g, 64.52%) as off white solid. ^{1}H NMR (DMSO-d$_6$): δ_H 6.61 (m, 2H), 6.24 (t, J = 7.8 Hz, 2H), 6.15 (s, 1H), 5.02 (s, 1H), 4.02 (s, 1H), 3.74 (s, 3H), 3.61 (s, 3H), 3.14 (s, 1H), 2.17 (m, 2H), 2.13 (m, 2H), 2.03 (m, 2H). ^{13}C NMR (DMSO-d$_6$): δc 183.8, 175.4, 162.9, 132.5, 129.1 (2C), 115.3 (2C),

92.5, 67.1, 57.4, 54.2,30.1 (2C), 15.3. ESI-MS *m/z* 325.31 (M+H)$^+$. Anal Calcd for C$_{15}$H$_{20}$N$_2$O$_4$S; C, 55.54; H, 6.21; N, 8.64; Found C, 55.61; H, 6.20; N, 8.65.

Methyl-2-(1-(3-(4-acetylphenyl)thioureido)cyclobutyl)-2-hydroxyacetate (RL_18): The compound was synthesized according to the above general procedure using methyl 2-(1-aminocyclobutyl)-2-hydroxyacetate **(RL_08)** (0.15g, 0.94mmol), 4-acetylphenyl isothiocyanate (0.17g, 0.94mmol) and triethylamine (0.14g, 1.41mmol) to afford **RL_18** (0.19g, 59.38%) as off white solid. ^{1}H NMR (DMSO-d$_6$): δ_H.7.47 (m, 2H), 6.37 (t, *J* = 7.4 Hz, 2H), 6.21 (s, 1H), 5.10 (s, 1H), 4.10 (s, 1H), 3.59 (s, 3H), 3.15 (s, 1H), 2.46 (s, 3H), 2.13 (m, 2H), 2.06 (m, 2H), 1.98 (m, 2H).^{13}C NMR (DMSO-d$_6$): δc 195.3, 181.5, 173.9, 144.3, 135.2, 129.8 (2C), 127.1 (2C), 91.2, 68.8, 54.2, 31.1 (2C), 25.3, 15.4. ESI-MS *m/z* 337.12 (M+H)$^+$. Anal Calcd for C$_{16}$H$_{20}$N$_2$O$_4$S; C, 57.12; H, 5.99; N, 8.33; Found C, 57.07; H, 6.01; N, 8.35.

Methyl-2-hydroxy-2-(1-(3-phenylureido)cyclobutyl)acetate (RL_19): The compound was synthesized according to the above general procedure using methyl 2-(1-aminocyclobutyl)-2-hydroxyacetate **(RL_08)** (0.15g, 0.94mmol), phenyl isocyanate (0.11g, 0.94mmol) and triethylamine (0.14g, 1.41 mmol) to afford **RL_19** (0.18g, 69.23%) as off white solid.^{1}H NMR (DMSO-d$_6$): δ_H.8.52 (s, 1H), 7.34 (m, 2H), 7.25 (t, *J* = 7.8 Hz, 2H), 6.95 (m, 1H),6.40 (s, 1H), 4.16 (s, 1H), 3.73 (s, 3H), 3.28 (s, 1H), 2.15 (m, 2H), 2.11 (m, 2H), 2.00 (m, 2H).^{13}C NMR (DMSO-d$_6$): δc 172.9, 153.8, 142.6, 130.2 (2C), 125.4, 119.7 (2C), 90.6, 62.5, 54.7, 25.2 (2C), 14.7. ESI-MS *m/z* 279.13 (M+H)$^+$. Anal Calcd for C$_{14}$H$_{18}$N$_2$O$_4$; C, 60.42; H, 6.52; N, 10.07; Found C, 60.45; H, 6.50; N, 10.05.

Methyl-2-(1-(3-(4-fluorophenyl)ureido)cyclobutyl)-2-hydroxy acetate (RL_20): The compound was synthesized according to the above general procedure using methyl 2-(1-aminocyclobutyl)-2-hydroxyacetate **(RL_08)** (0.15g, 0.94mmol), 4-fluorophenyl isocyanate (0.13g, 0.94mmol) and triethylamine (0.14g, 1.41 mmol) to afford **RL_ 20** (0.19g, 67.86%) as off white solid. ^{1}H NMR (DMSO-d$_6$): δ_H .8.53 (s, 1H), 7.33 (m, 2H), 7.01 (t, *J* = 8.0 Hz, 2H), 6.38 (s, 1H), 4.20 (s, 1H), 3.68 (s, 3H), 3.29 (s, 1H), 2.13 (m, 2H), 2.09 (m, 2H), 1.96 (m, 2H).^{13}C NMR (DMSO-d$_6$): δc 171.7, 164.9, 156.8, 137.4, 120.4 (2C), 116.3 (2C), 92.1, 62.4, 53.6, 30.5 (2C), 15.2. ESI-MS *m/z* 297.15 (M+H)$^+$. Anal Calcd for C$_{14}$H$_{17}$FN$_2$O$_4$; C, 56.75; H, 5.78; N, 9.45; Found C, 56.72; H, 5.80; N, 9.44.

Methyl-2-(1-(3-(4-chlorophenyl)ureido)cyclobutyl)-2-hydroxy acetate (RL_21): The compound was synthesized according to the above general procedure using methyl 2-(1-

aminocyclobutyl)-2-hydroxyacetate **(RL_08)** (0.15g, 0.94mmol), 4-chlorophenyl isocyanate (0.14g, 0.94mmol) and triethylamine (0.14g, 1.41mmol) to afford **RL_21** (0.21g, 72.41%) as off white solid. ^{1}H NMR (DMSO-d$_6$): δ_H 8.54 (s, 1H), 7.46 (m, 2H), 7.31 (t, J = 7.8 Hz, 2H), 6.41 (s, 1H), 4.18 (s, 1H), 3.70 (s, 3H), 3.26 (s, 1H), 2.11 (m, 2H), 2.09 (m, 2H), 1.98 (m, 2H).^{13}C NMR (DMSO-d$_6$): δc 172.1, 155.6, 136.2, 134.8, 131.2 (2C), 121.7 (2C), 91.4, 61.3, 53.8, 30.3 (2C), 14.4. ESI-MS m/z 313.08 (M+H)$^+$. Anal Calcd for $C_{14}H_{17}ClN_2O_4$; C, 53.77; H, 5.48; N, 8.96; Found C, 53.71; H, 5.47; N, 8.94.

Methyl-2-(1-(3-(4-bromophenyl)ureido)cyclobutyl)-2-hydroxy acetate (RL_22): The compound was synthesized according to the above general procedure using methyl 2-(1-aminocyclobutyl)-2-hydroxyacetate **(RL_08)** (0.15g, 0.94mmol), 4-bromophenyl isocyanate (0.19g, 0.94mmol) and triethylamine (0.14g, 1.41mmol) to afford **RL_22** (0.25g, 73.53%) as off white solid. ^{1}H NMR (DMSO-d$_6$): δ_H 8.49 (s, 1H), 7.41 (m, 2H), 7.35 (t, J = 7.4 Hz, 2H), 6.38 (s, 1H), 4.21 (s, 1H), 3.63 (s, 3H), 3.24 (s, 1H), 2.14 (m, 2H), 2.10 (m, 2H), 2.03 (m, 2H).^{13}C NMR (DMSO-d$_6$): δc 172.8, 156.2, 140.6, 133.5(2C), 124.6, 120.6 (2C), 90.1, 62.4, 54.5, 30.7(2C), 12.1. ESI-MS m/z 358.04 (M+H)$^+$. Anal Calcd for $C_{14}H_{17}BrN_2O_4$; C, 47.07; H, 4.80; N, 7.84; Found C, 47.00; H, 4.81; N, 7.82.

Methyl-2-hydroxy-2-(1-(3-(4-nitrophenyl)ureido)cyclobutyl)acetate (RL_23): The compound was synthesized according to the above general procedure using methyl 2-(1-aminocyclobutyl)-2-hydroxyacetate **(RL_08)** (0.15g, 0.94mmol), 4-nitrophenyl isocyanate (0.15g, 0.94mmol) and triethylamine (0.14g, 1.41mmol) to afford **RL_23** (0.25g, 80.65%) as yellow solid. ^{1}H NMR (DMSO-d$_6$): δ_H8.58 (s, 1H), 8.07 (m, 2H), 7.73 (t, J = 7.8 Hz, 2H), 6.46 (s, 1H), 4.28 (s, 1H), 3.64 (s, 3H), 3.17 (s, 1H), 2.18 (m, 2H), 2.15 (m, 2H), 2.04 (m, 2H).^{13}C NMR (DMSO-d$_6$): δc 172.5, 156.1, 147.2, 145.4, 125.6 (2C), 120.3 (2C), 91.6, 62.8, 54.1, 30.2(2C), 14.7. ESI-MS m/z 324.12 (M+H)$^+$. Anal Calcd for $C_{14}H_{17}N_3O_6$; C, 52.01; H, 5.30; N, 13.00; Found C, 52.08; H, 5.28; N, 13.01.

Methyl-2-hydroxy-2-(1-(3-(p-tolyl)ureido)cyclobutyl)acetate (RL_24): The compound was synthesized according to the above general procedure using methyl 2-(1-aminocyclobutyl)-2-hydroxyacetate **(RL_08)** (0.15g, 0.94mmol), p-tolyl isocyanate (0.13g, 1mmol) and triethylamine (0.14g, 1.41mmol) to afford **RL_24** (0.19g, 67.86%) as white solid. ^{1}H NMR (DMSO-d$_6$): δ_H 8.48 (s, 1H), 7.29 (m, 2H), 7.13 (t, J = 7.8 Hz, 2H), 6.35 (s, 1H), 4.12 (s, 1H), 3.70 (s, 3H), 3.24 (s, 1H), 2.28 (s, 3H), 2.11 (m, 2H), 2.06 (m, 2H), 1.96 (m, 2H).^{13}C NMR

(DMSO-d$_6$): δc 169.2, 153.7, 135.8, 135.1, 130.6 (2C), 122.7 (2C), 89.2, 58.3, 50.2, 29.4 (2C), 20.8, 12.6. ESI-MS m/z 293.15 (M+H)$^+$. Anal Calcd for C$_{15}$H$_{20}$N$_2$O$_4$; C, 61.63; H, 6.90; N, 9.58; Found C, 61.70; H, 6.89; N, 9.57.

Methyl-2-hydroxy-2-(1-(3-(4-methoxyphenyl)ureido)cyclobutyl)acetate (RL_25): The compound was synthesized according to the above general procedure using methyl 2-(1-aminocyclobutyl)-2-hydroxyacetate (**RL_08**) (0.15g, 0.94mmol), 4-methoxyphenyl isocyanate (0.14g, 0.94mmol) and triethylamine (0.14g, 1.41mmol) to afford **RL_25** (0.17g, 58.62%) as white solid. ^{1}H NMR (DMSO-d$_6$): δ_H 8.50 (s, 1H), 7.22 (m, 2H), 6.84 (t, J = 8.2 Hz, 2H), 6.32 (s, 1H), 4.20 (s, 1H), 3.79 (s, 3H), 3.65 (s, 3H), 3.18 (s, 1H), 2.12 (m, 2H), 2.07 (m, 2H), 1.98 (m, 2H).^{13}C NMR (DMSO-d$_6$): δc 174.1, 155.4, 151.6, 132.4, 120.6 (2C), 112.3 (2C), 90.7, 63.2, 57.3, 51.6, 25.3 (2C), 14.2. ESI-MS m/z 309.23 (M+H)$^+$. Anal Calcd for C$_{15}$H$_{20}$N$_2$O$_5$; C, 58.43; H, 6.54; N, 9.09; Found C, 58.49; H, 6.56; N, 9.07.

Methyl-2-(1-(3-(4-acetylphenyl)ureido)cyclobutyl)-2-hydroxy acetate (RL_26): The compound was synthesized according to the above general procedure using methyl 2-(1-aminocyclobutyl)-2-hydroxyacetate (**RL_08**) (0.15g, 0.94mmol), 4-acetylphenyl isocyanate (0.15g, 0.94mmol) and triethylamine (0.14g, 1.41mmol) to afford **RL_26** (0.18g, 60%) as off white solid. ^{1}H NMR (DMSO-d$_6$): δ_H 8.51 (s, 1H), 7.86 (m, 2H), 7.55 (t, J = 8.2 Hz, 2H), 6.38 (s, 1H), 4.22 (s, 1H), 3.72 (s, 3H), 3.21 (s, 1H), 2.42 (s, 3H), 2.08 (m, 2H), 2.02 (m, 2H), 1.94 (m, 2H).^{13}C NMR (DMSO-d$_6$): δc 196.4, 173.5, 156.2, 144.9, 138.3, 131.8 (2C), 122.3 (2C), 91.4, 61.5, 55.2, 29.7(2C), 25.8, 13.7. ESI-MS m/z 321.13 (M+H)$^+$. Anal Calcd for C$_{16}$H$_{20}$N$_2$O$_5$; C, 59.99; H, 6.29; N, 8.74; Found C, 59.93; H, 6.31; N, 8.76.

Procedure for the synthesis of Final compounds (RL_29-RL_44)

RL_09 - RL_26   RL_29 - RL_44

X = O,S
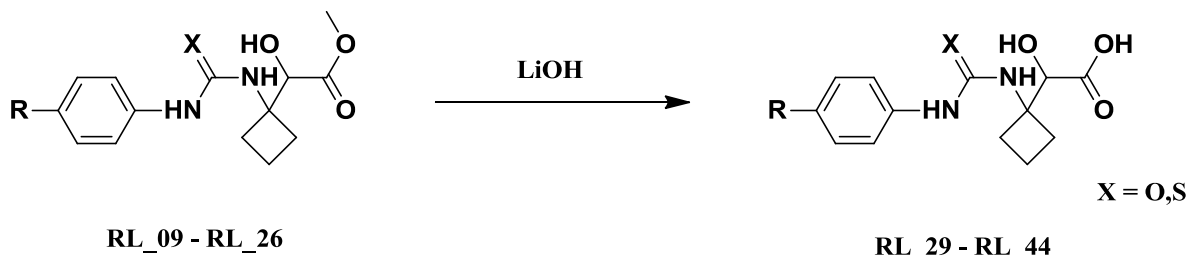
To solution of corresponding urea/ thiourea (1 mmol) in THF:water (3:1), LiOH (3 mmol) was added at 0 ^{o}C. The reaction mixture was allowed to stir at 30 ^{o}C for 6-8 hr (completion monitored through TLC and LCMS). The reaction mixture was concentrated under reduced pressure and diluted with water. The aqueous phase was washed with ethylacetate and then

acidified with 1N HCl. The acidic layer was extracted with ethylacetate (2*5ml) dried over anhydrous sodium sulphate and evaporated under reduced pressure to yield desired product as mentioned below.

Table 6.1: Physiochemical properties of the synthesized compounds **RL_27 – RL_44**
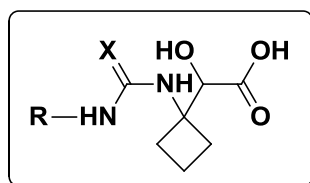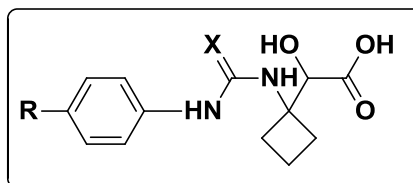
RL_27,28   RL_29-44

Cmpd.	R	X	Yield (%)	Molecular Formula	Molecular Weight
RL_27	(CH₃)₂CH-	S	68.73	$C_{10}H_{18}N_2O_3S$	246.33
RL_28	(CH₃)₂CH-	O	72.29	$C_{10}H_{18}N_2O_4$	230.26
RL_29	H	S	75.93	$C_{13}H_{16}N_2O_3S$	280.34
RL_30	F	S	66.67	$C_{13}H_{15}FN_2O_3S$	298.33
RL_31	Cl	S	45.33	$C_{13}H_{15}ClN_2O_3S$	314.79
RL_32	Br	S	45.44	$C_{13}H_{15}BrN_2O_3S$	359.24
RL_33	NO₂	S	66.67	$C_{13}H_{15}N_3O_5S$	325.34
RL_34	CH₃	S	66.67	$C_{14}H_{18}N_2O_3S$	294.37
RL_35	OCH₃	S	55.56	$C_{14}H_{18}N_2O_4S$	310.37
RL_36	COCH₃	S	77.78	$C_{15}H_{18}N_2O_4S$	322.38
RL_37	H	O	79.20	$C_{13}H_{16}N_2O_4$	264.28
RL_38	F	O	55.56	$C_{13}H_{15}FN_2O_4$	282.27
RL_39	Cl	O	45.44	$C_{13}H_{15}ClN_2O_4$	298.72
RL_40	Br	O	55.56	$C_{13}H_{15}BrN_2O_4$	343.17
RL_41	NO₂	O	77.78	$C_{13}H_{15}N_3O_6$	309.27
RL_42	CH₃	O	66.67	$C_{14}H_{18}N_2O_4$	278.30
RL_43	OCH₃	O	45.47	$C_{14}H_{18}N_2O_5$	294.30
RL_44	COCH₃	O	55.56	$C_{15}H_{18}N_2O_5$	306.31

6.1.3. Characterization of Synthesized compounds RL_27 - RL_44

2-Hydroxy-2-(1-(3-isopropylthioureido)cyclobutyl)acetic acid (RL_27): To solution of corresponding methyl-2-hydroxy-2-(1-(3-isopropylthioureido)cyclobutyl)acetate (**RL_09**) (0.1g, 0.38mmol) in THF:water (3:1), LiOH (0.05g, 1.14mmol) was added at 0 °C. The reaction mixture was allowed to stir at 30 °C for 6-8 h (completion monitored through TLC and LCMS). The reaction mixture was concentrated under reduced pressure and diluted with water. The aqueous phase was washed with ethylacetate and then acidified with 1N HCl. The acidic layer was extracted with ethylacetate (2*5ml) dried over anhydrous sodium sulphate and evaporated under reduced pressure and purified by column chromatography to yield **RL_27** (0.07g, 68.73%) as off white solid. ^{1}H NMR (DMSO-d$_6$): δ_H.11.98 (s, 1H), 6.13 (s, 1H), 5.00 (s, 1H), 4.63 (s, 1H),4.11 (s, 1H), 3.37 (s, 1H), 2.16 (m, 2H), 2.12 (m, 2H), 2.07 (m, 2H), 1.14 (s, 3H), 1.12 (s, 3H).^{13}C NMR (DMSO-d$_6$): δc 182.3, 175.6, 95.6, 69.5, 54.4, 32.7 (2C), 21.2 (2C), 12.5. ESI-MS m/z 245.11 (M-H)$^{+}$. Anal Calcd for $C_{10}H_{18}N_2O_3S$; C, 48.76; H, 7.37; N, 11.37; Found C, 48.74; H, 7.36; N, 11.39.

2-Hydroxy-2-(1-(3-isopropylureido)cyclobutyl)acetic acid (RL_28): To solution of methyl-2-hydroxy-2-(1-(3-isopropylureido)cyclobutyl)acetate (**RL_10**) (0.1g, 0.41mmol) in THF:water (3:1), LiOH (0.05g, 1.23mmol) was added at 0 °C. The reaction mixture was allowed to stir at 30 °C for 6-8 h (completion monitored through TLC and LCMS). The reaction mixture was concentrated under reduced pressure and diluted with water. The aqueous phase was washed with ethylacetate and then acidified with 1N HCl. The acidic layer was extracted with ethylacetate (2*5ml) dried over anhydrous sodium sulphate and evaporated under reduced pressure and purified by column chromatography to afford **RL_28** (0.07g, 72.29%) as off white solid. ^{1}H NMR (DMSO-d$_6$): δ_H. 11.82 (s, 1H),6.48 (s, 1H), 6.44 (s, 1H), 4.43 (s, 1H),4.21 (s, 1H), 3.38 (s, 1H), 2.23 (m, 2H), 2.19 (m, 2H), 2.03 (m, 2H), 1.40 (s, 3H), 1.38 (s, 3H).^{13}C NMR (DMSO-d$_6$): δc 177.8, 156.3, 90.6, 62.8, 46.8, 30.2 (2C), 19.6 (2C), 15.4. ESI-MS m/z 229.13 (M-H)$^{+}$. Anal Calcd for $C_{10}H_{18}N_2O_4$; C, 52.16; H, 7.88; N, 12.17; Found C, 52.09; H, 7.90; N, 12.18.

2-Hydroxy-2-(1-(3-phenylthioureido)cyclobutyl)acetic acid (RL_29): The compound was synthesized according to the above general procedure using methyl-2-hydroxy-2-(1-(3-phenylthioureido)cyclobutyl)acetate (**RL_ 11**)(0.1g, 0.34mmol) and LiOH (0.04g, 1.02mmol) to

afford **RL_29** (0.07g, 75.93%) as off white solid. ^{1}H NMR (DMSO-d$_6$): $\delta_{H.}$ 11.67 (s, 1H),7.55 (m, 2H), 7.14 (t, J = 8.2 Hz, 2H), 6.72 (m, 1H), 6.30 (s, 1H), 5.15 (s, 1H), 4.14 (s, 1H), 3.32 (s, 1H), 2.13 (m, 2H), 2.11 (m, 2H), 2.00 (m, 2H).^{13}C NMR (DMSO-d$_6$): δc 181.7, 172.5, 140.2, 132.4, 129.1 (2C), 124.2(2C), 94.6, 64.3, 32.4 (2C), 14.6. ESI-MS m/z 279.09 (M-H)$^+$. Anal Calcd for C$_{13}$H$_{16}$N$_2$O$_3$S; C, 55.70; H, 5.75; N, 9.99; Found C, 55.77; H, 5.76; N, 10.01.

2-(1-(3-(4-Fluorophenyl)thioureido)cyclobutyl)-2-hydroxyacetic acid (RL_30): The compound was synthesized according to the above general procedure using methyl**-**2-(1-(3-(4-fluorophenyl)thioureido)cyclobutyl)-2-hydroxyacetate (**RL_12**) (0.1g, 0.32mmol) and LiOH (0.04g, 0.96mmol) to afford **RL_30** (0.06g, 66.67%) as off white solid. ^{1}H NMR (DMSO-d$_6$): $\delta_{H.}$11.75 (s, 1H), 6.81 (m, 2H), 6.34 (t, J = 7.4 Hz, 2H), 6.22 (s, 1H), 5.08 (s, 1H), 4.04 (s, 1H), 3.28 (s, 1H), 2.14 (m, 2H), 2.11 (m, 2H), 2.03 (m, 2H).[13]C NMR (DMSO-d$_6$): δc 183.4, 171.3, 164.8, 133.2, 129.7 (2C), 114.7 (2C), 90.3, 64.2, 28.4 (2C), 12.9. ESI-MS m/z 297.10 (M-H)$^+$. Anal Calcd for C$_{13}$H$_{15}$FN$_2$O$_3$S; C, 52.34; H, 5.07; N, 9.39; Found C, 52.28; H, 5.05; N, 9.36.

2-(1-(3-(4-Chlorophenyl)thioureido)cyclobutyl)-2-hydroxyacetic acid (RL_31): The compound was synthesized according to the above general procedure using methyl**-**2-(1-(3-(4-chlorophenyl)thioureido)cyclobutyl)-2-hydroxyacetate (**RL_13**) (0.1g, 0.3mmol) and LiOH (0.04g, 0.9mmol) to afford **RL_31** (0.04g, 45.33%) as off white solid. ^{1}H NMR (DMSO-d$_6$): $\delta_{H.}$11.45 (s, 1H), 7.17 (m, 2H), 6.68 (t, J = 8.2 Hz, 2H), 6.21 (s, 1H), 5.07 (s, 1H), 4.24 (s, 1H), 3.21 (s, 1H), 2.16 (m, 2H), 2.12 (m, 2H), 2.04 (m, 2H).[13]C NMR (DMSO-d$_6$): δc 181.8, 169.3, 134.9, 132.7, 130.4 (2C), 128.2 (2C), 92.3, 66.4, 30.3 (2C), 11.2. ESI-MS m/z 313.05 (M-H)$^+$. Anal Calcd for C$_{13}$H$_{15}$ClN$_2$O$_3$S; C, 49.60; H, 4.80; N, 8.90; Found C, 49.55; H, 4.78; N, 8.92.

2-(1-(3-(4-Bromophenyl)thioureido)cyclobutyl)-2-hydroxyacetic acid (RL_32): The compound was synthesized according to the above general procedure using methyl**-**2-(1-(3-(4-bromophenyl)thioureido)cyclobutyl)-2-hydroxyacetate (**RL_14**) (0.1g, 0.27mmol) and LiOH (0.03g, 0.81mmol) to afford **RL_32** (0.04g, 45.44%) as off white solid. ^{1}H NMR (DMSO-d$_6$): $\delta_{H.}$11.62 (s, 1H), 7.26 (m, 2H), 6.70 (t, J = 7.2 Hz, 2H), 6.32 (s, 1H), 5.11 (s, 1H), 4.04 (s, 1H), 3.22 (s, 1H), 2.11 (m, 2H), 2.04 (m, 2H), 1.95 (m, 2H).[13]C NMR (DMSO-d$_6$): δc 181.4, 175.2, 138.4, 131.6 (4C), 121.4, 91.6, 64.3, 30.2 (2C), 13.6. ESI-MS m/z 358.00 (M-H)$^+$. Anal Calcd for C$_{13}$H$_{15}$BrN$_2$O$_3$S; C, 43.46; H, 4.21; N, 7.80; Found C, 43.51; H, 4.19; N, 7.81.

2-Hydroxy-2-(1-(3-(4-nitrophenyl)thioureido)cyclobutyl)acetic acid (RL_33): The compound was synthesized according to the above general procedure using methyl-2-hydroxy-2-(1-(3-(4-nitrophenyl)thioureido)cyclobutyl)acetate (**RL_15**) (0.1g, 0.29mmol) and LiOH (0.04g, 0.87mmol) to afford **RL_33** (0.06g, 66.67%) as yellow solid. ^{1}H NMR (DMSO-d$_6$): δ_{H} 11.65 (s, 1H), 8.02 (m, 2H), 6.45 (t, J = 7.8 Hz, 2H), 6.21 (s, 1H), 5.04 (s, 1H), 4.04 (s, 1H), 3.19 (s, 1H), 2.14 (m, 2H), 2.11 (m, 2H), 2.06 (m, 2H). ^{13}C NMR (DMSO-d$_6$): δc 181.7, 171.5, 143.8, 142.1, 122.5 (2C), 121.7 (2C), 90.4, 64.8, 32.4 (2C), 16.3. ESI-MS m/z 324.07 (M-H)$^+$. Anal Calcd for C$_{13}$H$_{15}$N$_3$O$_5$S; C, 47.99; H, 4.65; N, 12.92; Found C, 48.06; H, 4.63; N, 12.91.

2-Hydroxy-2-(1-(3-(p-tolyl)thioureido)cyclobutyl)acetic acid (RL_34): The compound was synthesized according to the above general procedure using methyl-2-hydroxy-2-(1-(3-(p-tolyl)thioureido)cyclobutyl)acetate (**RL_16**) (0.1g, 0.32mmol) and LiOH (0.04g, 0.96mmol) to afford **RL_34** (0.06g, 66.67%) as off white solid. ^{1}H NMR (DMSO-d$_6$): δ_{H} 11.47 (s, 1H), 6.84 (m, 2H), 6.24 (t, J = 8.0 Hz, 2H), 6.22 (s, 1H), 5.11 (s, 1H), 4.04 (s, 1H), 3.25 (s, 1H), 2.30 (s, 3H), 2.08 (m, 2H), 2.04 (m, 2H), 1.92 (m, 2H). ^{13}C NMR (DMSO-d$_6$): δc 184.6, 175.4, 136.2, 134.3, 130.4 (2C), 127.2 (2C), 94.5, 64.2, 32.1 (2C), 20.3,12.9. ESI-MS m/z 293.10 (M-H)$^+$. Anal Calcd for C$_{14}$H$_{18}$N$_2$O$_3$S; C, 57.12; H, 6.16; N, 9.52; Found C, 57.07; H, 6.15; N, 9.51.

2-Hydroxy-2-(1-(3-(4-methoxyphenyl)thioureido)cyclobutyl)acetic acid (RL_35): The compound was synthesized according to the above general procedure using methyl-2-hydroxy-2-(1-(3-(4-methoxyphenyl)thioureido)cyclobutyl)acetate (**RL_17**) (0.1g, 0.31mmol) and LiOH (0.04g, 0.93mmol) to afford **RL_35** (0.05g, 55.56%) as off white solid. ^{1}H NMR (DMSO-d$_6$): δ_{H} 11.63 (s, 1H), 6.58 (m, 2H), 6.22 (t, J = 8.0 Hz, 2H), 6.13 (s, 1H), 4.99 (s, 1H), 4.04 (s, 1H), 3.71 (s, 3H), 3.12 (s, 1H), 2.11 (m, 2H), 2.08 (m, 2H), 2.01 (m, 2H). ^{13}C NMR (DMSO-d$_6$): δc 184.3, 172.1, 155.4, 128.6, 125.8 (2C), 112.4 (2C), 90.2, 66.2, 57.4,30.4 (2C), 13.7. ESI-MS m/z 309.10 (M-H)$^+$. Anal Calcd for C$_{14}$H$_{18}$N$_2$O$_4$S; C, 54.18; H, 5.85; N, 9.03; Found C, 54.11; H, 5.87; N, 9.02.

2-(1-(3-(4-Acetylphenyl)thioureido)cyclobutyl)-2-hydroxyacetic acid (RL_36): The compound was synthesized according to the above general procedure using methyl-2-(1-(3-(4-acetylphenyl)thioureido)cyclobutyl)-2-hydroxyacetate (**RL_18**) (0.1g, 0.29mmol) and LiOH (0.04g, 0.87mmol) to afford **RL_36** (0.07g, 77.78%) as off white solid. ^{1}H NMR (DMSO-d$_6$): δ_{H} 11.64 (s, 1H), 7.45 (m, 2H), 6.34 (t, J = 8.2 Hz, 2H), 6.19 (s, 1H), 5.06 (s, 1H), 4.04 (s, 1H),

3.12 (s, 1H), 2.42 (s, 3H), 2.10 (m, 2H), 2.04 (m, 2H), 1.97 (m, 2H).^{13}C NMR (DMSO-d$_6$): δc 193.4, 184.6, 175.8, 142.8, 132.9, 127.2 (2C), 124.3 (2C), 88.4, 63.7, 25.6 (2C), 23.1, 11.5. ESI-MS m/z 321.10 (M-H)$^+$. Anal Calcd for C$_{15}$H$_{18}$N$_2$O$_4$S; C, 55.88; H, 5.63; N, 8.69; Found C, 55.95; H, 5.65; N, 8.71.

2-Hydroxy-2-(1-(3-phenylureido)cyclobutyl)acetic acid (RL_37): The compound was synthesized according to the above general procedure using methyl-2-hydroxy-2-(1-(3-phenylureido)cyclobutyl)acetate (**RL_19**) (0.1g, 0.36mmol) and LiOH (0.05g, 1.08mmol) to **RL_37** (0.08g, 79.20%) as off white solid. ^{1}H NMR (DMSO-d$_6$): δ_H 11.58 (s, 1H), 8.55 (s, 1H), 7.36 (m, 2H), 7.24 (t, J = 8.0 Hz, 2H), 6.92 (m, 1H), 6.43 (s, 1H), 4.24 (s, 1H), 3.32 (s, 1H), 2.16 (m, 2H), 2.14 (m, 2H), 2.01 (m, 2H).^{13}C NMR (DMSO-d$_6$): δc 171.8, 154.8, 140.6, 129.4 (2C), 128.2, 121.2 (2C), 94.8, 36.2, 31.2 (2C), 17.8. ESI-MS m/z 263.12 (M+H)$^+$. Anal Calcd for C$_{13}$H$_{16}$N$_2$O$_4$; C, 59.08; H, 6.10; N, 10.60; Found C, 59.14; H, 6.09; N, 10.58.

2-(1-(3-(4-Fluorophenyl)ureido)cyclobutyl)-2-hydroxy acetic acid (RL_38): The compound was synthesized according to the above general procedure using methyl-2-(1-(3-(4-fluorophenyl)ureido)cyclobutyl)-2-hydroxy acetate (**RL_20**) (0.1g, 0.34mmol) and LiOH (0.04g, 1.02mmol) to afford **RL_38** (0.05g, 55.56%) as off white solid. ^{1}H NMR (DMSO-d$_6$): δ_H 11.62 (s, 1H), 8.56 (s, 1H), 7.31 (m, 2H), 7.04 (t, J = 7.8 Hz, 2H), 6.34 (s, 1H), 4.22 (s, 1H), 3.31 (s, 1H), 2.12 (m, 2H), 2.11 (m, 2H), 1.98 (m, 2H).^{13}C NMR (DMSO-d$_6$): δc 172.3, 163.7, 155.4, 136.2, 118.6 (2C), 118.8 (2C), 93.7, 61.3, 29.1 (2C), 14.6. ESI-MS m/z 281.32 (M-H)$^+$. Anal Calcd for C$_{13}$H$_{15}$FN$_2$O$_4$; C, 55.32; H, 5.36; N, 9.92; Found C, 55.28; H, 5.37; N, 9.94.

2-(1-(3-(4-Chlorophenyl)ureido)cyclobutyl)-2-hydroxyacetic acid (RL_39): The compound was synthesized according to the above general procedure using methyl-2-(1-(3-(4-chlorophenyl)ureido)cyclobutyl)-2-hydroxy acetate (**RL_21**) (0.1g, 0.32mmol) and LiOH (0.04g, 0.96mmol) to afford **RL_39** (0.04g, 45.44%) as off white solid. ^{1}H NMR (DMSO-d$_6$): δ_H 11.51 (s, 1H), 8.52 (s, 1H), 7.43 (m, 2H), 7.28 (t, J = 7.8 Hz, 2H), 6.45 (s, 1H), 4.16 (s, 1H), 3.31 (s, 1H), 2.12 (m, 2H), 2.08 (m, 2H), 1.97 (m, 2H).^{13}C NMR (DMSO-d$_6$): δc 171.6, 155.3, 138.4, 135.2, 129.1 (2C), 123.5 (2C), 93.7, 59.4, 30.6 (2C), 11.8. ESI-MS m/z 297.10 (M-H)$^+$. Anal Calcd for C$_{13}$H$_{15}$ClN$_2$O$_4$; C, 52.27; H, 5.06; N, 9.38; Found C, 52.21; H, 5.07; N, 9.39.

2-(1-(3-(4-Bromophenyl)ureido)cyclobutyl)-2-hydroxyacetic acid (RL_40): The compound was synthesized according to the above general procedure using methyl-2-(1-(3-(4-bromophenyl)ureido)cyclobutyl)-2-hydroxy acetate (**RL_22**) (0.1g, 0.28mmol) and LiOH (0.04g, 0.84mmol) to afford **RL_40** (0.05g, 55.56%) as off white solid. ^{1}H NMR (DMSO-d$_6$): δ_H 11.49 (s, 1H), 8.52 (s, 1H), 7.38 (m, 2H), 7.38 (t, J = 8.4 Hz, 2H), 6.34 (s, 1H), 4.23 (s, 1H), 3.27 (s, 1H), 2.11 (m, 2H), 2.07 (m, 2H), 2.02 (m, 2H). ^{13}C NMR (DMSO-d$_6$): δc 174.1, 155.3, 139.2, 132.7 (2C), 120.3, 119.2 (2C), 91.7, 61.7, 29.6 (2C), 11.7. ESI-MS m/z 342.07 (M-H)$^+$. Anal Calcd for C$_{13}$H$_{15}$BrN$_2$O$_4$; C, 45.50; H, 4.41; N, 8.16; Found C, 45.44; H, 4.40; N, 8.18.

2-Hydroxy-2-(1-(3-(4-nitrophenyl)ureido)cyclobutyl)acetic acid (RL_41): The compound was synthesized according to the above general procedure using methyl-2-hydroxy-2-(1-(3-(4-nitrophenyl)ureido)cyclobutyl)acetate (**RL_23**) (0.1g, 0.31mmol) and LiOH (0.04g, 0.93mmol)to afford **RL_41** (0.07g, 77.78%) as yellow solid. ^{1}H NMR (DMSO-d$_6$): δ_H 11.72 (s, 1H),8.61 (s, 1H), 8.11 (m, 2H), 7.75 (t, J = 8.2 Hz, 2H), 6.43 (s, 1H), 4.25 (s, 1H), 3.20 (s, 1H), 2.16 (m, 2H), 2.13 (m, 2H), 2.03 (m, 2H). ^{13}C NMR (DMSO-d$_6$): δc 174.3, 155.7, 146.4, 144.2, 122.7 (2C), 117.8 (2C), 93.4, 61.4, 29.4 (2C), 12.9. ESI-MS m/z 308.10 (M-H)$^+$. Anal Calcd for C$_{13}$H$_{15}$N$_3$O$_6$; C, 50.49; H, 4.89; N, 13.59; Found C, 50.42; H, 4.88; N, 13.61.

2-Hydroxy-2-(1-(3-(*p*-tolyl)ureido)cyclobutyl)acetic acid (RL_42): The compound was synthesized according to the above general procedure using methyl-2-hydroxy-2-(1-(3-(*p*-tolyl)ureido)cyclobutyl)acetate (**RL_24**) (0.1g, 0.34mmol) and LiOH (0.04g, 1.02mmol) to afford **RL_42** (0.06g, 66.67%) as white solid. ^{1}H NMR (DMSO-d$_6$): δ_H 11.42 (s, 1H), 8.46 (s, 1H), 7.30 (m, 2H), 7.12 (t, J = 7.2 Hz, 2H), 6.32 (s, 1H), 4.14 (s, 1H), 3.27 (s, 1H), 2.31 (s, 3H), 2.14 (m, 2H), 2.10 (m, 2H), 2.04 (m, 2H). ^{13}C NMR (DMSO-d$_6$): δc 174.7, 155.2, 135.5, 134.8, 131.4 (2C), 123.2 (2C), 93.8, 62.4, 30.3 (2C), 22.5,14.2. ESI-MS m/z 277.10 (M-H)$^+$. Anal Calcd for C$_{14}$H$_{18}$N$_2$O$_4$; C, 60.42; H, 6.52; N, 10.07; Found C, 60.49; H, 6.51; N, 10.06.

2-Hydroxy-2-(1-(3-(4-methoxyphenyl)ureido)cyclobutyl)acetic acid (RL_43): The compound was synthesized according to the above general procedure using methyl-2-hydroxy-2-(1-(3-(4-methoxyphenyl)ureido)cyclobutyl)acetate (**RL_25**) (0.1g, 0.32mmol) and LiOH (0.04g, 0.96mmol) to afford **RL_43** (0.04g, 45.47%) as white solid. ^{1}H NMR (DMSO-d$_6$): δ_H 11.54 (s, 1H), 8.47 (s, 1H), 7.19 (m, 2H), 6.82 (t, J = 8.2 Hz, 2H), 6.30 (s, 1H), 4.18 (s, 1H), 3.81 (s, 3H), 3.15 (s, 1H), 2.09 (m, 2H), 2.04 (m, 2H), 1.95 (m, 2H). ^{13}C NMR (DMSO-d$_6$): δc 175.8, 162.7,

156.4, 135.2, 124.1(2C), 116.8 (2C), 95.9, 63.4, 56.4, 32.4 (2C), 15.4. ESI-MS *m/z* 293.10 (M-H)$^{+}$. Anal Calcd for $C_{14}H_{18}N_2O_5$; C, 57.13; H, 6.16; N, 9.52; Found C, 57.08; H, 6.17; N, 9.54.

2-(1-(3-(4-Acetylphenyl)ureido)cyclobutyl)-2-hydroxyacetic acid (RL_44): The compound was synthesized according to the above general procedure using methyl**-**2-(1-(3-(4-acetylphenyl)ureido)cyclobutyl)-2-hydroxy acetate (**RL_26**) (0.1g, 0.31mmol) and LiOH (0.04g, 0.93mmol) to afford **RL_44** (0.05g, 55.56%) as off white solid. ^{1}H NMR (DMSO-d$_6$): $\delta_{\text{H.}}$ 11.71 (s, 1H), 8.47 (s, 1H), 7.84 (m, 2H), 7.53 (t, *J* = 8.2 Hz, 2H), 6.39 (s, 1H), 4.24 (s, 1H), 3.22 (s, 1H), 2.44 (s, 3H), 2.06 (m, 2H), 2.01 (m, 2H), 1.92 (m, 2H).^{13}C NMR (DMSO-d$_6$): δc 192.1, 170.6, 158.7, 145.8, 132.8, 125.9(2C), 120.7 (2C), 88.2, 59.7, 27.3 (2C), 24.9, 11.5. ESI-MS *m/z* 305.12 (M-H)$^{+}$. Anal Calcd for $C_{15}H_{18}N_2O_5$; C, 58.82; H, 5.92; N, 9.15; Found C, 58.89; H, 5.90; N, 9.17.

6.1.4. *In vitro* LAT inhibitory assay, antimycobacterial potency and cytotoxicity studies of the synthesized molecules

LAT enzyme during dormancy is associated with regulation of amino acid pool which inturn regulates Guanosine 3$^{'}$,5$^{'}$ bispyrophosphate, key molecule in antibiotic resistance and bacterial persistence. LAT enzyme catalyses transfer of amine from lysine to ketoglutarate resulting in formation of piperidine-6-carboxylate and glutamate. The resultant products have absorbance maxima at 465 and 280 nm which is used for measuring inhibitory potential of synthesized compounds. All the synthesized compounds were evaluated for their inhibitory potency against LAT enzyme and 7 compounds were found to be potent when compared to lead compound (IC$_{50}$: 8.16 µM). 5 compounds have IC$_{50}$ lower than 5 µM. The results are final compounds were tabulated in **Table 6.2.** The most potent compound among the series was found to **RL_33** with an IC$_{50}$ of 2.09 ± 0.21µM, whose dose response curve has been given in **Fig 6.3**.

114
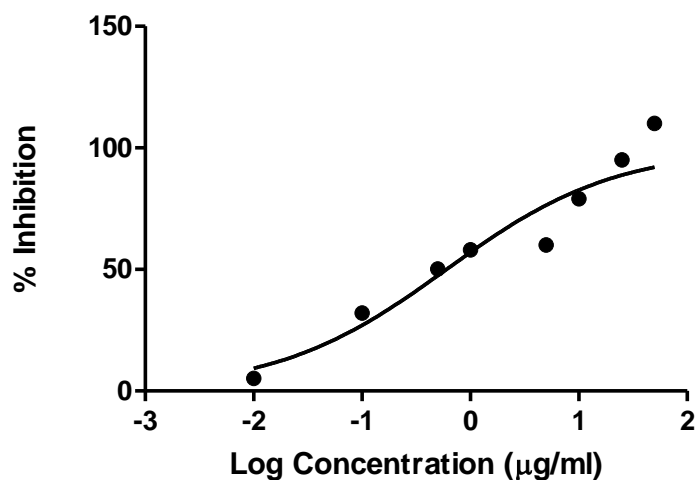
Fig 6.3: Dose response curve of active compound **RL_33**

The antimycobacterial potency of compounds was further evaluated by MABA assay and the MIC values were found to be in range of 2.46 – 76.48 μM. The compounds safety profile was analysed by testing against RAW cell lines at a concentration of 50 μg/ml. Percentage inhibition was found to be in range of 3.02 – 48.93 % so most of the compounds are devoid of cytotoxicity.

Table 6.2: *In vitro* biological evaluation of the synthesized compounds **RL_27 –44**
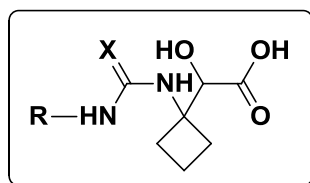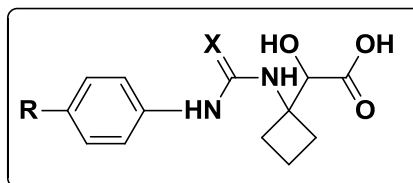
RL_27-28   RL_29-44

Cmpd.	R	X	LAT (IC$_{50}$) μM	MIC μM	Cytotoxicity (% inhi) at 50 μg/ml
RL_27	(CH$_3$)$_2$CH-	S	100.15 ±1.69	50.75	13.35 ±0.89
RL_28	(CH$_3$)$_2$CH-	O	3.26 ± 0.23	54.29	17.54 ±0.64
RL_29	H	S	14.83 ± 0.85	44.59	5.43 ±0.31
RL_30	F	S	>83.79 ±1.23	41.89	44.84 ±0.28

RL_31	Cl	S	2.47 ± 0.41	39.71	26.72 ±0.91
RL_32	Br	S	12.43 ± 0.64	8.69	26.92 ±1.31
RL_33	NO_2	S	2.09 ± 0.21	76.84	12.36 ±0.73
RL_34	CH_3	S	6.18 ± 0.51	10.62	16.42 ±0.47
RL_35	OCH_3	S	2.84 ± 0.17	20.14	48.93 ±0.93
RL_36	$COCH_3$	S	>77.55 ± 1.52	4.85	18.32 ±0.76
RL_37	H	O	5.83 ± 0.37	2.88	20.87 ±0.32
RL_38	F	O	18.59 ± 0.42	2.69	12.78 ± 0.48
RL_39	Cl	O	27.91 ± 0.76	2.54	21.03 ±0.63
RL_40	Br	O	2.44 ± 0.89	18.21	46.89 ±1.82
RL_41	NO_2	O	>80.84 ± 0.77	2.46	3.02 ±0.32
RL_42	CH_3	O	53.03 ± 0.81	5.61	48.93 ±0.96
RL_43	OCH_3	O	33.74 ± 0.94	21.24	44.32 ±0.72
RL_44	$COCH_3$	O	51.51 ± 1.62	2.48	13.35 ±0.33
INH			--	0.4	--
RIF			--	0.5	--

IC$_{50}$ – 50% inhibitory concentration, **MIC** – minimum inhibitory concentration, **inhi**- inhibition, **INH-** isoniazid, **RIF-** Rifampicin

Further to support the activity we performed docking for these compounds. All the compounds were docked in to the active site of *Mtb* LAT protein using programme Glide (Glide v5.7, Schrodinger, LLC, New York, NY). First the reference ligand α-ketoglutarate was re-docked into the active site of *Mtb* LAT to validate the active site cavity. The reference ligand exhibited highest glide score of -6.04 kcal/mol and was found in the vicinity of the Arg422, Gln274, Lys300, Arg170, Phe167, Glu243 amino acid residues. Further, re-docking results with ligand preparation showed that this ligand exhibited similar interactions as that of the original crystal structure with an RMSD of 0.24 Å as illustrated in **Fig 6.4**. The active site of the *Mtb* LAT protein is small, thus due to the inherent flexibility of this side chain, this is more likely simply a favourable electrostatic interaction. The hydrophobic pocket of *Mtb* LAT is defined by the side chains of Phe415, Leu414, Val63, and Phe167.

116
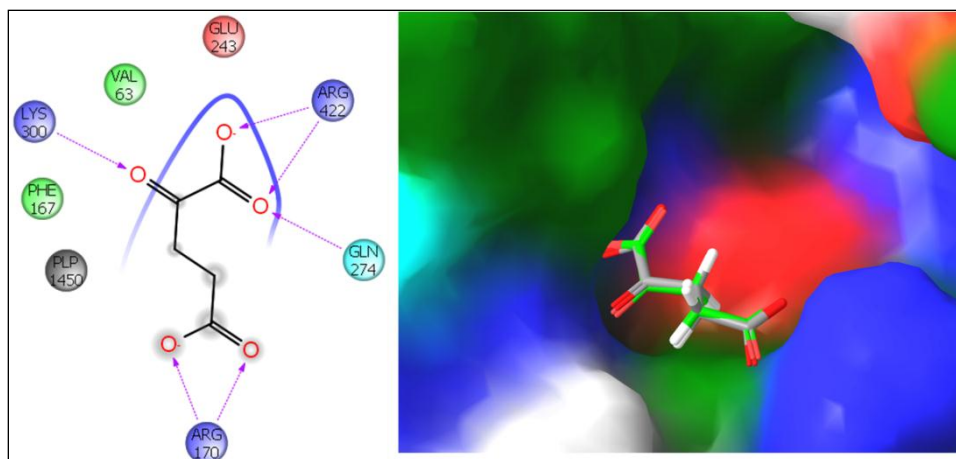
Fig 6.4: Interactions of reference inhibitor with the active site residues of *Mtb* LAT and superimposition of docked pose of the reference ligand to the original pose of the ligand.

Among the urea derivatives, at R position substitutions with Br and IPr at R exhibited good activity (**RL_40** and **RL_28**), while substitution with NO_2 (**RL_41**) group at R_1 showed moderate activity as compared to other substitutions. A closer look into the interaction profile of active molecules revealed that the O of urea and carboxylic acid was involved in a prominent hydrogen bonding interaction with Lys300, Arg170, Arg422 and Gln274 analogous to the observed in the crystal ligand. **RL_40** and **RL_28** also showed additional hydrophobic contact with Ile184, Phe167, Val63 and Pro145 due to which was found to display good binding with a docking score of -6.74 and -6.50 kcal/mol (**Fig 6.5**).
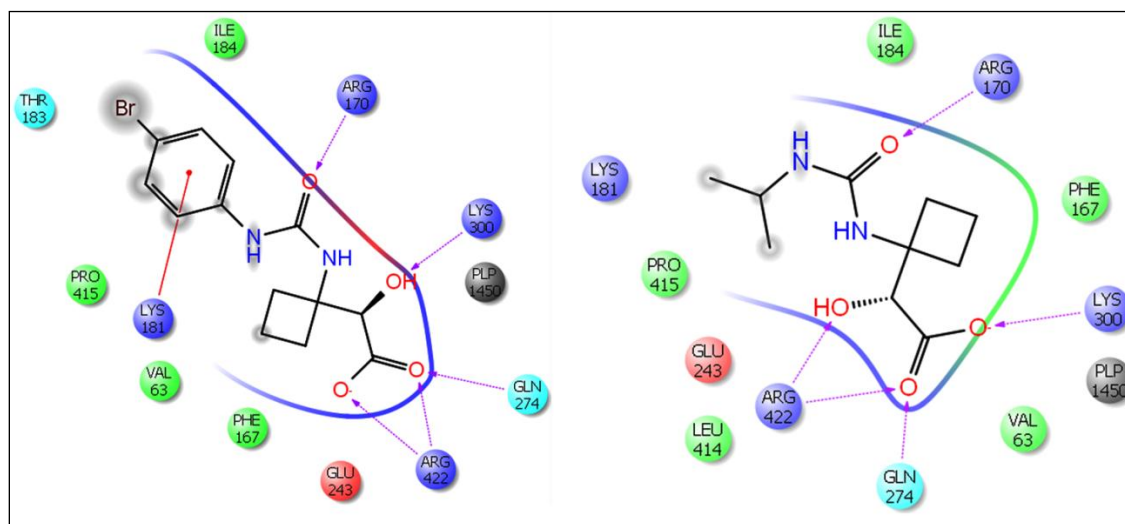
Figure 6.5: Binding pose and its interaction pattern of the **RL_40** and **RL_28.**

However it was surprising to note that replacement with NO_2 substituent (**RL_41**) on the R_1 position led to a reduction in the activity as indicated in their interaction profile where the molecule was found to be in a slightly different orientation/pose compared to that of **RL_ 40** and **RL_28** thereby losing the hydrogen bonding interaction with the protein as presented in **Fig 6.6**.
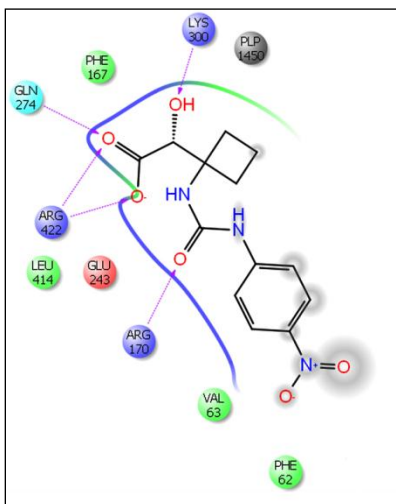
Fig 6.6: Binding pose and its interaction pattern of the **RL_41.**

In the next subset of synthesized compounds, thioureas the effects of similar substituent's were explored at R_1 positions on left and right sides of cyclobutyl having S (sulphur) group instead of O (oxygen) at the R position. Among the nine synthesized compounds in this set, three compounds where R_1 is substituted with OCH_3, Cl and NO_2 group (**RL_35, RL_31** and **RL_33**) inhibited *Mtb* LAT enzyme activity with sub micromolar range. *In silico* analysis of these compounds indicated that the molecules oriented in a similar manner as that of reference compound retaining hydrogen bonding with Lys300, Arg170, Arg422 and Gln274 and other significant hydrophobic interactions as shown in **Fig 6.7**. All the compounds were well inserted into the active site pocket which made these compounds better among all the compounds that showed good binding with the receptor (-6.78, -6.86 and -6.50 kcal/mol).
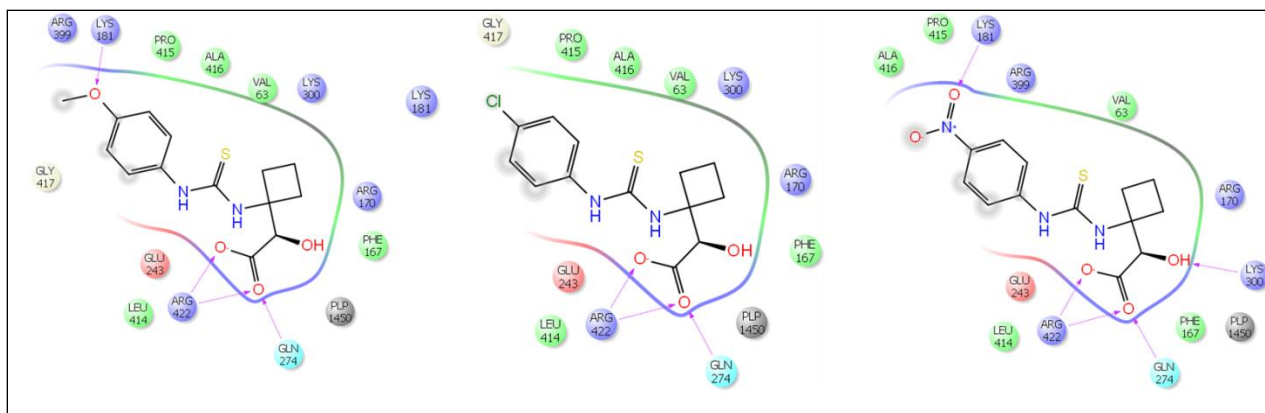
Fig 6.7: Binding pose and its interaction pattern of the **RL_ 35, RL_31** and **RL_33.**

Binding analysis of least active compounds from this set of compounds revealed that they were oriented differently when compared to active compounds. 4-Fluoro or Acetyl group at R_1 position was displaced out of the pocket due to which the activity of molecules (**RL_30** and **RL_36**) could have been affected, as shown in **Fig 6.8.**
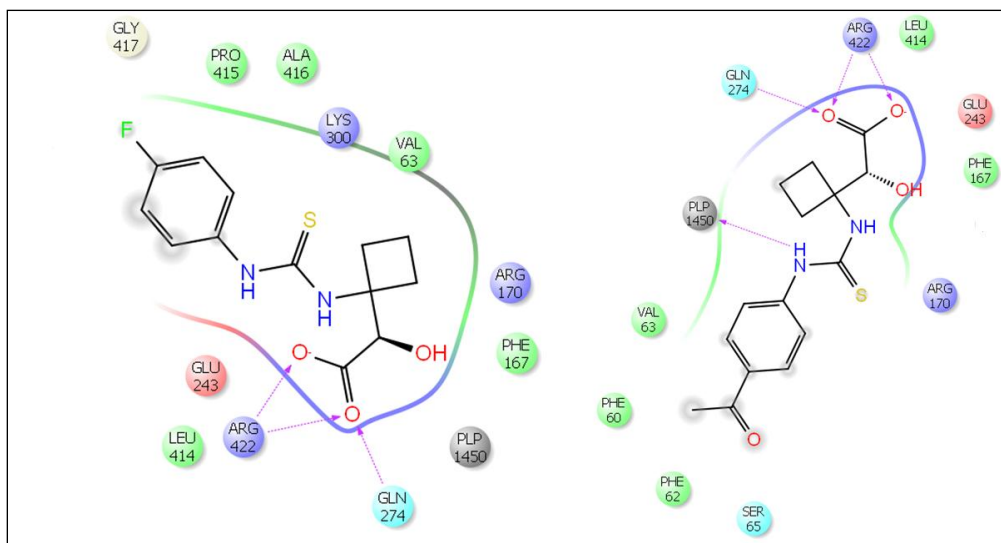
Fig 6.8: Binding pose and its interaction pattern of the **RL_30** and **RL_36.**

6.1.5. Nutrient starvation model

Dormant TB characterized by many changes in the phenotype as well as genotype. Phenotypic changes include drug tolerance, morphology, cell wall thickness and permeability. Genotype variations are downregulation of metabolic genes, replication machinery and upregulation of various enzymes. All these characteristics are observed in nutrient starvation model. As LAT

enzyme is involved in persistence and antibiotic tolerance it was found to 40 fold overexpressed in nutrient starvation model. Compounds were tested against 6 weeks starved *Mtb* culture at a concentration of 10 μg/ml. In this model **RL_37** emerged as most potent as it exhibited log reduction of 2.9 fold. **RL_34** also exhibited significant log reduction of 2.7 fold in this model. These two compounds were potent when compared to first line drugs Isoniazid (1.2 fold), Rifampicin (1.3 fold) and Moxifloxacin (2.2 fold). The most potent **RL_33** according to LAT inhibitory potential shows 2.0 fold reduction (**Fig 6.9**).
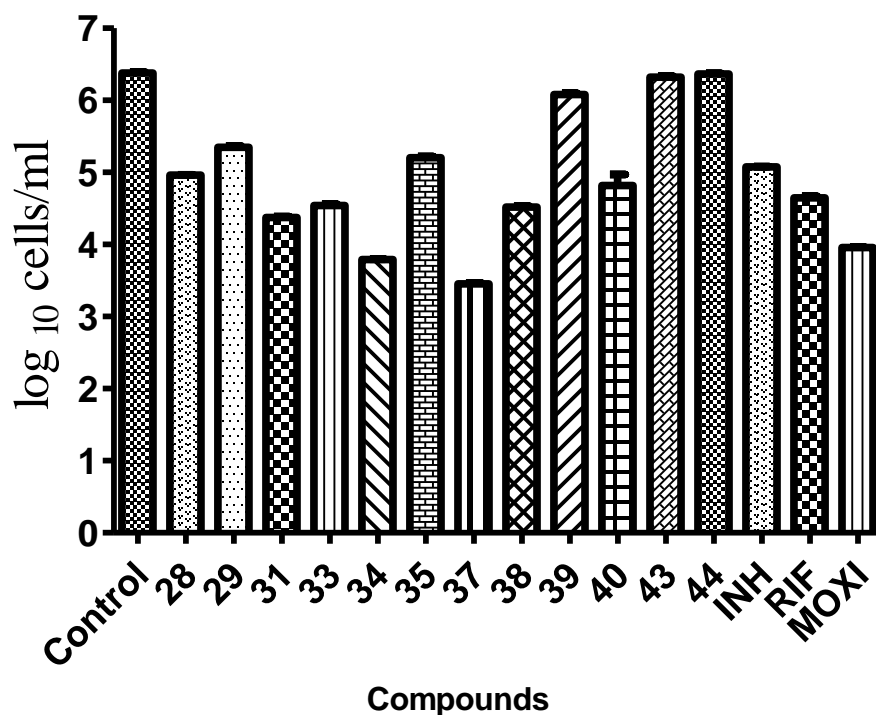
Fig 6.9: Biological activities of the synthesized compounds against *M. tuberculosis* in the nutrient starvation model. Bacterial count estimation (Mean ± S.D., n = 3) for control and treated groups conducted by using the MPN (most probable number) assay. Most of the compounds gave significant inhibition of growth of *M. tuberculosis* in this model as compared to the control ($p < 0.0001$, two way ANOVA usingGraphPad Prism Software).

6.1.6. Evaluation of potency of compound against biofilm forming Mycobacteria

To study the effect on persistent phase of bacteria compounds **RL_34** and **RL_37** (2.5 and 2.9 log reduction in nutrient starvation model) were evaluated against *Mtb* Biofilm i.e., a condition

which simulates lesion microenvironment in host granuloma. *M. tuberculosis* forms biofilms as a defined and distinct physiological state harbouring drug-tolerant persisters, we propose that biofilm development represents an excellent drug target. Identification of drugs that inhibit biofilm formation could enable the dramatic shortening of tuberculosis treatments using standard antibiotics, with substantial potential impact on global health and reduction of antibiotic resistance associated with non-compliance. Both compounds were found to be active against biofilms and exhibited a log reduction of 2.0 fold similar to standard drugs- Isoniazid (1.9 fold), Rifampicin (2 fold), Moxifloxacin (1.8 fold) (**Fig 6.10**).
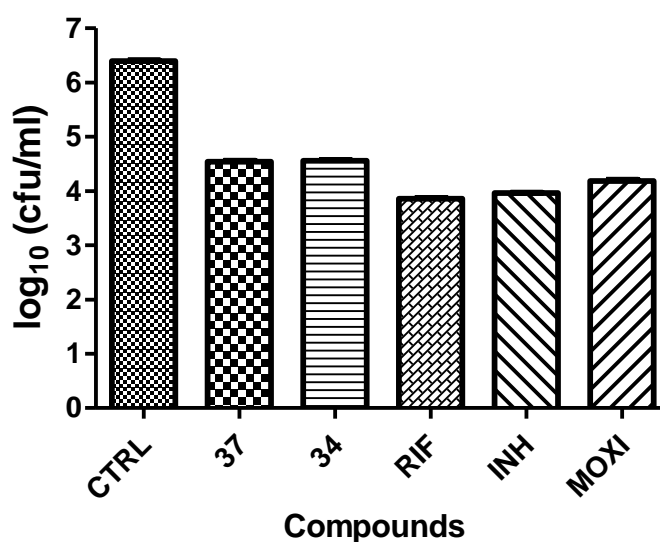
Fig 6.10: Biological activities of compounds **RL_20** and **RL_22** against biofilm forming *M. tuberculosis*. Bacterial count estimation (Mean ± S.D., n = 4) for control and treated groups conducted by using the MPN (most probable number) assay. Both compounds gave significant inhibition of growth of *M. tuberculosis* in this model as compared to the control ($p < 0.0001$, two way ANOVA using GraphPad Prism Software).

6.1.7. Kill kinetic curves under nutrient starved conditions

Preliminary study by nutrient starvation model over a period of 7 days treatment with compound **RL_37** gave a log reduction of 2.9 fold. Kill curve experiments give an insight on nature of kill (bactericidal or static) and kinetics of kill under nutrient starved conditions. For further evaluation on its mechanism of action persistors were evaluated at 0, 7, 14, 21 days after drug

treatment at varying drug concentrations (5, 10, 20 µg/ml). At all concentrations tested there was almost 3 fold log reduction on 21st day. To conclude, kill kinetic profiling against nutrient starved model of most potent compound **RL_37** was found to be dependent on concentration (**Fig 6.11**).
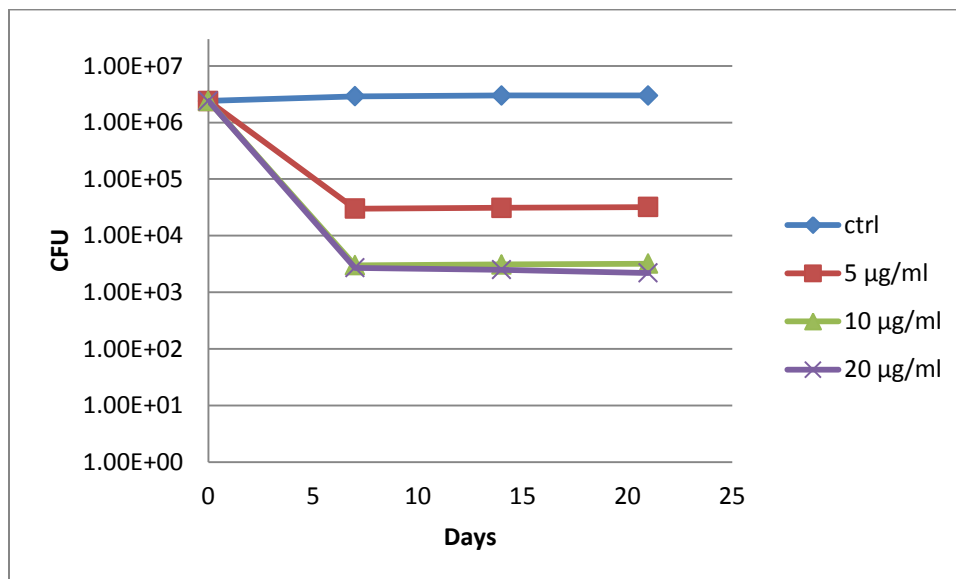
Fig 6.11: Kill kinetic curve of compound **RL_22** at 3 different concentrations.

6.1.8. *In vivo* antimycobacterial evaluation by *Mycobacterium marinum* induced zebra fish model

To further validate their *in vivo* antimycobacterial potency **RL_37** was tested in *M. marinum* induced zebra fish model. Zebra fish has genetic, physiological and immune (adaptive and innate) related similarities with mammalian host. When infected with *M.marinum* it forms granulomas with central necrosis and hypoxia similar to human. It also serves as a link between *in vitro* and *in vivo* models as it provides insight into pharmacokinetic and pharmacodynamics parameters. Activity and dosage of antimycobacterial compounds in zebrafish closely resemble characteristics in humans. It exhibited significant log reduction of 2.9 fold in bacterial count similar to first line drug- Isoniazid. The results suggest that **RL_37** has activity against active replicating stages of bacteria (**Fig 6.12**).
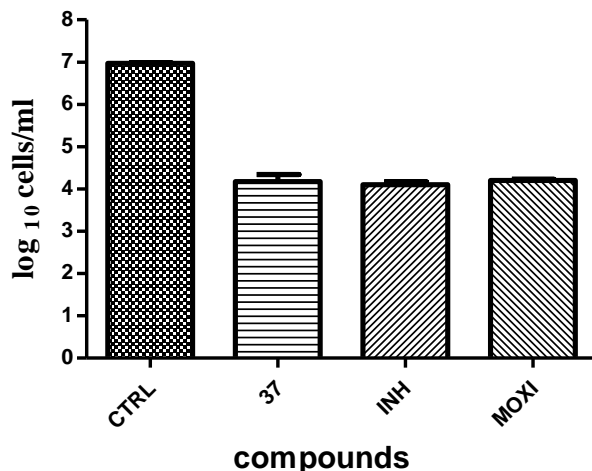
Fig 6.12: Bacterial count estimation (Mean ± S.E.M., n = 6) for control and treated groups conducted by using MPN (most probable number) assay. The statistical significance ($p < 0.001$) with respect to infected control group has been analyzed by Two-way ANOVA using GraphPad Prism Software.

6.1.9. Highlights of the study

Preidentified lead was derivatised and library of 18 compounds were synthesized, purified and characterized by well validated protocols. When they are evaluated for inhibitory potential against *Mtb* LAT enzyme **RL_33** emerged as most potent compound with an IC_{50} of 2.09 ± 0.21μM. **RL_34** and **RL_37** were found to be more effective in lowering bacterial load in nutrient starved model correlating with their LAT inhibitory potency. These compounds observed to be equally effective in persistent phase when evaluated against biofilm forming mycobacterium. The most potent compound **RL_37** in the series was found to be effective when evaluated in *M. marinum* induced zebra fish model. **RL_37** was found to have bactericidal effect and its action is concentration dependent. So **RL_37** is expected to act on both replicating and nonreplicating stages of Tb and is expected to lower duration of therapy.

123

LEAD EXPANSION

SCREENING OF MOLECULES

RL_37
LAT (IC$_{50}$) : 5.83 ± 0.37µM
MIC : 2.88 µM
Nutreint starvation: 2.9 fold
Biofilm : 2.0 fold
Zebra fish : 2.9 fold
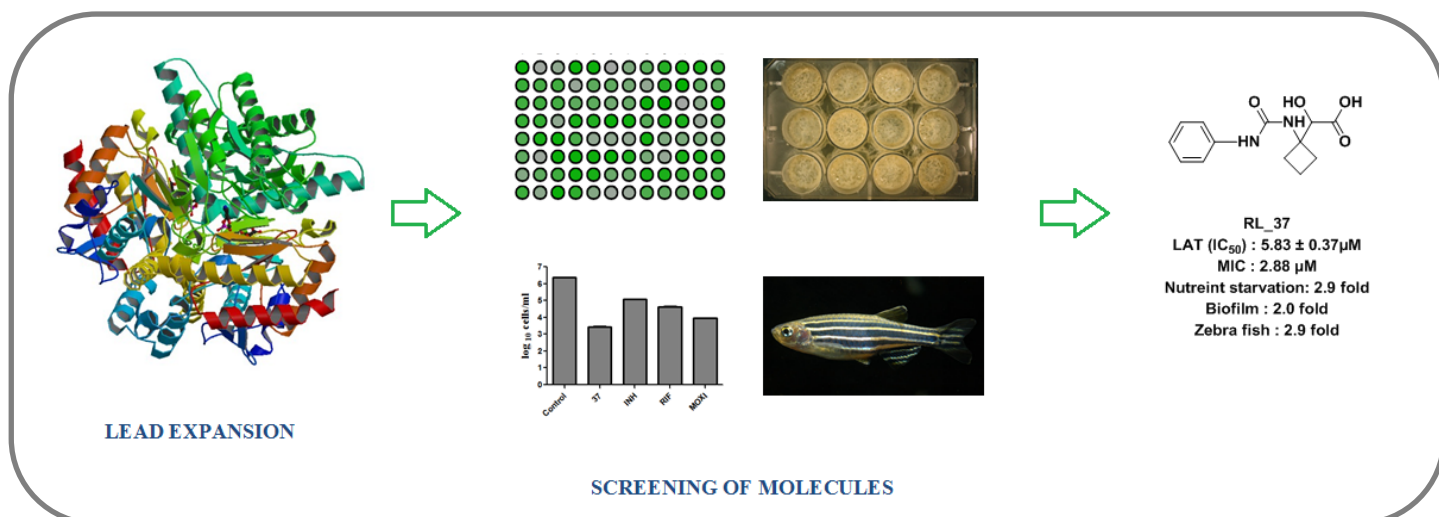
6.2. Design, synthesis and biological evaluation of substituted Benzthiazole derivatives as potent *Mycobacterium tuberculosis* Lysine aminotransferase inhibitors

6.2.1. Design of molecule

P Brindha Devi *et.al., (*2015) by employing e-pharmacophore approach for crystal structure of LAT from *Mtb* in internal aldimine form with bound substrate of α-ketoglutarate (PDB code: 2CJH) with 2.00 Å resolution; shortlisted 9 leads based on docking score and crucial ligand interactions. When evaluated for LAT inhibitory potency compound 1 (lead 9) was found to have an IC$_{50}$ of 10.38 µM. It was not only found to retain critical hydrogen bonding with Arg170, Arg422, Gln274 and Lys300 but also hydrophobic interactions in the active site. As the findings of the study are fascinating we attempted some modifications in compound **01** by introducing various changes in aromatic handle and the benzthiazole scaffold is unaltered (**Fig 6.13**). For SAR purpose various phenyl and heterocycles were introduced at R position and a library of 22 compounds were taken for further synthesis.
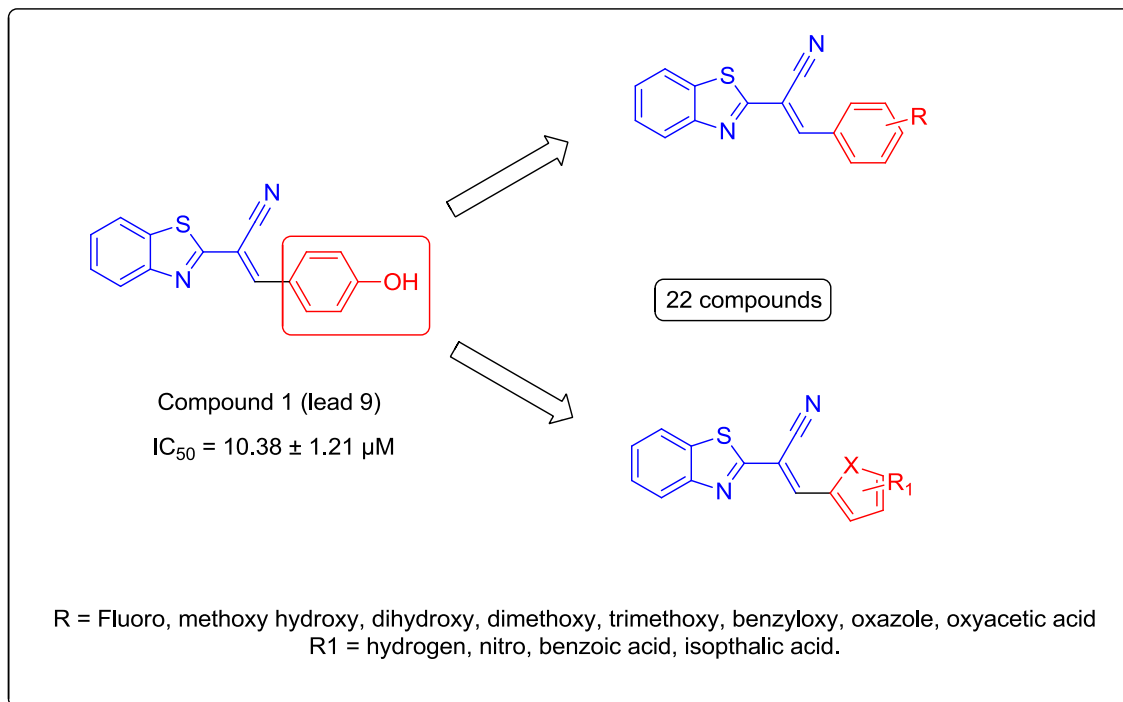
Fig 6.13: Design strategy employed for lead derivatization

6.2.2. Experimental procedures utilized for the synthesis of RR_01 – RR_22

Two steps synthetic protocols was utilized for the synthesis of target compounds, depicted in Scheme 1. Synthesis started with the construction of benzothiazole ring. This was achieved by condensation of 2-aminothiophenol with malononitrile using ethanol as solvent. In this step acetic acid is used in catalytic amount. The final step is knoevenagel condensation with substituted aldehydes [Lanke, S. K., et al., 2016]. The Knoevenagel reaction is a modified Aldol Condensation. In this step nucleophilic addition of active hydrogen from acetonitrile part with carbonyl group of substituted aldehydes followed by water elimination to form α-β unsaturated aldehydes (conjugated enone) as final compounds. In this step weak base piperidine used in catalytic amount [Gao, X., et al., 2015, Jeankumar, V. U., et al., 2016].

Preparation of 2-(benzo[d]thiazol-2-yl)acetonitrile (RR_c)
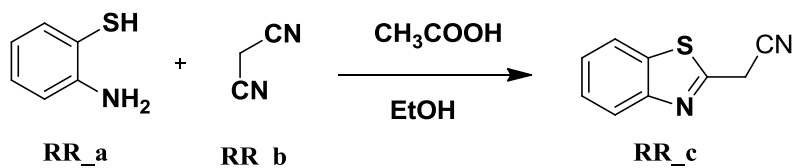
To solution of 2-aminobenzenethiol (**RR_a**) (2.5g, 19.97 mmol) in absolute ethanol (25ml), malanonitrile (**RR_b**) (1.32g, 19.97 mmol) was added, stirred and refluxed at 50 ^{0}C for 2 h along with catalytic amount of glacial acetic acid. the solvent was evaporated under reduced pressure and the residue was extracted with chloroform and purified by column chromatography using hexane–ethylacetate as eluent and decolourised with activated carbon to afford **RR_c** (0.23g, 66.11%) as yellow solid.

Preparation of final compounds RR_01 – RR_22
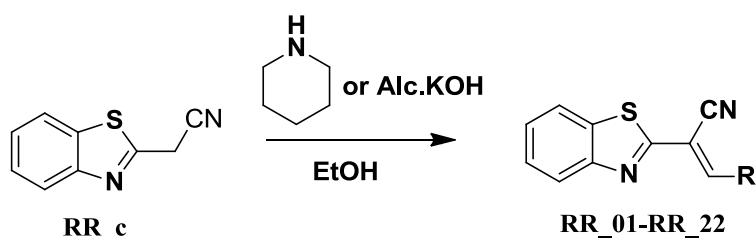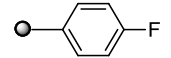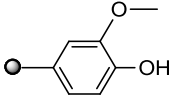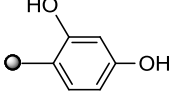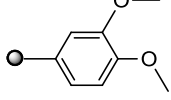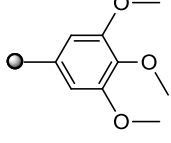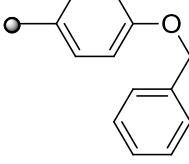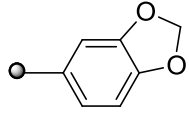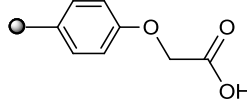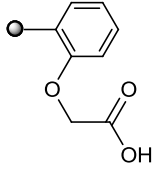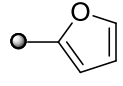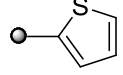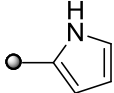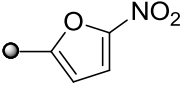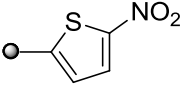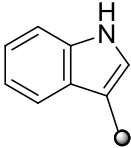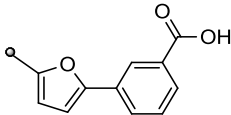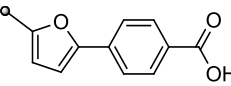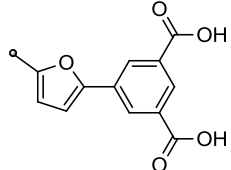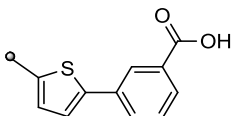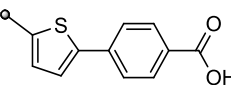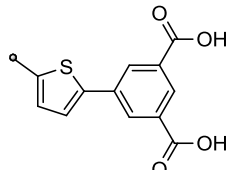
Procedure A: To a warm solution of the corresponding 2-(benzo[d]thiazol-2-yl) acetonitrile (**RR_c**) (1 mmol) in absolute ethanol (8 mL) was added the corresponding aldehyde (1 mmol) and catalytic amount of piperidine (0.2 mmol). The reaction mixture was then stirred and heated to 80 ^{o}C for 0.5-1 h, (as monitored by TLC and LCMS for completion), the precipitate formed was collected by suction and recrystallised from ethanol to give the desired product in good yield as mentioned below.

Procedure B: To a warm solution of the corresponding 2-(benzo[d]thiazol-2-yl) acetonitrile (**RR_c**) (1 mmol) in absolute ethanol (8 mL) was added the corresponding aldehyde (1 mmol) and catalytic amount of 10% methanolic KOH (0.2 mmol). The reaction mixture was then stirred and heated to 80 ^{o}C for 0.5-1 h, (as monitored by TLC and LCMS for completion), the precipitate formed was collected by suction and recrystallised from ethanol to give the desired product in good yield as mentioned below.

Table 6.3: Physicochemical properties of the synthesized compounds **RR_01 – RR_22**
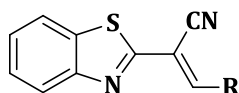
CODE	R	Yield (%)	MP (°C)	Molecular Formula	Molecular Weight
RR_01		80.2	218-220	$C_{16}H_{10}N_2OS$	278.33
RR_02		79.6	174-176	$C_{16}H_9FN_2S$	280.32
RR_03		88.04	175-177	$C_{17}H_{12}N_2O_2S$	308.35
RR_04		82.9	151-153	$C_{16}H_{10}N_2O_2S$	294.33
RR_05		58.32	147-149	$C_{18}H_{14}N_2O_2S$	322.38
RR_06		61.27	262-264	$C_{19}H_{16}N_2O_3S$	352.41
RR_07		69.94	217-219	$C_{23}H_{16}N_2OS$	368.45
RR_08		50.11	219-221	$C_{17}H_{10}N_2O_2S$	306.34
RR_09		55.9	231-233	$C_{18}H_{12}N_2O_3S$	336.36
RR_10		43.48	257-259	$C_{18}H_{12}N_2O_3S$	336.36
RR_11		77.78	137-139	$C_{14}H_8N_2OS$	252.29
RR_12		33.77	149-151	$C_{14}H_8N_2S_2$	268.36

RR_13		52.63	176-178	$C_{14}H_9N_3S$	251.31
RR_14		65.57	245-247	$C_{14}H_7N_3O_3S$	297.29
RR_15		71.27	260-262	$C_{14}H_7N_3O_2S_2$	313.35
RR_16		50.81	289-291	$C_{18}H_{11}N_3S$	301.37
RR_17		58.05	279-281	$C_{21}H_{12}N_2O_3S$	372.40
RR_18		65.54	109-111	$C_{21}H_{12}N_2O_3S$	372.40
RR_19		61.87	269-271	$C_{22}H_{12}N_2O_5S$	416.41
RR_20		64.60	283-285	$C_{21}H_{12}N_2O_2S_2$	388.46
RR_21		52.07	289-291	$C_{21}H_{12}N_2O_2S_2$	388.46
RR_22		61.19	281-283	$C_{22}H_{12}N_2O_4S_2$	432.47

6.2.3. Characterization of Synthesized compounds RR_01 - RL_22

(*E*)-2-(Benzo[*d*]thiazol-2-yl)-3-(4-hydroxyphenyl)acrylonitrile (RR_01): The compound was synthesized according to the above general procedure **A** using 2-(benzo[d]thiazol-2-yl) acetonitrile (**RR_c**) (0.25g, 1.44mmol), 4-hydroxy benzaldehyde(0.18g, 1.44mmol), piperidine

128

(0.025g, 0.29mmol) to afford **RR_01** (0.32g, 80.2%) as yellow coloured solid. M.p: 218-220°C. .
^{1}H NMR (DMSO-d$_6$): δ_H. 8.34 (s, 1H), 8.16 (t, J = 7.4Hz, 1H), 8.05 (t, J = 7.8Hz, 1H), 7.62 − 7.49 (m, 4H), 6.82 (m, 2H), 5.46 (s, 1H). ^{13}C NMR (DMSO-d6): δc. 163.4, 158.2, 152.5 (2C), 134.6, 130.3 (2C), 128.1, 126.6, 123.4 (2C), 122.3, 120.4, 116.3, 114.8, 105.7. ESI-MS m/z 279.3 (M+H)$^+$. Anal Calcd.for C$_{16}$H$_{10}$N$_2$OS; C, 69.04; H, 3.62; N, 10.06; Found: C, 69.13; H, 3.61; N, 10.07.

(*E*)-2-(Benzo[*d*]thiazol-2-yl)-3-(4-fluorophenyl)acrylonitrile (RR_02): The compound was synthesized according to the above general procedure **A** using 2-(benzo[*d*]thiazol-2-yl)acetonitrile (**RR_c**) (0.25g, 1.44mmol), 4-fluoro benzaldehyde(0.18g, 1.44mmol), piperidine (0.025g, 0.29mmol) to afford **RR_02** (0.32g, 79.6 %) as red coloured solid. M.p: 174-176°C. ^{1}H NMR (DMSO-d$_6$): δ_H. 8.37 (s, 1H), 8.18 (t, J = 8.0Hz, 1H), 8.04 (t, J = 8.2Hz, 1H), 7.84 - 7.53 (m, 4H), 7.25 (m, 2H). ^{13}C NMR (DMSO-d6): δc. 164.1, 162.4, 155.7 (2C), 138.7, 131.1 (2C), 125.6, 123.6, 122.8 (2C), 120.4, 118.7, 115.3 (2C), 106.5. ESI-MS m/z 281.4 (M+H)$^+$. Anal Calcd.for C$_{16}$H$_9$FN$_2$S; C, 68.55; H, 3.24; N, 9.99; Found: C, 68.38; H, 3.23; N, 10.01.

(*E*)-2-(Benzo[*d*]thiazol-2-yl)-3-(4-hydroxy-3-methoxyphenyl)acrylonitrile (RR_03): The compound was synthesized according to the above general procedure **A** using 2-(benzo[*d*]thiazol-2-yl)acetonitrile (**RR_c**) (0.25g, 1.44mmol), 4-hydroxy-3-methoxy benzaldehyde (0.218g, 1.44mmol), piperidine (0.025g, 0.29mmol) to afford **RR_03** (0.39g, 88.04%) as green coloured solid. M.p: 175-177°C. ^{1}H NMR (DMSO-d6): δ_H. 8.31 (s, 1H), 8.16 (t, J = 7.8Hz, 1H), 8.05 (t, J = 7.4Hz, 1H), 7.55 − 7.18 (m, 4H), 7.02 (d, J = 8.2Hz, 1H), 5.41 (s, 1H), 3.84 (s, 3H). ^{13}C NMR (DMSO-d6): δc. 161.2, 153.8(2C), 148.8, 148.3, 137.6, 129.4, 124.2, 123.6 (2C), 122.6, 119.6, 118.3, 115.9, 112.1, 107.5, 57.9. ESI-MS m/z 309.4 (M+H)$^+$. Anal Calcd.for C$_{17}$H$_{12}$N$_2$O$_2$S; 66.22; H, 3.92; N, 9.08; Found: C, 66.17; H, 3.91 N, 9.10.

(*E*)-2-(Benzo[*d*]thiazol-2-yl)-3-(2,4-dihydroxyphenyl)acrylonitrile (RR_04): The compound was synthesized according to the above general procedure **A** using 2-(benzo[*d*]thiazol-2-yl)acetonitrile (**RR_c**) (0.25g, 1.44mmol), 2,4-dihydroxy benzaldehyde (0.198g, 1.44mmol), piperidine (0.025g, 0.29mmol) to afford **RR_04** (0.35g, 82.9%) as orange coloured solid. M.p: 151-153°C. ^{1}H NMR (DMSO-d6): δ_H. 8.43 (s, 1H), 8.15 (t, J = 8.0Hz, 1H), 8.03 (t, J = 7.4Hz, 1H), 7.95 - 6.56 (m, 4H), 6.42 (s, 1H), 5.38 (s, 2H).^{13}C NMR (DMSO-d6): δc. 161.1, 160.2, 157.4, 153.9 (2C), 137.9, 131.4, 126.9, 124.2 (2C), 120.4, 118.7, 110.2, 108.6, 107.8, 103.2. ESI-

MS *m/z* 295.4 (M+H)$^+$. Anal Calcd.for $C_{16}H_{10}N_2O_2S$; C, 65.29; H, 3.42; N, 9.52; Found: C, 65.17; H, 3.43; N, 9.51.

(*E*)-2-(Benzo[*d*]thiazol-2-yl)-3-(3,4-dimethoxyphenyl)acrylonitrile (RR_05): The compound was synthesized according to the above general procedure **A** using 2-(benzo[*d*]thiazol-2-yl)acetonitrile (**RR_c**)(0.25g, 1.44mmol), 3,4-dimethoxy benzaldehyde (0.239g, 1.44mmol), piperidine (0.025g, 0.29mmol) to afford **RR_05** (0.27g, 58.32%) as orange coloured solid. M.p: 147-149^{0}C. ^{1}H NMR (DMSO-d6): δ_H 8.36 (s, 1H), 8.16 (t, *J* = 8.8Hz, 1H), 8.06 (t, *J* = 7.2Hz, 1H), 7.81 − 7.47 (m, 4H), 7.19 (d, *J* = 8.4Hz, 1H), 3.87 (s, 3H), 3.84 (s, 3H). ^{13}C NMR (DMSO-d6): δc. 163.3, 153.5, 152.8, 149.3, 146.8, 134.7, 126.8, 126.6, 125.7, 125.4, 123.3, 121.6, 117.1, 111.3, 111.1, 102.3, 56.1(2C). ESI-MS *m/z* 323.4(M+H)$^+$. Anal Calcd.for $C_{18}H_{14}N_2O_2S$; C, 67.06; H, 4.38; N, 8.69; Found: C, 66.92; H, 4.39 N, 8.71.

(*E*)-2-(Benzo[*d*]thiazol-2-yl)-3-(3,4,5-trimethoxyphenyl)acrylonitrile (RR_06): The compound was synthesized according to the above general procedure **A** using 2-(benzo[*d*]thiazol-2-yl)acetonitrile (**RR_c**) (0.25g, 1.44mmol), 3,4,5-trimethoxy benzaldehyde (0.283g, 1.44mmol), piperidine (0.025g, 0.29mmol) to afford **RR_06** (0.31g, 61.27%) as yellow coloured solid. M.p 262-264^{0}C. ^{1}H NMR (DMSO-d6): δ_H 8.16 (s, 1H), 8.07 (t, *J* = 7.2Hz, 1H), 8.05 (t, *J* = 7.6Hz, 1H), 7.57 − 7.32 (m, 4H), 3.95 (s, 3H), 3.94 (s, 6H). ^{13}C NMR (DMSO-d6): δc. 163, 153.7(2C), 153.5(2C), 135.0, 127.6, 127.1, 126.1, 123.6 (2C), 121.8, 117.0, 107.9, 104.1(2C), 61.2, 56.4 (2C). ESI-MS *m/z* 353.42 (M+H)$^+$. Anal Calcd.for $C_{19}H_{16}N_2O_3S$; C, 64.76; H, 4.58; N, 7.95; Found: C, 64.63; H, 4.57; N, 7.97.

(*E*)-2-(Benzo[*d*]thiazol-2-yl)-3-(4-benzyloxyphenyl)acrylonitrile (RR_07): The compound was synthesized according to the above general procedure **A** using 2-(benzo[*d*]thiazol-2-yl)acetonitrile (**RR_c**) (0.25g, 1.44mmol), benzyloxybenzaldehyde (0.31g, 1.44mmol), piperidine (0.025g, 0.29mmol) to afford **RR_07** (0.37g, 69.94%) as brown coloured solid. M.p 217-219 ^{0}C. ^{1}H NMR (DMSO-d6): δ_H 8.28 (s, 1H), 8.16 (t, *J* = 8.2Hz, 1H), 8.06 (t, *J* = 7.8Hz, 1H), 7.74 (d, *J* = 7.8Hz, 2H), 7.51 − 7.37 (m, 7H), 7.04 (d, *J* = 7.8Hz, 2H), 5.28 (s, 2H). ^{13}C NMR (DMSO-d6): δc. 162.3, 159.8, 157.4, 153.8(2C), 136.8, 135.9, 129.8 (2C), 128.6 (2C), 127.5 (2C), 127.4, 126.3, 124.2 (2C), 120.1, 118.8, 114.3(2C), 107.8, 69.7. ESI-MS *m/z* 369.45 (M+H)$^+$. Anal Calcd.for $C_{23}H_{16}N_2OS$; C, 74.98; H, 4.38; N, 7.60; Found: C, 75.08; H, 4.39; N, 7.62.

(*E*)-3-(Benzo[d][1,3]dioxol-5-yl)-2-(benzo[d]thiazol-2-yl)acrylonitrile   (**RR_08**):   The compound was synthesized according to the above general procedure **B** using 2-(benzo[*d*]thiazol-2-yl)acetonitrile (**RR_c**) (0.25g, 1.44mmol), alc. KOH (0.02g, 0.29mmol), piperidine (0.025g, 0.29mmol) to afford **RR_08** (0.22 g, 50.11%) as red coloured solid. M.p 219-221 ^{0}C.^{1}H NMR (DMSO-d6): δ_H. 8.30 (s, 1H), 8.15 (t, *J* = 7.8Hz, 1H), 8.07 (t, *J* = 7.2Hz, 1H), 7.83 (d, *J* = 7.4Hz, 1H), 7.60 (m, 2H), 7.37 (s, 1H), 7.02 (d, *J* = 7.6Hz, 1H), 6.12 (s, 2H). ^{13}C NMR (DMSO-d6): δc. 158.4, 154.4 (2C), 149.1, 147.8, 137.6, 129.1, 126.7, 123.3 (2C), 122.3, 119.2, 118.4, 112.1, 108.4, 107.3, 100.8. ESI-MS *m*/*z* 307.32 (M+H)$^+$. Anal.Calcd.for $C_{17}H_{10}N_2O_2S$; C, 66.65; H, 3.29; N, 9.14; Found: C, 66.59; H, 3.28; N, 9.12.

(*E*)-2-(-4-(2-(Benzo[d]thiazol-2-yl)-2-cyanovinyl)phenoxy)acetic   acid   (RR_09):   The compound was synthesized according to the above general procedure **A** using 2-(benzo[*d*]thiazol-2-yl)acetonitrile (**RR_c**) (0.25g, 1.44mmol), 4-formyl-phenoxy acetic acid(0.26 g, 1.44mmol), piperidine (0.025g, 0.29mmol) to afford **RR_9** (0.27g, 55.9%) as green coloured solid. M.p 231-233 ^{0}C. ^{1}H NMR (DMSO-d6): δ_H. 12.68 (s, 1H), 8.38 (s, 1H), 8.15 (t, *J* = 7.6Hz, 1H), 8.07 (d, *J* = 7.8Hz, 1H), 7.65 − 7.56 (m, 4H), 7.06 (d, *J* = 7.4Hz, 2H), 4.44 (s, 2H). ^{13}C NMR (DMSO-d6): δc. 169.7, 162.8, 157.6, 153.8 (2C), 137.6, 130.4 (2C), 127.4, 126.9, 123.1 (2C), 122.8, 118.7, 114.5 (2C), 107.9, 63.9. ESI-MS *m*/*z* 335.36 (M-H)$^+$. Anal Calcd.for $C_{18}H_{12}N_2O_3S$; C, 64.27; H, 3.60; N, 8.33; Found: C, 64.32; H, 3.61; N, 8.31.

(*E*)-2-(-2-(2-(Benzo[*d*]thiazol-2-yl)-2-cyanovinyl)phenoxy)acetic   acid   (RR_10):   The compound was synthesized according to the above general procedure **A** using 2-(benzo[*d*]thiazol-2-yl)acetonitrile (**RR_c**) (0.25g, 1.44mmol), 2-formyl-phenoxy acetic acid(0.26g, 1.44mmol), piperidine (0.025g, 0.29mmol) to afford **RR_10** (0.21g, 43.48%) as green coloured solid. M.p 257-259 ^{0}C. ^{1}H NMR (DMSO-d6): δ_H. 12.63 (s, 1H), 8.72 (s, 1H), 8.17 (t, *J* = 7.2Hz, 2H), 8.09 (d, *J* = 8.0Hz, 1H), 7.59 (t, *J* = 7.8Hz, 1H), 7.52 (t, *J* = 8.2Hz, 2H), 7.09 (t, *J* = 8.2Hz, 1H), 7.01 (d, *J* = 8.2Hz, 1H), 4.42 (s, 2H).^{13}C NMR (DMSO-d6): δc.170.7, 163.4, 158.8, 152.9 (2C), 143.3, 134.0, 127.7, 127.0, 126.1, 123.0, 122.4, 120.8, 120.0, 116.3, 113.6, 104.1, 68.5. ESI-MS *m*/*z* 335.36 (M-H)$^+$. Anal Calcd.for $C_{18}H_{12}N_2O_3S$; C, 64.27; H, 3.60; N, 8.33; Found: C, 64.22; H, 3.59; N, 8.34.

(*E*)-2-(Benzo[*d*]thiazol-2-yl)-3-(furan-2-yl)acrylonitrile (RR_11):   The compound was synthesized according to the above general procedure **B** using 2-(benzo[*d*]thiazol-2-

yl)acetonitrile (**RR_c**) (0.25g, 1.44mmol), furaldehyde (0.14g, 1.44mmol), alc. KOH (0.02g, 0.29mmol) to afford **RR_11** (0.28 g, 77.78%) as yellow coloured solid. M.p: 137-139°C. ^{1}H NMR (DMSO-d6): δ_H 8.22 (s, 1H), 8.14 (t, J = 7.8Hz, 1H), 8.07 (t, J = 8.0Hz, 1H), 7.82 (d, J = 7.2Hz, 1H), 7.52 (m, 2H), 7.03 (d, J = 8.0Hz, 1H), 6.67 (t, J = 8.2Hz, 1H). ^{13}C NMR (DMSO-d6): δc. 162.4, 152.2, 150.6, 144.8, 143.6, 135.3, 124.5, 123.4 (2C), 120.1, 118.9, 113.8, 112.9, 109.4. ESI-MS m/z 253.3(M+H)$^+$. Anal Calcd.for $C_{14}H_8N_2OS$; C, 66.65; H, 3.20; N, 11.10; Found: C, 66.58; H, 3.21; N, 11.12.

(E)-2-(Benzo[d]thiazol-2-yl)-3-(thiophen-2-yl)acrylonitrile (**RR_12**): The compound was synthesized according to the above general procedure **B** using 2-(benzo[*d*]thiazol-2-yl)acetonitrile (**RR_c**) (0.25g, 1.44mmol), 2-thiophenecarboxaldehyde (0.16g, 1.44mmol), alc. KOH (0.02g, 0.29mmol) to afford **RR_12** (0.13 g, 33.77%) as yellow coloured solid. M.p 149-151 °C. ^{1}H NMR (DMSO-d6): δ_H 8.26 (s, 1H), 8.13 (t, J = 8.2Hz, 1H), 8.05 (t, J = 7.8Hz, 1H), 7.73 (d, J = 8.2Hz, 1H), 7.59 (m, 2H), 7.26 (t, J = 8.8Hz, 1H), 7.11 (d, J = 7.6Hz, 1H). ^{13}C NMR (DMSO-d6): δc. 162.1, 154.7, 142.3, 137.6, 135.3, 133.2, 129.8, 128.6, 124.7, 123.2 (2C), 120.2, 118.3, 113.8. ESI-MS m/z 269.41 (M+H)$^+$. Anal.Calcd.for $C_{14}H_8N_2S_2$; C, 62.66; H, 3.00; N, 10.44; Found: C, 62.75; H, 2.99; N, 10.42.

(E)-2-(Benzo[d]thiazol-2-yl)-3-(1H-pyrrol -2-yl)acrylonitrile (RR_13): The compound was synthesized according to the above general procedure **B** using 2-(benzo[*d*]thiazol-2-yl)acetonitrile (**RR_c**) (0.25g, 1.44mmol), pyrrole-2-carboxaldehyde(0.14g, 1.44mmol), alc. KOH (0.02g, 0.29mmol) to afford **RR_13** (0.19g, 52.63%) as brown coloured solid. M.p: 176-178°C. ^{1}H NMR (DMSO-d6): δ_H 9.12 (s, 1H), 8.21 (s, 1H), 8.12 (t, J = 7.2Hz, 1H), 8.05 (t, J = 7.8Hz, 1H), 7.57 (m, 2H), 7.03 (d, J = 8.0Hz, 1H), 6.67 (d, J = 8.2Hz, 1H), 6.26 (t, J = 7.4Hz, 1H). ^{13}C NMR (DMSO-d6): δc. 162.6, 154.1, 145.4, 137.0, 126.6, 125.4 (2C), 122.8, 120.5, 118.7, 118.0, 113.9, 112.0, 107.9. ESI-MS m/z 252.4 (M+H)$^+$. Anal Calcd.for $C_{14}H_9N_3S$; C,66.91; H, 3.61; N, 16.72; Found: C, 66.87; H, 3.62; N, 16.74.

(E)-2-(Benzo[d]thiazol-2-yl)-3-(5-nitrofuran-2-yl)acrylonitrile (**RR_14**): The compound was synthesized according to the above general procedure **B** using 2-(benzo[*d*]thiazol-2-yl)acetonitrile (**RR_c**) (0.25g, 1.44mmol), 5-nitrofurfural (0.20g, 1.44mmol), KOH (0.02g, 0.29mmol) to afford **RR_14** (0.28g, 65.57%) as orange coloured solid. M.p 245-247 °C.^{1}H NMR (DMSO-d6): δ_H 8.26 (s, 1H), 8.15 (t, J = 7.2Hz, 1H), 8.04 (t, J = 7.8Hz, 1H), 7.64 – 7.58

(m, 3H), 6.97 (d, J = 8.0Hz, 1H). ^{13}C NMR (DMSO-d6): δc. 161.3, 155.9, 154.2, 153.9, 144.8, 137.6, 124.6, 123.7 (2C), 122.8, 118.1, 116.5, 114.8, 113.6. ESI-MS m/z 298.3 (M+H)$^+$. Anal.Calcd.for $C_{14}H_7N_3O_3S$; C, 56.56; H, 2.37; N, 14.13; Found: C, 56.48; H, 2.36; N, 14.12.

(*E*)-2-(Benzo[d]thiazol-2-yl)-3-(5-nitrothiophen-2-yl)acrylonitrile (**RR_15**): The compound was synthesized according to the above general procedure **B** using 2-(benzo[*d*]thiazol-2-yl)acetonitrile (**RR_c**) (0.25g, 1.44mmol), 5-nitrothiophene-2-carboxaldehyde (0.23g, 1.44mmol), KOH (0.02g, 0.29mmol) to afford **RR_15** (0.32g, 71.27%) as green coloured solid. M.p 260-262 ^{0}C.^{1}H NMR (DMSO-d6): δ_H. 8.20 (s, 1H), 8.18 (d, J = 8.0Hz, 1H), 8.14 (t, J = 7.2Hz, 1H), 8.06 (t, J = 7.8Hz, 1H), 7.50 (m, 2H), 7.41 (d, J = 8.0Hz, 1H). ^{13}C NMR (DMSO-d6): δc.162.2, 156.3, 154.7, 147.2, 141.8, 138.2, 135.3, 129.8, 126.8, 123.6 (2C), 119.7, 116.5, 111.2. ESI-MS m/z 314.37 (M+H)$^+$. Anal.Calcd.for $C_{14}H_7N_3O_2S_2$; C, 53.66; H, 2.25; N, 13.41; Found: C, 53.62; H, 2.24; N, 13.39..

(*E*)-2-(Benzo[*d*]thiazol-2-yl)-3-(1*H*-indol-3-yl)acrylonitrile (RR_16): The compound was synthesized according to the above general procedure **B** using 2-(benzo[*d*]thiazol-2-yl)acetonitrile (**RR_c**) (0.25g, 1.44mmol), indole-3-carboxaldehyde(0.21g, 1.44mmol), KOH (0.02g, 0.29mmol) to afford **RR_16** (0.22g, 50.81%) as green coloured solid. M.p: 289-291°C . ^{1}H NMR (DMSO-d6): δ_H. 11.52 (s, 1H), 8.31 (s, 1H), 8.10 (t, J = 7.8Hz, 1H), 8.02 (t, J = 7.2Hz, 1H), 7.82 (s, 1H), 7.73 – 7.62 (m, 3H), 7.12 – 7.05 (m, 3H). ^{13}C NMR (DMSO-d6): δc. 161.2, 154.1(2C), 137.3, 136.1, 129.4, 126.9, 125.0, 124.7 (2C), 123.2, 121.8, 119.6, 118.8, 117.9, 113.8, 111.3, 110.7. ESI-MS m/z 302.37 (M+H)$^+$. Anal Calcd.for $C_{18}H_{11}N_3S$; C,71.74; H, 3.68; N, 13.94; Found: C, 71.65; H, 3.67; N, 13.96.

(*E*)-3-(5-(2-(Benzo[*d*]thiazol-2-yl)-2-cyanovinyl)furan-2-yl)benzoic acid (RR_17): The compound was synthesized according to the above general procedure **A** using 2-(benzo[*d*]thiazol-2-yl)acetonitrile (**RR_c**) (0.25g, 1.44mmol), 3-(5-formyl furan-2-yl) benzoic acid (0.31g, 1.44mmol), piperidine (0.025g, 0.29mmol) to afford **RR_17** (0.31g, 58.05%) as orange coloured solid. M.p:279-281°C. ^{1}H NMR (DMSO-d6): δ_H. 13.12 (s, 1H), 8.65 (s, 1H), 8.53 (d, J = 7.2Hz, 1H), 8.21 (s, 1H), 8.23 – 8.13 (m, 2H), 8.06 (t, J = 7.2Hz, 1H), 7.84 (t, J = 8.2Hz,1H), 7.51 (m, 2H), 7.14 (d, J = 8.2Hz, 1H), 6.94 (d, J = 7.8Hz, 1H). ^{13}C NMR (DMSO-d6): δc. 171.3, 162.3, 156.3, 152.7, 150.8, 144.8, 137.3, 131.1, 130.9, 129.9, 129.8 (2C), 126.9,

124.2, 123.1(2C), 122.1, 118.6, 114.7, 110.2, 106.1. ESI-MS m/z 371.05 (M-H)$^+$. Anal Calcd.for C$_{21}$H$_{12}$N$_2$O$_3$S; C,67.73; H, 3.25; N, 7.52; Found: C, 67.69; H, 3.24; N, 7.50.

(*E*)-4-(5-(2-(Benzo[*d*]thiazol-2-yl)-2-cyanovinyl)furan-2-yl)benzoic acid (RR_18): The compound was synthesized according to the above general procedure **A** 2-(benzo[*d*]thiazol-2-yl)acetonitrile (**RR_c**) (0.25g, 1.44mmol), 4-(5-formyl furan-2-yl) benzoic acid(0.31g, 1.44mmol), piperidine (0.025g, 0.29mmol) to afford **RR_18** (0.35g, 65.54%) as yellow coloured solid. M.p:109-111°C . ^{1}H NMR (DMSO-d6): δ_H 13.07 (s, 1H), 8.27 (s, 1H), 8.19 − 8.07 (m, 6H), 7.51 (m, 2H), 7.16 (d, J = 8.0Hz, 1H), 6.96 (d, J = 8.2Hz, 1H). ^{13}C NMR (DMSO-d6): δc. 170.6, 161.0, 155.7, 153.3, 151.2, 143.2, 136.8, 134.3, 130.8, 126.9 (2C), 125.1, 124.4 (2C), 123.1(2C), 120.5, 117.7, 114.7, 110.8, 107.1. ESI-MS m/z 371.05 (M-H)$^+$. Anal Calcd.for C$_{21}$H$_{12}$N$_2$O$_3$S; C,67.73; H, 3.25; N, 7.52; Found: C, 67.81; H, 3.24; N, 7.50.

(*E*)-5-(5-(2-(Benzo[d]thiazol-2-yl)-2-cyanovinyl)furan-2-yl)isophthalic acid (**RR_19**): The compound was synthesized according to the above general procedure **A** using 2-(benzo[*d*]thiazol-2-yl)acetonitrile (**RR_c**) (0.25g, 1.44mmol), 5-(5-formylfuran-2-yl)isophthalic acid (0.38 g, 1.44 mmol),piperidine (0.025 g, 0.29 mmol) to afford **RR_19** (0.38 g, 61.87%) as yellow coloured solid. M.p: 269-271 ^{0}C. ^{1}H NMR (DMSO-d6): δ_H 12.96 (s, 1H), 12.87 (s, 1H), 9.27 (s, 2H), 8.67 (s, 1H), 8.31 (s, 1H), 8.15 (t, J = 7.2Hz, 1H), 8.03 (t, J = 7.0Hz,1H), 7.48 (m, 2H), 7.12 (d, J = 8.2Hz, 1H), 6.96 (d, J = 8.4Hz, 1H). ^{13}C NMR (DMSO-d6): δc. 170.9(2C), 161.8, 155.8, 154.6, 150.3, 144.8, 136.9, 135.9 (2C), 130.8(3C), 130.6, 126.2, 125.1 (2C), 120.4, 117.7, 114.9, 110.3, 106.6. ESI-MS m/z 415.41 (M-H)$^+$. Anal.Calcd.for C$_{22}$H$_{12}$N$_2$O$_5$S; C, 63.46; H, 2.90; N, 6.73; Found: C, 63.39; H, 2.89; N, 6.75.

(*E*)-3-(5-(2-(Benzo[*d*]thiazol-2-yl)-2-cyanovinyl)thiophen-2-yl)benzoic acid (RR_20): The compound was synthesized according to the above general procedure **A** using 2-(benzo[*d*]thiazol-2-yl)acetonitrile (**RR_c**) (0.25g, 1.44mmol), 3-(5-formyl thiophen-2-yl) benzoic acid (0.33g, 1.44mmol), piperidine (0.025g, 0.29mmol) to afford **RR_20** (0.36g, 64.6%) as brown coloured solid. M.p: 283-285°C . ^{1}H NMR (DMSO-d6): δ_H 13.32 (s, 1H), 8.63 (s, 1H), 8.25 (s, 1H), 8.16 (t, J = 8.0Hz, 1H), 8.12 - 7.98 (m, 4H), 7.86 (d, J = 4.0Hz, 1H), 7.64 − 7.50 (m, 3H). ^{13}C NMR (DMSO-d6): δc. 171.2, 162.4, 155.3, 144.5, 142.7, 139.7, 135.4, 133.5, 132.3, 130.2 (2C), 130.1, 129.9, 127.6, 125.6, 124.3, 122.8 (2C), 120.1, 118.2, 113.5. ESI-MS

m/z 387.1 (M-H)$^+$. Anal Calcd.for C$_{21}$H$_{12}$N$_2$O$_2$S$_2$; C, 64.93; H, 3.11; N, 7.21; Found: C, 64.98; H, 3.12; N, 7.23.

(*E*)-4-(5-(2-(Benzo[*d*]thiazol-2-yl)-2-cyanovinyl)thiophen-2-yl)benzoic acid (RR_21): The compound was synthesized according to the above general procedure **A** using 2-(benzo[*d*]thiazol-2-yl)acetonitrile (**RR_c**) (0.25g, 1.44mmol), 4-(5-formyl thiophen-2-yl) benzoic acid (0.33g, 1.44mmol), piperidine (0.025g, 0.29mmol) to afford **RR_21** (0.29g, 52.07%) as brown coloured solid. M.p: 289-291°C. ^{1}H NMR (DMSO-d6): δ_H. 13.01 (s, 1H), 8.34 (s, 1H), 8.20 (t, *J* = 7.2Hz, 1H), 8.16 (t, *J* = 8.0Hz, 1H), 8.11 − 7.87 (m, 4H), 7.67 (m, 2H), 7.28 (d, *J* = 8.0 Hz, 2H). ^{13}C NMR (DMSO-d6): δc. 170.1, 161.7, 152.4, 143.9, 141.5, 139.8, 138.4, 135.1, 131.0, 130.9, 128.4, 127.9, 126.8 (2C), 125.1, 124.9 (2C), 123.7, 120.4, 117.4, 113.2.ESI-MS *m/z* 387.51 (M-H)$^+$. Anal Calcd for C$_{21}$H$_{12}$N$_2$O$_2$S$_2$; C, 64.93; H, 3.11; N, 7.21; Found: C, 64.86; H, 3.12; N, 7.23.

(E)-4-(5-(2-(Benzo[d]thiazol-2-yl)-2-cyanovinyl)thiophen-2-yl)isophthalicacid (RR_22): The compound was synthesized according to the above general procedure **A** using 2-(benzo[*d*]thiazol-2-yl)acetonitrile (**RR_c**) (0.25g, 1.44mmol), 4-(5-formyl thiophen-2-yl) isophthalic acid (0.39g, 1.44mmol), piperidine (0.025g, 0.29mmol) to afford **RR_22** (0.38g, 61.19%) as yellow solid. M.p: 281-283°C. ^{1}H NMR (DMSO-d6): δ_H. 13.01 (s, 1H), 12.96 (s, 1H), 8.52 − 8.48 (m, 2H), 8.27 (s, 1H), 8.18 (m, 1H), 8.14 (t, *J* = 7.4Hz, 1H), 8.03 (d, *J* = 7.2Hz, 1H), 7.92 (d, *J* = 7.6Hz, 1H), 7.58 (m, 2H), 7.43 (d, *J* = 8.0Hz, 1H). ^{13}C NMR (DMSO-d6): δc. 170.4, 169.1, 158.3, 152.4, 144.2, 141.5, 139.2, 138.5, 135.4, 132.8, 131.3, 129.7 (2C), 128.4, 128.1, 126.8, 125.1, 124.2 (2C), 120.4, 117.4, 113.0. ESI-MS *m/z* 431.44 (M-H)$^+$. Anal Calcd for C$_{22}$H$_{12}$N$_2$O$_4$S$_2$; C, 61.10; H, 2.80; N, 6.48; Found: C, 61.14; H, 2.79; N, 6.50.

6.2.4. *In vitro* LAT inhibitory assay, antimycobacterial potency and cytotoxicity studies of the synthesized molecules

LAT catalyses reversible transamination from lysine to α-keto glutaric acid resulting in piperidine-6-carboxylic acid and glutamate. As the end products have absorbance maxima at 465 nm and 280 nm all compounds were evaluated for their *Mtb* LAT inhibitory potency by spectroscopic method reported earlier and the results are tabulated in **Table 6.4**. Five compounds exhibited IC$_{50}$ less than 5 μM and **RR_19** was found to be most potent among all compounds

with an IC_{50} value of 1.15 ± 0.27 μM. **RR_19** showed 10 fold reduction in IC_{50} when compared to lead i.e., **RR_01** (10.38 ± 1.21 μM). Out of 22 compounds, 8 compounds have more efficacy interms of LAT inhibitory potency than lead compound. **RR_09, 17** and **22** also exhibited good inhibitory potency of 3.08 ± 0.37, 3.74 ± 0.27, 2.62 ± 0.37 μM respectively.
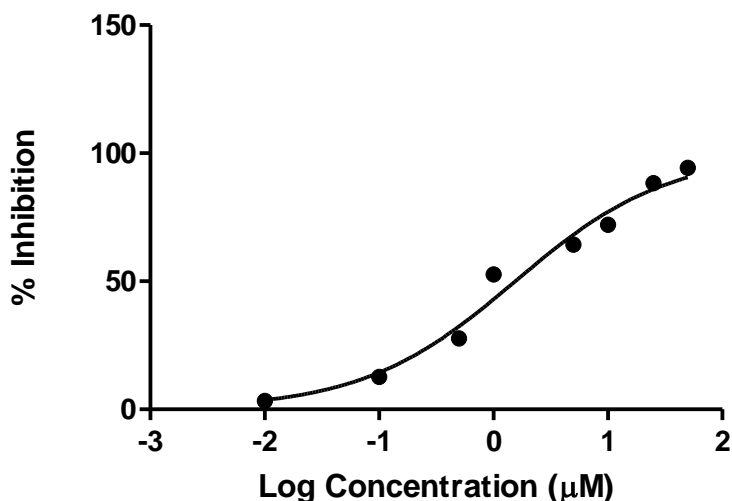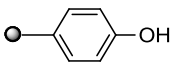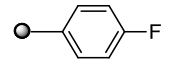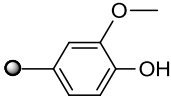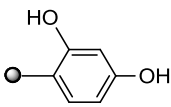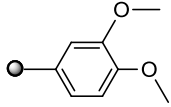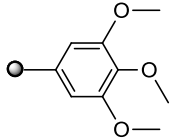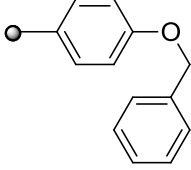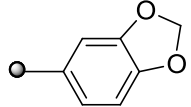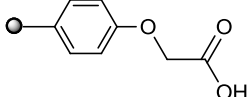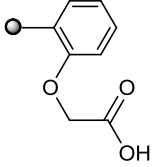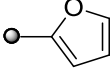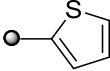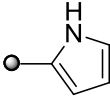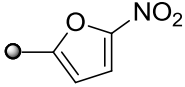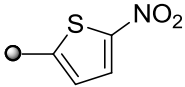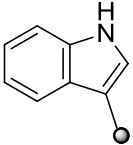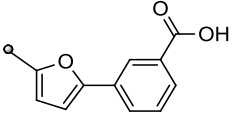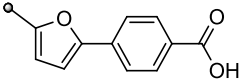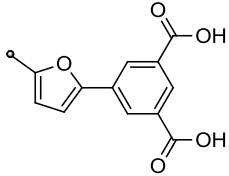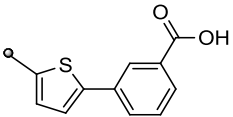
Fig 6.14: Dose response curve of active compound **RR_01**
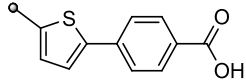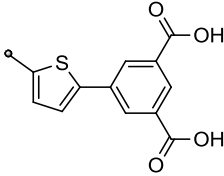
When tested against active forms of mycobacterium the MIC were in the range of 2.01 to 99.60 μM. surprisingly **RR_21** and **RR_09** has good action against both replicating and non replicating stages of bacteria as there MIC values are 2.01 and 4.64 μM respectively (**Table 6.4**). **RR_10** was found to be inactive against LAT enzyme but has low MIC of 2.32 μM indicating that its mechanism of action might be different. To know the toxic effect of compound on macrophages, the residence of parasite RAW cell lines were used for cytotoxicity studies. All the compounds were tested at a concentration of 50 μg/ml and the percentage inhibition were found to be in range of 2.26 to 60.31% (**Table 6.4**). Most of the compounds are devoid of cellular toxicity.

Table 6.4: *In vitro* biological evaluation of the synthesized compounds **RR_01 – RR_22**
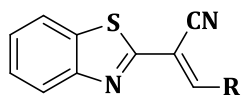
CODE	R	LAT (IC$_{50}$) μM	MIC μM	Cytotoxicity (% inhi) at 50 μg/ml
RR_01		10.38 ± 1.21	>89.93	2.26 ± 0.11
RR_02		4.11 ± 0.78	89.29	10.56 ± 0.63
RR_03		7.83 ± 0.31	20.29	34.78 ± 0.82
RR_04		23.19 ± 0.89	10.61	45.72 ± 0.21
RR_05		61.41 ± 1.56	>77.64	32.45 ± 0.92
RR_06		64.89 ± 2.31	>71.02	12.59 ± 0.38
RR_07		47.93 ± 1.82	67.95	22.82 ± 0.21
RR_08		65.98 ± 0.63	81.69	45.67 ± 0.91
RR_09		3.08 ± 0.37	4.64	12.67 ± 0.35

RR_10		53.78 ± 0.96	2.32	52.31 ± 1.92
RR_11		16.23 ± 0.26	49.60	47.31 ± 1.81
RR_12		92.57 ± 1.94	>93.28	17.34 ± 0.92
RR_13		17.05 ± 1.21	>99.60	56.42 ± 0.97
RR_14		19.59 ± 0.32	>84.18	19.64 ± 0.62
RR_15		54.76 ± 0.21	>79.87	60.31 ± 1.23
RR_16		37.91 ± 0.48	>83.06	45.69 ± 0.92
RR_17		3.74 ± 0.27	>67.20	3.12 ± 0.67
RR_18		14.06 ± 0.16	>67.20	15.24 ± 0.51
RR_19		1.15 ± 0.27	60.09	14.38 ± 0.82
RR_20		5.73 ± 0.79	64.43	18.94 ± 0.92

RR_21		6.72 ± 0.27	2.01	5.64 ± 0.76
RR_22		2.62 ± 0.37	>57.60	32.17 ± 1.56
INH		--	0.4	--
RIF		--	0.5	--

IC_{50} – 50% inhibitory concentration, **MIC** – minimum inhibitory concentration, **inhi**-inhibition, **INH-** isoniazid, **RIF-** Rifampicin

Our most active ligand **(E)-4-(5-(2-(benzo[d]thiazol-2-yl)-2-cyanovinyl)thiophen-2-yl)isophthalicacid (RR_22)** on docking gave a glide score of -6.12 kcal/mol. The ligand had four hydrogen bonding with Arg422, Lys300 and GLn274 with a well fitted pose in the active site. The ligand found in the hydrophobic pocket within the vicinity of Val30, Leu24, Met28, Leu28, Leu414, Pro415, Phe167 and Val63. The binding pattern within the active site pocket of the crystal ligand and reference ligand was quite similar and additionally the solvent exposure area around the ligand constituted for a stable binding profile of the molecule as shown in the **Fig 6.15**.
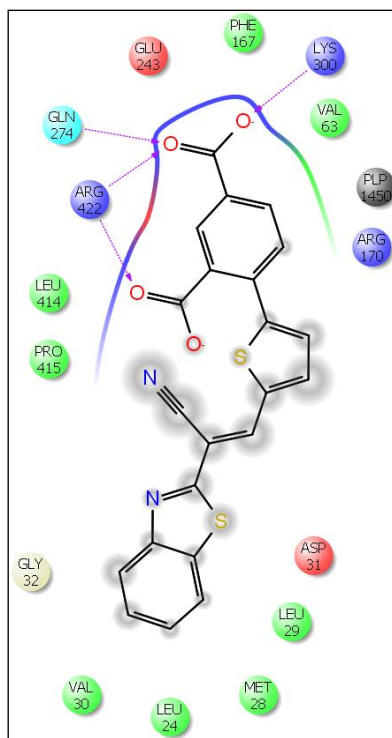
Fig 6.15: Interactions of most active inhibitor **RR_22** with the active site residues of MTB LAT.

SAR analysis revealed that when compared to substituted phenyl ring, heterocycles are favoring activity. Heterocycles attached with isophthalic acid were more promising hits than heterocycles attached to benzoic acid. When attempts were made to modify the benzthiazole ring with benzoxazole ring it resulted in complete loss of activity.

6.2.5. Nutrient starvation model

Nutrient starvation model was found to mimic microenvironment of granuloma as *Mtb* exhibits significantly reduced intracellular ATP levels, very low but continuous respiration and Loss of Ziehl-Neelsen staining characteristic. This model is also characterized by resistance to commonly used antibiotics (INH, RIF, Metronidazole, some Fluoroquinolines).After 96 h of starvation 323 genes involved in amino acid biosynthesis, biosynthesis of cofactors, prosthetic groups and carriers, DNA replication, repair, recombination and restriction/modification, energy metabolism, lipid biosynthesis, translation and post-translational modification and virulence were down regulated. Genes which are found to be upregulated are involved in antibiotic

production and resistance, insertion sequence (IS) elements, repeated sequences and phage, nucleotide biosynthesis and metabolism, putative enzymes and regulatory function. Lysine-ε aminotransferase expressed by Rv3290c gene was found to be upregulated 41.86 folds as it involved in antibiotic resistance. All compounds were evaluated for their activities against dormant phase of mycobacterium at 10 μg/ml. Most of the compounds have well correlation between enzyme inhibitory concentration values and log reduction in this model. **RR_20** and **RR_22** showed a log reduction of 2.9 fold and potent when compared to first line drugs Isoniazid (1.2 fold), Rifampicin (1.3 fold) and Moxifloxacin (2.2 fold). **RR_09, RR_14, RR_19** showed 2.8 fold reduction and are potent when compared to standard drugs (**Fig 6.16**).
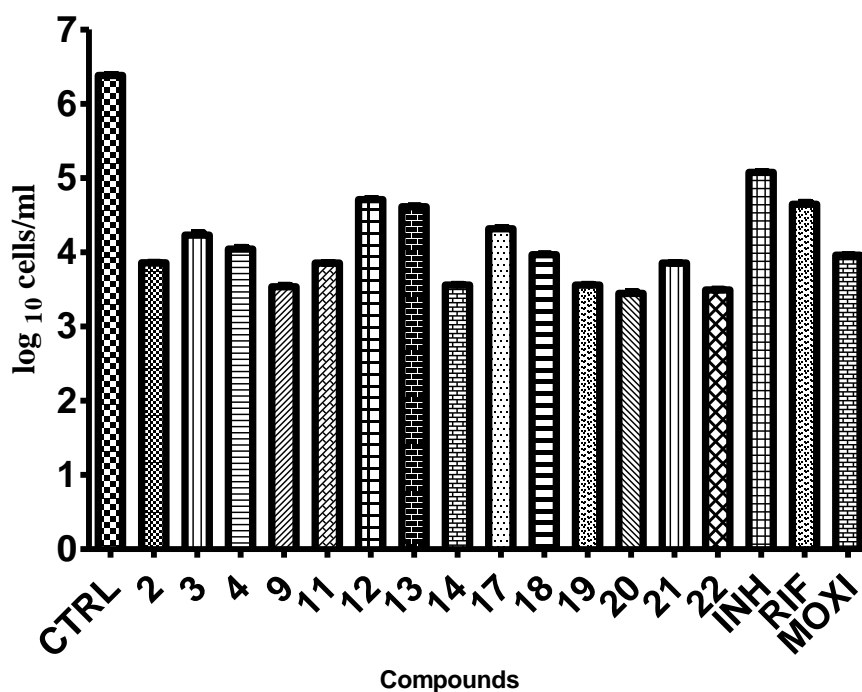
Fig 6.16: Biological activities of the synthesised compounds against *M. tuberculosis* in the nutrient starvation model. Bacterial count estimation (Mean ± S.D., n = 3) for control and treated groups conducted by using the MPN (most probable number) assay. Most of the compounds gave significant inhibition of growth of *M. tuberculosis* in this model as compared to the control (p < 0.0001, two way ANOVA usingGraphPad Prism Software).

6.2.6. Evaluation of potency of compound against biofilm forming Mycobacteria

Biofilm formation explains the reasons for long term persistence of *Mtb* in human host and longer duration of treatment to completely recover from TB. Biofilm is a structured community of persistent cells (low nutrients and oxygen) enclosed in a self-produced polymeric matrix and adherent to an inert or living surface. In case of *Mtb* bacilli are embedded in a lipid-rich extracellular matrix containing free methoxy mycolic acids resulting in drug tolerance (50 times higher than MIC) and persistence. Most active compounds **RR_20** and **RR_22** were tested against biofilms of *Mtb* by incubating at concentration of 10 µg/ml and exposure time was 7 days. Both compounds shown promising results and has 2.1 and 2.3 log reduction in bacterial count similar to standard drugs- Isoniazid (1.9 fold), Rifampicin (2 fold), Moxifloxacin (1.8 fold) as shown in **Fig 6.17**.
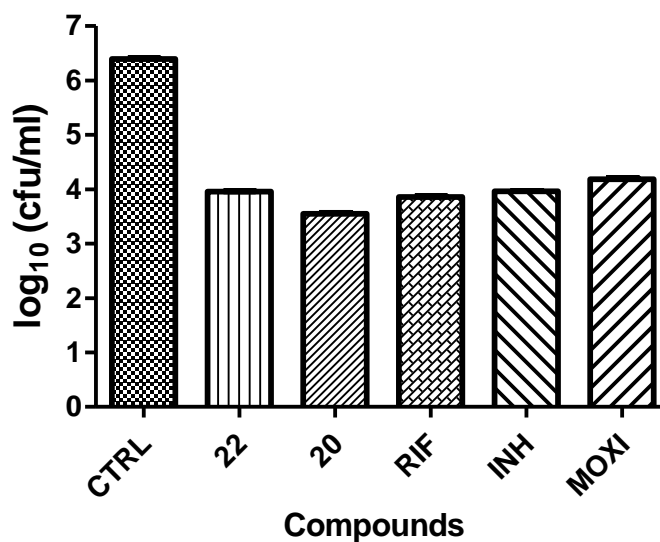
Fig 6.17: Biological activities of compounds **RR_20 and 22** against biofilm forming *M. tuberculosis*. Bacterial count estimation (Mean ± S.D., n = 4) for control and treated groups conducted by using the MPN (most probable number) assay. Both compounds gave significant inhibition of growth of *M. tuberculosis* in this model as compared to the standards (p < 0.0001, two way ANOVA usingGraphPad Prism Software).

6.2.7. Kill kinetic curves under nutrient starved conditions

Kill curve experiments give an insight on nature of kill (bactericidal or static) and kinetics of kill under given set of conditions. MBC is defined as the lowest concentration of compound needed to kill 3 logs of *M. tuberculosis* in 21 days under the given conditions. Compounds that are bactericidal may also exhibit time dependent killing or concentration-dependent killing. For compounds that have time-dependent kill, any concentration at or above the MBC will result in a constant rate of kill of the bacteria. For compounds that are concentration dependent, the rate of kill will increase as the concentration of compound increases. For further evaluation on its mechanism of action persistors obtained after 2 weeks starvation were evaluated at 0, 7, 14, 21 days after drug treatment at varying drug concentrations (5, 10, 20 µg/ml). At all concentrations tested there was almost 3 fold log reduction from 7th day to 21st day. Based on this observations kinetic profiling of **RR_22** against dormant forms of mycobacteria was neither dependent on concentration nor time as observed in the **Fig 6.18**. It also has bactericidal effect against non replicative stages of mycobacterium.
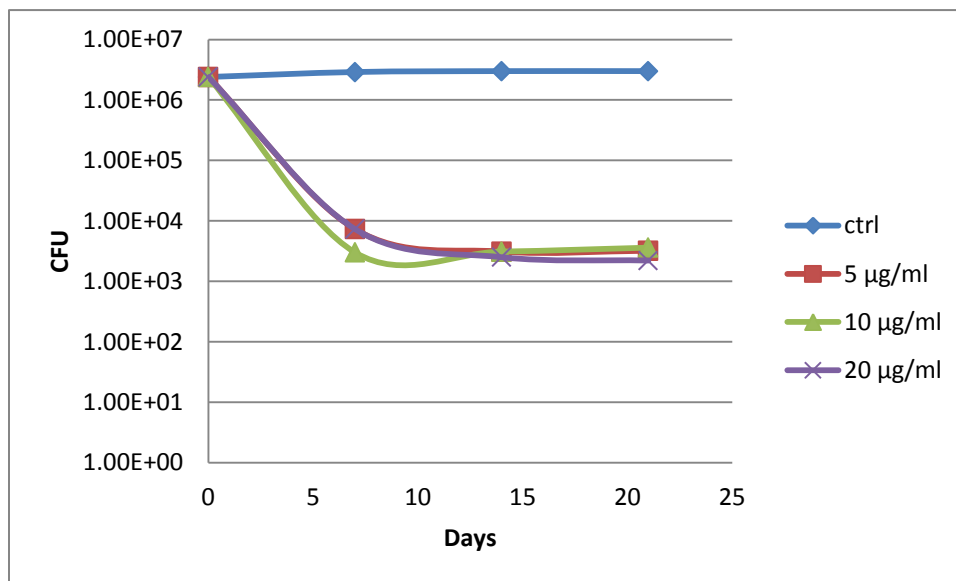
Fig 6.18: Kill kinetic curve of **RR_22** at 3 different concentrations

6.2.8. *In vivo* antimycobacterial evaluation by *Mycobacterium marinum* induced zebra fish model

When infected with *M.marinum* zebra fish forms granulomas with central necrosis and hypoxia similar to human. Oxidative stress stimulates the expression of bacterial efflux pumps in active stage of mycobacterium in zebra fish model. Crucial virulence factors, host genes and immune cell types implicated in human *Mtb* pathogenesis are retained in zebrafish–*M. marinum* model. The natural heterogeneity of the zebrafish population proved to be beneficial as it helps in understanding of genetic differences of different individuals. It also serves as a link between *in vitro* and *in vivo* models as it provides insight into pharmacokinetic and pharmacodynamics parameters. Most potent molecule in the series **RR_22** was tested for *in vivo* antimycobacterial potency by well validated *M. marinum* induced zebra fish model. The activity of compound is not much significant indicating that it acts through pathways involved in dormancy (**Fig 6.19**).
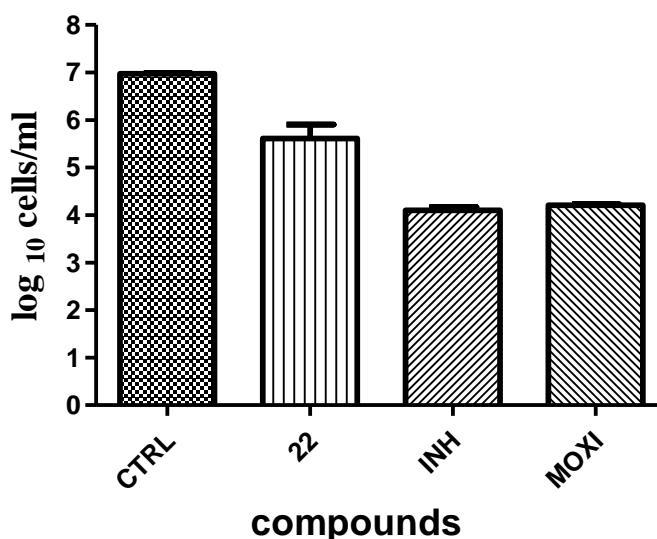
Fig 6.19: Bacterial count estimation (Mean ± S.E.M., n = 6) for control and treated groups conducted by using MPN (most probable number) assay. The statistical significance (p < 0.001) with respect to infected control group has been analyzed by Two-way ANOVA using GraphPad Prism Software.

6.2.9. Human *In vivo* 3D granuloma model

Human 3D granuloma model is a biomimetic model of human granuloma dormancy as well as reactivation in favourable conditions such as immunosuppression. The mycobacterium in this model exhibits characteristics of dormancy such as loss of acid fast staining, accumulation of fats, rifampicin tolerance and gene expression changes. After formation of 3D granuloma it was treated with **RR_22** for 4 days followed by Rifampicin for 3 days. Then the granuloma was hydrolysed followed by enumeration of % Rifampicin tolerant persisters and *Mtb* cfu. When the granuloma was treated with **RR_22** alone (30.85 $X10^5$) cfu were much higher but when treated incombination with Rif, the cfu counts were less (2.11X 10^5), as compared to the cfu counts for *Mtb* from granulomas treated with Rif alone (3.3$X10^5$) as shown in **Fig 6.20** and **6.21**. This indicates that **RR_22**, is a more effective killer in the presence of Rif.
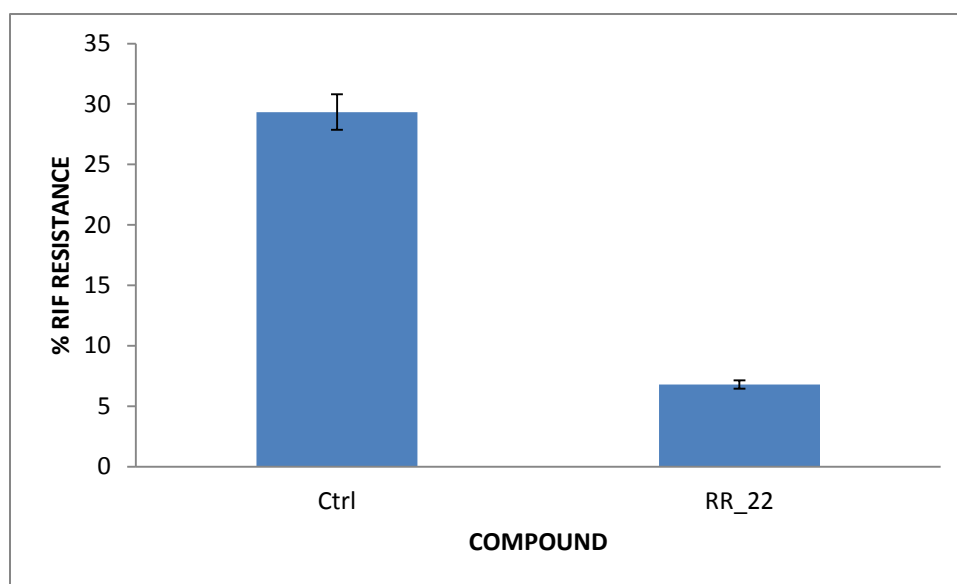
Fig 6.20: After the formation of granuloma, the granulomas were either left untreated or were treated with the **RR_22** for 4 days and then with Rif for further 3 days. The graph represents the % Rif resistance of *Mtb* recovered from these granulomas.
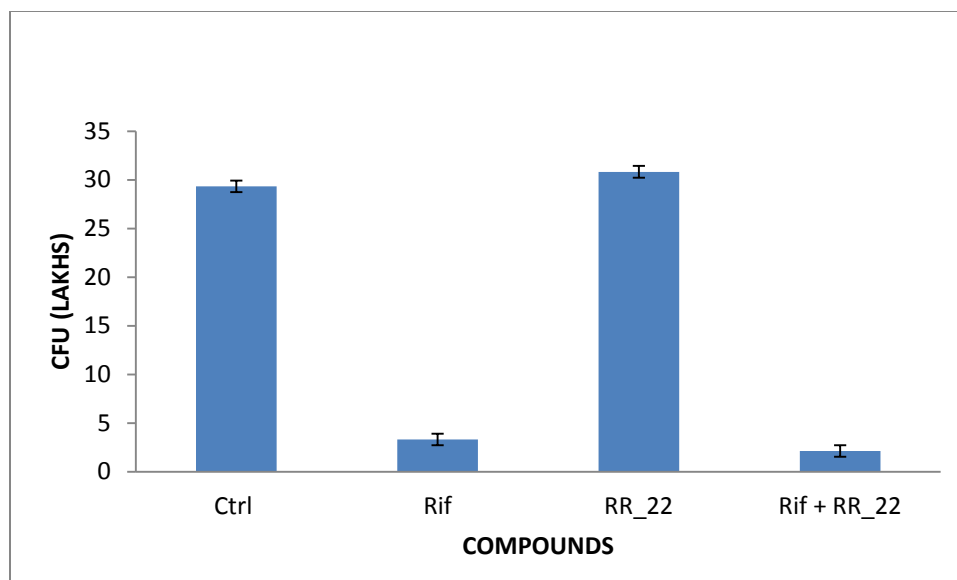
Fig 6.21: Data showing cfu counts for *Mtb* recovered from granulomas treated either with no drugs or treated with Rif, **RR_22** alone or treated with **RR_22**+ Rif.

6.2.10. Highlights of the study

In the present work, existing lead was modified to develop more active compound against *Mtb* LAT, a crucial enzyme for regulation of amino acid pool which in turn a key for antibiotic tolerance and persistence. In our attempts we also unexpectedly arrived at an interesting compound **RR_21 (*E*)-4-(5-(2-(benzo[*d*]thiazol-2-yl)-2-cyanovinyl)thiophen-2-yl)benzoic acid** which even though has moderate activity against persistent phase of mycobacterium it has significant potency against active phase. In the entire series, compound **RR_22 (E)-4-(5-(2-(benzo[d]thiazol-2-yl)-2-cyanovinyl)thiophen-2-yl)isophthalicacid** emerged as potent molecule with LAT IC_{50} of 2.62 μM. It has a significant log reduction of 2.9 and 2.3 fold against nutrient starved and biofilm forming mycobacteria. It was found to inactive against active *Mtb* and also in *M. marinum* induced zebra fish model indicating that it acts through dormant targets. It is also devoid of cytotoxicity. **RR_22** was also found to possess bactericidal effect which is independent of concentration and time. It was found to be effective in combination with Rifampicin in 3D granuloma model. All these parameters make it a better candidate for further development.

SCREENING OF MOLECULES
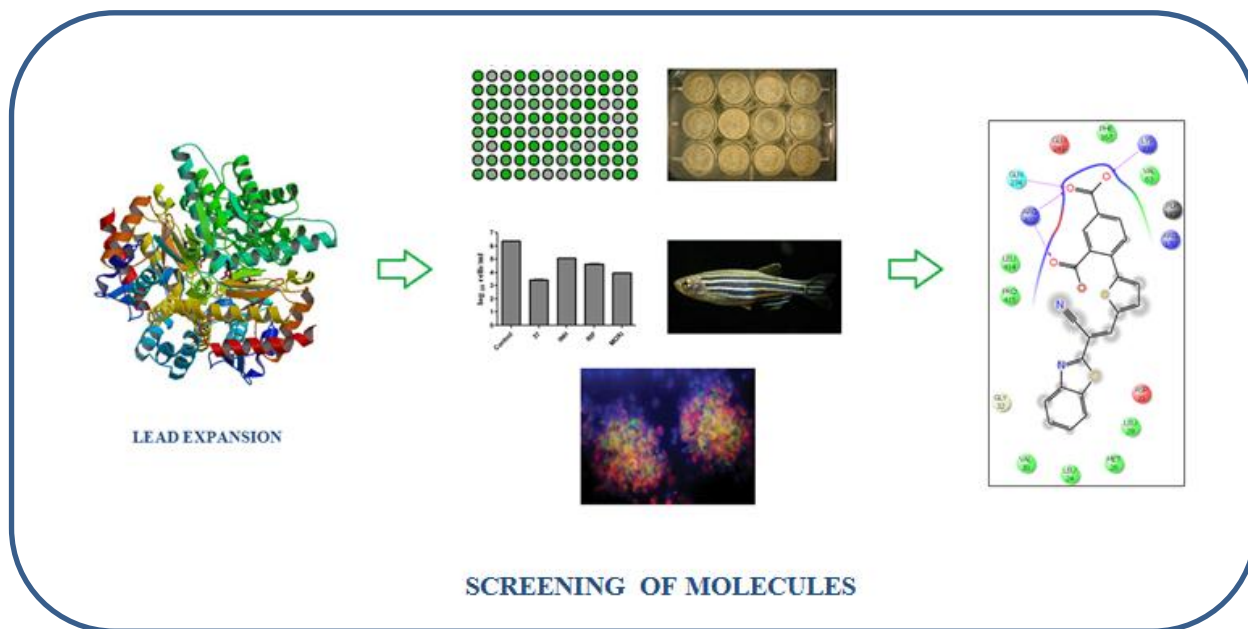
6.3. Design, synthesis and biological evaluation of substituted Quinoline derivatives as potent *Mycobacterium tuberculosis* Lysine Ɛ-aminotransferase inhibitors

6.3.1. Design of molecule

There are many evidences in literature supporting antimycobacterial potency of quinoline derivatives. In our previous study (Brindha D. P., *et. al.,* 2016) by screening of BITS inhouse database against lysine bound LAT enzyme (PDB id: 2CJD) we identified quinoline lead (lead-7) with IC_{50} of 23.33 μM. In present work we have taken this quinoline lead for lead expansion and synthesized a library of 21 derivatives as shown in **Fig 6.22** below.
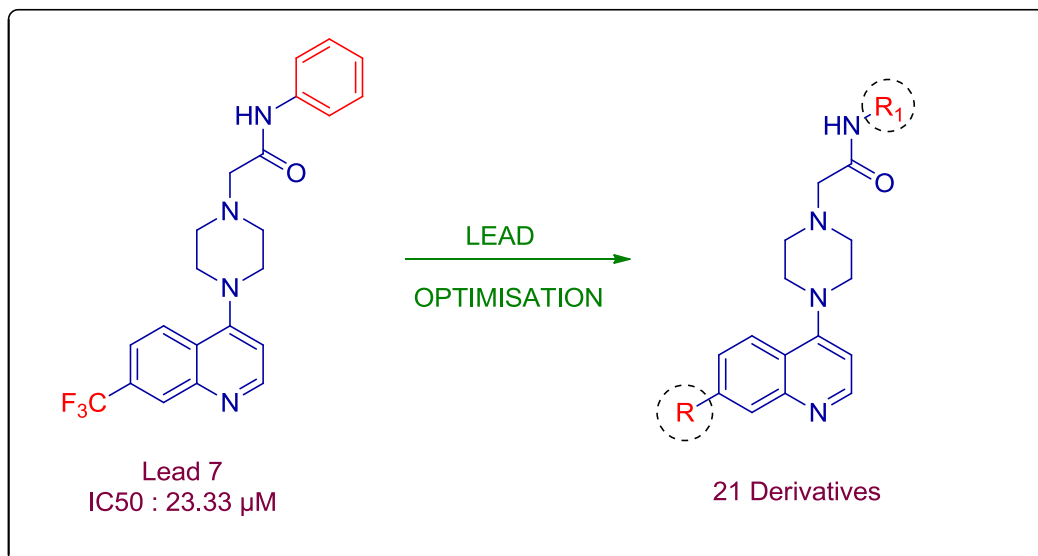
Fig 6.22: Design strategy employed

6.3.2. Experimental procedures utilized for the synthesis of RS_10 – RS_30

Synthesis started with commercially available 7 substituted 4 chloro quinolone. In the first step substituted 4 chloro quinolone under gone N alkylation with piperazine. This was achieved by using acetonitrile as solvent and K_2CO_3 as base. In order to prevent the formation of by product di substituted quinolone, reaction volume was increased to 200 volumes. Also equivalence of quinolone used was increased to double that of piperazine. Minor percentage of di substituted product formed was removed by manual column chromatographic technique. The first step product was taken for further N alkylation using methyl bromoacetate and K_2CO_3 as base. Subsequently the methyl ester was hydrolyzed to acid by weak base lithium hydroxide, water mixture at 60°C. Final target molecule was attained by reaction with substituted amines using T3p as coupling agent resulted in amide linkage [Jeankumar, V. U., et al., 2016].

General procedure for the synthesis of 4-(piperazin-1-yl)quinoline derivatives (RS_04 - RS_06):

To a suspension of 4-chloro quinoline derivative (1 mmol) and potassium carbonate (1.2 mmol) in acetonitrile (20 mL) was added piperazine (1 mmol) at 30°C. The reaction mixture was then heated to 80°C for 1-2 h (monitored by TLC and LCMS for completion), cooled to 30°C. The mixture was then filtered through celite bed, and acetonitrile was evaporated in vacuo. The resultant residue was diluted with water (10 mL) and dichloromethane (20 mL) and the layers

148

separated. The aqueous layer was re-extracted with dichloromethane (2x 25 mL).The combined organic extract was washed with brine, dried over sodium sulphate, and evaporated in vacuo. The resultant residue was the purified by column chromatography on neutral alumina using hexane:ethylacetate as eluent to give desired product as described below

Preparation of 4-(Piperazin-1-yl)quinolone (RS_04):
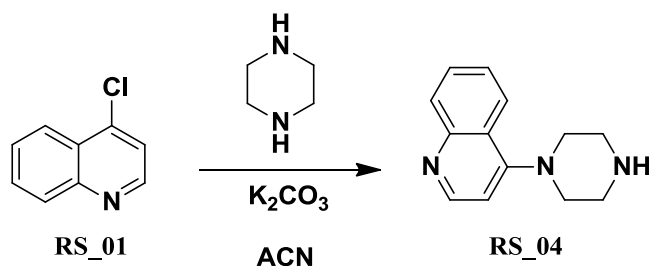
The compound was synthesized according to the above general procedure using 4-chloroquinoline (**RS_01**) (2.5g, 15.28mmol), potassium carbonate (2.54g, 18.34mmol) and piperazine (1.32g, 15.28mmol) to afford **RS_04** (1.82g, 55.83%) as an off-white solid. ^{1}H NMR (DMSO-d$_6$): δ_H 2.82 − 2.99 (m, 4H), 3.12 - 3.20, (m, 4H), 6.27 − 8.23 (m, 6H). ^{13}C NMR (DMSO-d$_6$): δc. 161.3, 154.3, 143.1, 133.1, 129.2, 126.5, 123.7, 115.4 (2C), 52.8 (2C), 45.3 (2C). ESI-MS m/z 214.13(M+1)$^{+}$. Anal Calcd for C$_{13}$H$_{15}$N$_3$; C, 73.21; H, 7.09; N, 19.70; Found: 73.15; H, 6.91; N, 19.72.

Preparation of 7-Chloro-4-(piperazin-1-yl)quinolone (RS_05):
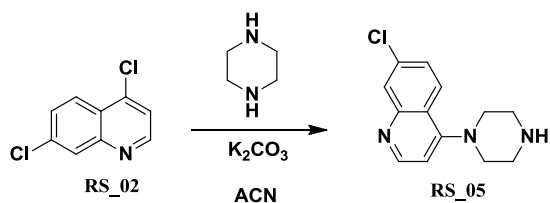
The compound was synthesized according to the above general procedure using 4,7-dichloroquinoline (**RS_02**) (2.5g, 12.62mmol), potassium carbonate (2.09, 15.14mmol) and piperazine (1.09g, 12.62mmol) to afford **RS_05** (1.9g, 60.7%) as an off-white solid. ^{1}H NMR (DMSO-d$_6$): δ_H2.92 - 3.03 (m, 4H), 3.05 - 3.13, (m, 4H), 6.95 − 8.67 (m, 5H).^{13}C NMR (DMSO-d$_6$): δc. 156.7, 152.1, 149.6, 133.4, 128, 125.9, 125.5, 121.3, 109.2, 52.8 (2C), 45.3 (2C). ESI-MS m/z 248.1(M+1)$^{+}$.Anal Calcd for C$_{13}$H$_{14}$ClN$_3$; C, 63.03; H, 5.70; N, 16.96; Found:63.05; H, 5.67; N, 16.93.

Preparation of 7-Trifluoromethyl-4-(piperazin-1-yl)quinolone (RS_06):
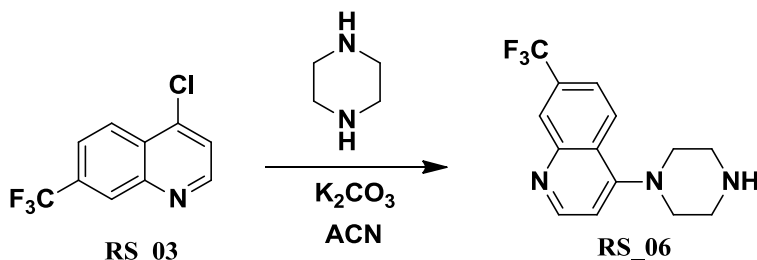
The compound was synthesized according to the above general procedure using 4-chloro-7-trifluoromethyl quinoline **(RS_03)** (2.5g, 10.79mmol), potassium carbonate (1.79g, 12.95mmol) and piperazine (0.93g, 10.79mmol) to afford **RS_06** (2.24g, 73.68%) as an off-white solid. ^{1}H NMR (DMSO-d$_6$): $\delta_{H.}$ 2.63 – 2.87 (m, 4H), 3.16 - 3.25 (m, 4H), 6.48 – 8.84 (m, 5H).^{13}C NMR (DMSO-d$_6$): δc. 161.5, 154.7, 145.2, 135.8, 130, 128.6, 124.1, 123.3, 119.7 (2C), 53.4 (2C), 43.7 (2C). ESI-MS m/z 282.12(M+1)$^+$. Anal Calcd for C$_{14}$H$_{14}$F$_3$N$_3$; C, 59.78; H, 5.02; N, 14.94; Found: 59.70; H, 4.93; N, 14.88.

General procedure for the synthesis of Methyl 2-(4-(7-substituted quinolin-4-yl)piperazin-1-yl)acetate derivatives (RS_7a-9a):

To a suspension of 4-(piperazin-1-yl)quinoline derivative (1mmol) and potassium carbonate (1.2mmol) in acetonitrile (20 mL) was added methylbromoacetate (1mmol) at 30°C. The reaction mixture was then heated to 60°C for 1h (monitored by TLC and LCMS for completion), cooled to 30°C. The mixture was then filtered through celite bed, and acetonitrile was evaporated in vacuo. The resultant residue was diluted with water and dichloromethane, and the layers separated. The aqueous layer was re-extracted with dichloromethane (2x 40 mL).The combined organic extract was washed with brine, driedoversodium sulphate, and evaporated in vacuo The resultant residue was the purified by column chromatography on neutral alumina using hexane: ethylacetate as eluent to to give desired product as described below

Preparation of Methyl 2-(4-(quinolin-4-yl)piperazin-1-yl)acetate (RS_7a):
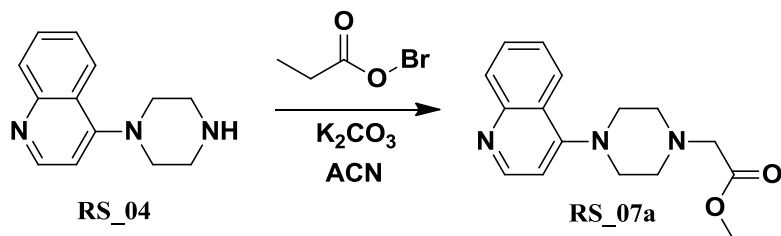
The compound was synthesized according to the above general procedure using 4-(piperazin-1-yl)quinolone (**RS_04**) (2.5g, 11.72mmol), potassium carbonate (1.94g, 14.06mmol) and methylbromoacetate (1.79g, 11.72mmol) to afford **RS_7a** (2.76g, 82.39%) as an off-white solid.^{1}H NMR (DMSO-d$_6$): δ_H 2.36–2.48 (m, 4H), 3.1 – 3.18 (m, 4H), 3.42 (s, 2H), 3.78 (s, 3H), 6.38 – 8.42 (m, 6H). ^{13}C NMR (DMSO-d$_6$): δc. 173.7, 161.8, 153.2, 139.6, 132.5, 129.2 (2C), 126.8, 124.9, 115.5, 57.6, 54.3 (2C), 52.0 (2C), 49.4. ESI-MS m/z 286.15(M+H)$^+$. Anal Calcd for C$_{16}$H$_{19}$N$_3$O$_2$; C, 67.35; H, 6.71; N, 14.73; Found: C, 67.21; H, 6.63; N, 14.69.

Preparation of Methyl 2-(4-(7-chloroquinolin-4-yl)piperazin-1-yl)acetate (RS_8a):

RS_05 → RS_08a
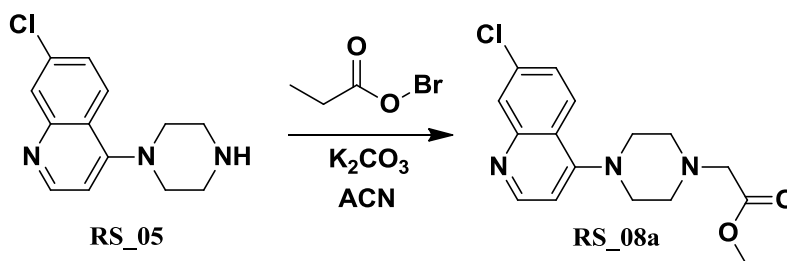
The compound was synthesized according to the above general procedure using 7-chloro-4-(piperazin-1-yl)quinolone (**RS_05**) (2.5g, 10.09mmol), potassium carbonate (1.67 g, 12.11mmol) andmethylbromoacetate (1.54 g, 10.09mmol) to afford **RS_8a** (2.23g, 69.04%) as an off-white solid.^{1}H NMR (DMSO-d$_6$): δ_H.2.73–2.82 (m, 4H), 3.01 – 3.12 (m, 4H), 3.36 (s, 2H), 3.68 (s, 3H), 6.93 – 8.61 (m, 5H).^{13}C NMR (DMSO-d$_6$): δc. 170.3, 156.5, 151.9, 149.7, 133.3, 128.1, 125.7, 125.3, 121.5, 118.9, 57.1, 55.3 (2C), 53.9 (2C), 51.2. ESI-MS m/z 320.11(M+H)$^+$. Anal Calcd for C$_{16}$H$_{18}$ClN$_3$O$_2$; C, 60.09; H, 5.67; N, 13.14; Found:C, 60.11; H, 5.64; N, 13.11.

Preparation of Methyl 2-(4-(7-trifluoromethylquinolin-4-yl)piperazin-1-yl)acetate (RS_9a):

RS_06 → RS_09a
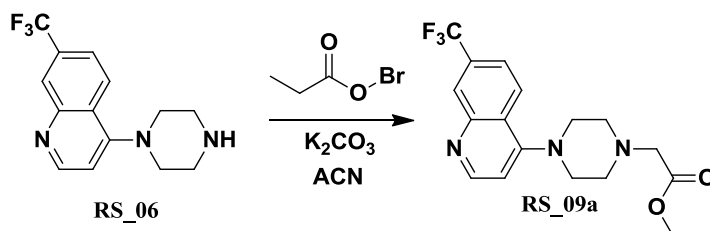
The compound was synthesized according to the above general procedure using7-trifluoromethyl-4-(piperazin-1-yl)quinolone (**RS_06**) (2.5g, 8.89mmol), potassium carbonate (1.47g, 10.67mmol) and methylbromoacetate (1.36g, 8.89mmol) to afford **RS_9a** (2.38g, 75.79%) as an off-white solid.^{1}H NMR (DMSO-d$_6$): δ_H 2.38–2.46 (m, 4H), 3.13 – 3.24 (m, 4H), 3.38 (s, 2H), 3.72 (s, 3H), 6.43 – 8.65 (m, 5H). ^{13}C NMR (DMSO-d$_6$): δc. 174.6, 162.3, 156.8, 150.1, 135.7, 130.1 (2C), 126.8, 124.3, 121.5, 118.5, 58.3, 54.8 (2C), 51.6 (2C), 50.4. ESI-MS

m/z 354.14(M+H)$^+$. Anal Calcd for $C_{17}H_{18}F_3N_3O_2$; C, 57.79; H, 5.13; N, 11.89; Found: C, 57.85; H, 5.08; N, 11.80.

General procedure for the synthesis of 2-(4-(quinolin-4-yl)piperazin-1-yl)acetic acid derivatives (RS_07 - RS_09): To a solution of methyl 2-(4-(quinolin-4-yl)piperazin-1-yl)acetatederivatives (1mmol) in THF:H$_2$O:CH$_3$OH system (1:1:1) was added lithium hydroxide (1.5mmol) at 0°C. The reaction mixture was slowly warmed to 30 ^{o}C then stirred at 30 ^{o}C for 3-4 h (monitored by TLC and LCMS for completion). The reaction mixture was then cooled to 0°C and acidified to a pH of 5-6 with 1N HCl. and extracted with dichloromethane (3 * 50mL). The combined organic extract was successively washed with water and brine,driedoversodium sulphate, and evaporated in vacuo to give desired product as mentioned below-

2-(4-(Quinolin-4-yl)piperazin-1-yl)acetic acid (RS_07):
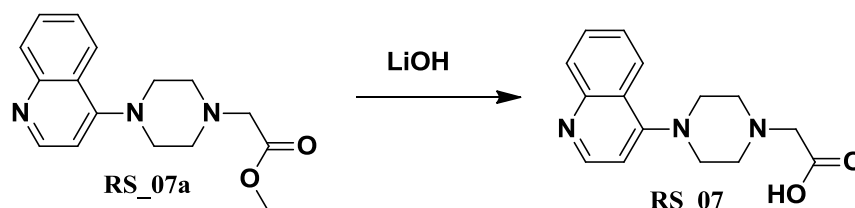
The compound was synthesized according to the above general procedure using methyl 2-(4-(quinolin-4-yl)piperazin-1-yl)acetate **(RS_7a)** (1.5g, 5.26 mmol)and lithium hydroxide (0.33g, 7.89mmol) to afford **RS_07** (0.87g, 60.84%)as white solid.^{1}H NMR (DMSO-d$_6$): δ_H 2.32 − 2.47 (m, 4H), 3.04 − 3.18 (m, 4H), 3.7 (s, 2H), 6.57 − 8.82 (m, 6H), 11.9 (s, 1H). ^{13}C NMR (DMSO-d$_6$): δc. 179.2, 163.7, 152.6, 141.4, 132.5, 129.8, 128.1, 126, 124.7, 117.2, 60.2, 53.8 (2C), 50.7 (2C). ESI-MS m/z 270.14 (M-H)$^+$. Anal Calcd for $C_{15}H_{17}N_3O_2$; C, 66.40; H, 6.32; N, 15.49; Found: C, 66.35; H, 6.41; N, 15.43.

2-(4-(7-Chloroquinolin-4-yl)piperazin-1-yl)acetic acid (RS_08):
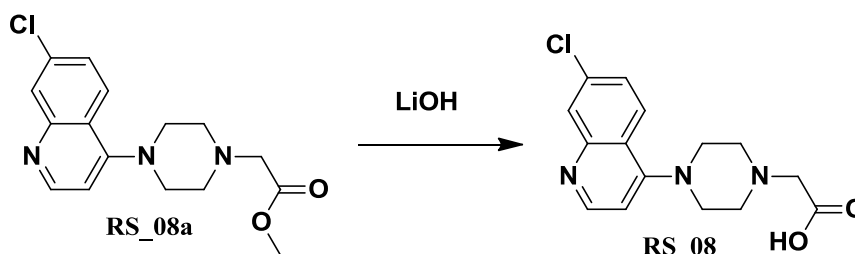
The compound was synthesized according to the above general procedure using methyl 2-(4-(7-chloroquinolin-4-yl)piperazin-1-yl)acetate **(RS_8a)** (1.5g, 4.69mmol) and lithium hydroxide (0.29g, 7.04mmol) to afford **RS_08** (0.7g, 48.95%) as white solid.^{1}H NMR (DMSO-d$_6$): δ_H 2.63

– 2.69 (m, 4H), 2.98 – 3.09 (m, 4H), 3.24 (s, 2H), 6.97 – 8.63 (m, 5H) 12.1 (s, 1H). ^{13}C NMR (DMSO-d$_6$): δc. 175.8, 156.9, 151.8, 149.3, 133.6, 127.8, 126, 125.6, 121.1, 109, 60.6, 55.6 (2C), 54.1 (2C). ESI-MS m/z 304.1 (M-H)[+]. Anal Calcd for C$_{15}$H$_{16}$ClN$_3$O$_2$; C, 58.92; H, 5.27; N, 13.74; Found:C, 58.89; H, 5.25; N, 13.76.

2-(4-(7-(Trifluoromethyl)quinolin-4-yl)piperazin-1-yl)acetic acid (RS_09):
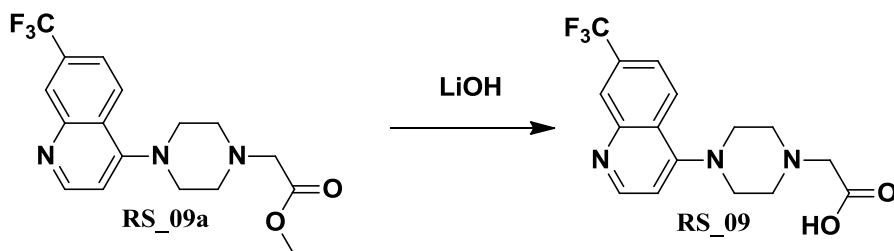
The compound was synthesized according to the above general procedure using methyl 2-(4-(7-(trifluoromethyl)quinolin-4-yl)piperazin-1-yl)acetate **(RS_9a)** (1.5g,4.25mmol) and lithium hydroxide (0.27g, 6.38mmol) to afford **RS_09** (0.69g, 47.92%) as white solid. ^{1}H NMR (DMSO-d$_6$): δ$_H$ 2.23 – 2.31 (m, 4H), 3.02 – 3.10 (m, 4H), 3.41 (s, 2H), 6.43 – 8.66 (m, 5H) 11.7 (s, 1H). ^{13}C NMR (DMSO-d$_6$): δc. 178.4, 161.3, 152.7, 145.9, 135.3, 130.6 (2C), 127.2, 123.8, 120.7, 118.5, 60.9, 54.1 (2C), 51.1 (2C). ESI-MS m/z 338.12 (M-H)[+]. Anal Calcd for C$_{16}$H$_{16}$F$_3$N$_3$O$_2$; C, 56.64; H, 4.75; N, 12.38; Found: C, 56.69; H, 4.72; N, 12.43.

General procedure for the synthesis of final compounds (RS_10- RS_30)
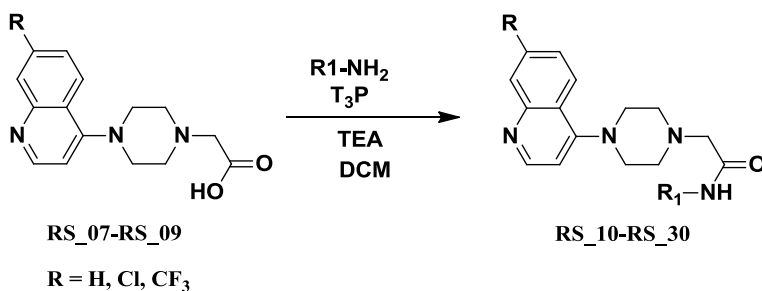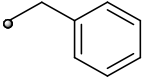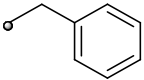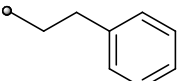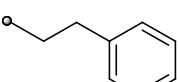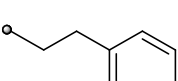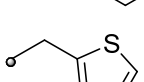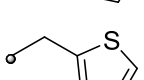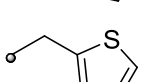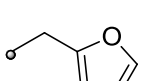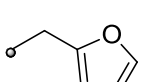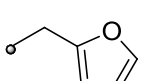
 To a solution of 2-(4-quinolin-4-yl)piperazin-1-yl)acetic acid derivatives (1 mmol) in dry dichloromethane (3mL) was added triethyl amine (1.5 mmol) and corresponding amine (1 mmol) at 0 °C. Propylphosphonic anhydride (2 mmol) was then added drop wise to the reaction mixture and the reaction mixture was stirred at rt for 6 h. (monitored by TLC & LCMS for completion). The reaction mixture was washed with water (2mL), brine (2mL), dried over anhydrous sodium sulphate and evaporated in vacuo to give the desired product as mentioned below.

Table 6.5: Physiochemical properties of the synthesized compounds **RS_10 – RS_30**
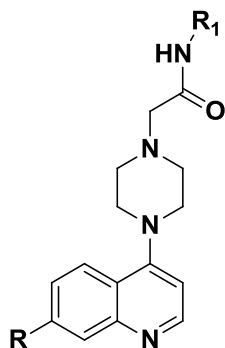
COMP.	R	R₁	Yield (%)	Molecular Formula	Molecular Weight
RS_10	H		69.7	$C_{21}H_{23}N_5O$	361.44
RS_11	Cl		75.0	$C_{21}H_{22}ClN_5O$	395.89
RS_12	CF₃		58.0	$C_{22}H_{22}F_3N_5O$	429.44
RS_13	H		60.1	$C_{22}H_{25}N_5O$	375.47
RS_14	Cl		73.5	$C_{22}H_{24}ClN_5O$	409.91
RS_15	CF₃		54.5	$C_{23}H_{24}F_3N_5O$	443.46
RS_16	H		64.8	$C_{21}H_{22}ClN_5O$	395.89
RS_17	Cl		57.1	$C_{21}H_{21}Cl_2N_5O$	430.33
RS_18	CF₃		67.6	$C_{22}H_{21}ClF_3N_5O$	463.88
RS_19	H		54.5	$C_{22}H_{24}N_4O$	360.45

RS_20	Cl		84.2	$C_{22}H_{23}ClN_4O$	394.90
RS_21	CF$_3$		47.7	$C_{23}H_{23}F_3N_4O$	428.45
RS_22	H		54.2	$C_{23}H_{26}N_4O$	374.48
RS_23	Cl		45.4	$C_{23}H_{25}ClN_4O$	408.92
RS_24	CF$_3$		54.6	$C_{24}H_{25}F_3N_4O$	442.48
RS_25	H		64.7	$C_{20}H_{22}N_4OS$	366.48
RS_26	Cl		64.0	$C_{20}H_{21}ClN_4OS$	400.92
RS_27	CF$_3$		46.8	$C_{21}H_{21}F_3N_4OS$	434.48
RS_28	H		81.2	$C_{20}H_{22}N_4O_2$	350.41
RS_29	Cl		59.0	$C_{20}H_{21}ClN_4O_2$	384.86
RS_30	CF$_3$		70.9	$C_{21}H_{21}F_3N_4O_2$	418.41

6.3.3. Characterization of Synthesized compounds RS_10 - RL_30

2-(4-(Quinolin-4-yl)piperazin-1-yl)-N-(pyridin-2-ylmethyl)acetamide (**RS_10**): The compound was synthesized according to the above general procedure using 2-(4-(quinolin-4-yl)piperazin-1-yl)acetic acid (**RS_07)** (0.25g, 0.92mmol), pyridin-2-ylmethanamine (0.099g mmol, 0.92mmol), triethylamine (0.14g, 1.38mmol), propylphosphonic anhydride (0.59g, 1.84mmol) to afford **RS_10** (0.23g, 69.7%) as off white solid.^{1}H NMR (DMSO-d$_6$): δ_H 2.54 (m, 4H), 3.07 (m, 4H), 3.37(s, 2H), 4.52 (s, 2H), 6.94 (d, J = 7.8 Hz,1H), 7.35 − 7.88 (m, 6H), 8.06 (s, 1H), 8.14 − 8.52 (m, 3H). ^{13}C NMR (DMSO-d$_6$): δc. 171.1, 157.3, 156, 151.6, 148.9, 140.4, 139.9, 130.6, 130, 128.7, 128.2, 127, 124.3, 121.1, 114.9, 60.1, 52.6 (2C), 47.8 (2C), 46.1. ESI-

MS *m/z* 362.19 (M+H)$^+$. Anal Calcd for $C_{21}H_{23}N_5O$;C, 69.78; H, 6.41; N, 19.38; Found: 69.84;H, 6.42; N, 19.36.

2-(4-(7-Chloroquinolin-4-yl)piperazin-1-yl)-N-(pyridin-2-ylmethyl)acetamide (**RS_11**): The compound was synthesized according to the above general procedure using 2-(4-(7-chloroquinolin-4-yl)piperazin-1-yl)acetic acid (**RS_08**) (0.25g, 0.82mmol), pyridin-2-ylmethanamine (0.09g,0.82mmol), triethylamine (0.13g, 1.23 mmol), propylphosphonic anhydride (0.52g, 1.64mmol) to afford **RS_11** (0.25g, 75%) as off white solid. ^{1}H NMR (DMSO-d$_6$): δ_H 2.69 (m, 4H), 3.07 (m, 4H), 3.36 (s, 2H), 4.51 (s, 2H), 6.93 (d, *J* = 5.2 Hz, 1H), 7.23 − 7.35 (m, 3H), 7.76 − 7.98 (m, 3H), 8.49 − 8.64 (m, 3H). ^{13}C NMR (DMSO-d$_6$): δc. 171.4, 156.9, 155.8, 152.7, 150.2, 149.3, 140, 136.9, 132.6, 128.6, 125.8, 124.3, 123.1, 121.2, 118.6, 60.3, 52.3 (2C), 47.6 (2C), 45.9. ESI-MS *m/z* 396.15 (M+H)$^+$. Anal Calcd for $C_{21}H_{22}ClN_5O$;C, 63.71; H, 5.60; N, 17.69; Found: C, 63.64; H, 5.61; N, 17.72.

**2-(4-(7-Trifluoromethyl quinolin-4-yl)piperazin-1-yl)-N-(pyridin-2-ylmethyl)acetamide** (**RS_12**): The compound was synthesized according to the above general procedure using 2-(4-(7-trifluoromethyl quinolin-4-yl)piperazin-1-yl)acetic acid (**RS_09**) (0.25g, 0.74mmol), pyridin-2-ylmethanamine (0.08g mmol,0.74mmol), triethylamine (0.11g, 1.11 mmol), propyphosphonic anhydride (0.47g, 1.48mmol) to afford **RS_12** (0.18g, 58%) as off white solid. ^{1}H NMR (DMSO-d$_6$): δ_H 2.71 (m, 4H), 2.99 (m, 4H), 3.43 (s, 2H), 4.67 (s, 2H), 6.95 (d, *J* = 7.0 Hz, 1H), 7.28 − 7.74 (m, 3H), 7.89 (s, 1H), 8.15 − 8.71 (m, 5H). ^{13}C NMR (DMSO-d$_6$): δc. 171.3, 157.7, 156.2, 152.9, 148.8, 147.9, 139.8, 132.7, 129.1, 128.8, 126.5, 124.3, 124.1, 121.8, 121, 120.4, 59.9, 52.4 (2C), 47.9 (2C), 46.1. ESI-MS *m/z* 430.21 (M+H)$^+$. Anal Calcd for $C_{22}H_{22}F_3N_5O$;C, 61.53; H, 5.16; N, 16.31; FoundC, 61.61; H, 5.17; N, 16.29.

2-(4-(Quinolin-4-yl)piperazin-1-yl)-N-(2-(pyridin-2-yl)ethyl)acetamide(RS_13): The compound was synthesized according to the above general procedure using 2-(4-(quinolin-4-yl)piperazin-1-yl)acetic acid (**RS_07)** (0.25g, 0.92mmol), 2-(pyridin-2-yl)ethanamine(0.11g, 0.92mmol), triethylamine (0.14g, 1.38 mmol), Propylphosphonic anhydride (0.59g, 1.84 mmol) to afford **RS_13** (0.21g, 60%) as off white solid. ^{1}H NMR (DMSO-d$_6$): δ_H 2.56 (m, 4H), 2.97 (t, J = 6.8 Hz, 2H), 3.07 (m, 4H), 3.32(s, 2H), 3.61 (m, 2H), 6.99 (d, *J* = 8.0 Hz,1H), 7.19 − 7.52 (m, 5H), 7.93 − 7.97 (m, 2H), 8.11 − 8.83 (m, 3H). ^{13}C NMR (DMSO-d$_6$): δc. 171.2, 159.8, 157.3, 150.8, 147.4, 142.7, 136.2, 131.8, 130.8, 128.7, 126, 124.8, 122.2, 120.1, 119.8, 60.7, 52.8 (2C),

50.4 (2C), 42.6, 33.7. ESI-MS m/z 376.21 (M+H)$^+$. Anal Calcd for $C_{22}H_{25}N_5O$;C, 70.38; H, 6.71; N, 18.65; Found: C, 70.49 ; H, 6.70 ; N, 18.67 .

2-(4-(7-Chloroquinolin-4-yl)piperazin-1-yl)-N-(2-(pyridin-2-yl)ethyl)acetamide(RS_14): The compound was synthesized according to the above general procedure using 2-(4-(7-chloroquinolin-4-yl)piperazin-1-yl)acetic acid (**RS_08**) (0.25g, 0.82mmol), 2-(pyridin-2-yl)ethanamine (0.1g mmol, 0.82mmol), triethylamine (0.13g, 1.23mmol), propyphosphonic anhydride (0.52 g, 1.64mmol) to afford **RS_14** (0.25g, 73.5%) as off white solid.^{1}H NMR (DMSO-d$_6$): δ_H 2.61 (m, 4H), 2.94 (t, J = 6.8 Hz, 2H), 3.02 (s, 2H), 3.16 (m, 4H), 3.53 (m, 2H), 6.99 (d, J = 5.2 Hz, 1H), 7.23 – 7.26 (m, 1H), 7.28 (d, J = 7.6 Hz, 1H), 7.57 − 8.01 (m, 5H), 8.51 − 8.73 (m,2H). ^{13}C NMR (DMSO-d$_6$): δc. 169.3, 159.7, 156.7, 152.6, 150.0, 149.5, 137.0, 134.0, 128.5, 126.5, 126.26, 123.7, 122.0, 121.8, 101.8, 61.6, 52.1 (2C), 39.4 (2C), 38.4, 37.4. ESI-MS m/z 410.17 (M+H)$^+$. Anal Calcd for $C_{22}H_{24}ClN_5O$;C, 64.46; H, 5.90; N, 17.09; Found: C, 64.37; H, 5.91; N, 17.11.

2-(4-(7-(Trifluoromethyl)quinolin-4-yl)piperazin-1-yl)-N-(2-(pyridin-2-yl)ethyl) acetamide (RS_15): The compound was synthesized according to the above general procedure using 2-(4-(7-(trifluoromethyl)quinolin-4-yl)piperazin-1-yl)acetic acid (**RS_09**) (0.25g, 0.74mmol), 2-(pyridin-2-yl)ethanamine (0.09g mmol,0.74mmol), triethylamine (0.11g, 1.11 mmol), Propylphosphonic anhydride (0.47g, 1.48mmol) to afford **RS_15** (0.18g, 54.55%) as off white solid. ^{1}H NMR (DMSO-d$_6$): δ_H 2.92 (m, 4H), 3.14 (m, 4H), 3.02 (t, J = 7.0 Hz, 2H), 3.27 (s, 2H), 3.58 (m, 2H), 7.06 (d, J = 8.0 Hz, 1H), 7.25 − 7.33 (m, 2H), 7.62 (s, 1H), 7.98 (s, 1H),8.18 −8.87 (m,5H). ^{13}C NMR (DMSO-d$_6$): δc. 171.5, 160.8, 158.2, 151.8, 148.1, 147, 135.9, 131.8, 129.3, 128.7, 126.7, 123.4, 122.3, 121.9, 119.7, 115.2, 60.7, 56.3 (2C), 50.7 (2C), 43.4, 35.1. ESI-MS m/z 444.19(M+H)$^+$. Anal Calcd for $C_{23}H_{24}F_3N_5O$;C, 62.29; H, 5.45; N, 15.79; Found: C, 62.37 ; H, 5.46 ; N, 15.77 .

2-(4-(Quinolin-4-yl)piperazin-1-yl)-N-((6-chloropyridin-3-yl)methyl)acetamide (RS_16): The compound was synthesized according to the above general procedure using 2-(4-(quinolin-4-yl)piperazin-1-yl)acetic acid (**RS_07**) (0.25g, 0.92mmol), (6-chloropyridin-3-yl)methanamine (0.13g mmol,0.92mmol), triethylamine (0.14g, 1.38 mmol), Propylphosphonic anhydride (0.59g, 1.84 mmol) to afford **RS_16** (0.24g, 64.87%) as off white solid. ^{1}H NMR (DMSO-d$_6$): δ_H 2.59 (m, 4H), 3.08 (m, 4H), 3.32 (s, 2H), 4.23 (s, 2H), 7.03 (d, J = 7.2 Hz,1H), 7.52 − 7.88 (m, 4H),

8.02 (s, 1H), 8.14 – 8.82 (m, 4H).^{13}C NMR (DMSO-d$_6$): δc. 171.8, 162.4, 151.3, 149.9, 146.8, 140.3, 139.3, 133.7, 130.2, 129.8, 128.4, 127.5, 125.2, 121.9, 116.3, 60.4, 55.9 (2C), 53.1 (2C), 43.2. ESI-MS m/z 396.15 (M+H)$^+$. Anal Calcd for C$_{21}$H$_{22}$ClN$_5$O;C, 63.71; H, 5.60; N, 17.69; Found: C, 63.81; H, 5.61; N, 17.71.

2-(4-(7-Chloroquinolin-4-yl)piperazin-1-yl)-N-((6-chloropyridin-3-yl)methyl)acetamide

(RS_17): The compound was synthesized according to the above general procedure using 2-(4-(7-chloroquinolin-4-yl)piperazin-1-yl) acetic acid (**RS_08**) (0.25g, 0.82mmol), (6-chloropyridin-3-yl)methanamine (0.12g,0.82mmol), triethylamine (0.13g, 1.23mmol), Propylphosphonic anhydride (0.52g, 1.64mmol) to afford **RS_17** (0.20g, 57.14%) as off white solid.^{1}H NMR (DMSO-d$_6$): $\delta$$_H$ 2.62 (m, 4H), 3.11 (m, 4H), 3.32 (s, 2H), 4.48 (s, 2H), 6.98 (d, J = 5.0, 1H), 7.42 - 7.82 (m, 3H), 8.01 – 8.53 (m, 4H), 8.86 (s,1H). ^{13}C NMR (DMSO-d$_6$): δc. 169.3, 160.3, 154.2, 151.2, 150.9, 147.5, 142.1, 137.5, 130.8, 129.9, 127, 124.8, 120.4, 118.4, 115.8, 61.6, 53.8 (2C), 51.6 (2C), 43.9. ESI-MS m/z 431.11 (M+H)$^+$. Anal Calcd for C$_{21}$H$_{21}$Cl$_2$N$_5$O; C, 58.61; H, 4.92; N, 16.27; Found: C, 58.55; H, 4.91; N, 16.29.

2-(4-(7-(Trifluoromethyl)quinolin-4-yl)piperazin-1-yl)-N-((6-chloropyridin-3-yl)methyl)

acetamide (RS_18): The compound was synthesized according to the above general procedure using2-(4-(7-(trifluoromethyl)quinolin-4-yl)piperazin-1-yl) acetic acid (**RS_09)** (0.25g, 0.74mmol), (6-chloropyridin-3-yl)methanamine (0.11g mmol,0.74mmol), triethylamine (0.11g, 1.11mmol), Propylphosphonic anhydride (0.47g, 1.48mmol) to afford **RS_18** (0.23g, 67.65%) as off white solid.^{1}H NMR (DMSO-d$_6$): $\delta$$_H$ 2.83 (m, 4H), 3.07 (m, 4H), 3.27 (s, 2H), 4.52 (s, 2H), 6.92 (d, J = 7.8 Hz, 1H), 7.40 – 7.38 (m, 1H), 7.91 (s, 1H), 8.19 – 8.27 (m, 4H), 8.72 – 8.82 (m,2H). ^{13}C NMR (DMSO-d$_6$): δc. 172.0, 160.4, 152.1, 151.6, 148.9, 146.4, 139.3, 134.5, 133.7, 130.6, 130.1, 125.4, 123.2, 122.6, 121.5, 119.6, 61.2, 53.2 (2C), 50.3 (2C), 43.1. ESI-MS m/z 464.14(M+H)$^+$. Anal Calcd for C$_{22}$H$_{21}$ClF$_3$N$_5$O;C, 56.96; H, 4.56; N, 15.10; Found: C,57.09; H, 4.57; N, 15.08.

N-(Benzyl)-2-(4-(quinolin-4-yl)piperazin-1-yl)acetamide (RS_19): The compound was synthesized according to the above general procedure using 2-(4-(quinolin-4-yl)piperazin-1-yl)aceticacid (**RS_07**) (0.25g, 0.92mmol), phenylmethanamine (0.098g mmol,0.92mmol), triethylamine (0.14g, 1.38 mmol), Propylphosphonic anhydride (0.59g, 1.84 mmol) to afford **RS_19** (0.18g, 54.55%) as solid.^{1}H NMR (DMSO-d$_6$): $\delta$$_H$ 2.62 (m, 4H), 3.11 (m, 4H), 3.28 (s,

2H), 4.27 (s, 2H), 7.01 (d, J = 6.8 Hz,1H), 7.26 – 7.74 (m, 7H), 7.91 – 8.26 (m, 4H). ^{13}C NMR (DMSO-d$_6$): δc. 172.5, 160.8, 152.8, 139.3, 136.4, 131.6, 130.2, 128.2, 128.8 (3C), 127.1 (2C), 126.8, 124.2, 117.4, 59.1 (2C), 54.7 (2C), 49.7, 43.8. ESI-MS m/z 361.2 (M+H)$^+$. Anal Calcd for C$_{22}$H$_{24}$N$_4$O;C, 73.31; H, 6.71; N, 15.54; Found: C, 73.24; H, 6.70; N, 15.56.

N-Benzyl-2-(4-(7-chloroquinolin-4-yl)piperazin-1-yl)acetamide (RS_20): The compound was synthesized according to the above general procedure using 2-(4-(7-chloroquinolin-4-yl)piperazin-1-yl)aceticacid (**RS_08)** (0.25g, 0.82mmol), phenylmethanamine (0.09g mmol,0.82mmol), triethylamine (0.13g, 1.23mmol), propylphosphonic anhydride (0.52g, 1.64mmol) to afford **RS_20** (0.27g, 84%) as solid.^{1}H NMR (DMSO-d$_6$): $\delta_{H.}$ 2.70 (m, 4H), 3.12 (s, 2H), 3.23 (m, 4H), 4.50 (s, 2H), 7.02 (d, J = 5.2, 1H), 7.27 – 7.38 (m, 6H), 7.57 (m, 1H), 8.01 (m, 1H), 8.50 – 8.71 (m,2H). ^{13}C NMR (DMSO-d$_6$): δc. 169.5, 156.7, 152.6, 150.1, 143.2, 134.0, 128.8, 128.5, 127.6, 127.1 (2C), 126.5 (2C), 126.2, 121.3, 109.8, 61.4, 53.1 (2C), 52.0 (2C), 37.4. ESI-MS m/z 395.16 (M+H)$^+$. Anal Calcd for C$_{22}$H$_{23}$ClN$_4$O;C, 66.91; H, 5.87; N, 14.19; Found: C, 67.00; H, 5.88; N, 14.21.

N-(Benzyl)-2-(4-(7-(trifluoromethyl)quinolin-4-yl)piperazin-1-yl)acetamide (RS_21): The compound was synthesized according to the above general procedure using2-(4-(7-(trifluoromethyl)quinolin-4-yl)piperazin-1-yl) acetic acid (**RS_09)** (0.25g, 0.74mmol), phenyl methanamine(0.08g mmol,0.74mmol), triethylamine (0.11g, 1.11 mmol), Propylphosphonicanhydride (0.47g, 1.48mmol) to afford **RS_21** (0.15g, 47.75%) as solid. ^{1}H NMR (DMSO-d$_6$): $\delta_{H.}$ 2.72 (m, 4H), 3.08 (m, 4H), 3.28 (s, 2H), 4.16 (s, 2H), 7.05 (d, J = 8.0, 1H), 7.21 – 7.37 (m, 5H), 7.92 (s, 1H), 8.19 – 8.28 (m, 3H), 8.85 (d, J = 7.2 Hz,1H). ^{13}C NMR (DMSO-d$_6$): δc. 170.8, 158.4, 153.4, 145.3, 136.2, 132.7, 129.4, 128.0, 128.6 (2C), 126.2 (2C), 125.7, 125.1, 124.5, 122.9, 119.6, 60.3, 55.6 (2C), 53.2 (2C), 43.1. ESI-MS m/z 429.18 (M+H)$^+$. Anal Calcd for C$_{23}$H$_{23}$F$_3$N$_4$O;C, 64.48; H, 5.41; N, 13.08; Found: C, 64.41; H, 5.40; N, 13.06.

N-Phenethyl-2-(4-(quinolin-4-yl)piperazin-1-yl)acetamide (RS_22): The compound was synthesized according to the above general procedure using 2-(4-(quinolin-4-yl)piperazin-1-yl)aceticacid (**RS_07)** (0.25g, 0.92mmol), phenylethanamine (0.11g, 0.92mmol), triethylamine (0.14g, 1.38 mmol), Propylphosphonic anhydride (0.59g, 1.84 mmol) to afford **RS_22** (0.19g, 54.29%) as solid.^{1}H NMR (DMSO-d$_6$): $\delta_{H.}$ 2.57 (m, 4H), 2.86 (t, J = 6.8 Hz, 2H), 3.10 (m, 4H), 3.28 (s, 2H), 3.42 (m, 2H), 6.96 (d, J = 7.0 Hz,1H), 7.28 – 7.73 (m, 7H), 7.92 - 8.06 (m, 2H),

8.22 – 8.31 (m, 2H). ^{13}C NMR (DMSO-d$_6$): δc. 169.8, 162.7, 153.6, 142.6, 140.7, 133.4, 131.8, 130.2, 129.7, 128.7 (2C), 126.4 (2C), 126.0, 123.8, 120.7, 59.4, 55.9 (2C), 53.8 (2C), 40.4, 34.8. ESI-MS m/z 375.21 (M+H)$^+$. Anal Calcd for C$_{23}$H$_{26}$N$_4$O; C, 73.77; H, 7.00; N, 14.96; Found: C,73.85 ; H, 6.99 ; N, 14.98.

N-Phenethyl-2-(4-(7-chloroquinolin-4-yl)piperazin-1-yl)acetamide (RS_23): The compound was synthesized according to the above general procedure using 2-(4-(7-chloroquinolin-4-yl)piperazin-1-yl) acetic acid (**RS_08)** (0.25g, 0.82mmol), phenyl ethanamine (0.099g, 0.82mmol), triethylamine (0.13g, 1.23mmol), Propylphosphonic anhydride (0.52g, 1.64mmol) to afford **RS_23** (0.15g, 45.46%) as solid.^{1}H NMR (DMSO-d$_6$): $\delta_{H.}$ 2.52 (m, 4H), 2.86 (t, J = 7.0 Hz, 2H), 3.12 (m, 6H), 3.30 (m, 2H), 7.00 (d, J = 5.4 Hz, 1H), 7.22 – 7.38 (m, 6H), 7.93 - 7.89 (m, 1H), 8.08 (s, 1H), 8.21 – 8.55 (m,2H). ^{13}C NMR (DMSO-d$_6$): δc. 171.4, 160.9, 154.8, 150.3, 140.4, 137.8, 131.3, 129.5, 129.0, 128.3 (2C), 125.7 (2C), 124.2, 121.8, 119.2, 59.1, 53.2 (2C), 50.8 (2C), 41.6, 33.7. ESI-MS m/z 409.17 (M+H)$^+$. Anal Calcd for C$_{23}$H$_{25}$ClN$_4$O; C, 67.55; H, 6.16; N, 13.70; Found: C, 67.66; H, 6.18; N, 13.68.

N-Phenethyl-2-(4-(7-(trifluoromethyl)quinolin-4-yl)piperazin-1-yl)acetamide (RS_24): The compound was synthesized according to the above general procedure using 2-(4-(7-(trifluoromethyl)quinolin-4-yl)piperazin-1-yl) acetic acid (**RS_09**) (0.25g, 0.74mmol), phenyl ethanamine (0.09g, 0.74mmol), triethylamine (0.11g, 1.11mmol), Propylphosphonic anhydride (0.47g, 1.48mmol) to afford **RS_24** (0.18g, 54.55%) as solid.^{1}H NMR (DMSO-d$_6$): $\delta_{H.}$ 2.51 (m, 4H), 2.91 (t, J = 6.8 Hz, 2H), 3.11 (m, 4H), 3.31 (s, 2H), 3.37 (m, 2H), 6.99 (d, J = 7.4 Hz, 1H), 7.25 – 7.40 (m, 5H), 7.81 (s, 1H), 8.24 – 8.32 (m, 3H), 8.78 (d, J = 6.8 Hz, 1H). ^{13}C NMR (DMSO-d$_6$): δc. 169.8, 158.3, 154.2, 147.9, 142.5, 133.7, 130.4, 129.7, 128.4 (2C), 126.4 (2C), 125.2, 124.8, 123.2, 121.6, 120.2, 59.3, 54.8 (2C), 51.4 (2C), 41.4, 34.9. ESI-MS m/z 443.2 (M+H)$^+$. Anal Calcd for C$_{24}$H$_{25}$F$_3$N$_4$O; C, 65.15; H, 5.69; N, 12.66; Found: C, 65.23; H, 5.68; N, 12.64.

2-(4-(Quinolin-4-yl)piperazin-1-yl)-N-(thiophen-2-ylmethyl)acetamide (RS_25): The compound was synthesized according to the above general procedure using 2-(4-(quinolin-4-yl)piperazin-1-yl)acetic acid (**RS_07**) (0.25g, 0.92mmol), thiophen-2-ylmethanamine (0.10g,0.92mmol), triethylamine (0.14g, 1.38 mmol), Propylphosphonic anhydride (0.59g, 1.84mmol) to afford **RS_25** (0.22g, 64.71%) as pale brown solid.^{1}H NMR (DMSO-d$_6$): $\delta_{H.}$ 2.61

(m, 4H), 3.15 (m, 4H), 3.34(s, 2H), 5.14 (s, 2H), 6.95 (m, 1H), 7.04 (d, J = 7.2 Hz, 1H), 7.08 – 7.77 (m, 4H), 7.97 - 8.33 (m, 4H). ^{13}C NMR (DMSO-d$_6$): δc. 174.4, 161.6, 153.2, 140.5, 139.8, 131.4, 129.4, 128.2, 127.8 (2C), 127, 125.4, 123.2, 120.3, 59.1, 54.7 (2C), 51.3 (2C), 44.7. ESI-MS m/z 367.15 (M+H)$^+$. Anal Calcd for C$_{20}$H$_{22}$N$_4$OS;C, 65.55; H, 6.05; N, 15.29; Found: C, 65.62; H, 6.06; N, 15.31.

2-(4-(7-Chloroquinolin-4-yl)piperazin-1-yl)-N-(thiophen-2-ylmethyl)acetamide (**RS_26**): The compound was synthesized according to the above general procedure using2-(4-(7-chloroquinolin-4-yl)piperazin-1-yl)acetic acid (**RS_08)** (0.25g, 0.82mmol), thiophen-2-ylmethanamine (0.09g mmol,0.82mmol), triethylamine (0.13g, 1.23mmol), propylphosphonic anhydride (0.52g, 1.64mmol) to afford **RS_26** (0.21g, 64%) as pale brown solid. ^{1}H NMR (DMSO-d$_6$): δH. 2.56 (m, 4H), 2.91 (m, 4H), 3.23 (s, 2H), 5.02 (s, 2H), 6.83 (d, J = 5.6 Hz, 1H), 7.11 – 7.82 (m, 5H), 8.08 (s, 1H), 8.26 – 8.49 (m, 2H). ^{13}C NMR (DMSO-d$_6$): δc. 171.1, 157.4, 152.8, 149.7, 141.1, 133.2, 129.8, 129, 127.2, 126.6, 125.8, 125.3, 122.9, 119.8, 59.8, 52.7 (2C), 47.6 (2C), 42.8. ESI-MS m/z 401.31(M+H)$^+$. Anal Calcd for C$_{20}$H$_{21}$ClN$_4$OS;C, 59.91; H, 5.28; N, 13.97; Found: C, 59.83; H, 5.29; N, 13.95.

2-(4-(7-(Trifluoromethyl)quinolin-4-yl)piperazin-1-yl)-N-(thiophen-2-ylmethyl)acetamide (RS_27): The compound was synthesized according to the above general procedure using 2-(4-(7-(trifluoromethyl)quinolin-4-yl)piperazin-1-yl) acetic acid (**RS_09)** (0.25g, 0.74mmol), thiophen-2-ylmethanamine (0.084g, 0.74mmol), triethylamine (0.11g, 1.11 mmol), Propylphosphonicanhydride (0.47g, 1.48mmol) to afford **RS_27** (0.15g, 46.88%) as pale brown solid.^{1}H NMR (DMSO-d$_6$): δH. 2.68 (m, 4H), 3.18 (m, 4H), 3.29 (s, 2H), 5.04 (s, 2H), 6.97 (m, 1H), 7.08 (d, J = 7.8 Hz,1H), 7.09 – 7.42 (m, 2H), 7.76 (s, 1H), 8.18 – 8.29 (m, 3H), 8.81 (d, J = 7.0 Hz, 1H).^{13}C NMR (DMSO-d$_6$): δc. 173.5, 160.4, 154.3, 149.8, 139.6, 133.7, 129.5, 129, 127.8, 126.8, 125.8, 125.3, 123.2, 121.4, 118.5, 59.8, 55.3 (2C), 52.6 (2C), 42.9. ESI-MS m/z 435.14 (M+H)$^+$. Anal Calcd for C$_{21}$H$_{21}$F$_3$N$_4$OS;C, 58.05; H, 4.87; N, 12.90; Found: C, 57.97; H, 4.86; N, 12.92.

2-(4-(Quinolin-4-yl)piperazin-1-yl)-N-(furan-2-ylmethyl)acetamide (RS_28): The compound was synthesized according to the above general procedure using 2-(4-(quinolin-4-yl)piperazin-1-yl)aceticacid (**RS_07**) (0.25g, 0.92mmol), furan-2-ylmethanamine (0.089g mmol,0.92mmol), triethylamine (0.14g, 1.38 mmol), Propylphosphonic anhydride (0.59g, 1.84 mmol) to afford

RS_28 (0.26g, 81.25%) as solid. ^{1}H NMR (DMSO-d$_6$): δ_H 2.62 (m, 4H), 3.15 (m, 4H), 3.27(s, 2H), 4.56 (s, 2H), 6.24 - 6.42 (m, 2H), 7.05 (d, J = 7.8 Hz,1H), 7.62 – 7.97 (m, 5H), 8.20 – 8.31 (m, 2H). ^{13}C NMR (DMSO-d$_6$): δc. 170.2, 160.8, 152.5, 146.3, 142.5, 139.6, 131.7, 129.0, 128.9, 127.1, 126.4, 117.3, 110.4, 109.8, 59.8, 54.2 (2C), 51.3 (2C), 37.2. ESI-MS m/z 351.17 (M+H)$^+$. Anal Calcd for C$_{20}$H$_{22}$N$_4$O$_2$;C, 68.55; H, 6.33; N, 15.99; Found: C, 68.45; H, 6.34; N, 16.01 .

2-(4-(7-Chloroquinolin-4-yl)piperazin-1-yl)-N-(furan-2-ylmethyl)acetamide (**RS_29**): The compound was synthesized according to the above general procedure using 2-(4-(7-chloroquinolin-4-yl)piperazin-1-yl)aceticacid (**RS_08**) (0.25g, 0.82mmol), furan-2-ylmethanamine (0.08g mmol,0.82mmol), triethylamine (0.13g, 1.23mmol), propylphosphonic anhydride (0.52g, 1.64mmol) to afford **RS_29** (0.19g, 59%) as solid. ^{1}H NMR (DMSO-d$_6$): δ_H 2.82 (m, 4H), 3.07 (m, 4H), 3.31 (s, 2H), 4.40 (d, J = 8.2 Hz, 2H), 6.24 - 6.45 (m, 2H), 6.91 (d, J = 5. Hz, 1H), 7.34 – 7.88 (m, 4H), 8.25 – 8.52 (m,2H). ^{13}C NMR (DMSO-d$_6$): δc. 170.8, 157.2, 152.7, 149.9, 146.3, 141.8, 133.4, 129.8, 129, 125.8, 122.6, 118.3, 110.1, 109.7, 59, 52.5 (2C), 47.2 (2C), 36.8. ESI-MS m/z 385.23 (M+H)$^+$. Anal Calcd for C$_{20}$H$_{21}$ClN$_4$O$_2$;C, 62.42; H, 5.50; N, 14.56; Found: C, 62.54; H, 5.51; N, 14.54.

2-(4-(7-(Trifluoromethyl)quinolin-4-yl)piperazin-1-yl)-N-(furan-2-ylmethyl)acetamide (RS_30): The compound was synthesized according to the above general procedure using 2-(4-(7-(trifluoromethyl)quinolin-4-yl)piperazin-1-yl) acetic acid (**RS_09**) (0.25g, 0.74mmol), furan-2-ylmethanamine (0.072g,0.74mmol), triethylamine (0.11g, 1.11 mmol), Propylphosphonic anhydride (0.47g, 1.48mmol) to afford **RS_30** (0.22g, 70.97%) as solid. ^{1}H NMR (DMSO-d$_6$): δ_H 2.77 (m, 4H), 3.16 (m, 4H), 3.33 (s, 2H), 4.33 (d, J = 8.0, 2H), 6.23 (m, 1H), 6.41 (m, 1H), 7.15 (d, J = 7.2 Hz, 1H), 7.57 (s, 1H), 7.81 – 8.30 (m, 4H), 8.83 (d, J = 7.4 Hz, 1H). ^{13}C NMR (DMSO-d$_6$): δc. 172.4, 160.3, 154.2, 148.1, 145.3, 141.3, 131.4, 129.7, 128, 127.2, 123.2, 120.3, 118.4, 110.1, 109.2, 60.5, 54.2 (2C), 51.8 (2C), 35.6. ESI-MS m/z 419.16 (M+H)$^+$. Anal Calcd for C$_{21}$H$_{21}$F$_3$N$_4$O$_2$;C, 60.28; H, 5.06; N, 13.39; Found: C, 60.32; H, 5.05; N, 13.41.

6.3.4. *In vitro* LAT inhibitory assay, antimycobacterial potency and cytotoxicity studies of the synthesized molecules

As LAT enzyme is involved in transferring amine from lysine to ketoglutarate resulting in formation of piperidine-6-carboxylate and glutamate. The resultant products have absorbance

maxima at 465 and 280 nm which was used for measuring inhibitory potential of synthesized compounds. Among 21 compounds, 13 compounds exhibited IC_{50} less than lead compound (23.33 μM). 9 compounds were found to have IC_{50} less than 5 μM and most potent compounds among series are **RS_18, RS_21** and **RS_30** with IC_{50} values of 0.89 ± 0.35, 0.74 ± 0.16 and 0.74 ± 0.34 μM respectively.
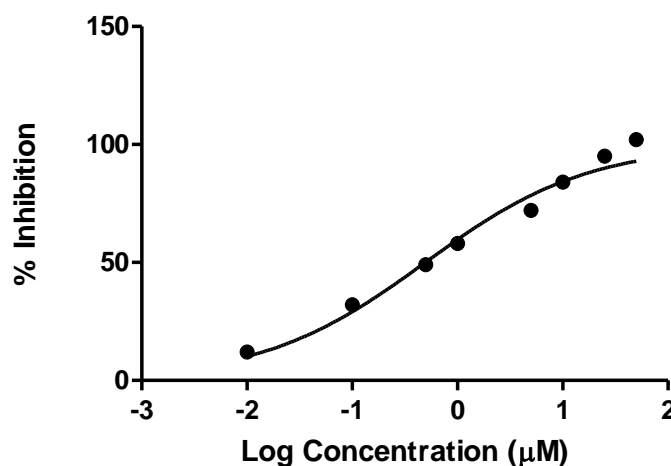
Fig 6.23: Dose response curve of active compound **RS_30**
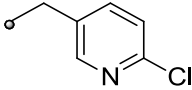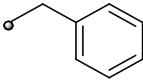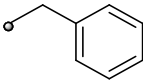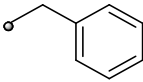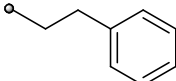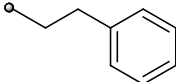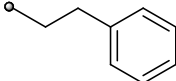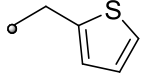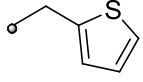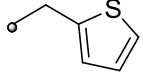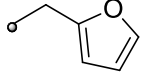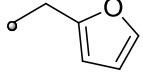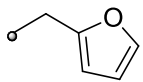
As quinoline moiety was reported earlier for antimycobacterial potency all synthesized derivatives were tested against active replicating forms of *Mtb* by MABA method. MIC is defined as the minimum concentration which inhibits the colour change. All the compounds in series show MIC values in range of $1.64 - 33.42$ μM. the most active compounds was found to possess trifluoromethyl substitution at R position and 2-chloro-5-methyl pyridine at R_1 position.

As *Mtb* primarily resides in macrophages all synthesized were evaluated for their toxicity against RAW cell lines at a concentration of 50 μg/ml. The percentage of inhibition was found to be in range of $11.26 - 62.84$. Results indicate that most of the compounds are devoid of cytotoxicity.

Table 6.6: *In vitro* biological evaluation of the synthesized compounds **RS_10 – RS_30**
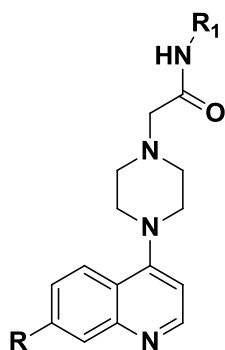
COMP.	R	R₁	IC₅₀ (μM)	MIC (μM)	Cytotoxicity (% inhi) at 50 μg/ml
RS_10	H		1.04 ± 0.38	2.11	26.32 ± 0.73
RS_11	Cl		6.72 ± 0.85	1.92	50.21 ± 0.85
RS_12	CF₃		1.67 ± 0.54	3.64	14.32 ± 1.21
RS_13	H		>25	16.67	23.67 ± 0.96
RS_14	Cl		>25	7.64	22.75 ± 1.13
RS_15	CF₃		>25	14.11	32.64 ± 1.27
RS_16	H		2.68 ± 0.76	3.95	62.84 ± 0.69
RS_17	Cl		1.26 ± 0.51	3.63	11.26 ± 0.82

			IC$_{50}$	MIC	% inhi
RS_18	CF$_3$		0.89 ± 0.35	1.64	50.85 ± 1.56
RS_19	H		1.24 ± 0.28	2.11	45.67 ± 1.78
RS_20	Cl		4.92 ± 1.27	1.93	38.29 ± 0.83
RS_21	CF$_3$		0.74 ± 0.16	1.78	56.74 ± 1.92
RS_22	H		>25	33.42	45.84 ± 1.34
RS_23	Cl		>25	30.64	49.32 ± 0.94
RS_24	CF$_3$		>25	14.14	50.16 ± 1.68
RS_25	H		>25	4.26	21.85 ± 0.42
RS_26	Cl		12.36 ± 0.99	15.63	27.35 ± 0.86
RS_27	CF$_3$		>25	1.75	54.91 ± 0.32
RS_28	H		5.69 ± 0.81	35.7	55.67 ± 0.78
RS_29	Cl		7.51 ± 1.24	8.13	46.32 ±0.82
RS_30	CF$_3$		0.74 ± 0.34	29.90	12.73 ± 0.48
INH			--	0.4	--
RIF			--	0.5	--

IC$_{50}$ – 50% inhibitory concentration, **MIC** – minimum inhibitory concentration, **inhi**- inhibition, **INH-** isoniazid, **RIF-** Rifampicin

Lead 7 emerged as a strong inhibitor with IC$_{50}$ of 23.33 μM. Docking results of Lead 7 within the active site of the *Mtb* LAT protein is illustrated in **Fig 6.24**. The predicted docking pose of Lead 7 showed hydrogen bonding with Lys300 amino acid residue and also it was well inserted into the active site cavity where exhibited various hydrophobic interactions with Pro415, Leu414, Val63, Phe167, Val132, Ala129, Ile184 and Ala416 amino acid residues. In addition to hydrogen bonding interactions the phenyl ring was found to interact *via* pi-pi stacking with Phe167 and cation-pi interaction with Arg170 amino acid residue. The predicted docking score of Lead 7 was found to be -5.12 kcal/mol and was well inserted into the active site cavity of the protein making this compound promising for further lead optimization.
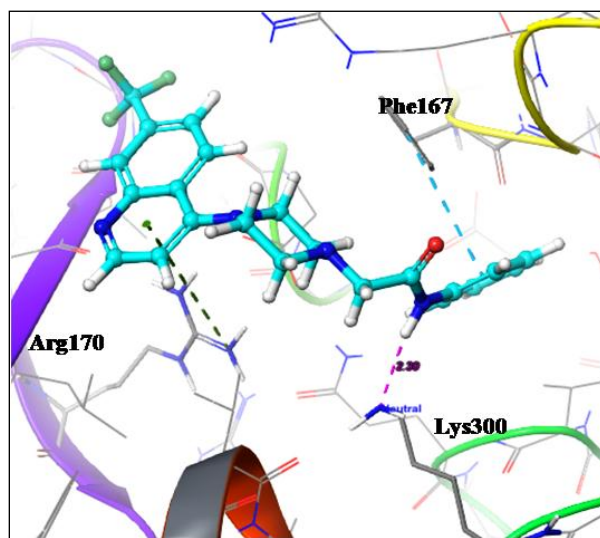
Fig 6.24: Binding mode of Lead compound.

Based on the identified Lead 7, we undertook synthesis of 21 analogues and evaluated for its biological activity against *Mtb* LAT enzyme for establishing structure-activity relationship. Substitutions are made at 7th position of quinoline (R= H or Cl or CF3) and at R$_1$ various aromatic amines are introduced, the chain length is varied (one or two carbon) like benzyl, phenethyl, pyridyl ethyl, pyridyl methyl and hetero aromatic amines (furan methyl and thiophene methyl) are introduced. Closer analyses of all the compounds in the *Mtb* LAT protein revealed that the compounds with one carbon chain length have shown good activity, while introducing two carbon chain lengths led to decreased the activity of compounds. Introducing furan ring favored the *Mtb* LAT activity, while substituting with thiophene ring also led to decrease the *Mtb* LAT activity.

Closer analyses of some of the active compounds (**RS_10, RS_11, RS_12**) in the *Mtb* LAT protein revealed that they could make favorable interactions with important amino acid residues such as Arg170, Ash271, and Thr180. In addition to these interactions, the phenyl ring interacted *via* pi-pi interaction with Phe167, analogues to the one observed with the crystal ligand. All the compounds were well inserted in to the active site cavity, with good fitness, which could make stable protein-ligand complexes (**Fig 6.25**).
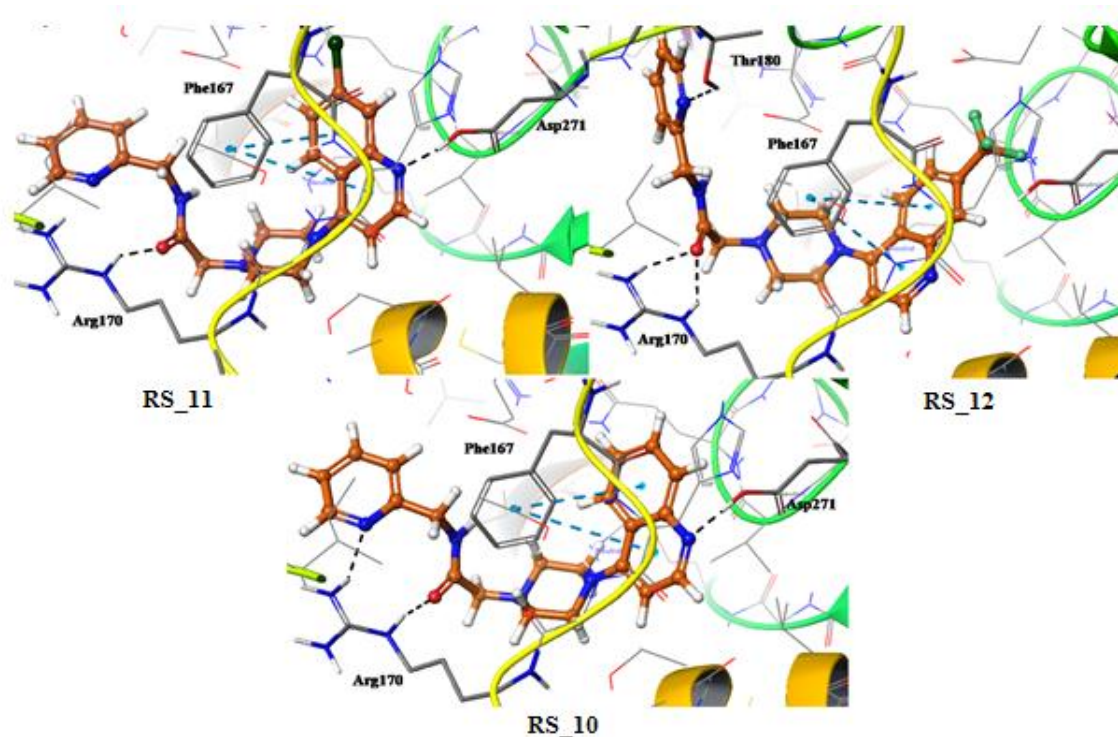
Fig 6.25: Binding mode of **RS_10, RS_11, RS_12**.

Further replacement of Cl and H substitutions of quinoline ring at R_1 position (**RS_16-21**) also resulted in the good activity in *Mtb* LAT protein. These compounds were also interacting in a similar manner as the other active compounds interact with the *Mtb* LAT protein.

Binding analysis of inactive compounds (**RS_13-15, RS_22-24**) in the active site of *Mtb* LAT protein revealed that due to extra carbon chain length the compounds were taken as a different orientation which will led to lose the important interactions with the protein (**Fig 6.26**)
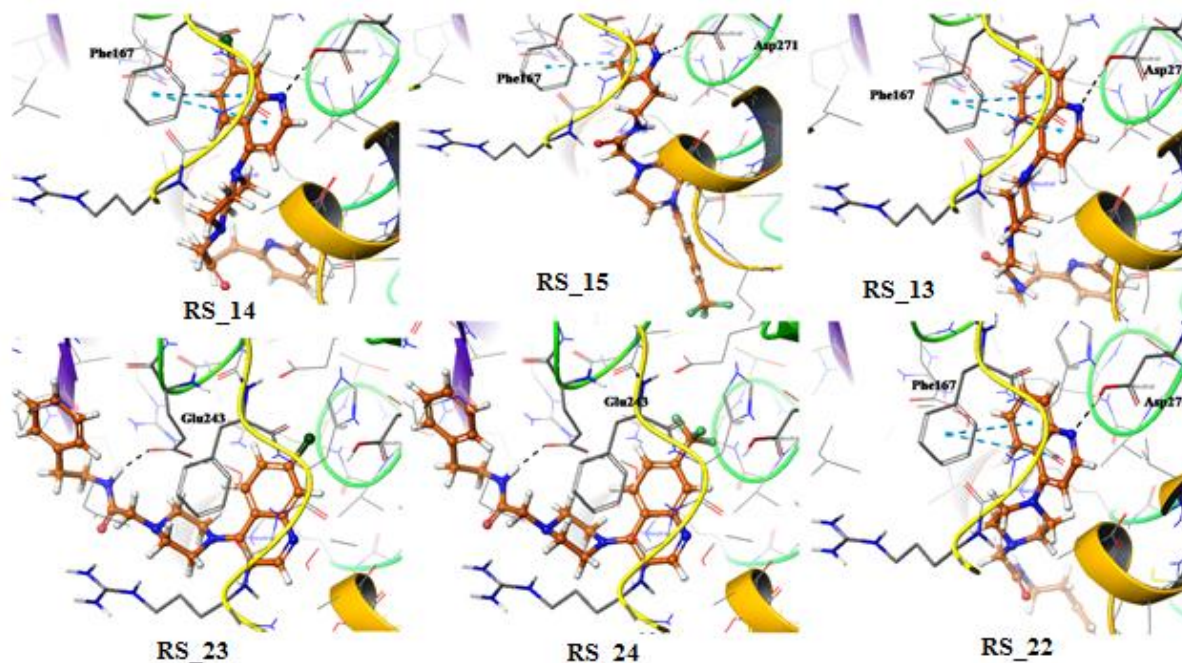
Fig 6.26: Binding Mode of inactive compounds (**RS_13-15, RS_22-24**).

As mention above introducing furan ring is showing good activity (IC$_{50}$ = 0.74±7.51 µM), while substituting with thiophene ring will led to a reduction in the activity (IC$_{50}$ = >25 µM). The binding analysis revealed that in compounds (**RS_28-30**) which fully occupies the active site pocket and also maintains the crucial hydrogen bonding as well as pi–pi interaction with important amino acid residues (**Fig 6.27**). On the other side other compounds (**RS_25-27**) were losing some important interactions also these compounds were slightly away from the active site (**Fig 6.28**).
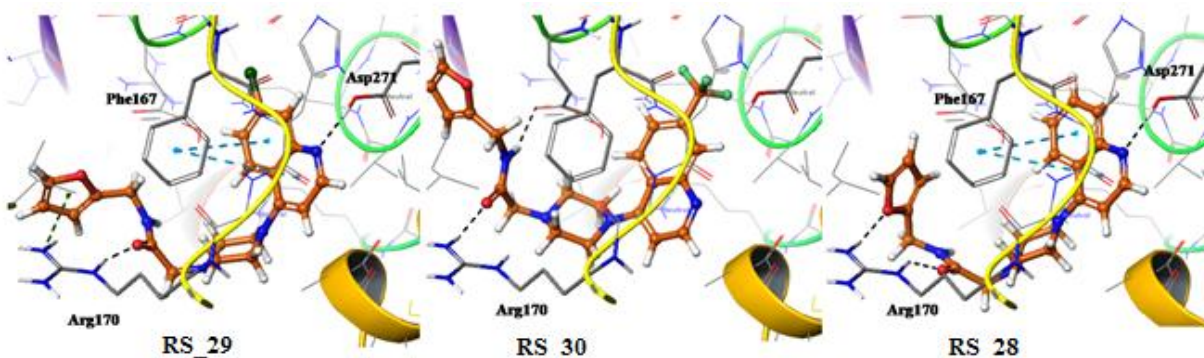
Fig 6.27: Binding Mode of **RS_28-30**.
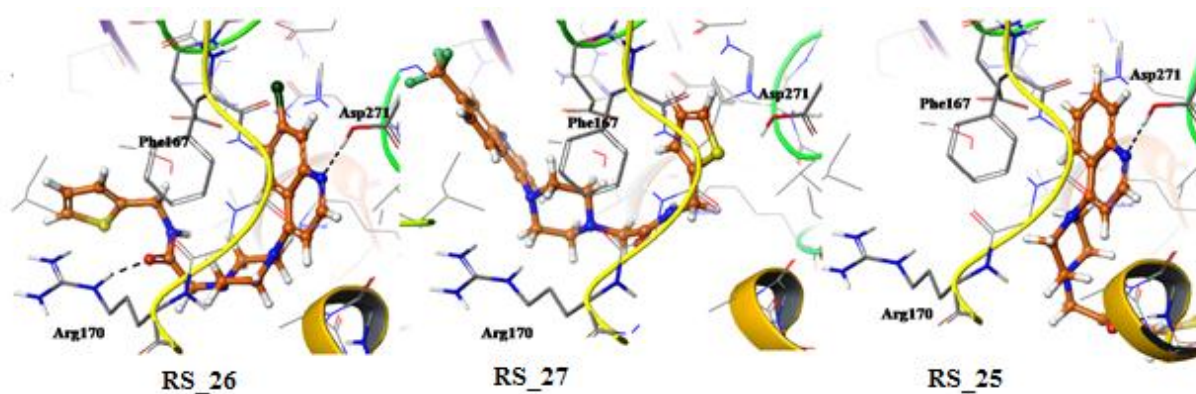
Fig 6.28: Binding Mode of **RS_25-27**.

6.3.5. Nutrient starvation model

Compounds which showed considerable action against LAT enzyme were taken for further testing against nutrient starved dormant model as reported by J.C. Bett et.al. Nutrient starvation is one of major stress faced by *Mtb* in granuloma environment of the host. The advantage of this model is its simplicity, reliability and it exhibits most of phenotypic and genotypic characteristics of dormancy. The *Mtb* culture in this model is starved for 6 weeks in PBS resulting in reduced intracellular ATP levels, very low but continuous respiration and Loss of Ziehl-Neelsen staining characteristics. The other advantage of this model is Lysine-ε aminotransferase expressed by Rv3290c gene was found to be upregulated 41.86 folds as it involved in antibiotic resistance. All compounds were evaluated for their activities against dormant phase of mycobacterium at 10 μg/ml. Most of the compounds have well correlation between enzyme inhibitory concentration values and log reduction in this model. **RS_10** showed a log reduction of 2.1 fold and potent when compared to first line drugs Isoniazid (1.2 fold), Rifampicin (1.3 fold) and equipotent to Moxifloxacin (2.2 fold). **RS_11, RS_19, RS_20, RS_21, RS_28** were also effective when compared to Isoniazid and rifampicin but less potent than moxifloxacin (**Fig 6.29**).

169
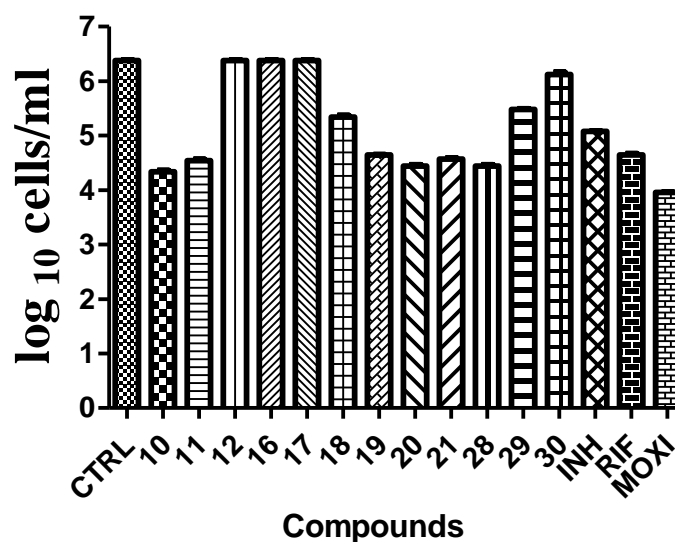
Fig 6.29: Biological activities of the synthesised compounds against *M. tuberculosis* in the nutrient starvation model. Bacterial count estimation (Mean ± S.D., n = 3) for control and treated groups conducted by using the MPN (most probable number) assay. Most of the compounds gave significant inhibition of growth of *M. tuberculosis* in this model as compared to the control (p < 0.0001, two way ANOVA usingGraphPad Prism Software).

6.3.6. Evaluation of potency of compound against biofilm forming Mycobacteria

Recent findings in *Mtb* infected Guinea pig lungs suggest the role of biofilm in persistence in granuloma environment. Biofilm formation helps in long term survival of mycobacterium in host, and also protects the *Mtb* from antibiotics and environmental stress prolongating the duration of therapy. In case of *Mtb* this acellular matrix is composed of free methoxy mycolic acids resulting in increase in MIC by 50 times than usual MIC. Biofilm also plays a vital role in transmission, infection, persistence, chronic nature of disease, virulence, immunomodulation and relapse of TB. Identification of drugs that inhibit biofilm formation could enable the dramatic shortening of tuberculosis treatments using standard antibiotics, with substantial potential impact on global health and reduction of antibiotic resistance associated with non-compliance. **RS_10** and **RS_20** which exhibited significant log reduction in nutrient starved dormant model were tested against biofilm formation. The drugs were tested at concentration of 10 μg/ml and exposure time was maintained as 7 days. When the frequency of drug tolerant persisters were enumerated by MPN assay **RS_10** and **RS_20** shown log reduction of 3 and 1.9 fold

170

respectively. **RS_10** was found to be effective when compared to marketed drugs namely Isoniazid (2.4 fold), Rifampicin (2.5 fold), Moxifloxacin (2.3 fold). These results make it evident that **RS_10** is an effective agent against persistent stage of *Mtb* (**Fig 6.30**).
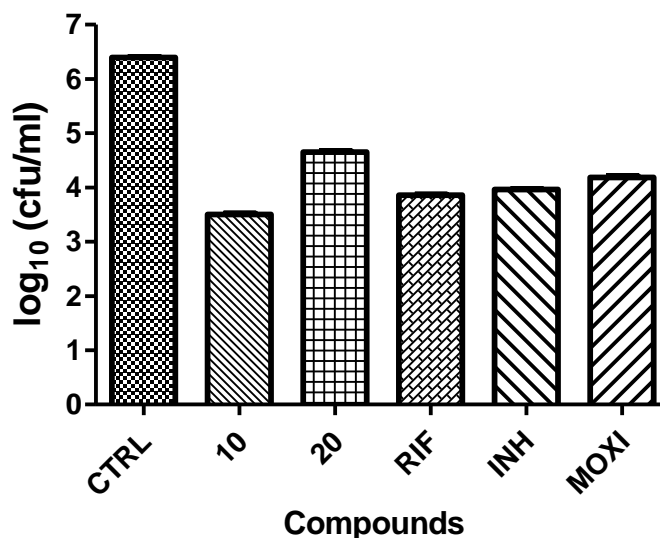
Fig 6.30: Biological activities of compounds **RS_10 and 20** against biofilm forming *M. tuberculosis*. Bacterial count estimation (Mean ± S.D., n = 4) for control and treated groups conducted by using the MPN (most probable number) assay. Both compounds gave significant inhibition of growth of *M. tuberculosis* in this model as compared to the control (p < 0.0001, two way ANOVA usingGraphPad Prism Software).

6.3.7. Kill kinetic curves under nutrient starved conditions

Kill curve experiments give an insight on nature of kill (bactericidal or static) and kinetics of kill under given set of conditions. Knowledge of nature of kill and factors effecting kill can be related to pharmacokinetic parameters and is very much crucial in deciding appropriate antibiotic for therapy. To study the nature of kill of active compound *Mtb* culture was starved in PBS-tyloxapol for 2 weeks. Starved culture was then treated with drug and frequency of persisters was determined at 0, 7, 4, 21 days. **Fig 6.31** shows that nature of kill is dependent on both concentration and time. At concentration of 20 µg/ml **RS_10** shows 3 log reduction indicating its bactericidal action.

171
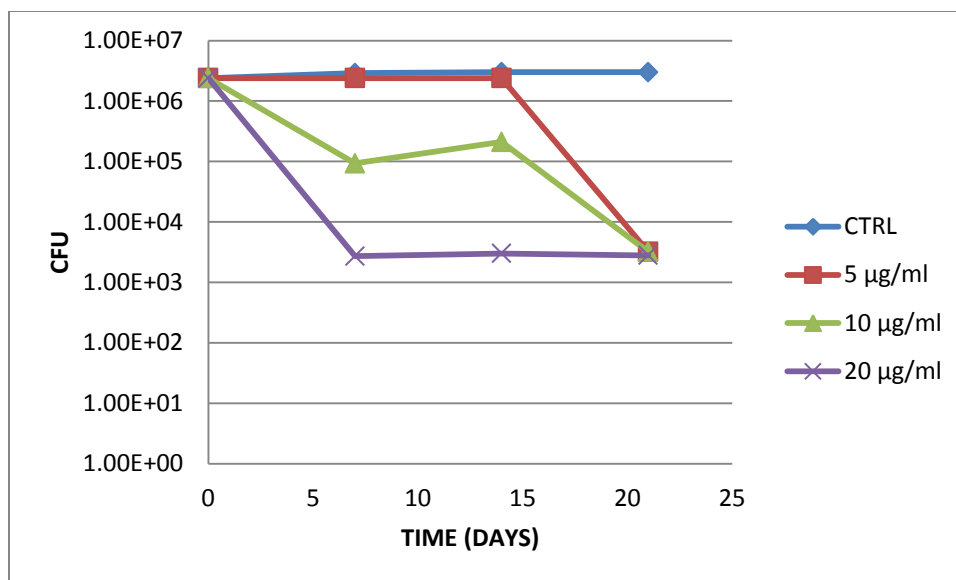
Fig 6.31: Kill kinetic curve of **RS_10** at 3 different concentrations

6.3.8. *In vivo* antimycobacterial evaluation by *Mycobacterium marinum* induced zebra fish model

M. marinum is relatively safe to humans as it is restricted to topical lesions, has genetic similarity to *Mtb* and also has higher replication rate than *M. tuberculosis*. Activity and dosage of antimycobacterial compounds in zebrafish closely resemble characteristics in humans. Owing to all the mentioned advantages and ease of handling, cost effectiveness zebra fish model can be used for highthroughput screening of antimycobacterial agents. The most effective compound among the series **RS_10** was evaluated for its antimycobacterial potency against *M. marinum* induced zebra fish model at dose of 10 mg/kg. It was observed to cause 2.2 log fold in bacterial load similar to standard drugs Isoniazid (2.4 fold) and Moxifloxacin (2.3 fold) at same dose tested (**Fig 6.32**).

172
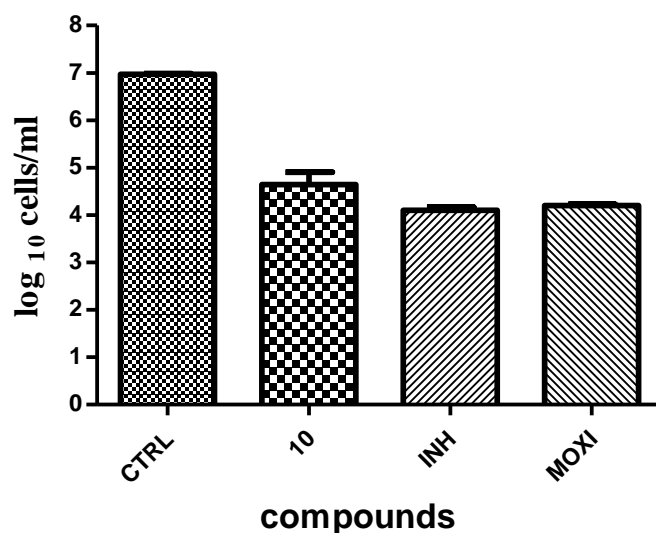
Fig 6.32: Bacterial count estimation (Mean ± S.E.M., n = 6) for control and treated groups conducted by using MPN (most probable number) assay. The statistical significance (p < 0.001) with respect to infected control group has been analyzed by Two-way ANOVA using GraphPad Prism Software.

6.3.9. Human 3D granuloma model

The features of model which makes it a replica of human granuloma are as follows- granuloma formation, multinucleated giant cell formation, decrease in CD4 T cell counts, unchanged CD8 T cell values, increase in CD4$^+$ CD25 $^+$ T cells, decrease in activated macrophage cells, increase in cytokine and chemokine secretion by host immune cells in response to *Mtb* infection, and resuscitation upon immunosuppression by treatment with anti-TNFa mAbs. After formation of 3D granuloma it was treated with **RS_10** for 4 days followed by Rifampicin for 3 days. Then the granuloma was hydrolysed followed by enumeration of % rifampicin tolerant persisters and *Mtb* cfu. The cfu counts for *Mtb* recovered from granulomas treated with **RS_10** alone was less (18X10^5) as compared to the cfu counts for *Mtb* recovered from granulomas that were left untreated (29.33X 10^5) This suggests that **RS_10** alone can kill *Mtb* even though not effective as Rifampicin (3.3X10^5). In combination with Rifampicin **RS_10** has synergistic action (**Fig 6.33**).

173
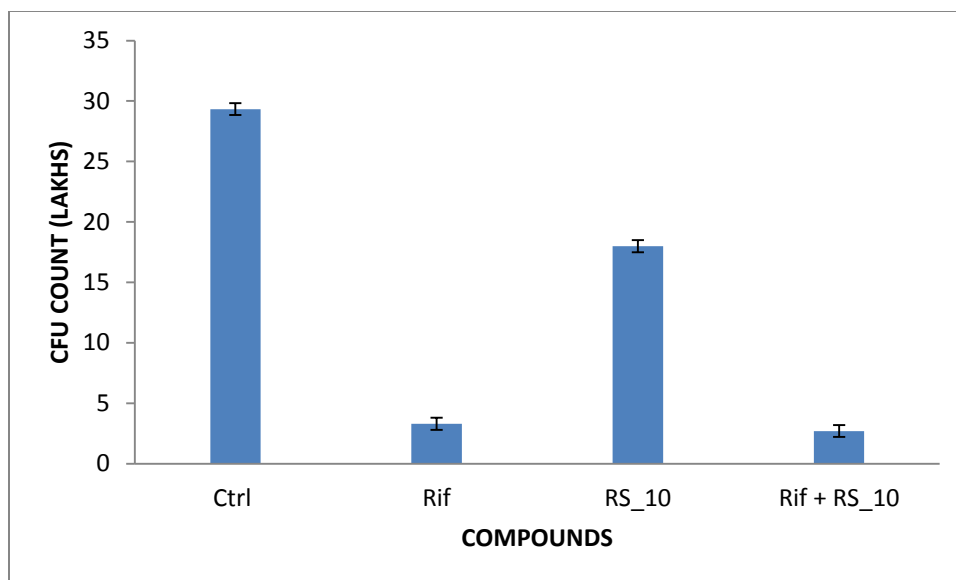
Figure 6.33: Data showing cfu counts for *Mtb* recovered from granulomas treated either with no drugs or treated with **RS_10,** Rif, alone or treated with **RS_10** + Rif.

6.3.10. Highlights of the study

Approval of bedaquiline for MDR TB has shifted the attention of researchers towards this class of antibiotics. In present work we attempted to modify quinoline leads to increase efficiency against persistent phase of *Mycobacterium tuberculosis* by targeting LAT enzyme. We were able to identify compounds which has efficacy against both replicating and nonreplicating stages of *Mtb*. **RS_10** results shows that it is equally effective as standard drugs against active stage of TB additionally it has advantage of potency against persistent phase of TB by inhibiting dormant target LAT. As the urge for new antitubercular drugs is increasing day by day the present class of drugs would be suitable class for further drug development studies.

LEAD EXPANSION

SCREENING OF MOLECULES
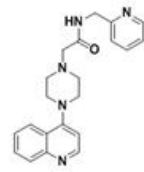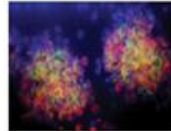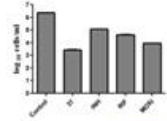
RS_10
LAT (IC$_{50}$) : 1.04 ± 0.38µM
MIC : 2.11µM
Nutreint starvation: 2.1 fold
Biofilm: 3.0 fold
zebra fish: 2.2 fold

175

Findings of government review on antimicrobial resistance revealed that one person in every three seconds will be affected with superbugs which accounts for 10 million lives by 2050. Superbugs are nothing but microbes which acquired resistance to all available antibiotics. E.coli, tuberculosis and malaria would cause devastating blow on mankind as superbugs. All these observations throw limelight on need for development of new drugs especially in case of Tuberculosis. Despite END TB Strategy efforts by WHO TB still remains among top 10 leading causes of deaths worldwide.

About one third of world population has been infected with latent TB and has lifetime risk of 10% to develop into active TB. Risk factors such as coinfection with HIV, use of immunosuppressant, smoking will aggravate condition of latent TB. Current treatment regimens for latent TB are too long and have associated side effects. New drugs are required in TB with enhanced efficacy against resistant forms and which can reduce treatment duration due to their potency to eliminate persistent phase of TB. Literature review shows that Cysteine synthase M and Lysine ɛ-aminotransferase are attractive and less exploited targets for dormant forms of *Mtb*.

In first section we reported identification and characterization of potent inhibitors of CysM, a critical enzyme in cysteine biosynthesis during dormancy. A screening campaign of 17 312 compounds identified ligands that bind to the active site with micromolar affinity. These were characterized in terms of their inhibitory potencies and structure − activity relationships through hit expansion guided by three-dimensional structures of enzyme − inhibitor complexes. The top compound (**RK_01)** binds to CysM with 300 nM affinity and displays selectivity over the mycobacterial homologues CysK1 and CysK2. Notably, two inhibitors (**RK_01** and **RK_03)** show significant potency in a zebra fish model, nutrient-starvation model of dormancy of *Mycobacterium tuberculosis*, good MIC values with little or no cytotoxicity toward mammalian cells.

We synthesized total of 61 compounds by lead derivatization technique for LAT and evaluated them by various biological assays. In Cyclobutyl series **RL_33** emerged as most potent compound with an IC$_{50}$ of 2.09 ± 0.21 μM. **RL_34** and **RL_37** were found to be more effective

in lowering bacterial load in nutrient starved model and biofilm model correlating with their LAT inhibitory potency. Compound **RL_37** in the series was found to be effective when evaluated in *M. marinum* induced zebra fish model. **RL_37** was found to have bactericidal effect and its action was concentration dependent. So **2-hydroxy-2-(1-(3-phenyl ureido) cyclobutyl) acetic acid (RL_37)** is acting on both replicating and non replicating stages of TB and is expected to lower duration of therapy.

In Benzthiazole series compound **(E)-4-(5-(2-(benzo[d]thiazol-2-yl)-2-cyanovinyl) thiophen-2-yl) isophthalicacid (RR_22)** emerged as potent molecule with LAT IC_{50} of 2.62 μM. It had a significant log reduction of 2.9 and 2.3 fold against nutrient starved and biofilm forming mycobacteria. It was found to be inactive against active *Mtb* and also in *M. marinum* induced zebra fish model indicating that it acted through dormant targets. It was also devoid of cytotoxicity. **RR_22** was also found to possess bactericidal effect which was independent of concentration and time. It was found to be effective in combination with Rifampicin in 3D granuloma model. All these parameters make it a better candidate for further development.

In Quinoline series **RS_18, RS_21** and **RS_30** were found to be potent with IC_{50} values of 0.89 ± 0.35, 0.74 ± 0.16 and 0.74 ± 0.34 μM respectively. In nutrient starvation model and biofilm **2-(4-(quinolin-4-yl)piperazin-1-yl)-N-(pyridin-2-ylmethyl)acetamide** (**RS_10**) showed a log reduction of 2.1 fold and 3.0 fold respectively. Results are correlating with its efficacy in 3D granuloma model. **RS_10** was also found to possess bactericidal effect which was dependent on concentration and time. In zebra fish model it exhibited 2.2 fold log reduction indicating its activity against replicative and non replicating stages of *Mtb*.

Our studies open a new window to a set of NCE which can be further developed into a novel drug candidate.
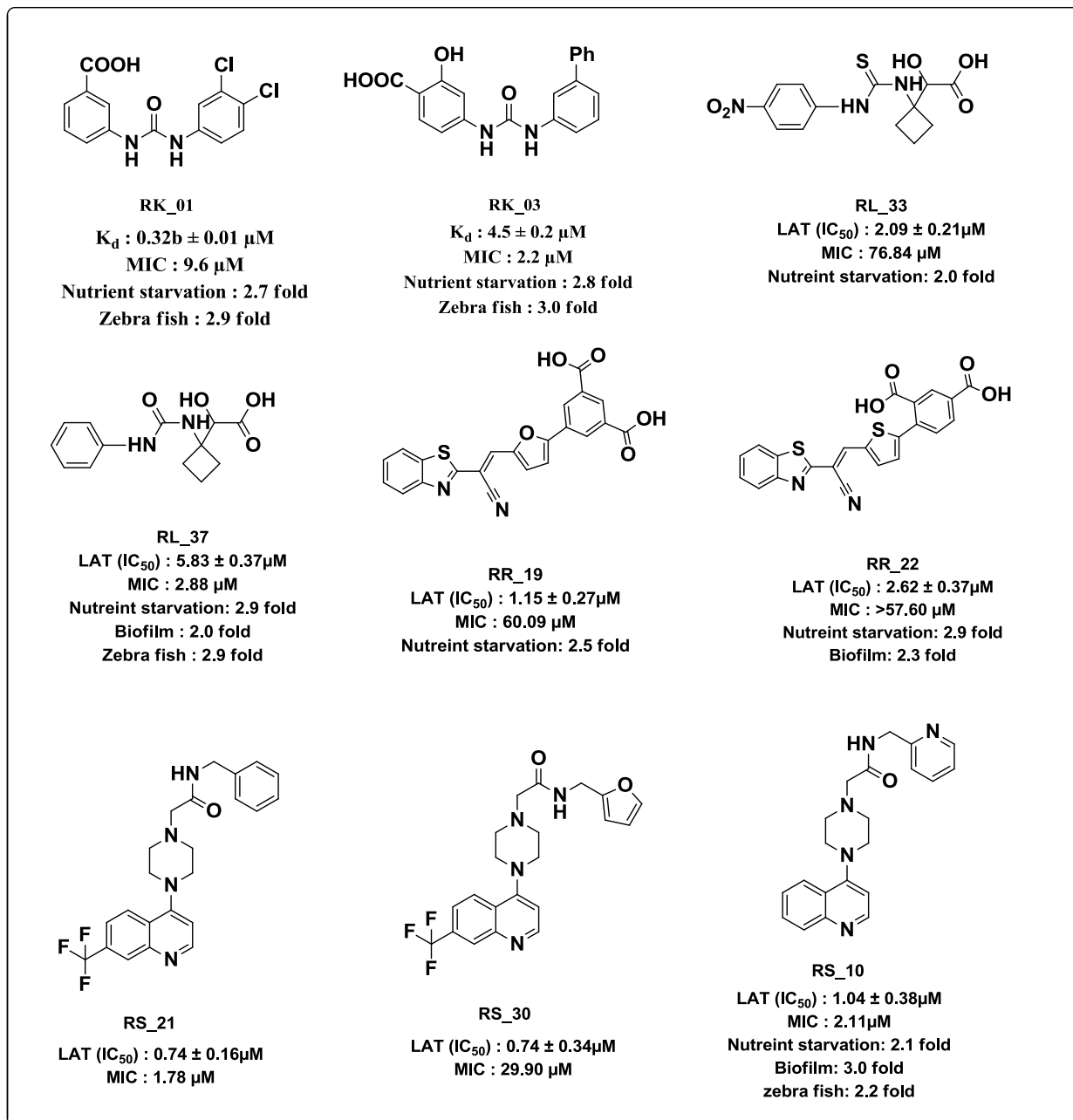
Fig 7.1.: Structures of most potent compounds from each series

Future perspectives

The cysteine and Lysine Ɛ-aminotransferase biosynthetic pathways are absent in humans but essential in microbial pathogens, suggesting that it provides potential targets for the development of novel antibacterial compounds with minimal mammalian toxicity. The present study focused on utilizing the less and unexploited targets such as Lysine Ɛ-aminotransferase and Cysteine synthase M as potential anti-tubercular target thus offering an excellent opportunity to address the ever increasing problem of latent tuberculosis.

The compounds reported here displayed excellent enzyme inhibitory potency and potency against *M. tuberculosis* H37Rv strain. Compounds were found to be more effective in dormant models such as nutrient starvation model, biofilm model, Nutrient starved kill kinetics and 3D granuloma. Although these results are encouraging, further optimization is still needed.

Also some of the active anti-mycobacterial compounds reported in this thesis were screened for their *in vivo* activity using adult zebra fish. Extensive pharmacodynamics and pharmacokinetic studies of the safer compounds have to be undertaken in higher animal models.

Extensive toxic and side effect profile of all the synthesized compounds may be studied. Further X-ray crystallisation studies (for LAT inhibitors), mutational studies and macrophage infection studies can be done for synthesised compounds.

The advancement of any of the candidate molecules presented in this thesis along a drug development track would require a substantial investment in medicinal chemistry, preclinical and clinical studies.

Cost effective and minimizing the number of steps involved in the synthesis of compounds reported in this thesis should be optimized.

References

Ågren, D., Schnell, R., & Schneider, G. (2009). The C-terminal of CysM from *Mycobacterium tuberculosis* protects the aminoacrylate intermediate and is involved in sulfur donor selectivity. *FEBS letters*, *583*(2), 330-336.

Ågren, D., Schnell, R., Oehlmann, W., Singh, M., & Schneider, G. (2008). Cysteine synthase (CysM) of *Mycobacterium tuberculosis* is an O-phosphoserine sulfhydrylase evidence for an alternative cysteine biosynthesis pathway in mycobacteria. *Journal of Biological Chemistry*, *283*(46), 31567-31574.

Amori, L., Katkevica, S., Bruno, A., Campanini, B., Felici, P., Mozzarelli, A., & Costantino, G. (2012). Design and synthesis of trans-2-substituted-cyclopropane-1-carboxylic acids as the first non-natural small molecule inhibitors of O-acetylserine sulfhydrylase. *MedChemComm*, *3*(9), 1111-1116.

Ayesa, S., Ersmark, K., Grabowska, U., Hewitt, E., Jönsson, D., Kahnberg, P., Klasson, B., Lind, P., Lundgren, S., Odèn L. and Parkes K.. (2014). *U.S. Patent 8,815,809.*

Ayesa, S., Grabowska, U., Hewitt, E., Jonsson, D., Klasson, B., Kahnberg, P., Lundgren, S., Tejbrant, J. and Wiktelius, D., Medivir. Uk Ltd, (2014). *U.S. Patent 8,859,505.*

Baell, J. B., & Holloway, G. A. (2010). New substructure filters for removal of pan assay interference compounds (PAINS) from screening libraries and for their exclusion in bioassays. *Journal of medicinal chemistry*, *53*(7), 2719-2740.

Baykov, A. A., Evtushenko, O. A., & Avaeva, S. M. (1988). A malachite green procedure for orthophosphate determination and its use in alkaline phosphatase-based enzyme immunoassay. *Analytical biochemistry*, *171*(2), 266-270.

Betts, H. M., Khan, I., & Robins, E. G. (2012). *U.S. Patent Application No. 14/001,952.*

Betts, J. C., Lukey, P. T., Robb, L. C., McAdam, R. A., & Duncan, K. (2002). Evaluation of a nutrient starvation model of *Mycobacterium tuberculosis* persistence by gene and protein expression profiling. *Molecular microbiology*, *43*(3), 717-731.

Bhaskar, A., Chawla, M., Mehta, M., Parikh, P., Chandra, P., Bhave, D., ... & Singh, A. (2014). Reengineering redox sensitive GFP to measure mycothiol redox potential of *Mycobacterium tuberculosis* during infection. *PLoS Pathog*, *10*(1), e1003902.

Burki, T. (2014). Improving the health of the tuberculosis drug pipeline. *The Lancet Infectious Diseases*, *14*(2), 102-103.

Burns, K. E., Baumgart, S., Dorrestein, P. C., Zhai, H., McLafferty, F. W., & Begley, T. P. (2005). Reconstitution of a New Cysteine Biosynthetic Pathway in *Mycobacterium t uberculosis*. *Journal of the American Chemical Society*, *127*(33), 11602-11603.

Centers for Disease Control and Prevention. (2012). The difference between latent TB infection and TB disease. *CDC Report*.

Chen, V. B., Arendall, W. B., Headd, J. J., Keedy, D. A., Immormino, R. M., Kapral, G. J., ... & Richardson, D. C. (2010). MolProbity: all-atom structure validation for macromolecular crystallography. *Acta Crystallographica Section D: Biological Crystallography*, *66*(1), 12-21.

Collins, L., & Franzblau, S. G. (1997). Microplate alamar blue assay versus BACTEC 460 system for high-throughput screening of compounds against *Mycobacterium tuberculosis* and *Mycobacterium avium*. *Antimicrobial agents and chemotherapy*, *41*(5), 1004-1009.

Coxon, G. D., Cooper, C. B., Gillespie, S. H., & McHugh, T. D. (2012). Strategies and challenges involved in the discovery of new chemical entities during early-stage tuberculosis drug discovery. *Journal of Infectious Diseases*, jis191.

D'Ambrosio, L., Centis, R., Sotgiu, G., Pontali, E., Spanevello, A., & Migliori, G. B. (2015). New anti-tuberculosis drugs and regimens: 2015 update. *ERJ Open Research*, *1*(1), 00010-2015.

Daniel, T. M. (2006). The history of tuberculosis. *Respiratory Medicine*, *100*(11), 1862-1870.

De Man, J. C. (1975). The probability of most probable numbers. *European journal of applied microbiology and biotechnology*, *1*(1), 67-78.

Devi, K., & Sarma, R. J. (2014). Exploring urea–fluoride interactions in the vicinity of a tryptophan residue. *RSC Advances*, *4*(19), 9551-9555.

Devi, P. B., Sridevi, J. P., Kakan, S. S., Saxena, S., Jeankumar, V. U., Soni, V., ... & Sriram, D. (2015). Discovery of novel lysine ε-aminotransferase inhibitors: An intriguing potential target for latent tuberculosis. *Tuberculosis*, *95*(6), 786-794.

Dheda, K., Warren, R. M., Zumla, A., & Grobusch, M. P. (2010). Extensively drug-resistant tuberculosis: epidemiology and management challenges.*Infectious Disease Clinics of North America*, *24*(3), 705-725.

Dorhoi, A., Reece, S. T., & Kaufmann, S. H. (2011). For better or for worse: the immune response against *Mycobacterium tuberculosis* balances pathology and protection. *Immunological reviews*, *240*(1), 235-251.

Dover, L. G., & Coxon, G. D. (2011). Current status and research strategies in tuberculosis drug development: miniperspective. *Journal of Medicinal Chemistry*, *54*(18), 6157-6165.

Duan, X., Li, Y., Du, Q., Huang, Q., Guo, S., Xu, M., ... & Xie, J. (2016). Mycobacterium Lysine ε-aminotransferase is a novel alarmone metabolism related persister gene via dysregulating the intracellular amino acid level. *Scientific reports*, *6*.

Dube, D., Tripathi, S. M., & Ramachandran, R. (2008). Identification of in vitro inhibitors of *Mycobacterium tuberculosis* Lysine ε-aminotransferase by pharmacophore mapping and three-dimensional flexible searches. *Medicinal Chemistry Research*, *17*(2-7), 182-188.

Dubos, R. J., & Davis, B. D. (1946). Factors affecting the growth of tubercle bacilli in liquid media. *The Journal of experimental medicine*, *83*(5), 409.

Emsley, P., Lohkamp, B., Scott, W. G., & Cowtan, K. (2010). Features and development of Coot. *Acta Crystallographica Section D: Biological Crystallography*, *66*(4), 486-501.

Franzblau, S. G., Witzig, R. S., McLaughlin, J. C., Torres, P., Madico, G., Hernandez, A., ... & Gilman, R. H. (1998). Rapid, low-technology MIC determination with clinical *Mycobacterium tuberculosis* isolates by using the microplate Alamar Blue assay. *Journal of clinical microbiology*, *36*(2), 362-366.

Gao, X., Gao, C., & Gao, R. (2015). Knoevenagel Condensation Reaction Using Ionic Liquid [ADPQ][CF^ sub 3^ SO^ sub 3^] as Green and Reusable Catalyst. *Asian Journal of Chemistry*, *27*(6), 2145.

Gerlier, D., & Thomasset, N. (1986). Use of MTT colorimetric assay to measure cell activation. *Journal of immunological methods*, *94*(1-2), 57-63.

Ginsberg, A. M., & Spigelman, M. (2007). Challenges in tuberculosis drug research and development. *Nature*, *13*(3), 290-294.

Green, K., & Garneau-Tsodikova, S. (2013). Resistance in tuberculosis: what do we know and where can we go?. *Frontiers in Microbiology*, *4*, 208.

Guirado, E., & Schlesinger, L. (2013). Modeling the *Mycobacterium tuberculosis* granuloma–the critical battlefield in host immunity and disease. *Frontiers in immunology*, *4*, 98.

Gupta, P., Hameed, S., & Jain, R. (2004). Ring-substituted imidazoles as a new class of anti-tuberculosis agents. *European Journal of Medicinal Chemistry*, *39*(9), 805-814.

Hayashi, H. (1995). Pyridoxal enzymes: mechanistic diversity and uniformity. *Journal of biochemistry*, *118*(3), 463-473.

Haydel, S. E. (2010). Extensively drug-resistant tuberculosis: a sign of the times and an impetus for antimicrobial discovery. *Pharmaceuticals*, *3*(7), 2268-2290.

Irwin, J. J., Duan, D., Torosyan, H., Doak, A. K., Ziebart, K. T., Sterling, T., ... & Shoichet, B. K. (2015). An aggregation advisor for ligand discovery. *Journal of medicinal chemistry*, *58*(17), 7076-7087.

Jasmer, R. M., Nahid, P., & Hopewell, P. C. (2002). Latent tuberculosis infection. *New England Journal of Medicine*, *347*(23), 1860-1866.

Jeankumar, V. U., Reshma, R. S., Vats, R., Janupally, R., Saxena, S., Yogeeswari, P., & Sriram, D. (2016). Engineering another class of anti-tubercular lead: Hit to lead optimization of an intriguing class of gyrase ATPase inhibitors. *European Journal of Medicinal Chemistry*, *122*, 216-231.

Jeankumar, V. U., Saxena, S., Vats, R., Reshma, R. S., Janupally, R., Kulkarni, P., ... & Sriram, D. (2016). Structure-Guided Discovery of Antitubercular Agents That Target the Gyrase ATPase Domain. *ChemMedChem*.

Kabsch, W. (2010). Xds. *Acta Crystallographica Section D: Biological Crystallography*, *66*(2), 125-132.

Kapoor, N., Pawar, S., Sirakova, T. D., Deb, C., Warren, W. L., & Kolattukudy, P. E. (2013). Human granuloma in vitro model, for TB dormancy and resuscitation. *PLoS One*, *8*(1), e53657.

Knechel, N. A. (2009). Tuberculosis: pathophysiology, clinical features, and diagnosis. *Critical Care Nurse*, *29*(2), 34-43.

Kulka, K., Hatfull, G., & Ojha, A. K. (2012). Growth of *Mycobacterium tuberculosis* biofilms. *JoVE* , (60), e3820-e3820.

Lanke, S. K., & Sekar, N. (2016). Pyrazole based solid state emissive NLOphores with TICT characteristics: synthesis, DFT and TDDFT studies. *Dyes and Pigments*, *126*, 62-75.

Lienhardt, C., Raviglione, M., Spigelman, M., Hafner, R., Jaramillo, E., Hoelscher, M., ... & Gheuens, J. (2012). New drugs for the treatment of tuberculosis: needs, challenges, promise, and prospects for the future. *Journal of Infectious Diseases*, *205*(suppl 2), S241-S249.

Lienhardt, C., Vernon, A., & Raviglione, M. C. (2010). New drugs and new regimens for the treatment of tuberculosis: review of the drug development pipeline and implications for national programmes. *Current Opinion in Pulmonary Medicine*, *16*(3), 186-193.

Lin, P. L., & Flynn, J. L. (2010). Understanding latent tuberculosis: a moving target. *The Journal of Immunology*, *185*(1), 15-22.

Lipinski, C. A. (2004). Lead-and drug-like compounds: the rule-of-five revolution. *Drug Discovery Today: Technologies*, *1*(4), 337-341.

Lyon, R. H., Lichstein, H. C., & Hall, W. H. (1963). Effect of Tween 80 on the growth of tubercle bacilli in aerated cultures. *Journal of bacteriology*, *86*(2), 280-284.

McCorvie, T. J., Kopec, J., Hyung, S. J., Fitzpatrick, F., Feng, X., Termine, D., ... & Bulawa, C. (2014). Inter-domain Communication of Human Cystathionine β-Synthase Structural Basis Of S-Adenosyl-L-Methionine Activation. *Journal of Biological Chemistry*, *289*(52), 36018-36030.

Meijer, A. H. (2016, March). Protection and pathology in TB: learning from the zebrafish model. In *Seminars in immunopathology* 38(2), 261-273.

Murshudov, G. N., Skubák, P., Lebedev, A. A., Pannu, N. S., Steiner, R. A., Nicholls, R. A., ... & Vagin, A. A. (2011). REFMAC5 for the refinement of macromolecular crystal structures. *Acta Crystallographica Section D: Biological Crystallography*, *67*(4), 355-367.

Neshich, I. A., Kiyota, E., & Arruda, P. (2013). Genome-wide analysis of lysine catabolism in bacteria reveals new connections with osmotic stress resistance. *The ISME journal*, *7*(12), 2400-2410.

O'Donnell, M. R., Padayatchi, N., Kvasnovsky, C., Werner, L., Master, I., & Horsburgh Jr, C. R. (2013). Treatment outcomes for extensively drug-resistant tuberculosis and HIV co-infection. *Emerg Infect Dis*, *19*(3), 416-424.

Parida, S. K., Axelsson-Robertson, R., Rao, M. V., Singh, N., Master, I., Lutckii, A., ... & Maeurer, M. (2015). Totally drug-resistant tuberculosis and adjunct therapies. *Journal of Internal Medicine*, *277*(4), 388-405.

Parish, T., & Stoker, N. G. (Eds.). (1998). Mycobacteria protocols pg 269-279.

Parthiban, B. D., Saxena, S., Chandran, M., Jonnalagadda, P. S., Yadav, R., Srilakshmi, R. R., ... & Dharmarajan, S. (2016). Design and Development of *Mycobacterium tuberculosis* Lysine ε-Aminotransferase Inhibitors for Latent Tuberculosis Infection. *Chemical biology & drug design*, *87*(2), 265-274.

Payne, D. J., Gwynn, M. N., Holmes, D. J., & Pompliano, D. L. (2007). Drugs for bad bugs: confronting the challenges of antibacterial discovery. *Nature Reviews Drug Discovery*, *6*(1), 29-40.

Pieroni, M., Annunziato, G., Beato, C., Wouters, R., Benoni, R., Campanini, B., ... & Costantino, G. (2016). Rational Design, Synthesis, and Preliminary Structure–Activity Relationships of α-

Substituted-2-Phenylcyclopropane Carboxylic Acids as Inhibitors of Salmonella typhimurium O-Acetylserine Sulfhydrylase. *Journal of medicinal chemistry*, *59*(6), 2567-2578.

Poyraz, O., Jeankumar, V. U., Saxena, S., Schnell, R., Haraldsson, M., Yogeeswari, P., ... & Schneider, G. (2013). Structure-guided design of novel thiazolidine inhibitors of O-acetyl serine sulfhydrylase from *Mycobacterium tuberculosis*. *Journal of medicinal chemistry*, *56*(16), 6457-6.

Rabeh, W. M., Alguindigue, S. S., & Cook, P. F. (2005). Mechanism of the addition half of the O-acetylserine sulfhydrylase-A reaction. *Biochemistry*, *44*(14), 5541-5550.

Rubin, E. J. (2009). The granuloma in tuberculosis—friend or foe?. *New England Journal of Medicine*, *360*(23), 2471-2473.

Sakamoto, K. (2012). The pathology of *Mycobacterium tuberculosis* infection. *Veterinary Pathology Online*, *49*(3), 423-439.

Salina, E., Ryabova, O., Kaprelyants, A., & Makarov, V. (2014). New 2-thiopyridines as potential candidates for killing both actively growing and dormant *Mycobacterium tuberculosis* cells. *Antimicrobial agents and chemotherapy*, *58*(1), 55-60.

Salsi, E., Bayden, A. S., Spyrakis, F., Amadasi, A., Campanini, B., Bettati, S., ... & Roderick, S. L. (2009). Design of O-acetylserine sulfhydrylase inhibitors by mimicking nature. *Journal of medicinal chemistry*, *53*(1), 345-356. 466.

Samala, G., Kakan, S. S., Nallangi, R., Devi, P. B., Sridevi, J. P., Saxena, S., ... & Sriram, D. (2014). Investigating structure–activity relationship and mechanism of action of antitubercular 1-(4-chlorophenyl)-4-(4-hydroxy-3-methoxy-5-nitrobenzylidene) pyrazolidine-3, 5-dione [CD59]. *International journal of mycobacteriology*, *3*(2), 117-126.

Sareen, D., Newton, G. L., Fahey, R. C., & Buchmeier, N. A. (2003). Mycothiol is essential for growth of *Mycobacterium tuberculosis* Erdman. *Journal of bacteriology*, *185*(22), 6736-6740.

Schnappinger, D., Ehrt, S., Voskuil, M. I., Liu, Y., Mangan, J. A., Monahan, I. M., ... & Schoolnik, G. K. (2003). Transcriptional adaptation of *Mycobacterium tuberculosis* within macrophages insights into the phagosomal environment. *The Journal of experimental medicine*, *198*(5), 693-704.

Schnell, R., Oehlmann, W., Singh, M., & Schneider, G. (2007). Structural Insights into Catalysis and Inhibition of O-Acetylserine Sulfhydrylase from *Mycobacterium tuberculosis* Crystal Structures Of The Enzyme A-Aminoacrylate Intermediate And An Enzyme-Inhibitor Complex. *Journal of Biological Chemistry*, *282*(32), 23473-23481.

Schnell, R., Sandalova, T., Hellman, U., Lindqvist, Y., & Schneider, G. (2005). Siroheme-and [Fe4-S4]-dependent NirA from *Mycobacterium tuberculosis* is a sulfite reductase with a covalent Cys-Tyr bond in the active site. *Journal of Biological Chemistry*, *280*(29), 27319-27328.

Schnell, R., Sriram, D., & Schneider, G. (2015). Pyridoxal-phosphate dependent mycobacterial cysteine synthases: Structure, mechanism and potential as drug targets. *Biochimica et Biophysica Acta (BBA)-Proteins and Proteomics*, *1854*(9), 1175-1183.

Scudiero, D. A., Shoemaker, R. H., Paull, K. D., Monks, A., Tierney, S., Nofziger, T. H., ... & Boyd, M. R. (1988). Evaluation of a soluble tetrazolium/formazan assay for cell growth and drug sensitivity in culture using human and other tumor cell lines. *Cancer research*, *48*(17), 4827-4833.

Shehzad, A., Rehman, G., Ul-Islam, M., Khattak, W. A., & Lee, Y. S. (2013). Challenges in the development of drugs for the treatment of tuberculosis. *Brazilian Journal of Infectious Diseases*, *17*(1), 74-81.

Silva Miranda, M., Breiman, A., Allain, S., Deknuydt, F., & Altare, F. (2012). The tuberculous granuloma: an unsuccessful host defence mechanism providing a safety shelter for the bacteria?. *Clinical and Developmental Immunology*, *2012*.

Smith, I. (2003). *Mycobacterium tuberculosis* pathogenesis and molecular determinants of virulence. *Clinical microbiology reviews*, *16*(3), 463-496.

Sridevi, J. P., Anantaraju, H. S., Kulkarni, P., Yogeeswari, P., & Sriram, D. (2014). Optimization and validation of *Mycobacterium marinum*-induced adult zebrafish model for evaluation of oral anti-tuberculosis drugs. *International journal of mycobacteriology*, *3*(4), 259-267.

Steiner, E. M., Böth, D., Lössl, P., Vilaplana, F., Schnell, R., & Schneider, G. (2014). CysK2 from *Mycobacterium tuberculosis* is an O-phospho-L-serine-dependent S-sulfocysteine synthase. *Journal of bacteriology*, *196*(19), 3410-3420.

Sundqvist, G., Stenvall, M., Berglund, H., Ottosson, J., & Brumer, H. (2007). A general, robust method for the quality control of intact proteins using LC–ESI-MS. *Journal of Chromatography B*, *852*(1), 188-194.

Swaim, L. E., Connolly, L. E., Volkman, H. E., Humbert, O., Born, D. E., & Ramakrishnan, L. (2006). *Mycobacterium marinum* infection of adult zebrafish causes caseating granulomatous tuberculosis and is moderated by adaptive immunity. *Infection and immunity*, *74*(11), 6108-6117.

Tripathi, S. M., & Ramachandran, R. (2006). Direct evidence for a glutamate switch necessary for substrate recognition: crystal structures of lysine ε-aminotransferase (Rv3290c) from *Mycobacterium tuberculosis* H37Rv. *Journal of molecular biology*, *362*(5), 877-886.

Tripathi, S. M., & Ramachandran, R. (2006). Overexpression, purification and crystallization of lysineε-aminotransferase (Rv3290c) from *Mycobacterium tuberculosis* H37Rv. *Acta Crystallographica Section F: Structural Biology and Crystallization Communications*, *62*(6), 572-575.

Vagin, A., & Teplyakov, A. (2010). Molecular replacement with MOLREP. *Acta Crystallographica Section D: Biological Crystallography*, *66*(1), 22-25.

Velick, S. F., & Vavra, J. (1962). A kinetic and equilibrium analysis of the glutamic oxaloacetate transaminase mechanism. *Journal of Biological Chemistry*, *237*(7), 2109-2122.

Villemagne, B., Crauste, C., Flipo, M., Baulard, A. R., Déprez, B., & Willand, N. (2012). Tuberculosis: the drug development pipeline at a glance. *European Journal of Medicinal Chemistry*, *51*, 1-16.

Voskuil, M. I., Visconti, K. C., & Schoolnik, G. K. (2004). *Mycobacterium tuberculosis* gene expression during adaptation to stationary phase and low-oxygen dormancy. *Tuberculosis*, *84*(3), 218-227.

Wang, F., Sambandan, D., Halder, R., Wang, J., Batt, S. M., Weinrick, B., ... & Hassani, M. (2013). Identification of a small molecule with activity against drug-resistant and persistent tuberculosis. *Proceedings of the National Academy of Sciences*, *110*(27), E2510-E2517.

Winn, M. D., Ballard, C. C., Cowtan, K. D., Dodson, E. J., Emsley, P., Evans, P. R., ... & McNicholas, S. J. (2011). Overview of the CCP4 suite and current developments. *Acta Crystallographica Section D: Biological Crystallography*, *67*(4), 235-242

World Health Organization. (2010). *Treatment of Tuberculosis: guidelines*. World Health Organization.

World Health Organization. (2016). *Global Tuberculosis Report 2016*. World Health Organization.

Young, D., Stark, J., & Kirschner, D. (2008). Systems biology of persistent infection: tuberculosis as a case study. *Nature Reviews Microbiology*, *6*(7), 520-528.

Zeng, L., Shi, T., Zhao, Q., & Xie, J. (2013). Mycobacterium sulfur metabolism and implications for novel drug targets. *Cell biochemistry and biophysics*, *65*(2), 77-83.

Zhang, J. H., Chung, T. D., & Oldenburg, K. R. (1999). A simple statistical parameter for use in evaluation and validation of high throughput screening assays. *Journal of biomolecular screening*, *4*(2), 67-73.

Zumla, A. I., Gillespie, S. H., Hoelscher, M., Philips, P. P., Cole, S. T., Abubakar, I., ... & Nunn, A. J. (2014). New antituberculosis drugs, regimens, and adjunct therapies: needs, advances, and future prospects. *The Lancet Infectious Diseases*, *14*(4), 327-340.

Zumla, A., Nahid, P., & Cole, S. T. (2013). Advances in the development of new tuberculosis drugs and treatment regimens. *Nature Reviews Drug discovery*, *12*(5), 388-404.

LIST OF PUBLICATIONS

From Thesis work

- Brunner, K., Maric, S., **Reshma, R. S.**, Almqvist, H., Seashore-Ludlow, B., Gustavsson, A. L., & Sriram, D. (2016). Inhibitors of the cysteine synthase CysM with antibacterial potency against dormant *Mycobacterium tuberculosis*. *Journal of Medicinal Chemistry*, *59*(14), 6848-6859.

- **Reshma, R. S.**, Yogeeswari, P., & Sriram, D. (2016). Design and development of novel inhibitors for the treatment of latent tuberculosis. *International Journal of Mycobacteriology*.

- **Reshma, R. S.,** Saxena, S., Jeankumar, V. U., Bobesh, K. A Nidhi K., Pappachan E K. , Sriram D. (2017) Modification of Benzthiazole lead against Mycobacterium tuberculosis LAT a potential target in dormancy. Bioorganic & Medicinal Chemistry Communicated.

- **Reshma, R. S.,** Saxena, S., Jeankumar, V. U., Bobesh, K. A Nidhi K., Pappachan E K. , Sriram D. (2017) Modulation of cyclobutyl based lead targeting persistent phase of Mycobacterium tuberculosis through lysine-ε aminotransferase. Chem Med Chem Communicated.

- **Reshma, R. S.,** Saxena, S., Jeankumar, V. U., Bobesh, K. A Nidhi K., Pappachan E K. , Sriram D. (2016) Morphed Quinoline Leads As New Horizon For Treatment Of Latent Tuberculosis. Tuberculosis Communicated.

Other publications

- **Reshma, R. S.**, Saxena, S., Bobesh, K. A., Jeankumar, V. U., Gunda, S., Yogeeswari, P., & Sriram, D. (2016). Design and development of new class of *Mycobacterium tuberculosis* l-alanine dehydrogenase inhibitors. *Bioorganic & Medicinal Chemistry*, *24*(18), 4499-4508.

- Jeankumar, V. U. [*], **Reshma, R. S.** [*], Vats, R., Janupally, R., Saxena, S., Yogeeswari, P., & Sriram, D. (2016). Engineering another class of anti-tubercular lead: Hit to lead optimization of an intriguing class of gyrase ATPase inhibitors. *European Journal of Medicinal Chemistry*, *122*, 216-231. ([*] Equal contribution)

- Jeankumar, V. U., **Reshma, R. S.**, Janupally, R., Saxena, S., Sridevi, J. P., Medapi, B., ... & Sriram, D. (2015). Enabling the (3+ 2) cycloaddition reaction in assembling newer anti-tubercular lead acting through the inhibition of the gyrase ATPase domain: lead optimization and structure activity profiling. *Organic & biomolecular chemistry*, *13*(8), 2423-2431.

- Jeankumar, V. U., Saxena, S., Vats, R., **Reshma, R. S.**, Janupally, R., Kulkarni, P., ... & Sriram, D. (2016). Structure-Guided Discovery of Antitubercular Agents That Target the Gyrase ATPase Domain. *ChemMedChem*.

- Parthiban, B. D., Saxena, S., Chandran, M., Jonnalagadda, P. S., Yadav, R., **Srilakshmi, R. R.**, ... & Dharmarajan, S. (2016). Design and Development of *Mycobacterium tuberculosis* Lysine ε-Aminotransferase Inhibitors for Latent Tuberculosis Infection. Chemical biology & drug design, 87(2), 265-274.

- Bobesh, K. A., Renuka, J., **Srilakshmi, R. R.**, Yellanki, S., Kulkarni, P., Yogeeswari, P., & Sriram, D. (2016). Replacement of cardiotoxic aminopiperidine linker with piperazine moiety reduces cardiotoxicity? *Mycobacterium tuberculosis* novel bacterial topoisomerase inhibitors.*Bioorganic & Medicinal Chemistry*, *24*(1), 42-52.

191

Papers presented at National/International Conferences

- **Reshma Srilakshmi R**, Bobesh KA, Shalini S, Yogeeswari P, Sriram D, Morphed Benzthiazole lead as new horizon for treatment of latent tuberculosis. ATMOS held at BITS-Pilani Hyderabad Campus, 14 Oct 2016 (Won the best paper presentation)

- **Reshma Srilakshmi R**, Bobesh KA, Shalini S, Yogeeswari P, Sriram D, Development of Cyclobutyl derivatives as potent *Mtb* Lysine Aminotransferase inhibitors targeting Latent Tuberculosis. 6th International Symposium on "Current Trends in Drug Discovery & Research", CSIR-CDRI, Lucknow, Feb. 25th – 28th, 2016

- **Reshma Srilakshmi R**, Bobesh KA, Shalini S, Yogeeswari P, Sriram D, Development of Quinoline derivatives as potent *Mtb* Lysine Amino transferase inhibitors targeting Latent Tuberculosis. Drug Discovery & Development – Global scenario – Indian Perspective at NIPER- Hyderabad, Nov. 20th - 21th , 2015.

- **Reshma Srilakshmi R**, Bobesh KA, Shalini S, Yogeeswari P, Sriram D, Design, Synthesis and Biological evaluation of Benzothiazole derivatives as *Mtb* Lysine aminotransferase inhibitors. National conference on Drug Discovery and Development in Chemistry- Applications in Pharma Industry (DDDC-2015) at S.V. University, Tirupathi, Sep. 14th - 15th, **2015**.

- National Symposium on Human Diseases at BITS-Pilani, Hyderabad Campus, Hyderabad, Mar. 15th - 16th, **2014.**

BIOGRAPHY OF D. SRIRAM

D. Sriram is presently working in the capacity of Professor at Department of Pharmacy, Birla Institute of Technology & Science, Pilani, Hyderabad campus. He received his Ph.D. in 2000 from Banaras Hindu University (IIT-Varanasi), Varanasi. He has been involved in teaching and research for last 16 years. He has 327 peer-reviewed research publications, 5 patents and 1 book to his credit. He has collaborations with various national and international organizations such as Karolinska Institute, Sweden; Institute of Science and Technology for Tuberculosis, Porto Allegre, Brazil; National Institute of Immunology, New Delhi etc. He was awarded the Young Pharmacy Teacher of the year award of 2006 by the Association of Pharmacy Teachers of India. He received ICMR Centenary year award in 2011. Prof. D Sriram has been selected for the prestigious Tata Innovation Fellowship of the Department of Biotechnology, Government of India for the year 2015-16 in recognition of his outstanding research contributions.He has guided 19 Ph.D. students and 8 students are pursuing Ph.D. currently. His research is funded by agencies like the UGC, CSIR, ICMR, DBT and DST.

BIOGRAPHY OF R. RESHMA SRI LAKSHMI

Ms. R. Reshma Sri Lakshmi completed her Bachelor of Pharmacy from GITAM Institute of Pharmacy, Visakhapatnam (GITAM University, A.P). She has obtained her Master of Pharmacy form BITS-Pilani Hyderabad campus. She has been appointed as DST-Inspire Junior Research Fellow from Aug 2014 onwards at Birla Institute of Technology & Science, Pilani, and Hyderabad campus under the supervision of Prof. D. Sriram. She has published eight scientific papers in well-renowned international journals and also presented papers at national and international conferences.